THESIS APPROVAL

The abstract and thesis of April Ann Herb for the Master of Science in Geology were presented January 14, 2000, and accepted by the thesis committee and the department.

COMMITTEE APPROVALS:

_____
Curt Peterson, Chair

_____
Kenneth Cruikshank

_____
Michael Roberts

_____
Trevor Smith
Representative of the Office of Graduate Studies

DEPARTMENTAL APPROVAL:

_____
Ansel Johnson, Chair
Department of Geology

ABSTRACT

An abstract of the thesis of April Ann Herb for the Master of Science in Geology presented January 14, 2000.

Title: Holocene Stratigraphy and Sediment Volumes for the Columbia River Littoral Cell, Pacific Northwest, USA

Historical erosion in parts of the Columbia River Littoral cell (160 km) has sparked research into the rates and mechanisms for deposition in the cell. In this study, sand deposition rates for the last 10,000 years have been calculated, and depositional processes inferred.

In order to accomplish this task drill holes, water wells, geotechnical boring logs, GPR traces and surf zone vibracores were used to establish changes in lithology with depth, specifically the erosional truncation and lag that occurred as the surf zone transgressed. This ravinement surface delineates the base of marine sediments deposited in the last 7000 years. Radiocarbon dating of selected samples allowed for validation of field observations.

Twenty across-shore cross-sections were constructed in order to calculate beach and shelf sediment volumes. The total sediment volume was converted to a long-term sedimentation rate using an average age of 6000 years for the whole cell. A total of 7.8 x 10^9 m^3 of sediment has accumulated to make the modern barrier beach plains of the Columbia River Littoral cell, at an average rate of 1.3 x 10^6 m^3 per year.

Accumulation of sediment occurred in Clatsop and Longbeach subcells first, due

to increased accommodation space caused by lowstand valley incision and large scale tectonic uplift in the northern subcell.

HOLOCENE STRATIGRAPHY AND SEDIMENT VOLUMES FOR THE COLUMBIA RIVER LITTORAL CELL, PACIFIC NORTHWEST, USA

by

April Ann Herb

A thesis submitted in partial fulfillment of the
requirements for the degree of

MASTER OF SCIENCE
in
GEOLOGY

Portland State University
2000

ACKNOWLEDGMENTS

I would like to sincerely acknowledge the USGS and Guy Gelfenbaum for the financial funding that made this project possible and Paul See who gave the initial ravinement depth estimates and the idea to drill to find the surface. I would also like to acknowledge Curt Peterson, my graduate advisor for all the advice, support and needed discipline that got me through this project. I also thank Mike Roberts, Sandy Vanderburgh and our team of drillers for their help and expertise in the field. Many thanks go to David Percy for his expertise with the more technical aspects of this project and to Dave Twichell for the shared information and ideas that allowed for a more complete understanding of this area, across the low water mark.

I would also like to acknowledge my parents, for their unfailing support during this endeavor.

TABLE OF CONTENTS

Page

ACKNOWLEDGMENTS I

TABLE OF CONTENTS II

LIST OF TABLES IV

LIST OF FIGURES V

INTRODUCTION 1

BACKGROUND 6

The Columbia River Littoral Cell **6**
Pre-Holocene Geology **8**
Holocene Processes **10**
Sea Level Rise 10
Wave Climate and Sand Mineralogy 11
Tephra Chronology 12
Geophysics Explorations **13**
Ground Penetrating Radar 13
Subsurface Shelf Studies 15
Previous Subsurface Studies **15**
Sequence Stratigraphy **21**

METHODS 23

Sampling Strategy **23**
Drilling **27**
Radiocarbon 28
Grain Size 28
Instrumental Neutron Activation Analysis (INAA) 29
Water Well and Geotechnical borehole Data **29**
Ground Penetrating Radar **30**
Cross-section Construction **31**
Volume Calculations **34**

RESULTS 40

Facies Descriptions **40**
Lithology 40
Grain Size 41

Longshore variability 42
Radiocarbon Dates 47
Tephra Deposits 64
Descriptive Stratigraphic Logs 70
Interpreted Stratigraphic Logs 70
Water Well and Geotechnical Borehole Data 76
Ground Penetrating Radar / Offshore Seismic 76
Surfzone Vibracores 76
Cross-sections 76
Methodology 76
Clatsop Subcell 81
Longbeach Subcell 84
Grayland Subcell 89
Ocean Shores Subcell 94
DISCUSSION 105

Transgressive Stratigraphy 105
Sediment Volumes 108
Sediment Volume Comparison 111
CONCLUSIONS 113

Ravinement Surface 113
Transgressive Patterns 113
Sediment Supply and Dispersal 113
REFERENCES 114

APPENDIX A-GRAIN SIZE DATA 119

APPENDIX B- RADIOCARBON DATES 129

APPENDIX C-TEPHRA CHEMISTRY 130

APPENDIX D-DETAILED CORE LOGS 137

APPENDIX E-CROSS-SECTION DATA 163

APPENDIX F-VOLUME CALCULATIONS 177

APPENDIX G-CORE LOG SCHEMATIC SECTIONS 178

LIST OF TABLES

Table *Page*

Table 1. Holocene volcanic eruptions…….. 13

Table 2. Total weight percent-gravel, sand and mud…… 40

Table 3. Grain Size for each facies……. 41

Table 4. Mean grain size at each site…….. 42

Table 5. Radiocarbon dates…… 47

Table 6. Cross-sections unaffected by channel migration……. 107

Table 7. Volumes of beach and shelf sediment for each facies…… 108

LIST OF FIGURES

Figure *Page*

Figure 1. Map of whole Columbia River littoral Cell……. 2

Figure 2. Map of Columbia River littoral cell with back edge dates

for each subcell……. 7

Figure 3. Distribution of Pleistocene terraces: Willapa Bay, Washington…….. 9

Figure 4. Clatsop Plains pre-Holocene geology……. 10

Figure 5. Grays Harbor Sea level curve…… 11

Figure 6. Off shore seismic trackline locations……. 16

Figure 7. Shelf sediment thickness isopach…….. 17

Figure 8. Water wells from Smith *et al*. (1999)…… 18

Figure 9. Smith et al. (1999) core locations…….. 19

Figure 10. Water well locations…… 23

Figure 11. GPR line locations…….. 24

Figure 12. Drill hole locations (this study)…….. 25

Figure 13. GPR with base of beach shown……. 31

Figure 14. Cross-section locations……. 32

Figure 15. Uninterpreted cross-section…….. 34

Figure 16. Interpreted cross-section…… 35

Figure 17. Cross-section with graphic logs…… 36

Figure 18. Map view with volume calculation cells…….. 37

Figure 19. Cross-section with volume shaded……... 38

Figure 20. Mean grain size at each site……. 43

Figure 21. Beach and Shelf grain size…… 44

Figure 22. Ravinement grain size at each site…… 45

Figure 23. Ravinement onset ages……. 48

Figure 24. Copr-1 core log…… 49

Figure 25. Mocl-1 core log…… 49

Figure 26. Grbe core log…… 50

Figure 27. Goul core log…… 51

Figure 28. Oyst core log …….. 52

Figure 29. Klip core log…… 53

Figure 30. Pcyd core log…… 54

Figure 31. 67th core log ……. 55

Figure 32. Mchu core log…….. 56

Figure 33. Sunb core log…….. 57

Figure 34. Delr core log…… 59

Figure 35. Delm core log…….. 60

Figure 36. Oyhut-1 core log……. 61

Figure 37. Ncov core log..…… 62

Figure 38. Tephra sites…… 64

Figure 39. Bayr core log…….. 65

Figure 40. Photomicrographs of tephra…….. 66

Figure 41. INAA chemistry plot- Sm-La……. 67

Figure 42. INAA chemistry plot- La-Ce…….. 67

Figure 43. INAA chemistry plot- Sm-Ce…… 68

Figure 44. Copr-2 core log …… 70

Figure 45. Roosevelt core site logs ……... 71

Figure 46. Glen core log……. 72

Figure 47. Delm core log…… 73

Figure 48. Smit core log…….. 74

Figure 49-a. Cross-section with reduced vertical exaggeration (20x)……. 78

Figure 49-b. Clatsop-1 Cross-section……. 79

Figure 50. Clatsop-2 Cross-section…… 81

Figure 51. Clatsop-3 Cross-section…… 82

Figure 52. Longbeach-1 Cross-section……... 84

Figure 53. Longbeach-2 Cross-section…….. 85

Figure 54. Longbeach-3 Cross-section…….. 86

Figure 55. Longbeach-4 Cross-section…….. 87

Figure 56. Grayland-1 Cross-section……. 89

Figure 57. Grayland-2 Cross-section……. 90

Figure 58. Grayland-3 Cross-section……. 91

Figure 59. Grayland-4 Cross-section…… 92

Figure 60. Ocean Shores-1 Cross-section……. 95

Figure 61. Ocean Shores-2 Cross-section…….. 96

Figure 62. Ocean Shores-3 Cross-section…….. 97

Figure 63. Ocean Shores-4 Cross-section…….. 98

Figure 64. Ocean Shores-5 Cross-section…….. 99

Figure 65. Ocean Shores-6 Cross-section…….. 100

Figure 66. Ocean Shores-7 Cross-section……. 101

Figure 67. Ocean Shores-8 Cross-section……. 102

Figure 68. Ocean Shores-9 Cross-section……. 103

INTRODUCTION

Recent concern about declining sand supply for beaches in southwest Washington (Phipps and Smith, 1978; Phipps, 1990) and developing erosional "hotspots" (Kaminsky *et al*., 1997) has prompted a study of sediment supply for the Columbia River Littoral Cell (Figure 1). This stretch of coastline, from Pt. Grenville, Washington to Tillamook Head, Oregon, has accreted an average rate of 2.6-3.3 m/yr in the historic time period (1880 AD to 1997 AD) but, only 0.5-0.7 m/yr for the prehistoric time period (~4500 BP to 1880 AD) (Woxell, 1998). For the past 75 years, erosion has occurred at Cape Shoalwater (Washaway Beach) and within the past decade, erosion at Cape Disappointment and Ocean Shores has begun. The result of this erosion is loss of property and millions of dollars in expense for protection measures (Gelfenbaum *et al*., 1997). A better understanding of how this system operated prior to anthropogenic influences is necessary to adequately respond to the erosion, which is threatening both private property and public infrastructure.

The Columbia River Littoral Cell extends 163 km between the bounding headlands Point Grenville, Washington, and Tillamook Head, Oregon (Peterson *et al*., 1991). The cell is divided into four subcells by major water bodies- the Columbia River, Willapa Bay and Grays Harbor. The beaches of the cell are characteristically backed by wide progradational barrier-beach plains, except for the area north of Copalis, Washington, where the beaches are backed by cliffs. The offshore and coastal sediment mineralogical signatures match those of Columbia River sediment suggesting the source of sediment to the cell is primarily from the Columbia River (Whetten *et al*., 1969; Scheidegger *et al*.,

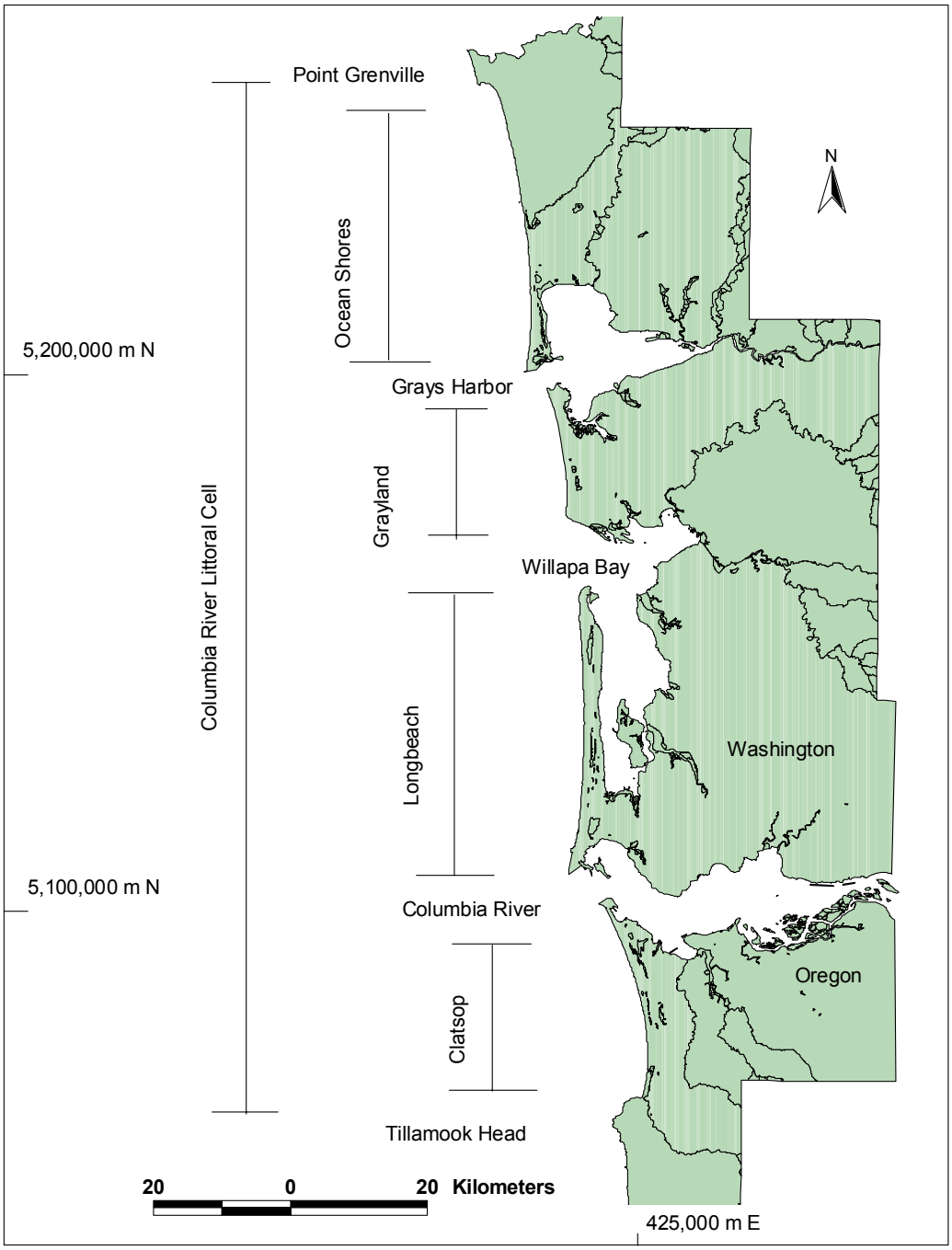

Figure 1: Map of Columbia River Littoral Cell, located on the Pacific Northwest coast of the United States. Subcell are shown from north to south: Ocean Shores, Grayland, Longbeach and Clatsop.

1976, and Sternberg, 1986).

Previous sediment budget work in the area consists of barrier accretion rates for the late historic and prehistoric time periods (Woxell, 1998) and dune correlation in Clatsop and Longbeach for the prehistoric time period (Cooper, 1958; Rankin, 1983). Offshore sedimentation rates have been estimated by Nittrouer (1978) and Sternberg (1986).

Historic sedimentation patterns (i.e., since 1880) can be explained in two ways: Either by natural changes in coastal processes and sediment supply, or as the result anthropogenic activity such as dam and jetty construction or intensive agricultural and forestry practices that yield increased sediment supply.

In order to predict future shoreline behavior and to model shoreline processes occurring today, the cause of historic and recent sedimentation pattern changes must be established. This objective can be achieved by comparing the net prehistoric sediment supply and dispersal to present conditions. The prehistoric sand supply to the cell can be determined by measuring the amount of sand deposited during the latest transgressive period.

The goals of this study are 1) to determine the amount of sand accumulated in the inner shelf, beach, and dune facies of the barrier beach plains and 2) to establish the time intervals during which the sand accumulation occurred.

Specific objectives of this project are as follows:

- Compilation of water well, geotechnical and borehole information for the Columbia River Littoral Cell.
- Determination of the depth and timing of facies transitions between dune, beach

and shelf deposits.

- Characterization of the ravinement surface and overlying facies.
- Radiocarbon dating of the post ravinement deposits.
- Computation of sand volume with time and space throughout the cell.

Results from these objectives will provide a history of Holocene sand accumulation in the cell.

Subsurface sampling and core logging were performed, during the summer of 1998, using solid stem auger and mud rotary drilling techniques. A total of 357 samples were taken from 25 boreholes. These samples were utilized for grain size analysis and lithologic characterization. A smaller number of samples were selected for radiocarbon dating.

The logs collected and interpreted during this field work along with ground penetrating radar (GPR) (collected by Dr. Harry Jol, University of Wisconsin Eau Claire) and selected water well and geotechnical logs have been used to interpret dune, beach and inner shelf facies distribution in the Columbia River Littoral Cell. Sand volumes for each subcell were calculated by constructing east to west cross-sections at representative alongshore intervals. Sand accumulation rates for the barrier beach plains are compared to sand budgets predicted for the Columbia River (Gates, 1994), shelf and bays (Gelfenbaum *et al*., 1999).

The three surfaces interpreted on the cross-sections are the beach-shelf contact, the ravinement surface and the lowstand surface (where information is available). The beach-shelf transition is based on a change in ground penetrating radar facies, which mimics the

change in bedding observed in surfzone Vibracores (Peterson unpublished data, 1998). This surface is a regressional feature that resulted from an increase in sediment supply relative to sea level rise. The ravinement surface, or transgressive erosive surface has cut into pre-existing material through landward and upward shoreface translation or beach erosion (Nummendal *et al*., 1987). This surface marks the time progressive march of the sea over land. It separates subaerial material from subaqueous material and becomes shallower and younger in the landward direction. The lowstand surface is the subaerial surface that was exposed during the last sea level low stand. In several cases this surface is overlain by either subaerial or subaqueous deposits that predate ravinement.

BACKGROUND

The Columbia River Littoral Cell

The Columbia River Littoral Cell (CRLC) is located along the northwest coastline of the United States (Figure 1) at the tectonically active Cascadia margin. The cell is 163 km long and is delimited by Point Grenville, Washington in the north and Tillamook Head, Oregon in the south. The CRLC is separated into four subcells; Ocean Shores, Grayland, Long Beach and Clatsop (Figure 1). Tidal basin inlets; Grays Harbor, Willapa Bay, and Columbia River separate the subcells.

Littoral cells are defined as coastal segments bounded by restricted alongshore sand transport (Terich and Schwartz, 1991). These cells can be identified in the Pacific Northwest where abrupt changes in alongshore sediment grain size or mineralogy trends occur on either side of a protruding headland (Peterson *et al*., 1991). Point Grenville and Tillamook Head, act as barriers to alongshore sand transport at the present sea level (Terich and Schwartz, 1991; Peterson *et al*., 1991). The subcell boundaries; at the mouth of the Columbia River, Willapa Bay and Grays Harbor, are justified on the basis of a difference in back edge barrier accretion dates between the subcells. Woxell (1998) presents back edge accretion dates, or ages of the most landward portion of the barriers, of 4000 y.b.p. for Clatsop and Longbeach subcells, 2000 y.b.p. for Grayland and 1000 y.b.p. for Ocean shores (Figure 2).

These back edge dates imply sediment accretion occurring at each subcell as a function of the distance from the source (Columbia River). The gaps in time for the start of sediment accumulation between the subcells are hypothesized to occur because of a lack of transport across subcell boundaries. The cause of which has not been resolved, but

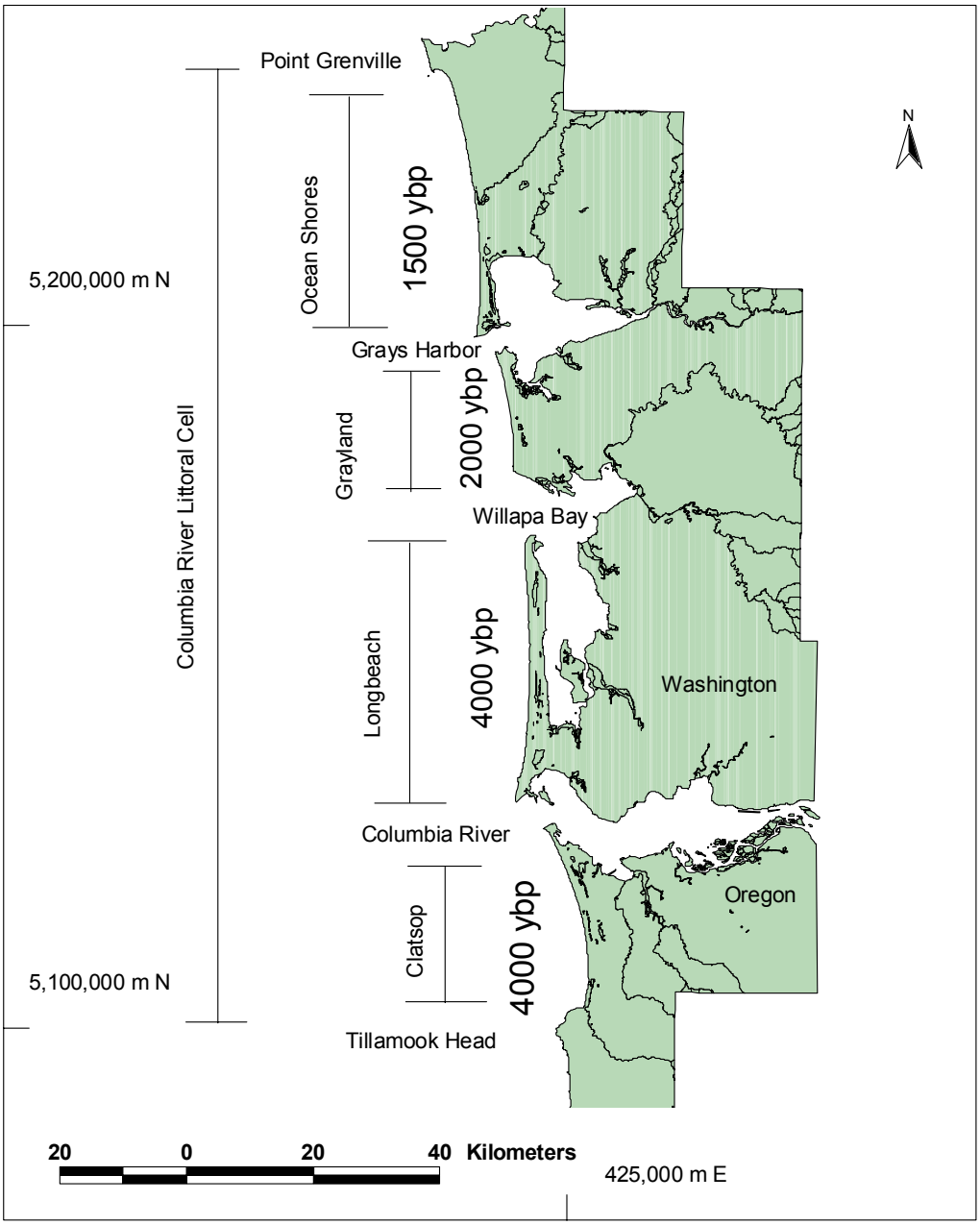

Figure 2: Back Edge dates (Woxell, 1998) showing the estimated date for onset of seaward barrier accretion for each subcell.

possibly is related to losing sediment to estuarine deposition and/or the routing of sediment offshore at the ebb tidal deltas.

Pre-Holocene Geology

Pleistocene terraces back the Holocene beaches and bays of the Columbia River Littoral cell (CRLC) (Figure 3). Investigations of Pleistocene terrace deposits around Willapa Bay show several different ages of deposition (Clifton, 1983). Two of these units have been distinguished with radiocarbon dating; both are overlain by Holocene terrace deposits. The older of which are more indurated, discontinuous and poorly defined spatially. Ages of Pliocene to early Pleistocene have been estimated based on the occurrence of mollusk, *Mytilus condoni* Dall, (Addicott, 1974). The younger Pleistocene deposits are dated at 100 to 200 ka by amino acid racemization (Kvenvolden *et al*., 1979). They are less indurated and directly underlie a more defined terrace of approximately 13 m in height. Both deposits consist of cyclic sedimentary units of sand, mud and gravel interpreted to have been deposited at or near sea level. The lack of evidence of open-marine deposition to the east of Willapa Bay indicates that the shoreline did not progress inland significantly from it's present location in Pleistocene time (Clifton, 1983).

Pre-Holocene geology in the Clatsop subcell is less well known. According to Schlicker *et al*. (1972) the pre-Holocene geology south of the Columbia River is comprised of marine terrace deposits of Pleistocene age and upper Miocene sandstone, which overlie undifferentiated sedimentary rock of Oligocene to middle Miocene age

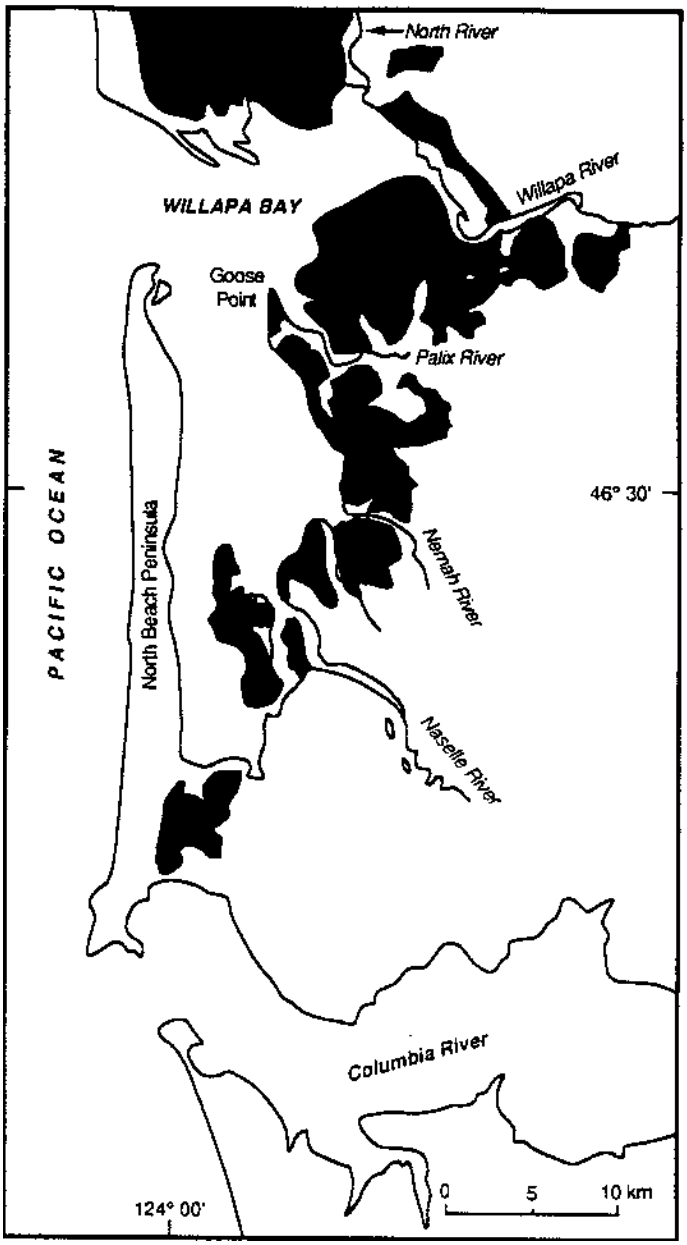

Figure 3: Pleistocene terrace distribution (shaded) surrounding Willapa Bay, Washington (modified from Clifton, 1984).

(Figure 4). The Tertiary bedrock consists of massive tuffaceous siltstone and claystone with lesser amounts of sandstone and shale. Tertiary basalts occur at depths of up to 120 m. Previous water well drilling in the Clatsop Plains area has shown unconsolidated

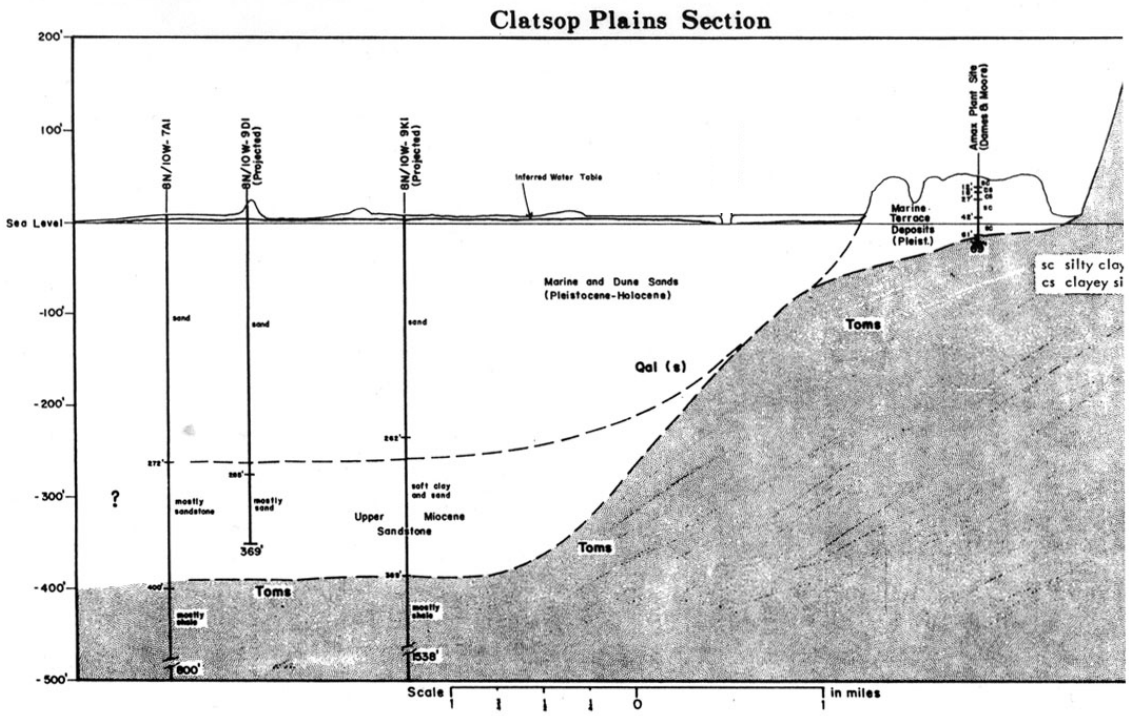

Figure 4: Cross-section for Clatsop subcell showing morphology of Quaternary deposits (from Schlicker et al., 1972). Qal : Quaternary deposits, Toms: Tertiary unit.

materials that locally reach 91 m below the surface (Frank, 1970; Schlicker *et al*., 1972).

Holocene Processes

Sea Level Rise

The beginning of Holocene time is defined as 10,000 years before present (ybp). At that time, the late Wisconsin glacial ice sheet cover had been reduced by 50% of its maximum extent and sea level was 30-50 m below present sea level (Bloom, 1983). The Holocene has been characterized as a global marine transgression created by melt from the remaining Wisconsin ice sheet. Rate of sea level rise varies locally, but has been shown to follow the general path of rapid sea level rise 10,000 ybp to 5,000 ybp and

slower sea level rise from 5,000 ybp to present (Bloom, 1983).

Local sea-level rise for the Columbia River Littoral Cell has been studied and interpreted at Grays Harbor (Peterson and Phipps, 1992). High resolution seismic, core drilling and radiocarbon dating were used to interpret Holocene filling of Grays Harbor and a corresponding sea level curve (Figure 5). Results indicate that the rate of sedimentation and eustatic sea level rise at Grays Harbor decreased substantially from 1.2 cm/yr for 10-7.5 ka to 0.1 cm/yr for 5-0 ka.

Wave Climate and Sand Mineralogy

Dominant southwesterly wind and wave attack during the stormy winter months is thought to drive sediment transport to the north in the CRLC. Significant wave heights ($H_{1/3}$) of 5 to 7 m during this time of year provide wave energy sufficient to mobilize and transport sediment northward along the coast of the pacific northwest (Komar *et al*., 1976). Midshelf transport of finer sediments is to the north-northwest as well (Nittrouer, 1978).

Sediments of the Columbia River Littoral Cell are characterized by high hypersthene to augite ratios that correlate to the mineralogy of the Columbia River Sediments (Scheidegger *et al*, 1976; Ballard, 1964). The Columbia River is well established as a dominant source of sand for the Long Beach barrier as is shown in multiple studies of the area (Ballard, 1964; Li, 1991; Li and Komar, 1992; Luepke, 1982; Scheidegger *et al*., 1971; Sternberg, 1986; Whetten *et al*., 1969). Columbia River sand is also a significant portion of the sediment in Grays Harbor (Scheidegger and Phipps, 1976). From both sediment transport and mineralogy, it can be assumed that the

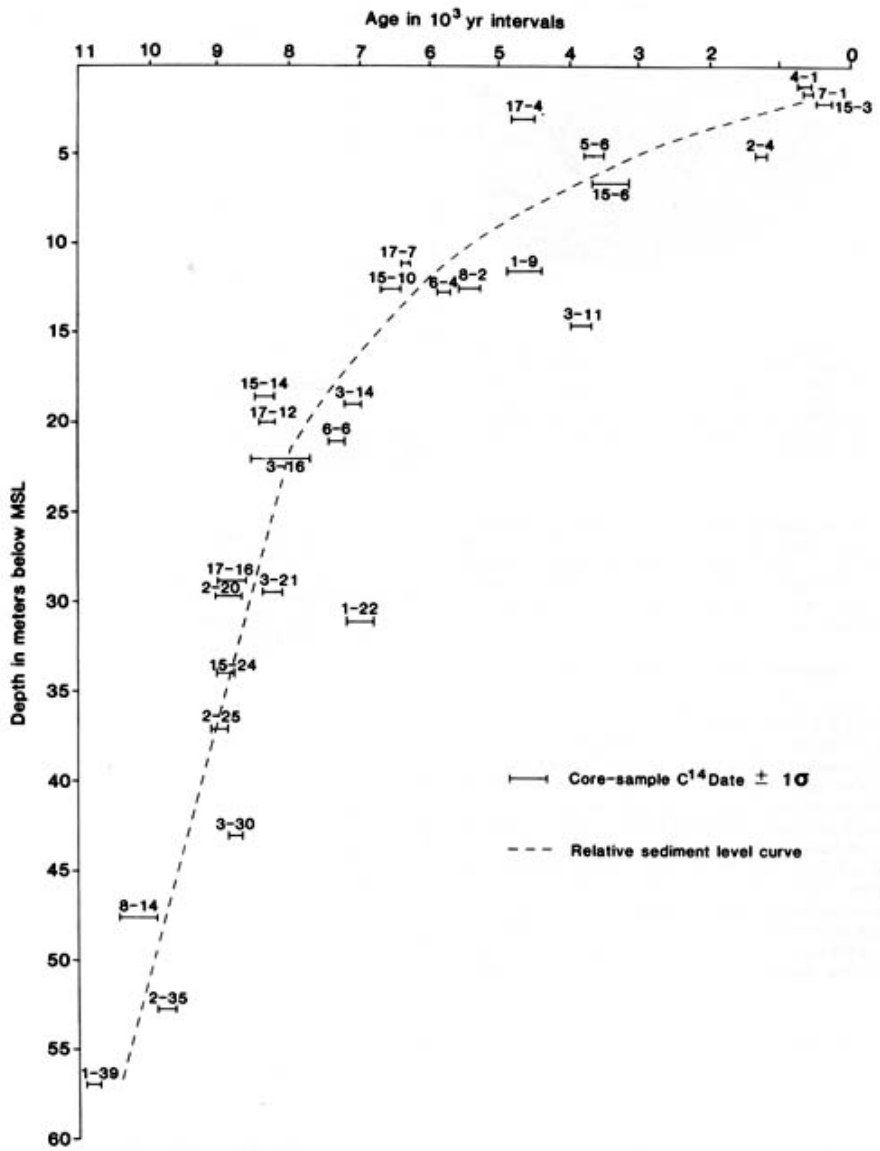

Figure 5: Sea-level curve at Grays Harbor, Washington (from Peterson and Phipps, 1992). Depth is depth of sediment level (thought to be close to sea level). Note change in rate of sea-level rise between 8000-6000 ybp.

Columbia River supplies the majority of the sediment found on the beaches of the CRLC.

Tephra Chronology

Gates (1994) has found Holocene tephra from the climax eruption of Mount Mazama in the Lower Columbia River basin. Ash from this event has been dated at 6845

Radiocarbon Years before Present (RCYBP) and has been found at a depth of 18.1 m, at a lower Columbia River site near Skamokowa, Washington. Thickness of these water lain silty ash deposits were found to be variable throughout the lower Columbia River valley. Sarna-Wojcicki et al. (1983) summarize the significant volcanic events during Holocene time in the following table (Table 1).

Table 1- VOLCANIC ASH LAYERS OF MODERATE TO LARGE VOLUME ERUPTED DURING HOLOCENE TIME (data from Sarna-Wojcicki *et al*., 1983)

Age	Ash Layer Set	Volcanic Source Area
1980	D	Mt. St. Helens, WA
180 ya	T	Mt. St. Helens, WA
500	We, Wn	Mt. St. Helens, WA
1150-1350	-	Newberry Volcano, OR
2580-2930	P	Mt. St. Helens, WA
3350-3510	Ye, Yn	Mt. St. Helens, WA
6700-7000	O (Mazama)	Crater Lake, OR
8300-11,700	J	Mt. St. Helens, WA

Near source tephra and ash layers from the volcanoes listed in Table 1 have been analyzed with Instrumental Neutron Activation Analysis (INAA) by Randle *et al*. (1970); Borchardt *et al*. (1971); Bacon and Druitt (1988) and Gates (1994). Gates (1994) found rare earth element ratios (La-Sm, Ce-Sm and Ce-La) to be good indicators of source for Mazama ash layers in Columbia River sediment. Randle *et al*. (1970) cite rare earth elements as good indicators of provenance for Cascade eruptions and suggest ratios between light rare earth elements and heavier rare earths as good discriminates. INAA methods were modeled after Gates (1994) for this study.

Geophysics Explorations

Ground Penetrating Radar

Procedure

Ground penetrating radar transmits radar pulses into the subsurface by a surface

antenna. The radar energy is reflected off layers or objects in the subsurface that have differences in conductance. A receiving antenna at the surface then detects the returning energy. Two-way travel time of the radar waves is recorded and manipulated by a computer to yield a time-depth cross-section along the traverse. This method works well for subsurface strata of sand and gravel. Salt water and muddy material inhibit penetration and reflection of the radar waves. Greater depth of radar penetration (up to 20 m) is achieved by using lower frequencies (100 or 50 MHz), but resolution is then sacrificed. For shallower subsurface studies a resolution of several centimeters scale is possible (300 MHz yields penetration less than 5 m) (Conyers and Goodman, 1997).

Findings

The upper 10 m of Holocene stratigraphy of the Long Beach Spit was interpreted from GPR traverses by Meyers (1994) and Jol *et al*., (1998) as dune forms and storm generated beachface reflectors. Meyers used water well logs, vibracoring and trenching to ground truth the Long Beach GPR database. The GPR profiles document subsurface scarps that define past shoreline positions following great subduction zone earthquakes (Smith *et al*., 1999; Jol *et al*., 1998; Doyle, 1996; Meyers, 1994). Ground truthing of GPR traces in the CRLC was performed by Woxell (1998) using Australian Sand Auger and vibracore methods (this study shares the GPR data set used by Woxell (1998) and collected by Jol et al., (1998) as well as additional GPR traces collected by Dr. Harry Jol during the summer of 1998).

These radar surveys found evidence for buried erosional scarps and accretionary, westward dipping, shoreface reflectors in the shallow subsurface (<10 meters depth)

(Meyers, 1994; Jol *et al*., 1995).

Subsurface Shelf Studies

Twichell and Cross at USGS Woods Hole are currently studying shelf deposits of the CRLC. Seismic reflection, side scan sonar, bottom videography and surface sampling were performed during cruises in 1997 and 1998 (Cross *et al*., 1999). Grain size analysis and interpretation of geophysical tracklines have since been performed. Seismic tracklines and a shelf sediment isopach map are presented here in Figures 6 and 7. Point interpretations of ravinement locations offshore (Cross *et al*., 1999; personal communication Twichell, 1999) are included in the cross-sections produced for this thesis. (For data tables see Appendix E)

Inner shelf seismic reflection data show folding of offshore Tertiary basement north of Willapa Bay. Deformation increases north of Grays Harbor and overlying shelf sediments decrease from 20 m to less than 2 m in thickness between Willapa Bay and Point Grenville (Twichell, 1997). The deformed basement was truncated to form a wave cut platform during the Holocene transgression. The regional decrease in Holocene shelf sediment thickness to the north is thought to represent a combination of greater tectonic uplift in the north and greater depth of river incision, during low stand, to the south (off shore of the Columbia River mouth) (Peterson *et al*., 1999).

Previous Subsurface Studies

Smith (1999) has conducted previous subsurface studies in the Longbeach area. This study contains three deep-water well logs that were logged during installation and have radiocarbon dates listed (Figures 8-9). Smith *et al.* hypothesize that the Longbeach

spit has approximately 25 m of sand above the ravinement. They also show a thin muddy layer beneath the ravinement and mention the absence of landward dipping GPR reflectors or ‘washovers’ on the east side of the spit. Back barrier erosion is sited as a possible cause for this lack of classic washover features.

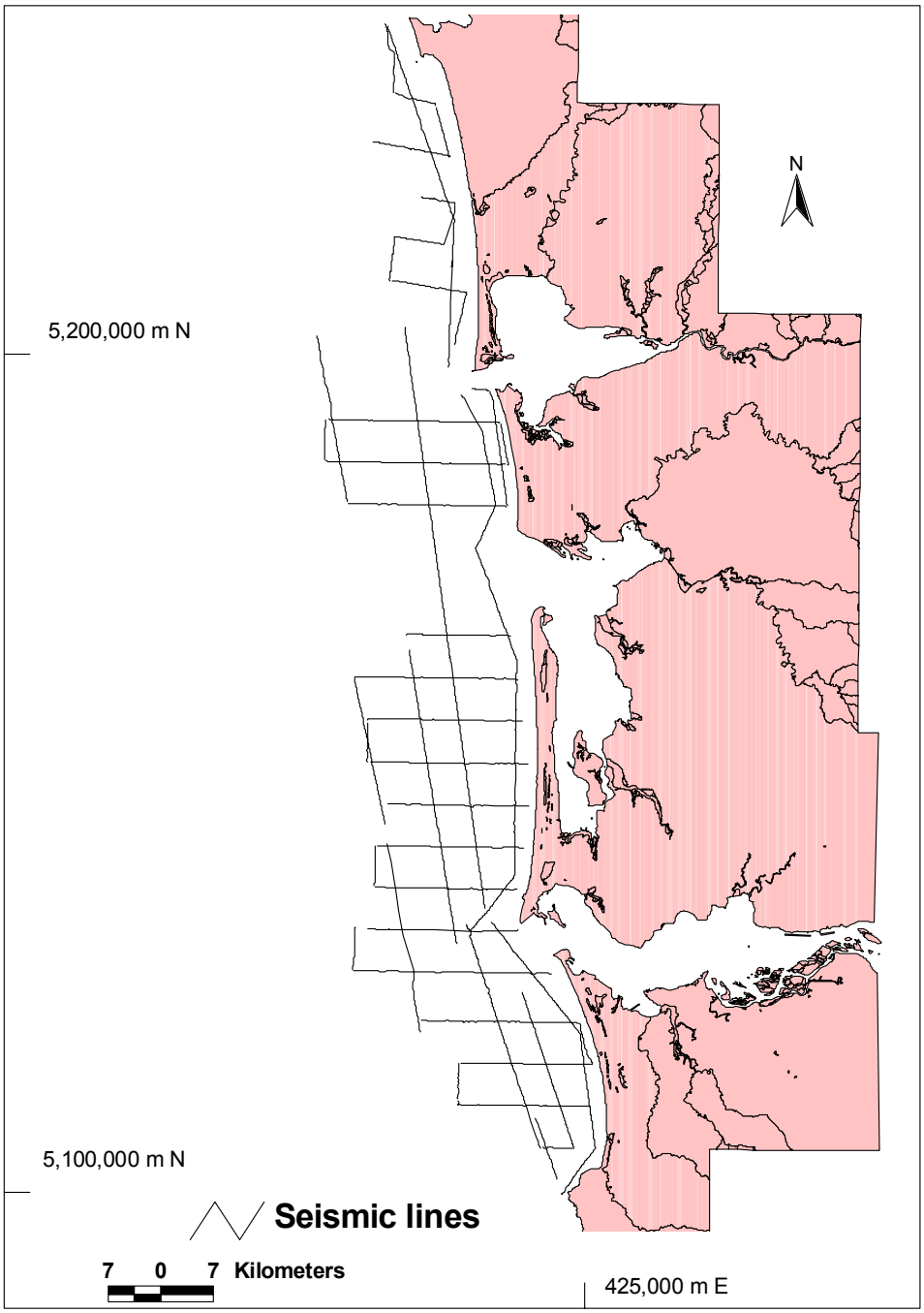

Figure 6: Tracklines for offshore seismic (from Cross et al., 1999).

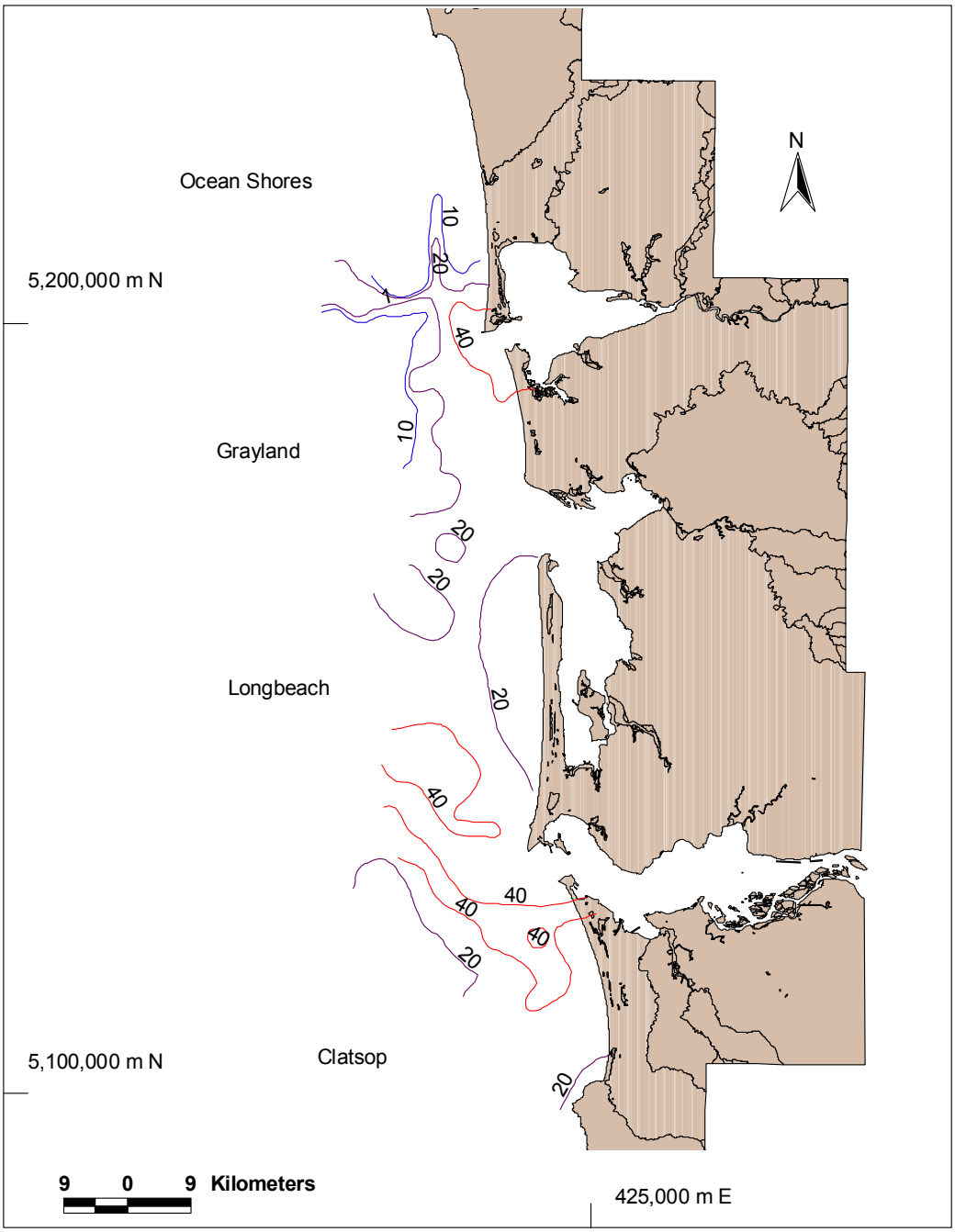

Figure 7: Shelf sediment isopach map interpreted from offshore seismic lines (thickness in meters below sea level)(Twichell, personal communication 1998).

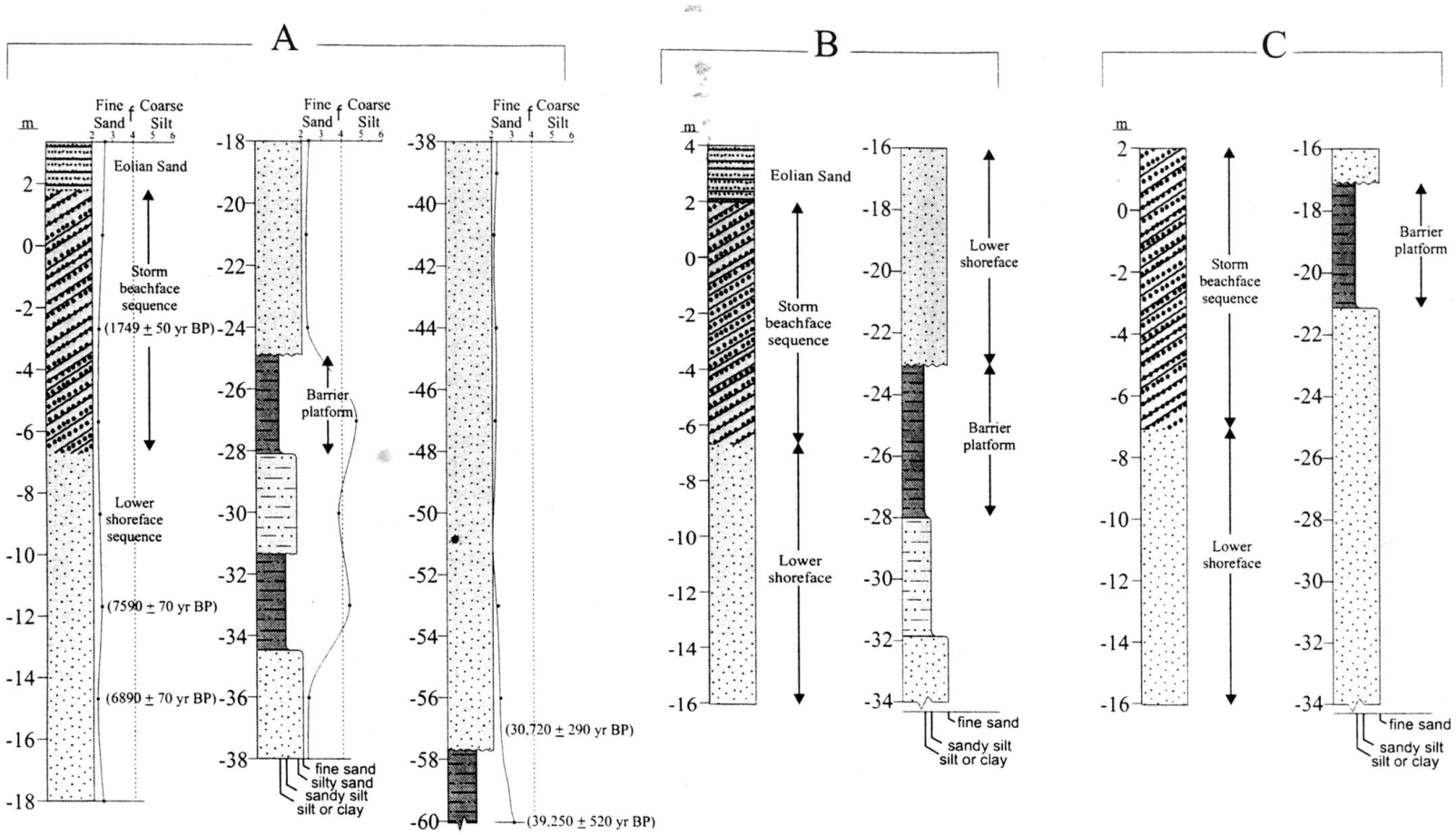

Figure 8: Smith *et al*. (1999) logs, Longbeach, Washington; showing the base of post-ravinement sediments at the top of the 'barrier platform'. A) Surfside (25 m), B) Ocean Park (23 m), C) A.Shawa (17 m).

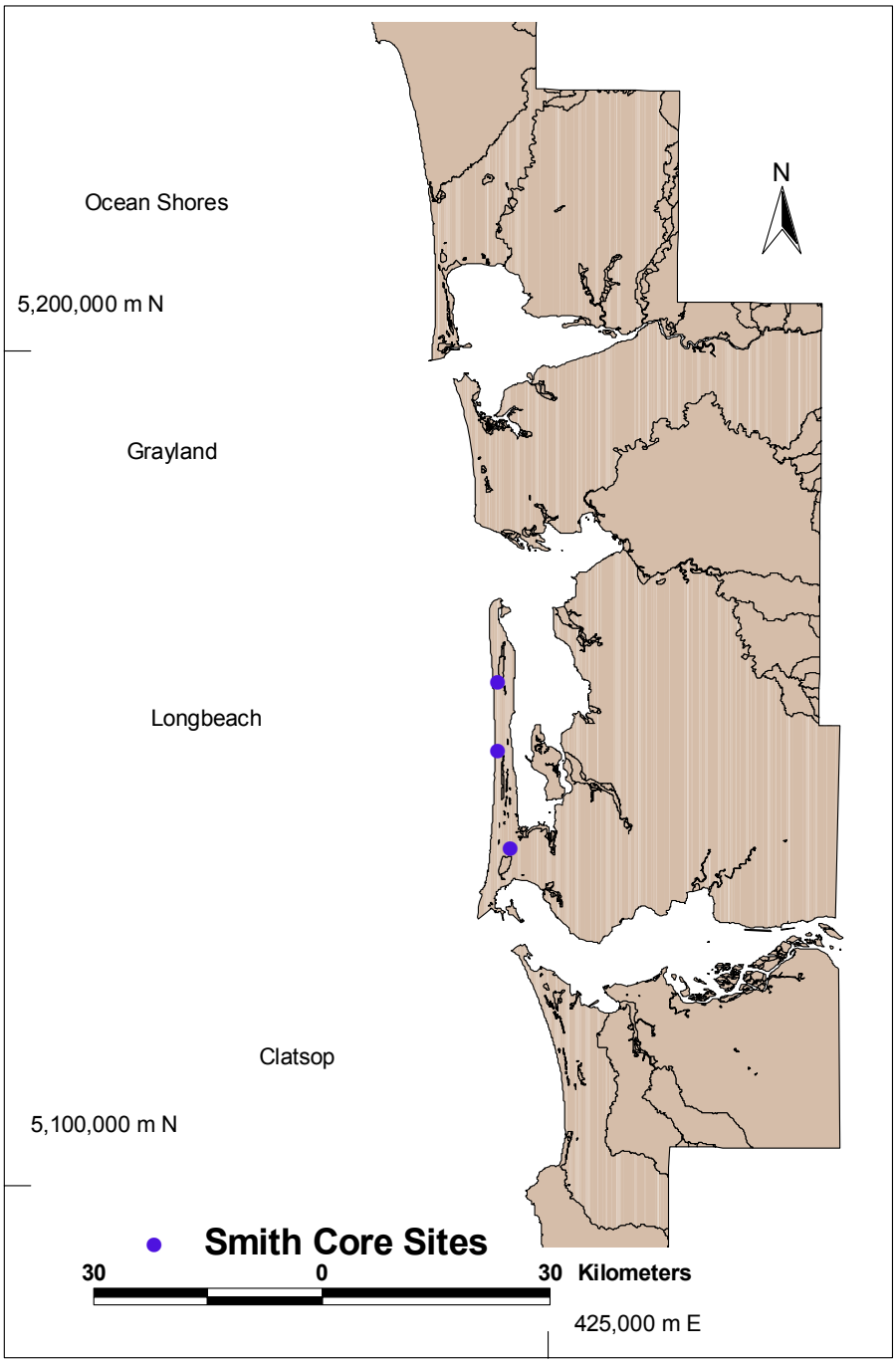

Figure 9: Smith *et al*. (1999) core locations, Longbeach Penninsula.

Sequence Stratigraphy

Stratigraphic relations resulting from sea level rise and fall are not universal around the world. Factors that contribute to differences in the preserved stratigraphy are tectonic activity, sediment supply, bedrock geology, rate of sea level rise, shelf incised valley and fill patterns, and wave strength. Sequence stratigraphy models have been developed only recently by Mitchum, *et al*., 1977, and refined by Mitchum, Vail, and coworkers at Exxon Production Research Company, (e.g., Posamentier, *et al*., 1988; Van Wagoner *et al*., 1988; 1990). These models are relatively well constrained for passive margin coastlines with barrier island stratigraphy. Smith *et al.* (1999) describe the CRLC as having thicker barrier sands (17-25 m), than passive margin coastlines (4-10 m). Thus, the thick barrier sands and thick off-shore deposits of the CRLC (Cross *et al*., 1999) do not conform to the thin transgressive sequences observed for other high energy coastlines. Since the Holocene stratigraphy of the CRLC is thicker than what is observed elsewhere, the mechanisms for and conditions of cell development in this system are presumably different and of great interest.

The base of transgressive stratigraphy is documented throughout the world as an erosive ravinement surface or depositional flooding surface. The transition is recognizable in several locations with transgressive stratigraphy preserved: the Late Cretaceous Cape Sebastian Sandstone in southwestern Oregon (Bourgeois, 1980); Late Cretaceous of the central California Coast Ranges (Howell *et al*., 1977) and Pleistocene marine terrace deposits at central Monterey Bay, California (Dupre, 1984). There are not many other examples of transgressive beach stratigraphy in geologic history because they are

relatively rarely preserved during shoreline retreat (Davis and Clifton, 1987).

This erosion during sea level rise yields the formation of a ravinement surface or erosional lag deposit on the inner shelf (Stamp, 1922; Swift, 1968; and Demarest and Kraft, 1987). The lithologic characteristics, slope, and depth of the transgressive surface is variable. It generally dips seaward at 1-2° and consists of poorly sorted sandy gravel overlying an unconformity. The difference in grain size between the transgressive surface and the overlying material represents a rapid change in sediment entrainment properties and the inferred paleo-environment (Demarest and Kraft, 1987).

In contrast, low lying areas, such as low stand channels or valleys, accumulate silt and mud as they are flooded with seawater. Such flooding surfaces are recorded by changes in lithology that represent a rapid deepening of the water. Often, some or all of this sediment is eroded as the surf zone transgresses over the area.

Ravinement recognition is difficult where pre-Holocene topography or underlying sediment types are unknown. It is then easy to mistake local flooding events or channel migrations for the ravinement surface. A different type of problem arises in the inlets and at locations where there is a lack of coarse sediment. In these cases, the grain size difference is insufficient to define a ravinement surface because of either high fluid power or a lack of grain size variation. Thus, in these locations recognition of the base of Holocene sediment is particularly difficult (Demarest and Kraft, 1987). In this study, radiocarbon dating, and tephra chronology have been employed to help interpret the base of Holocene sands in the CRLC.

METHODS

For this study the Simon Fraser University (SFU) Mobile B-53 drill rig was used to explore the subsurface stratigraphy of Holocene sediments. Both solid stem flight auger and mud rotary drilling methods were used. Existing water well logs (Figure 10) and ground penetrating radar traces (Figure 11) were used to help select hole locations and estimate depth to facies transitions prior to drilling. A total of 357 samples were taken from 25 boreholes (Figure 12). Coordinates of the borehole sites are given in Appendix F.

Sampling Strategy

The drilling strategy consisted of even placement of holes in the north-south direction and at least one east-west transect for each subcell (Figure 12). Drilling locations were picked using the criteria of spatial distribution, proximity to inlets and site accessibility. Borehole sites were selected away from inlets and bay mouths in order to avoid drilling channel forms or sediments that have accumulated in historic time. The greatest constraint on site selection was site accessibility. For the beach sites, both a suitable access road and 'hard' sands were needed in order to drive the rig out on the beach and for stability during drilling. Selection of mid-barrier sites was constrained by road access and private property ownership. Locations were selected away from overhead and underground utilities. Downhole sample collection was determined by three criterions: equally spaced intervals for grain size analysis in the lab, facies characterization and radiocarbon dating. Where lithology changed significantly, separate grain size samples were taken in addition to the regular interval samples. Radiocarbon samples were taken at all depths where datable materials, such as shell, detrital wood

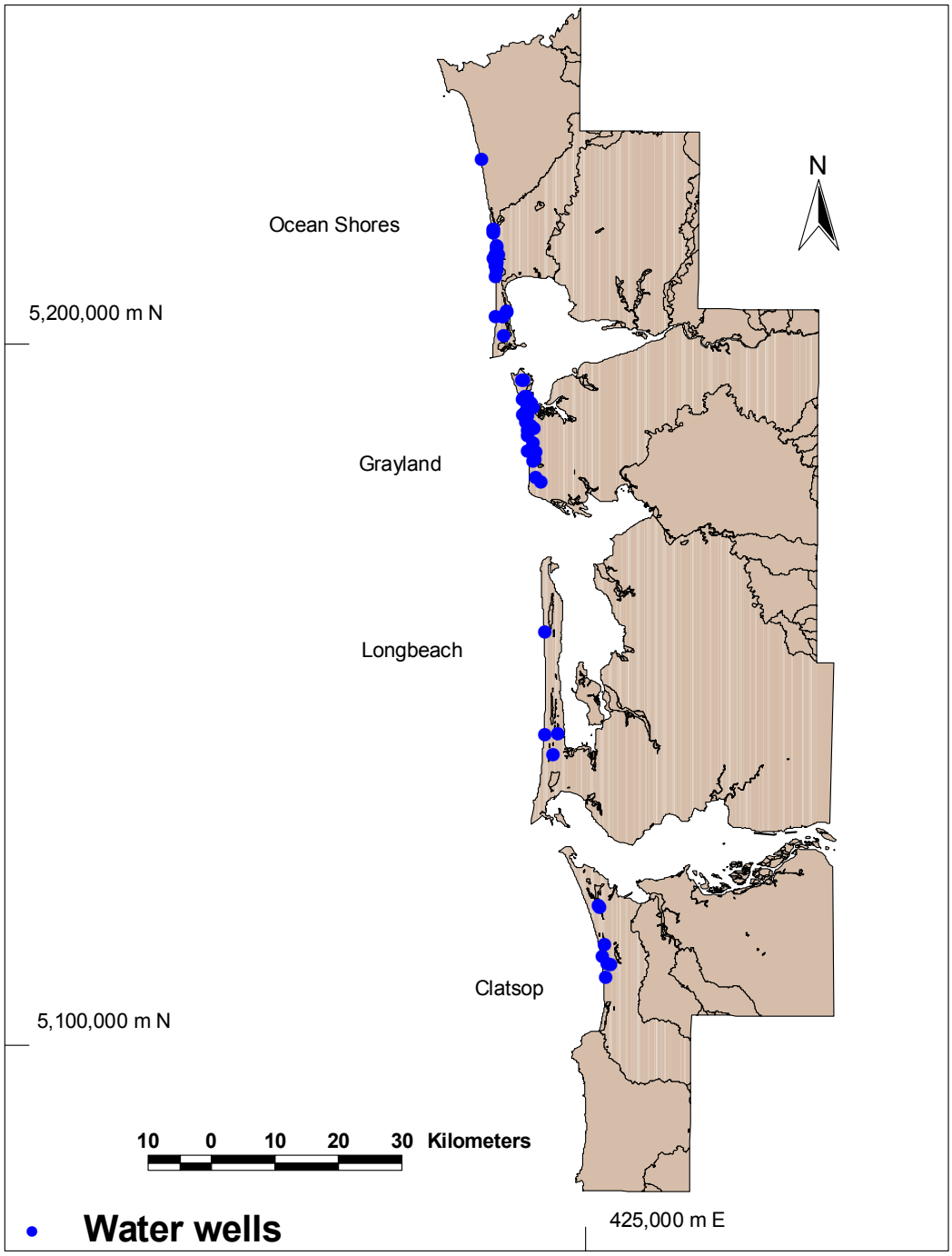

Figure 10: Water well locations in CRLC used for this study.

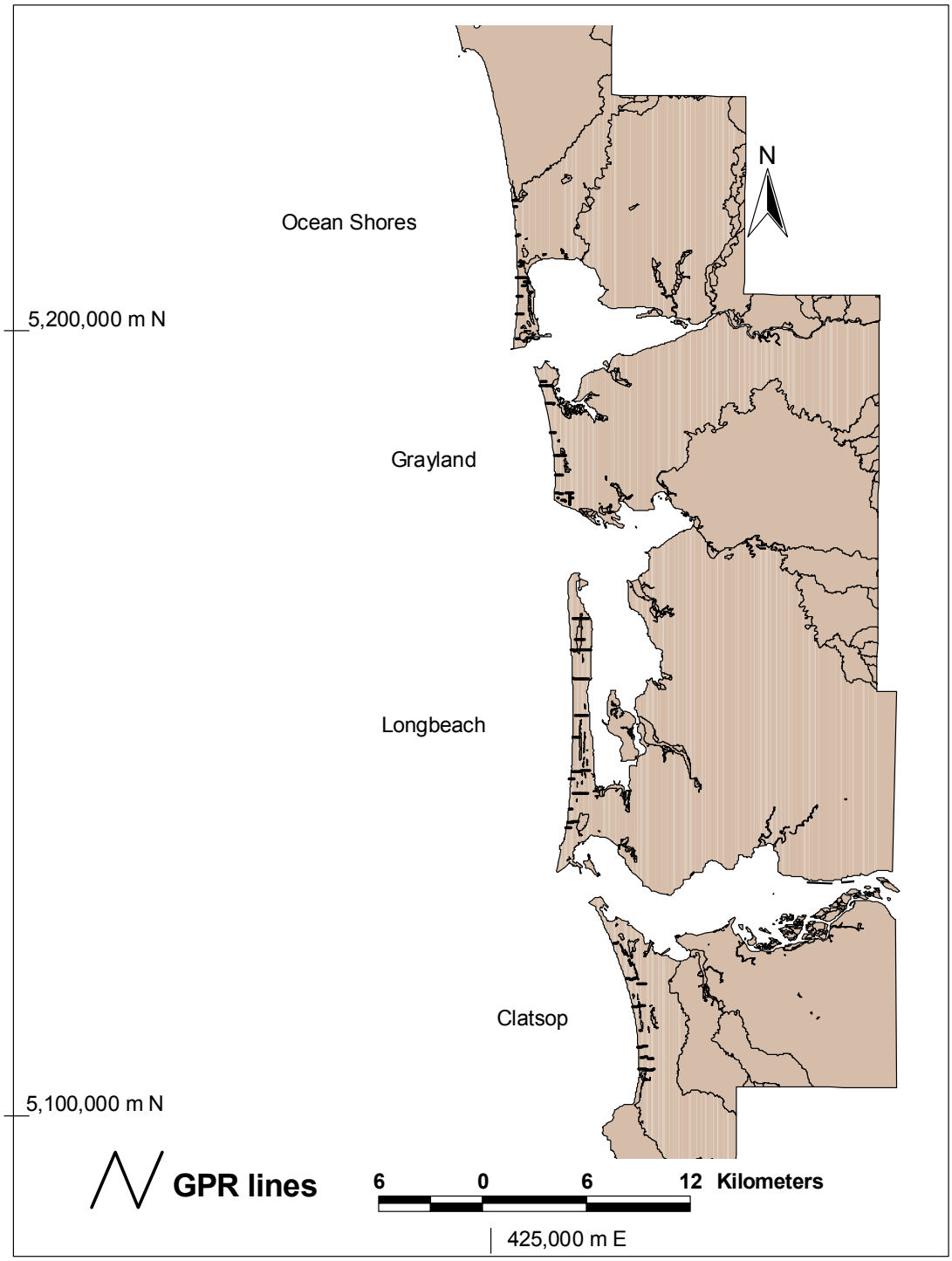

Figure 11: Ground Penetrating Radar line locations used for this study.

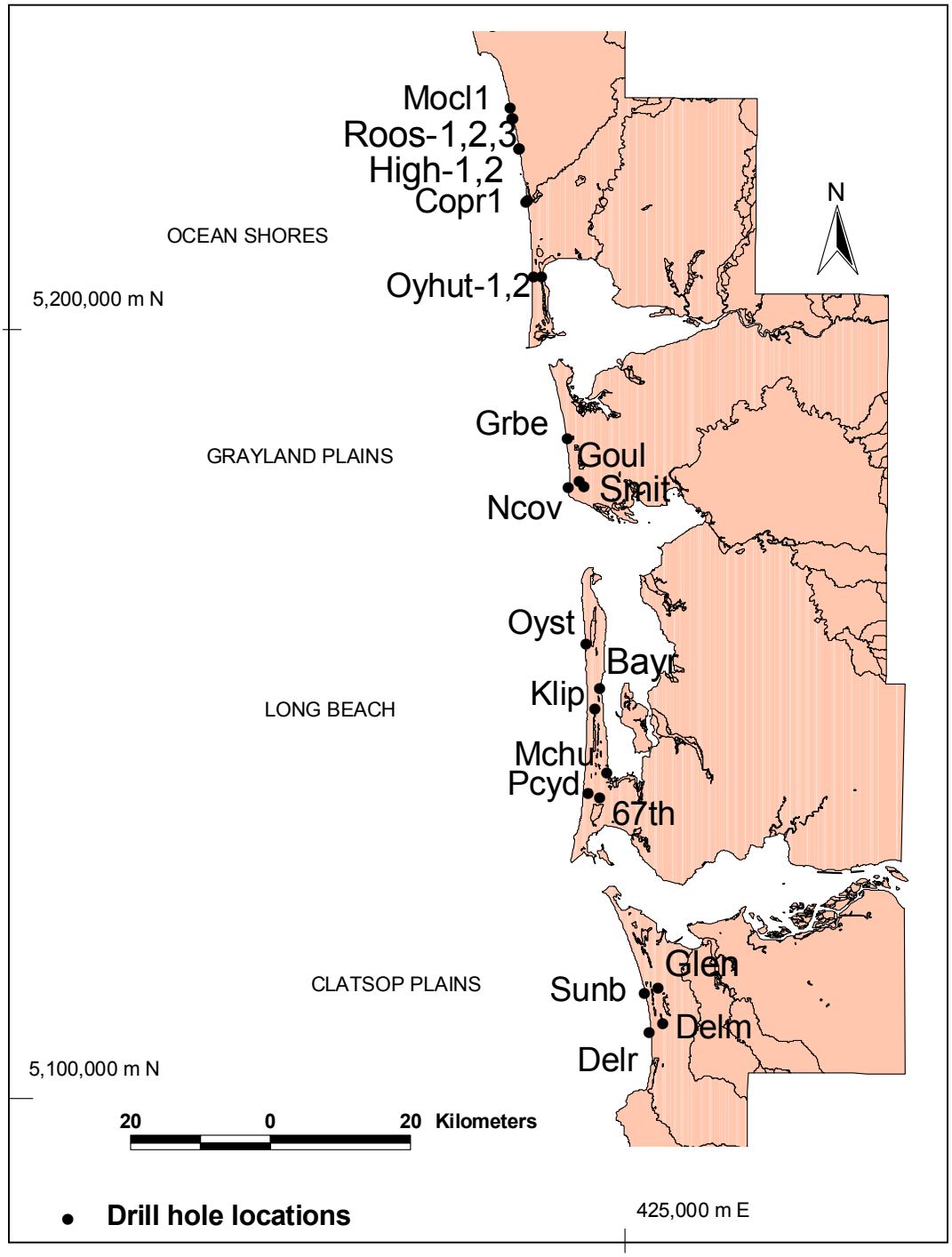

Figure 12: Drill Hole locations for this study.

fragments or peat were found.

Grain size analysis was performed on 309 of the 357 samples that were collected for characterization. Twenty radiocarbon samples were selected for timing of the ravinement / flooding event, and sedimentation rates for shelf sediments. Thirteen radiocarbon samples were chosen specifically to date the ravinement surface. These samples were selected within or just above the ravinement package and are distributed among at least three boreholes per subcell. Another seven samples from these boreholes were selected to constrain post-ravinement deposition rates.

Drilling

Dr. Mike Roberts and Dr. Sandy Vanderburg operated the SFU B-53 drill rig with the help of two undergraduate assistants. Solid stem flight auger drilling was the method of choice because continuous core return was necessary to distinguish subtle facies characteristics and lithologic changes. This method is, however, labor intensive and risky at depths greater than 50-70 feet (~16-22m). Therefore, mud rotary drilling was utilized at the base of holes Oyst and Ncov to reach or approach the ravinement surface.

Auger flights were drilled in five-foot intervals, and then brought to the surface for logging and sampling. The auger flight was placed on a plastic tarp and the core was pulled away from the stem for logging. A metal tape measure was used to record the core length in feet and inches. (English units were used to ensure accurate depth measurements and for ease in the field. Depths were later converted to metric.) Measured core logs were compared for each flight with the reported drill depths to assure accurate depth measurements. Materials on the outside edge of the core and near the top of the flight sections were potentially contaminated by up hole caving and thus these materials were

not logged. After scraping off the questionable material, the core was logged to the nearest half inch (1.27 cm), in the field. Photographs were taken of significant cores before sampling. Samples were placed in Ziploc™ freezer bags and labeled with the hole number, depth and contents. Two to four flights were laid out at a time to compare color and grain size trends. After the sediment was logged and sampled, the core material was disposed of on site.

Laboratory Analysis of Samples

Radiocarbon

Beta Analytic Laboratories (Miami, Florida) performed radiocarbon age dating of submitted material (wood and shell fragments). Radiocarbon samples were kept in freezer storage until processed. All radiocarbon samples were wet sieved, dried and hand picked to separate the sample from sources of contamination. Both bulk analysis and Accelerated Mass Spectrometry (AMS) methods were used.

Grain Size

Grain size analysis was performed on 309 samples to determine gravel, sand and mud weight percent ratios and grain size distribution within the sand size fraction (using the Wentworth scale). Samples were dried, weighed, wet sieved at 2 mm and 0.0625 mm, dried, and dry sieved at ¼ phi intervals for the sand size fraction. Thirty-three of these samples were selected randomly for statistical comparison of percent mud fraction. Comparison samples were wet sieved over a basin and the rinse was retained and settled for at least two days. The supernate then was poured off and the mud dried and weighed.

Statistical analysis was performed using Moment Statistics (Krumbein and Pettijohn, 1938) and modal analysis (Appendix A).

Instrumental Neutron Activation Analysis (INAA)

Instrumental Neutron Activation Analysis (INAA) was performed on pumice collected from tephra laminae observed during auguring. The pumice grains were hand picked from unwashed samples and identified with both binocular and petrographic microscope for volcanic glass. Photomicrographs were taken of each sample under the petrographic microscope for documentation. Samples were processed for INAA uncrushed (i.e., no glass separation). Due to the small sample size, unequal amounts of sample were analyzed. Samples were placed in clean polyvials and heat-sealed.

The samples were irradiated at the Reed College reactor (Portland, Oregon). They were exposed to a flux of 2.0×10^{12} neutrons cm^{-2} sec^{-1} at 250 kW for one hour. Gamma ray spectra were obtained using a high purity Germanium coaxial photon detection system. Spectra were collected first at 1000 seconds live time and later at 3000 seconds live time, after irradiation. Elemental concentration peaks and percent errors were obtained with the use of the EG&G ORTEC 92x Spectrum Master program package. The USGS standards, Coal Fly Ash, Andesite, Rhyolite and Gabbro were also analyzed in order to check accuracy. Trace, light and rare earth element abundances were plotted and compared to known eruptive sources and previous work in the study area such as Gates (1994).

Water Well and Geotechnical borehole Data

Water well logs and geotechnical borehole logs were used to help identify facies between drill sites. Water well logs were collected from Washington Department of Ecology for the extent of the cell in Washington State. Water well logs were collected from the Oregon Department of Water Resources for the Clatsop Plains subcell.

Geotechnical borehole logs were obtained from Washington and Oregon Departments of Transportation for selected portions of the cell. Geotechnical borehole logs are typically more detailed and more accurate than water well logs. However, they are restricted in number in this study area due to localized infrastructure development.

Selection of suitable water well and geotechnical logs was aided by examining location, locatability, depth of hole, and recognizable facies transitions. Water well and geotechnical borehole sites were limited to locations on the Holocene barriers, i.e., not on Pleistocene terrace deposits. The range of uncertainty for location was determined to be the nearest ¼ ¼ section (1/16th of a square mile) or approximately 400 m. Water wells used for cross-section construction were located within this range of uncertainty. More exact placement of the well sites was based on topographic features or proximity to housing developments. In some cases, the exact locations of the well or borehole sites were given by measurements from section corners, or street addresses. Holes with insufficient depth and holes that did not have sufficient data to define facies transitions were not used for cross-section construction.

Ground Penetrating Radar

Ground penetrating radar traces collected by Jol *et al*. (1998) were used to approximate the progradational beach-shelf contact. As noted in the Background section, the beach GPR facies are characterized by low angle seaward dipping reflectors (Jol, 1996). In comparison, inner shelf GPR facies are characterized by planar bedding and a lack of seaward dipping reflectors.

Sixty-two measurements were made from thirty-two radar lines (Figure 11) to pick

the depths of the transition between seaward dipping reflectors and chaotic to horizontal reflectors. Specifically, the lower beach contact was defined as the lowest continuous low angle seaward dipping reflector. Depths were measured from the ground surface, to the midpoint of the lowermost dipping reflector. This bottom reflector represents the *minimum* depth of the beach facies since either a change in facies or signal attenuation with depth may cause the termination of the dipping reflectors. An example GPR line is shown in Figure 13.

Cross-section Construction

Synthesis of the subsurface data was accomplished by constructing 20 east-west cross-sections (Figure 14). The cross-sections are placed at appropriate alongshore intervals to maximize data coverage. Topographic data was obtained digitally from 7.5 minute USGS Digital Elevation Model (DEM) series in the form of a Geographic Information Systems (GIS) coverage from the Washington state Department of Ecology. This coverage is based on interpolation of USGS quadrangle topographic maps with contour intervals of 20 ft. The DEM data was then converted to two dimensional x and z coordinates with ESRI ArcView GIS Spatial Analyst software in order to construct topographic profiles.

The average alongshore projection distance for subsurface data to the cross-section is 900 m. The maximum distance used to bring available subsurface records into the nearest cross-section was 5.3 Km. Where GPS (global positioning system) topographic measurements of hole elevation did not agree with the DEM data, the depth data were adjusted to the DEM topographic surface.

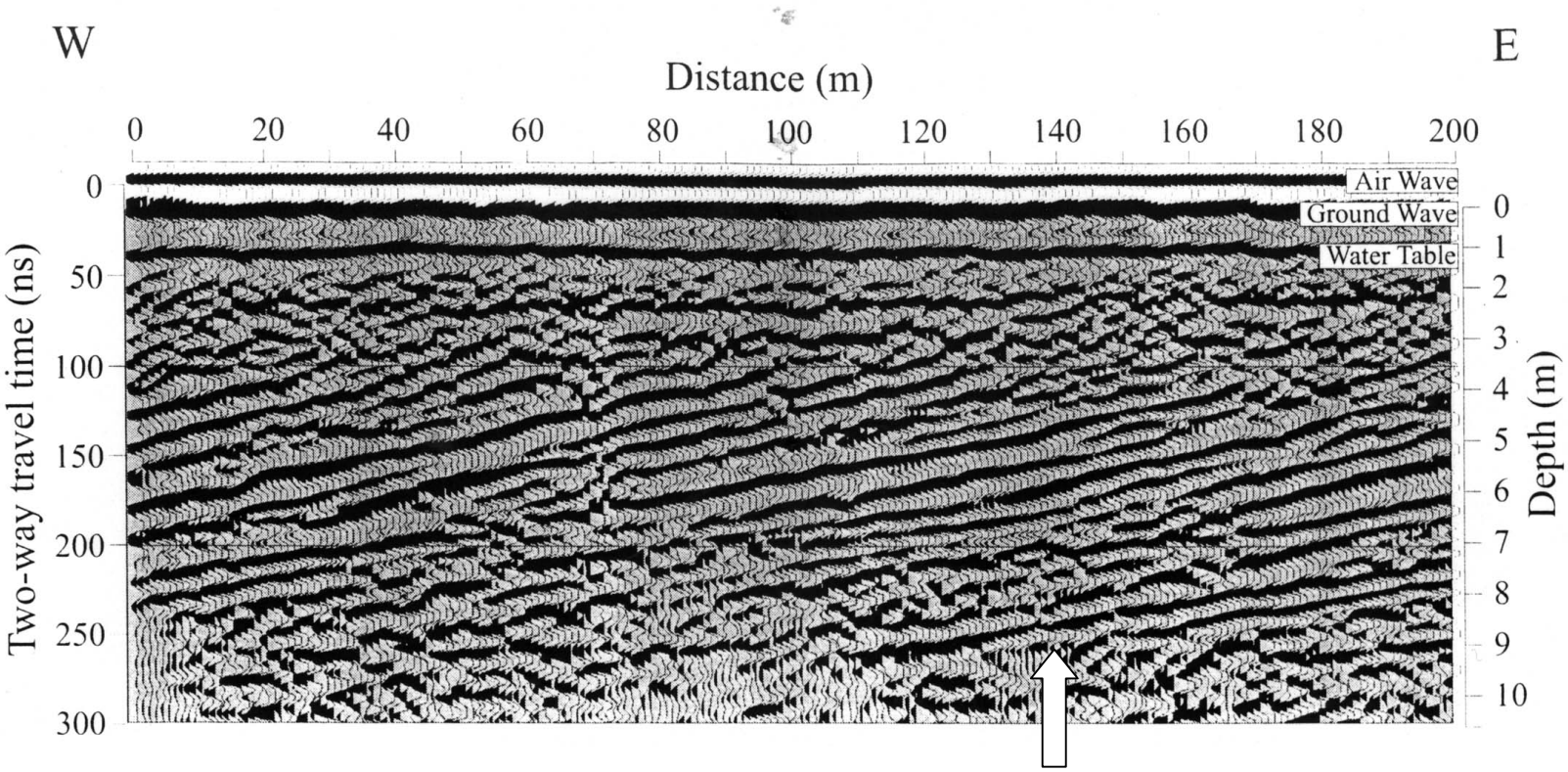

Figure 13: Ground Penetrating Radar example showing base of seaward dipping reflectors.

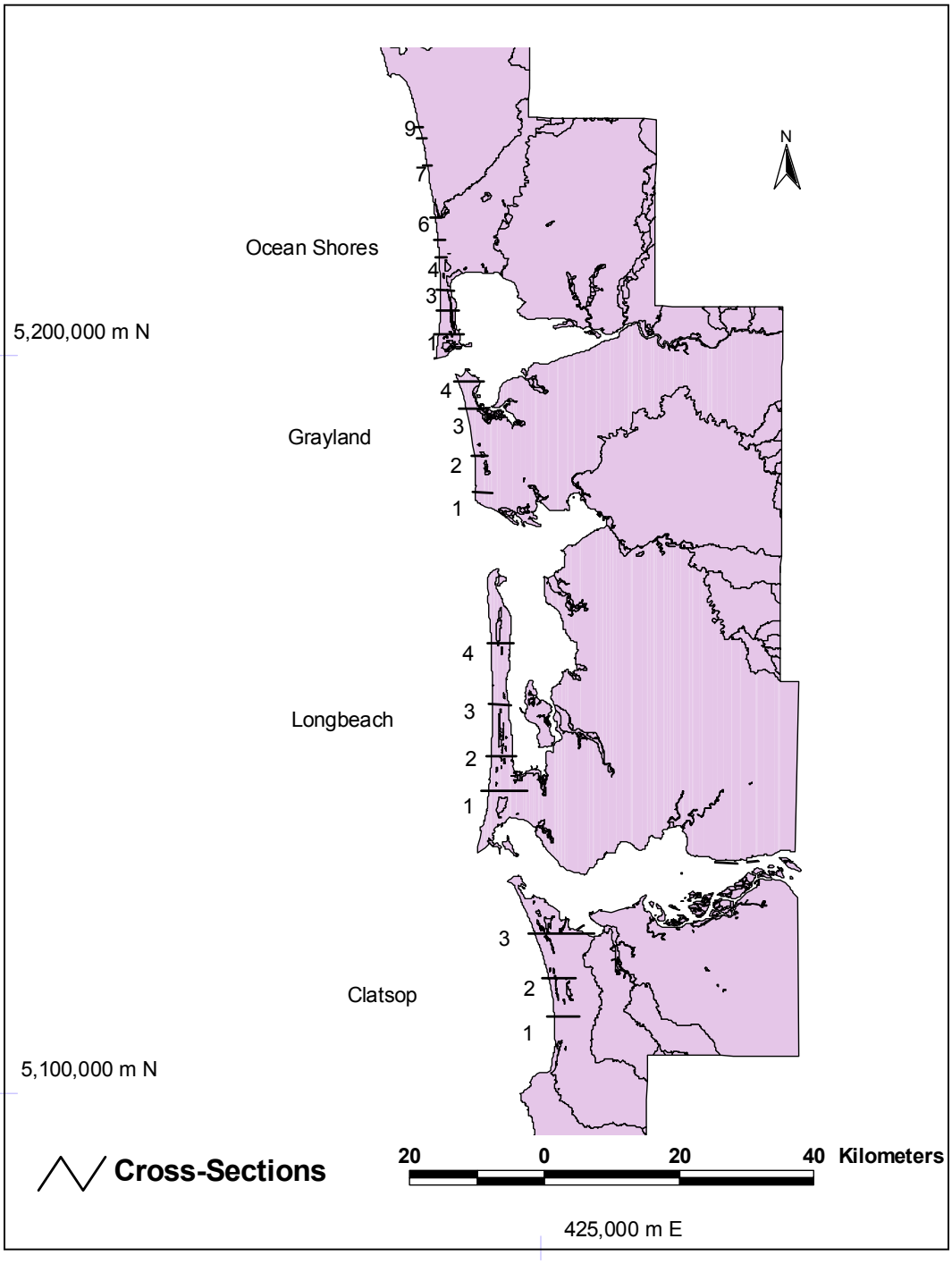

Figure 14: Cross-section location map.

Hole locations and depths to lithologic changes are plotted on each cross-section (Figure 15). Facies transitions are based on these data points. The symbols plotted on the cross-sections represent the base of lithologic changes; lines representing the bounds of each facies are plotted on each cross-section as well (Figure 16). For clarity, an example cross-section is presented here showing the graphic representation for two drill holes on the cross-section (Figure 17). Note that the line between beach and shelf facies is not shown as a change in lithology in the graphic logs.

Volume Calculations

Beach and Shelf facies volume calculations are based on the cross-sections mentioned above. Each subcell has been subdivided into longshore segments, which are represented geologically by the nearest cross-section (Figure 18). Volume calculations were performed for the combined units of beach and dune, and the shelf (depositional environment that is located below present barriers only). The seaward extent of this area was taken to be directly below the edge of the beach deposits, as delineated by surfzone vibracoring (Figure 19). Channel deposits have been included in the shelf volume on the basis that both deposits are subaqueous.

Cross-sections were used to calculate a representative cross-sectional volume for each longshore segment. The sections were digitized and area computed. This area was then multiplied by the length of the geologically representative longshore segment. Although crude, this provides the best estimate at this time for the volume of sediment located on and below the present day barriers. The use of more sophisticated modeling techniques by other workers is anticipated with the release of this data set.

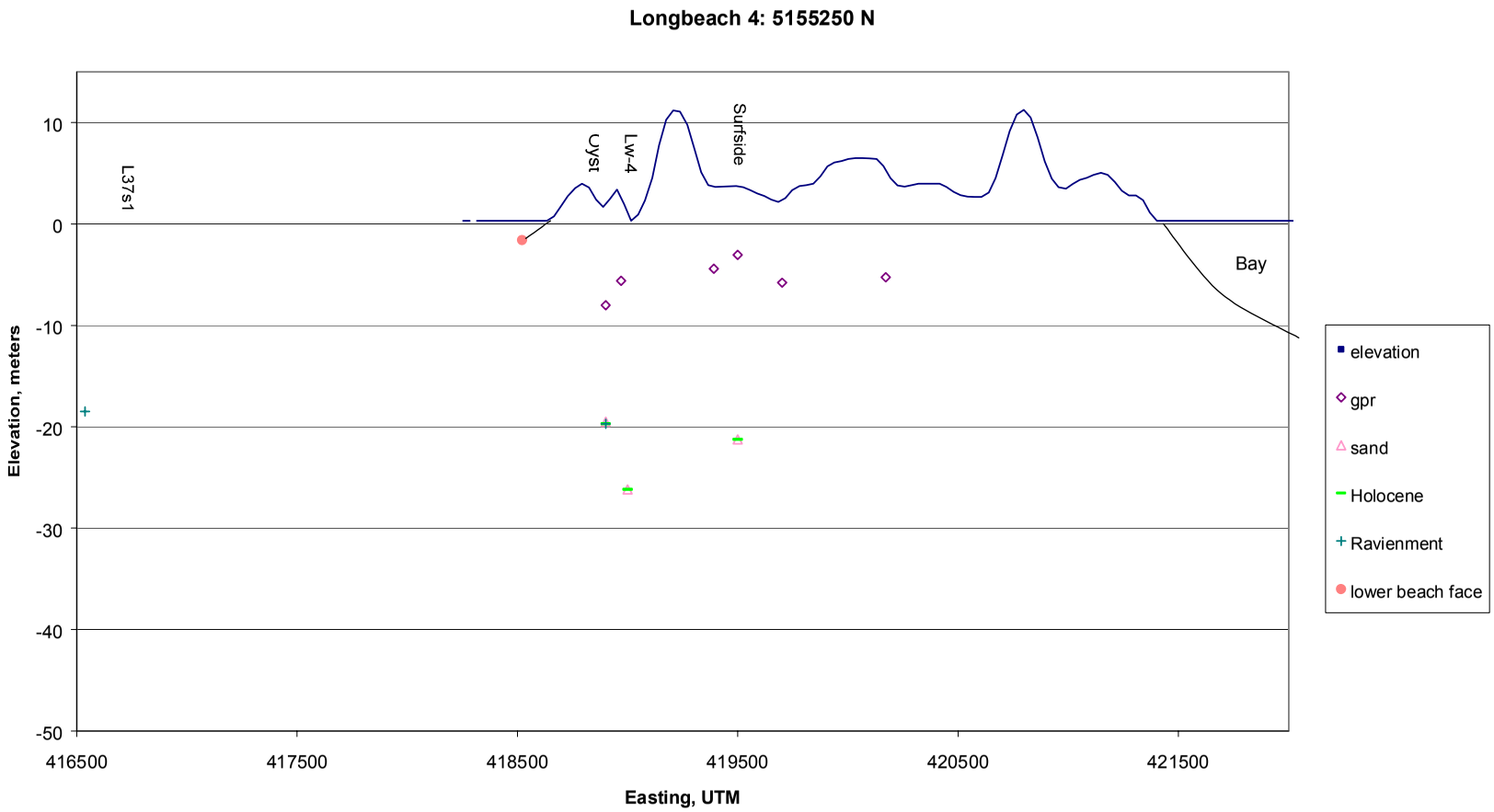

Figure 15: Uninterpreted cross-section, northern Longbeach subcell.

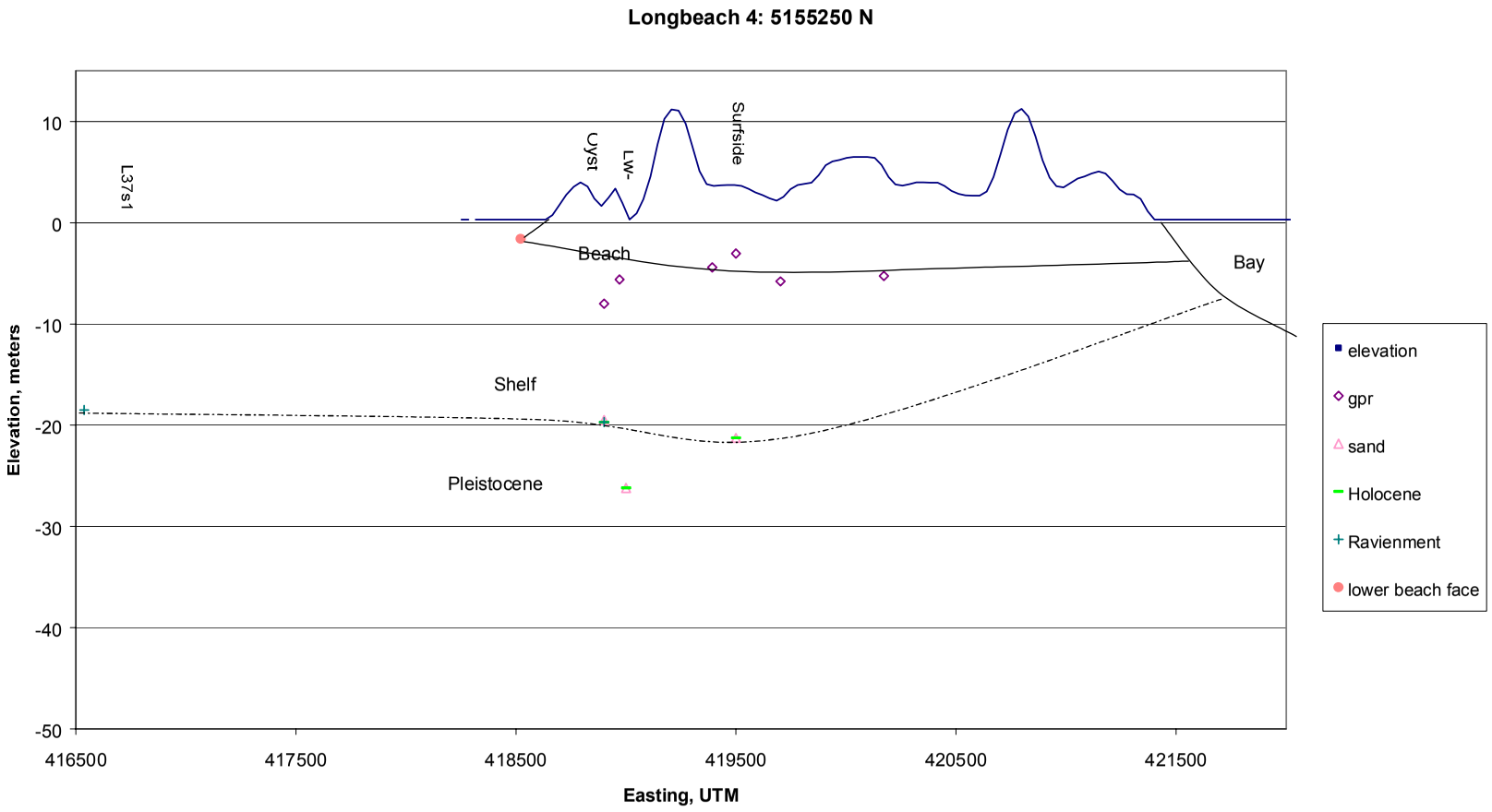

Figure 16: Interpreted cross-section, northern Longbeach subcell.

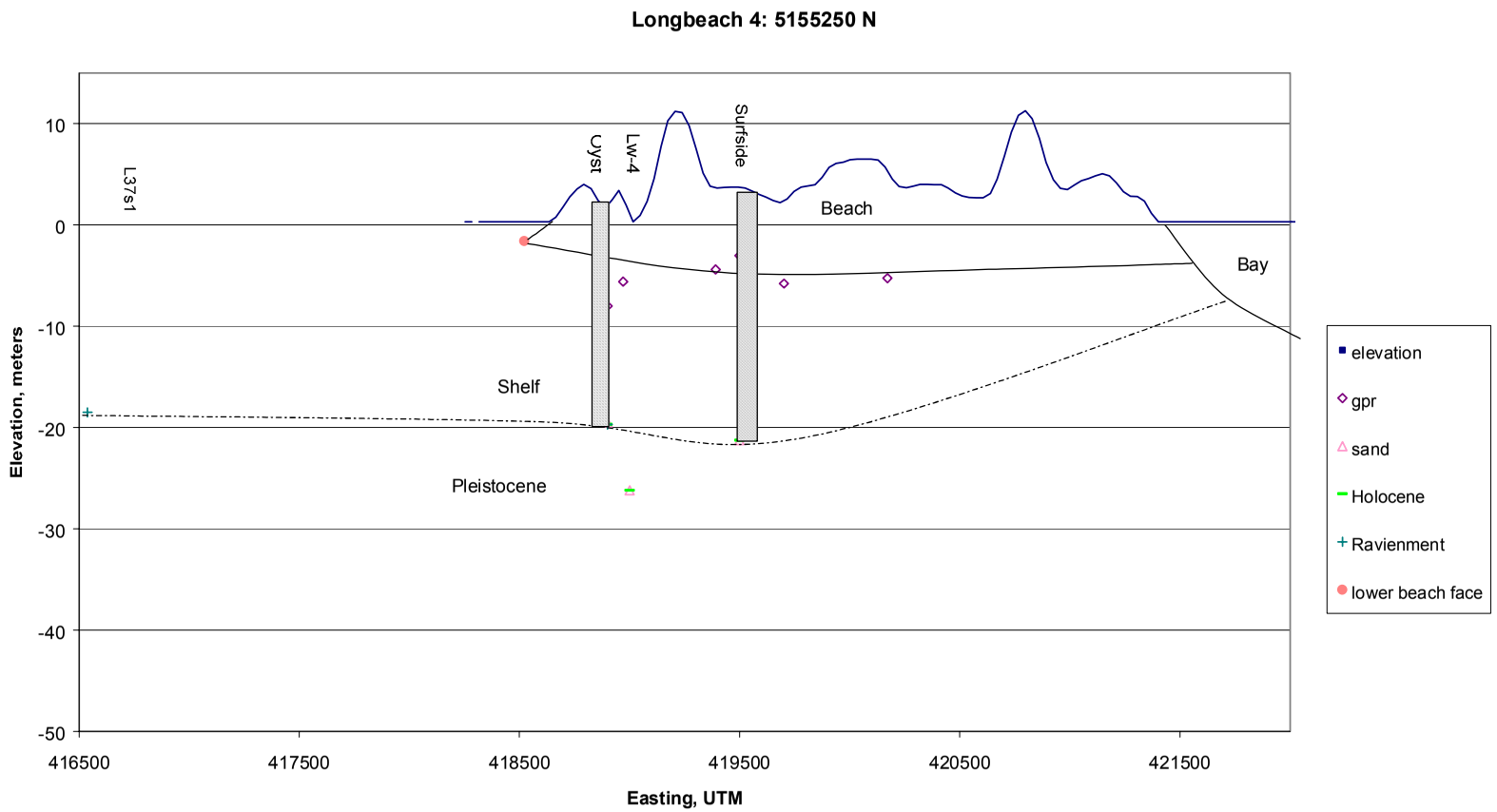

Figure 17: Cross-section with graphic log representation, northern Longbeach subcell.

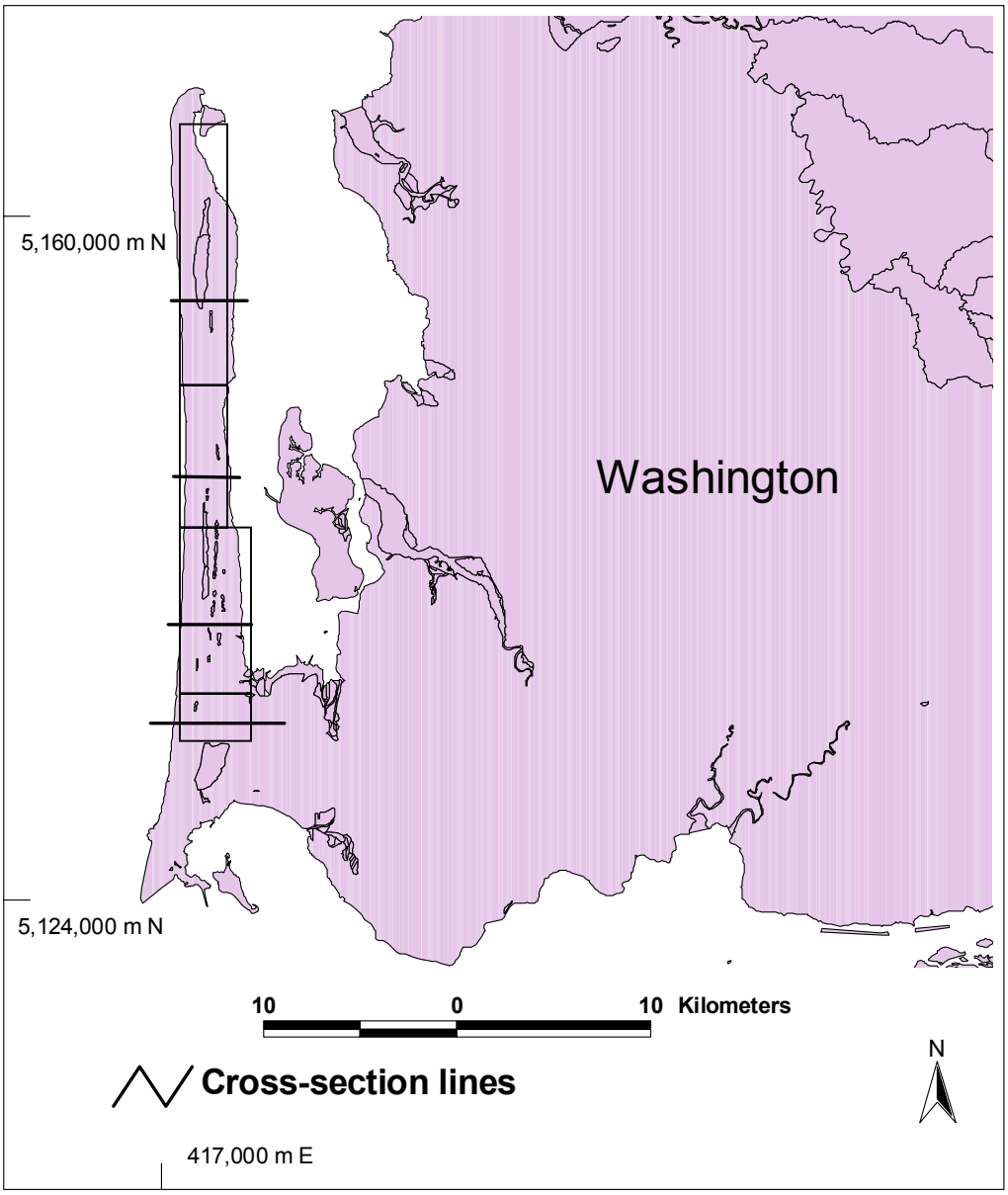

Figure 18: Map view of extent used for sediment volume calculations, Longbeach subcell.

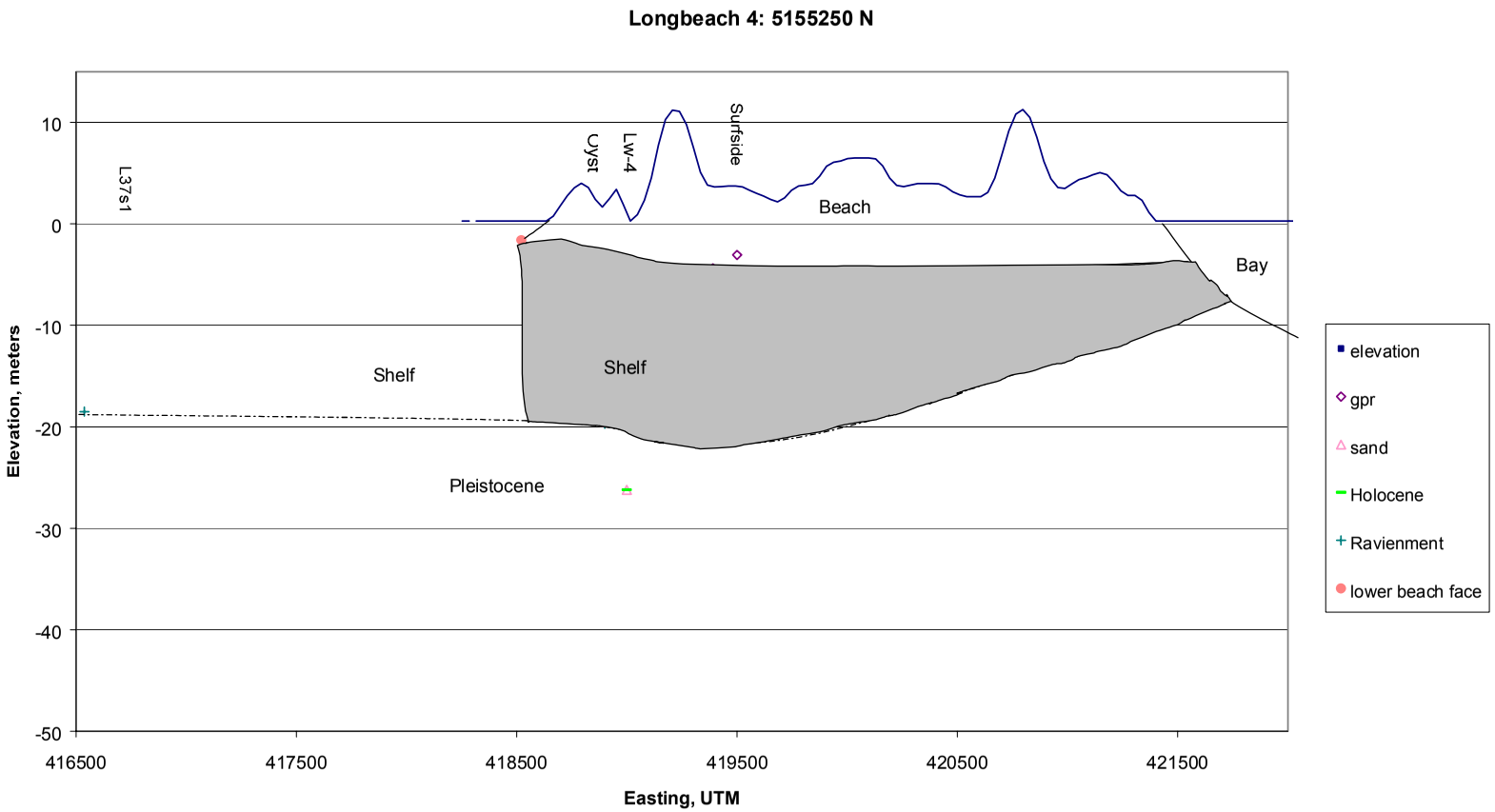

Figure 19: Cross-section with area used for volume calculations shaded. Note, extent of shelf volume for this study extends west only to the lower beach face contact, which is an arbitrary cut off.

RESULTS

Facies Descriptions

Lithology

Three Holocene units will be defined for the purpose of sediment reservoir partitioning in this project. The three units are: bay-lagoon, dune-beach and inner-shelf. In addition, the ravinement basal lag which is located at the base of either the beach or inner-shelf units will be described.

The bay-lagoon facies is comprised of sediment deposited in protected or low energy depositional environments. The bay-lagoon is comprised of clay, mud, and silt with some fine sand. In some cases, peaty mud and bay clams *Macoma sp.* shell fragments were observed. Detailed grain size partitioning, for the size fraction below 0.062 mm (fine sand), was not measured in the laboratory due to time constraints.

The dune-beach and inner-shelf units have a similar lithologic appearance. Both units consist of fine sand (mean: 0.2 mm), with occasional pebbles (4 mm to 10 mm). Wood fragments and thick walled shell fragments (*Clinocardium sp.* and Sand dollars) are present in both units without regularity or uniformity. Grading and layering was observed on rare occasions between fine, medium and coarse sands. Possible mud draped ripples were observed in the beach or inner-shelf facies in a few localities.

The base of the beach and shelf units contains an anomalous coarse lag in several locations. This layer is up to 1.5 m thick. The basal lag is distinguishable from both the underlying bay-lagoon and the overlying shelf and beach deposits by its larger modal grain size and poor sorting. It consists of gravel up to 7 cm in diameter, shell fragments, detrital wood fragments, sand and mud. In most cases this basal lag also contained

oxidized sediments and mud or peat rip-up clasts.

Grain Size

Weight percentages for gravel, sand and mud size fractions are calculated for each sample from the barrier borehole sites (Appendix A). Average values for all 309 samples are 6-7 % gravel, 80 % sand and 14 % mud (Table 2). This data shows that the majority (80%) of sediment beneath the barriers is sand.

Individual sample means are plotted on the interpreted stratigraphic logs (Figures 24-37, 39, and 44-48) to show down hole variability. The percent mud values are based on calculated values, which average 3 % greater mud weight percent than the measured values. This difference is considered insignificant for the total sand volume calculations.

TABLE 2- TOTAL WEIGHT PERCENT CALCULATIONS; GRAVEL, SAND AND MUD FOR ALL SAMPLES.

	Mean Weight %	Standard Deviation (wt. %)
Gravel	6	14
Sand	80	20
Mud	14	17

Note: This gives the mean distribution of grain size for all material cored.

Calculation of mean and mode (most common grain size) values for the beach, shelf ravinement and bay show that bay and ravinement are easily distinguished by mean grain size and mode (Table 3). Beach and shelf are less easily distinguished from one another by mean grain size and are indistinguishable by mode. Thus, three units are determinable by grain size alone, bay, beach-shelf, and ravinement.

TABLE 3A- GRAIN SIZE MEANS FOR EACH FACIES

Facies	Mean grain size (mm)	Standard deviation (mm)	Skewness	Kurtosis
Bay/Lagoon	0.14	0.262	6.977	118.492
Beach	0.173	0.101	-0.146	7.766
Shelf	0.289	0.421	3.729	92.72
Ravinement	1.963	1.911	1.248	15.024

TABLE 3B- MOST COMMON GRAIN SIZE FOR EACH FACIES

Facies	Most Common grain size (mm)	Standard deviation (mm)
Bay/Lagoon	0.064	0.061
Beach	0.181	0.062
Shelf	0.171	0.056
Ravinement	3.042	5.408

TABLE 3C- WEIGHT PERCENT IN THE MOST COMMON GRAIN SIZE

Facies	Weight Percent (mm)	Standard deviation (mm)
Bay/Lagoon	61.92	25.1
Beach	32.90	5.3
Shelf	33.12	8.5
Ravinement	35.80	13.0

Longshore variability

Mean grain size for each site is shown in Table 4. Detailed data for mean grain size, standard deviation, skewness and kurtosis are presented in Appendix A. Detailed modal grain size (most common size) is presented in Appendix A.

This measure of site-averaged mean grain size represents the average grain size through time that has been deposited at each site and indicates the presence of long term, long shore trends in grain size. The site-averaged mean grain size is much greater in the northernmost subcell of Ocean Shores near Grays Harbor. Small increases in grain size can be seen at the southern boundaries of both Grayland and Longbeach (Figure 20).

Grain size within each facies is plotted with position alongshore in Figures 21 and

TABLE 4- MEAN GRAIN SIZE PER AUGER SITE: DOWNHOLE COMPOSITE

Subcell	Site Name	Mean Grain Size, mm
North Ocean Shores Subcell	Roos	1.374
	Mocl	1.899
	High	6.336
Ocean Shores Subcell	Copr-1	0.859
(dunes present)	Copr-2	0.765
	Oyhut-1	1.988
	Oyhut-2	5.305
Grayland Subcell	Grbe	0.184
	Goul	1.112
	Smit	0.305
	Ncov	0.198
Longbeach Subcell	Oyst	0.328
	Bayr	0.178
	Klip	0.176
	Mchu	0.177
	Pcyd	0.217
	67th	0.651
Clatsop Subcell	Sunb	0.241
	Glen	0.452
	Delr	0.41
	Delm	0.366

Note: See Figure 12 for site locations.

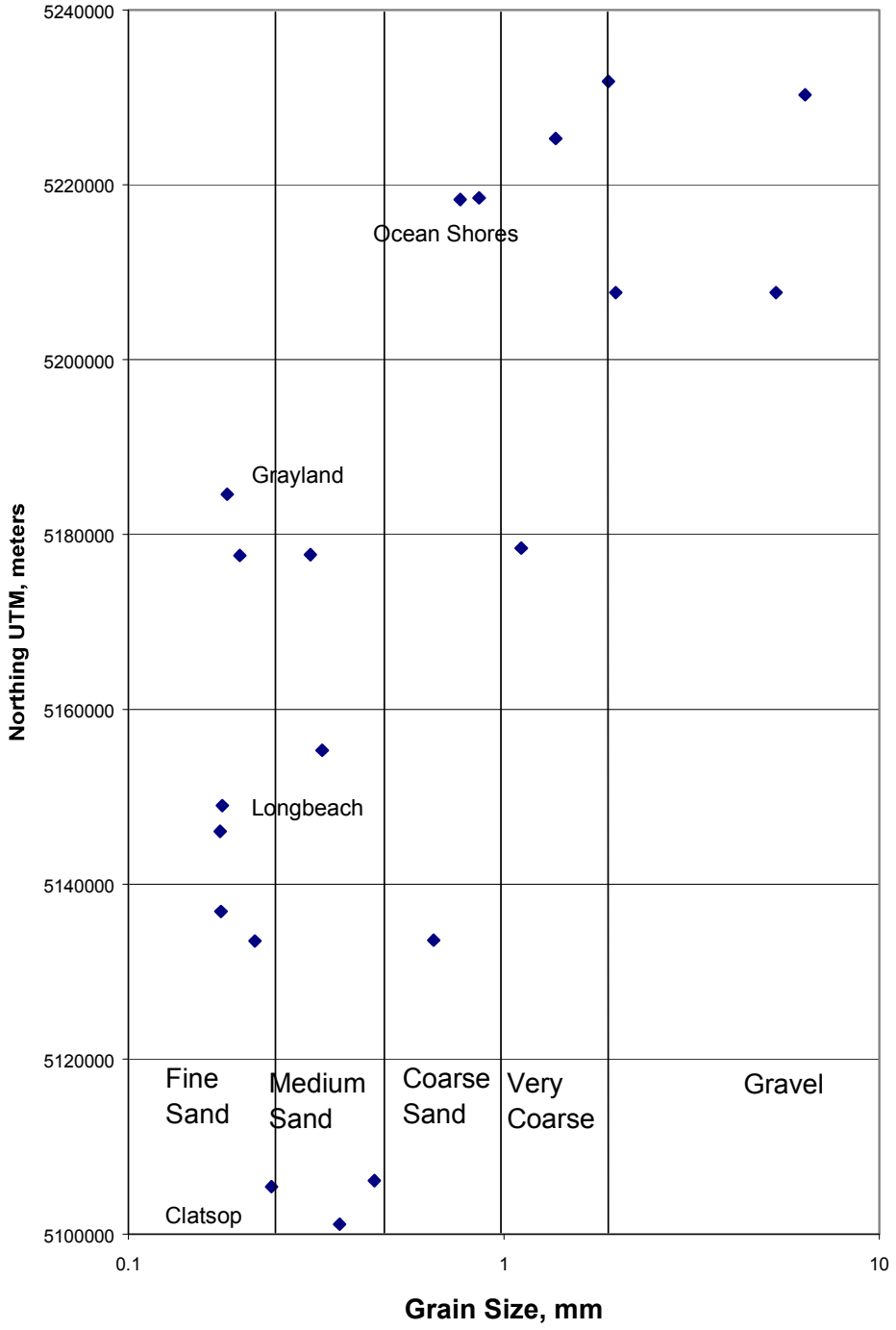

Figure 20: Mean Grain Size plotted alongshore to show increase in grain size to the north.

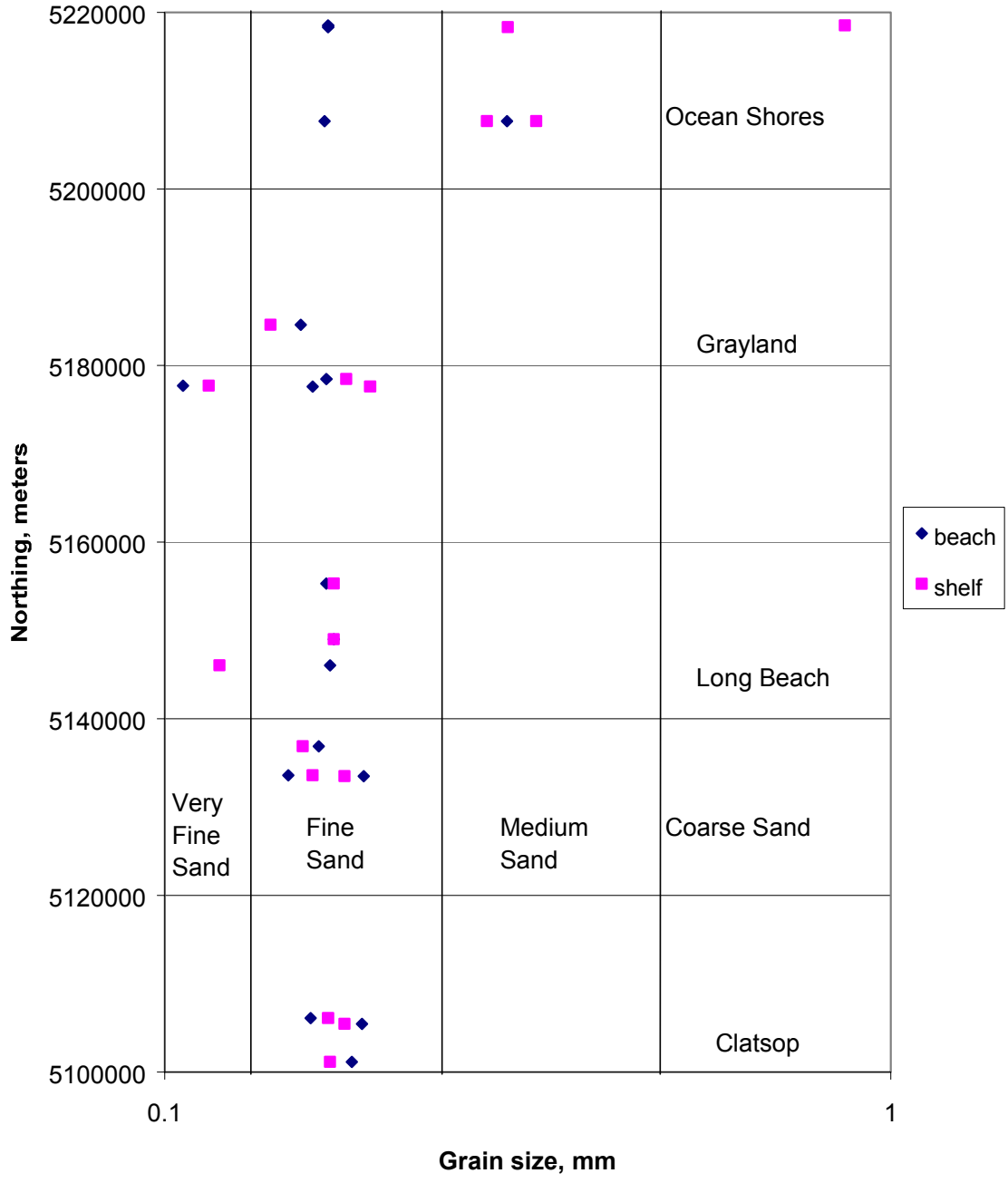

Figure 21: Beach versus Shelf grain size plotted alongshore to show the increase in grain size to the north and similarity of beach and shelf facies.

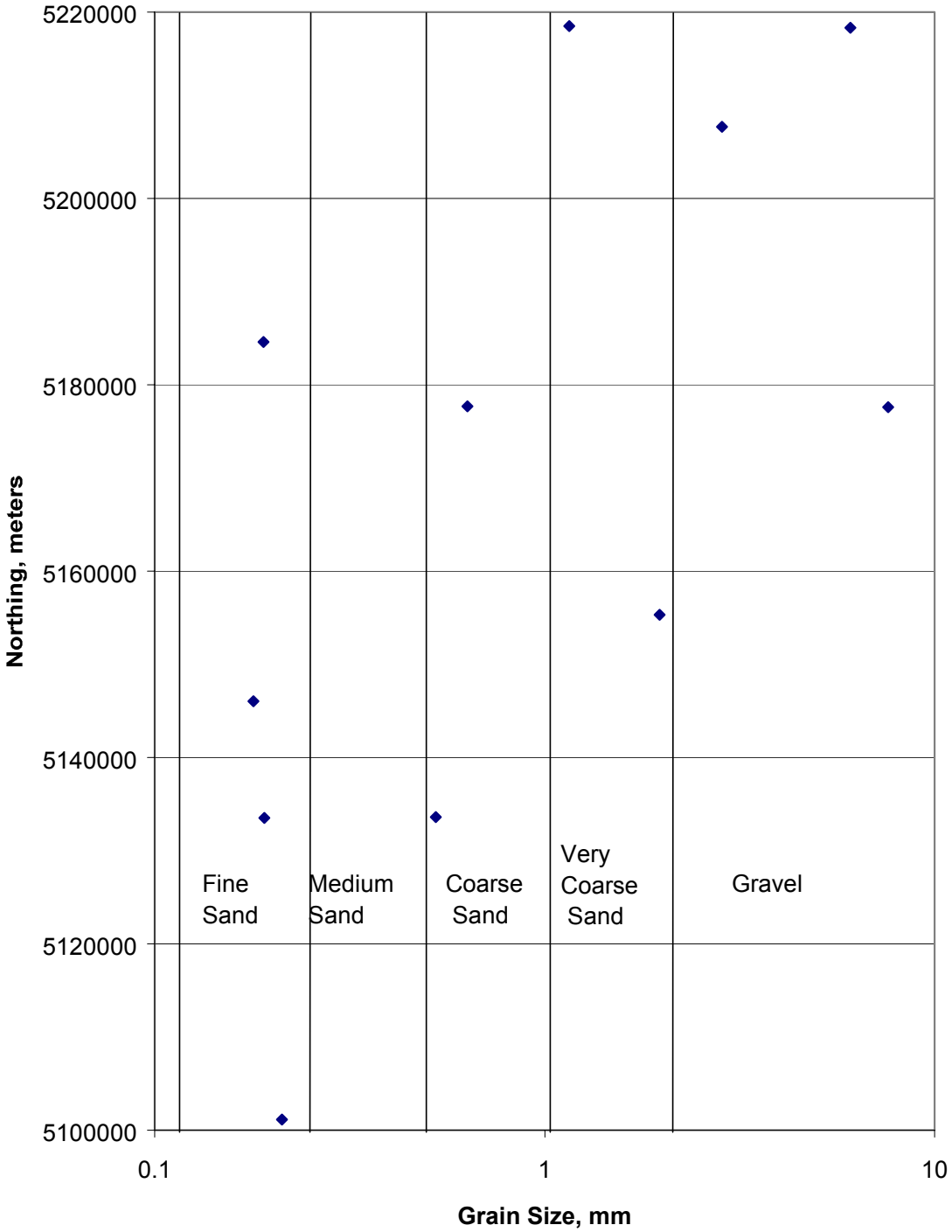

Figure 22: Ravinement grain size plotted alongshore to show increase in grain size to the north and larger grain sizes than beach and shelf facies.

22. Both beach and shelf sediments increase slightly in grain size in the northernmost subcell, Ocean Shores. Mean grain size for the basal layer increases in the northern half of the Columbia River Littoral cell though it is more varied than the beach and shelf units.

Radiocarbon Dates

Radiocarbon conventional ages are presented in Table 5. Shell or wood material deposited at or near the ravinement surface is indicated with an asterisk. The age of this material is dependent on its position from east to west. The estimated age of first ravinement (beneath present barriers) varies between subcells (Figure 23).

The northernmost subcell, Ocean Shores, has the youngest material at or near the ravinement surface. The southern portion of this subcell, from the north Grays Harbor jetty to the Copalis River has a ravinement age of ~1500 Radiocarbon Years Before Present (RCYBP) (Figure 24). North of the Copalis River dune forms are not present and radiocarbon dates show that the sand just above the ravinement is early historic to modern in age (Figure 25).

The Grayland subcell has a dated sample above the ravinement surface that is ~4000 RCYBP at site Grbe (Figure 26). There is also a ~7400 RCYBP dated sample, Goul, that was picked just below the ravinement surface (Figure 27). In the Grayland subcell, the age of ravinement is thus constrained between 4000 and 7400 years ago.

The Longbeach subcell shows the oldest age for dated materials located above, below, or at, the ravinement surface. Ages are older for more westerly sites and decrease for midbarrier sites. The most western site Oyst has a ravinement age of 7520 RCYPB (Figure 28). The average age for ravinement at the midbarrier sites, Klip (Figure 29),

TABLE 5- RADIOCARBON DATES FOR SAMPLES, Beta Analytic, Inc.

Sample #	beta #	Depth, m	Conventional C14	Type of sample	Relative Placement**
Mocl1	129512	1.3	108.4 +/- 0.5%	shell	R
Copr1	129521	7.2	1730 +/- 40	shell	R
Oyhut2	129526	2.7	20 +/- 60	wood	A
Oyhut1	129513	8.5	930 +/- 40	shell	A
Oyhut1	129520	11.1	1290 +/- 40	shell	A*
Grbe	129516	7.9	1550 +/- 40	shell	A
Grbe	129511	10.6	1460 +/- 40	shell	A
Grbe	129531	13.2	3920 +/- 70	peat	R
Goul	129524	11.9	7400 +/- 60	wood	B*
Ncov	129515	9.8	870 +/- 40	shell	A
Oyst	129514	21.9	7520 +/- 60	wood	R
Klip	129519	17.9	4710 +/- 70	peat	R
Mchu	129525	10.6	5240 +/- 60	wood	B
Mchu	129518	13.1	39,300 +/- 530	wood	B
67th	129523	10.1	4630 +/- 50	wood	R
Pcyd	129517	11.6	3170 +/- 50	wood	A
Pcyd	129530	14.2	3780 +/- 80	peat	R
Pcyd	131122	15.2	7060 +/- 110	shell	B*
Sunb	129529	10.9	2520 +/- 60	wood	A
Sunb	129527	16.8	3740 +/- 80	peat	A
Sunb	129522	21.0	3840 +/- 50	wood	A
Delm	129532	11.1	4260 +/- 80	peat	A*
Delr	129509	13.1	2160 +/- 40	shell	A

* Close to Ravinement
** R = Ravinement
A = Above Ravinement
B = Below Ravinement

Pcyd (Figure 30) and 67th (Figure 31), is ~4600 RCYBP. Mchu, a back bay site (Figure 32), has material dated at 39,3000 RCYBP which is 'radiocarbon dead' indicating a Pleistocene age the platform at this location. Mchu also has a ~5000 year old date in mud deposits just below the ravinement surface, which indicates that there was a bay-like environment behind the southern end of the Longbeach spit 5000 years ago (prior to ravinement).

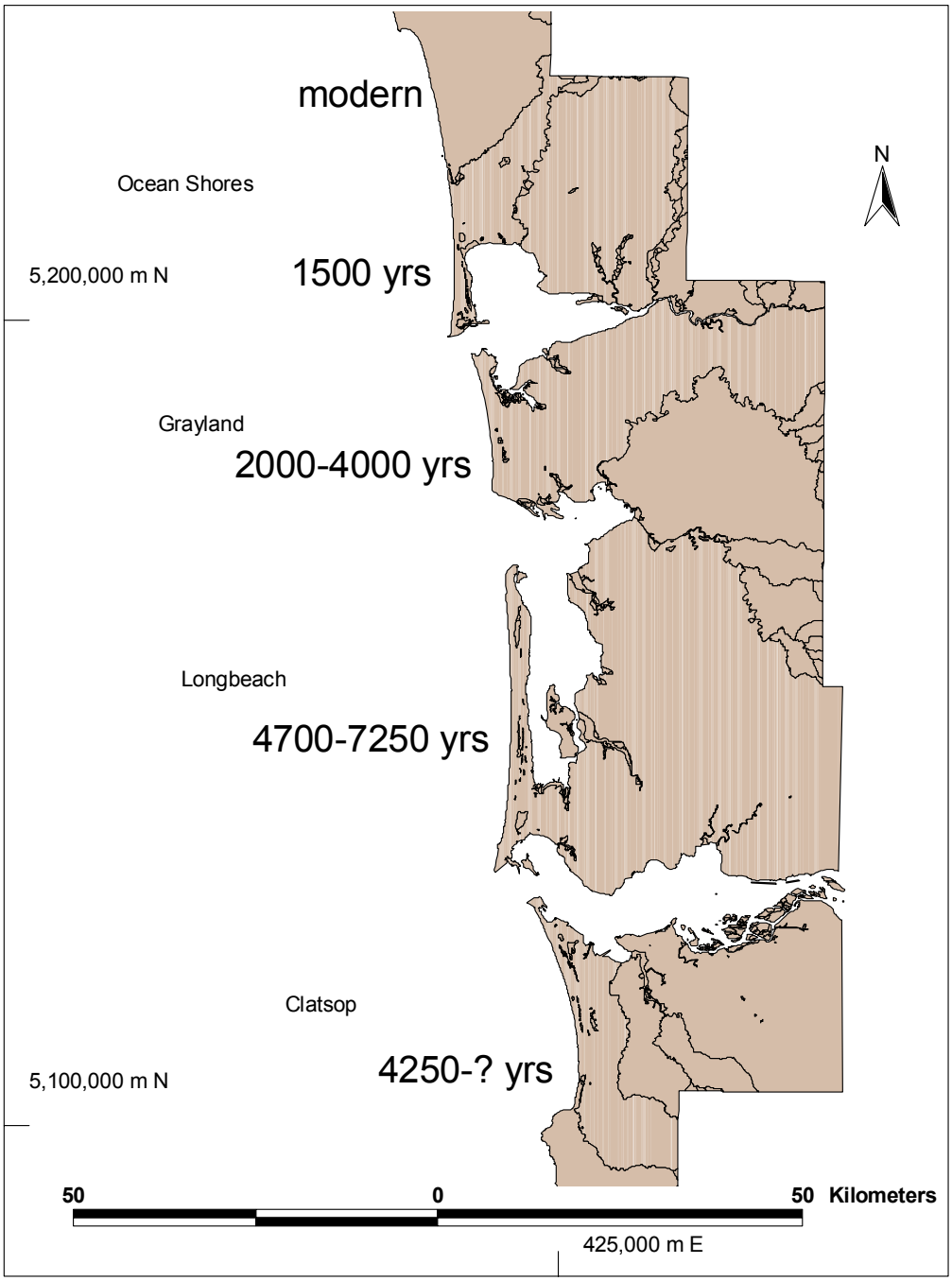

Figure 23: Map with 'estimated first onset of ravinement' ages listed for each subcell.

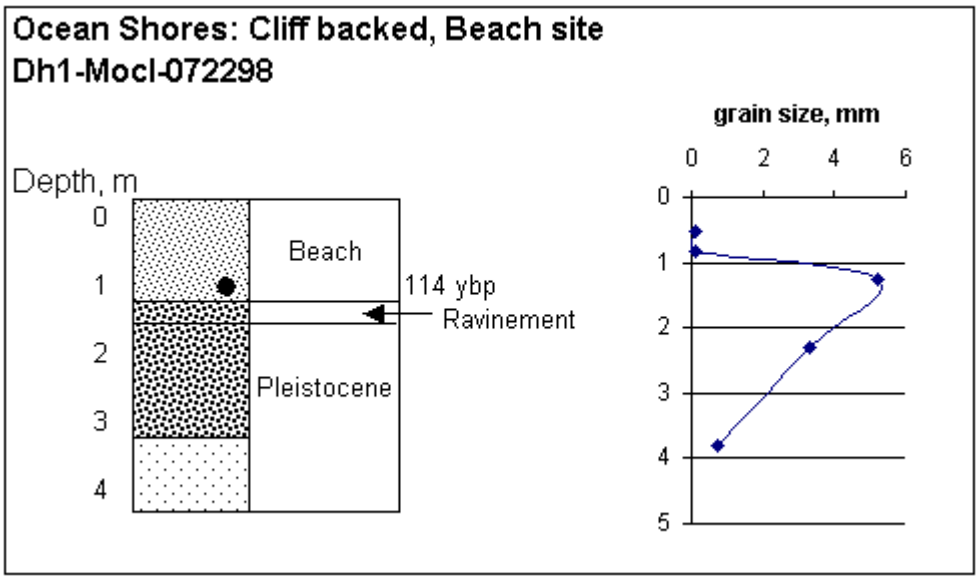

Figure 24: Copr-1 core log

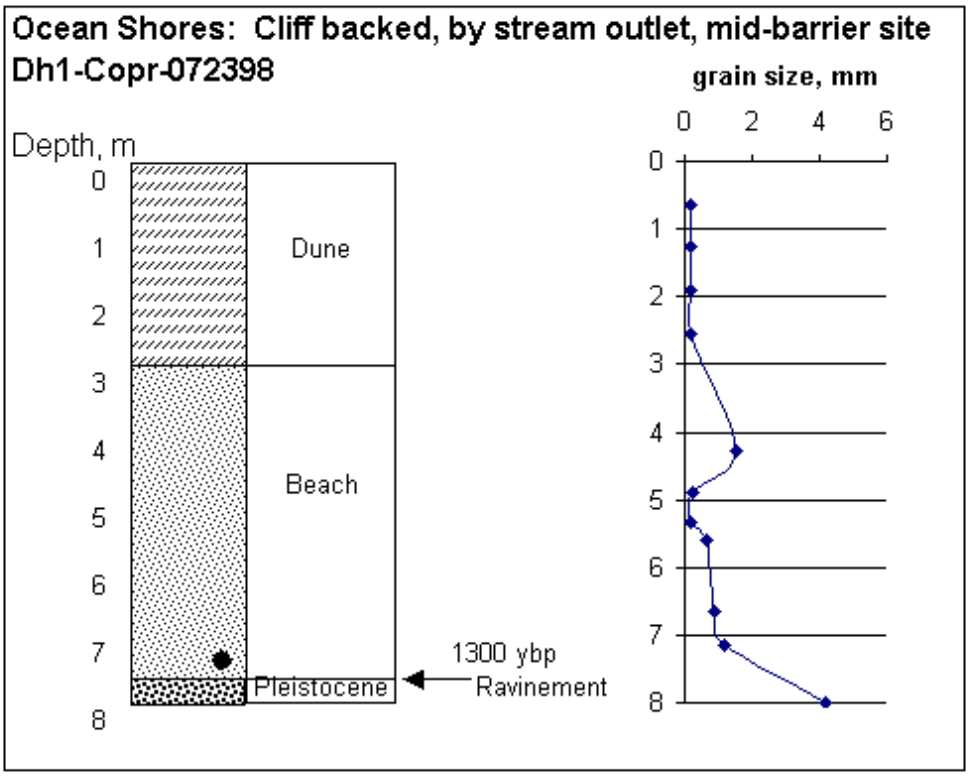

Figure 25: Mocl-1 core log.

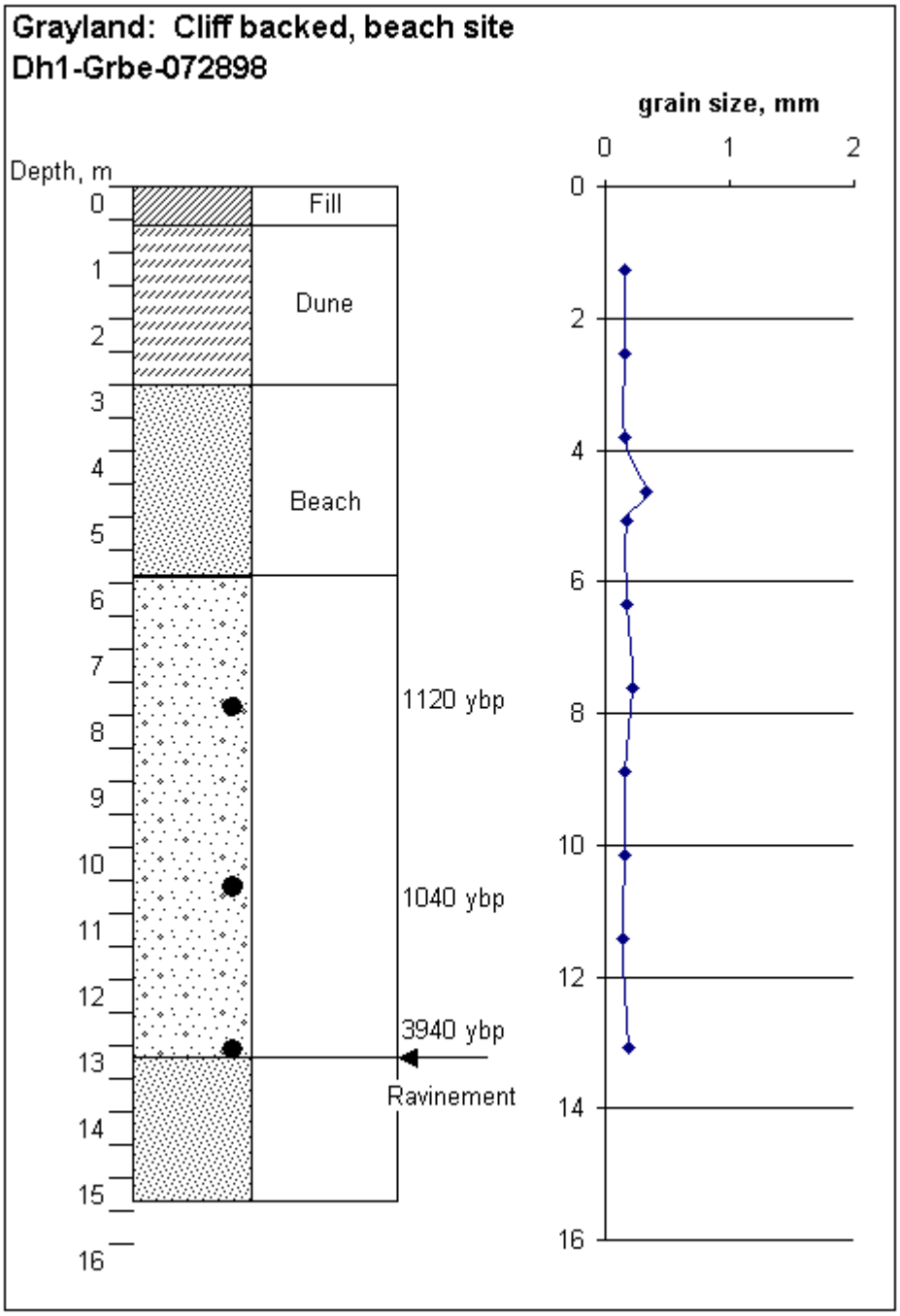

Figure 26: Grbe core log.

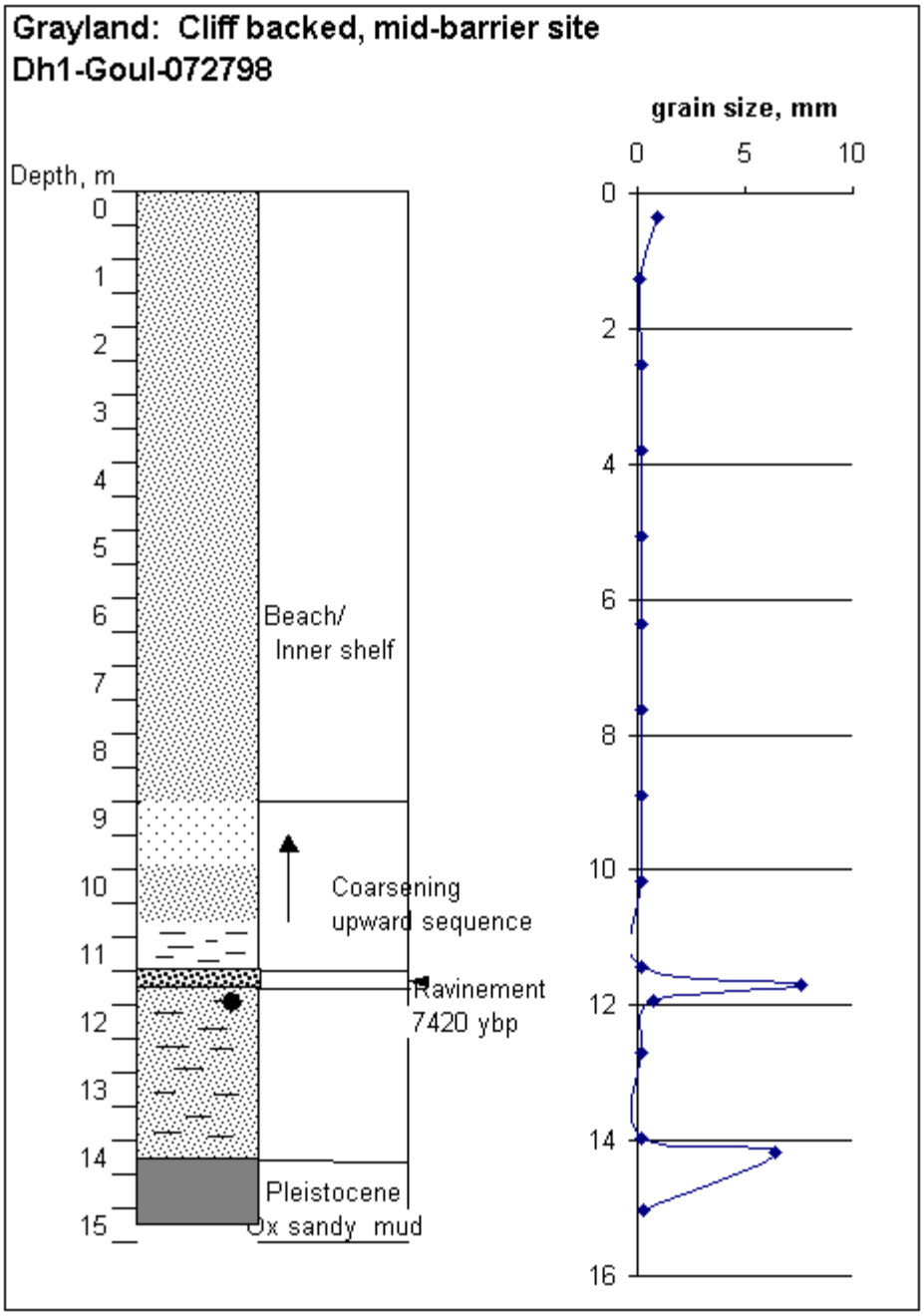

Figure 27: Goul core log.

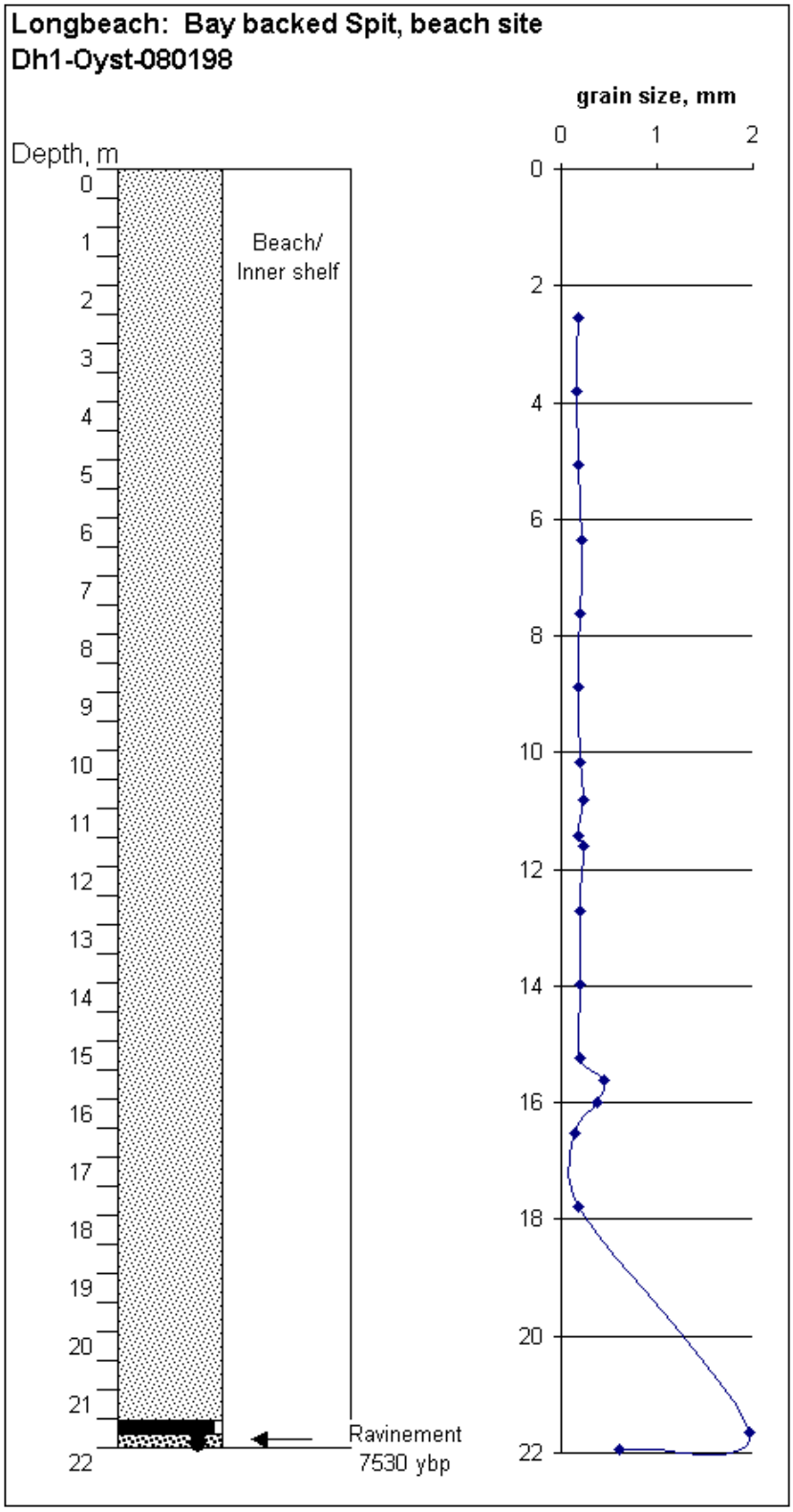

Figure 28: Oyst core log.

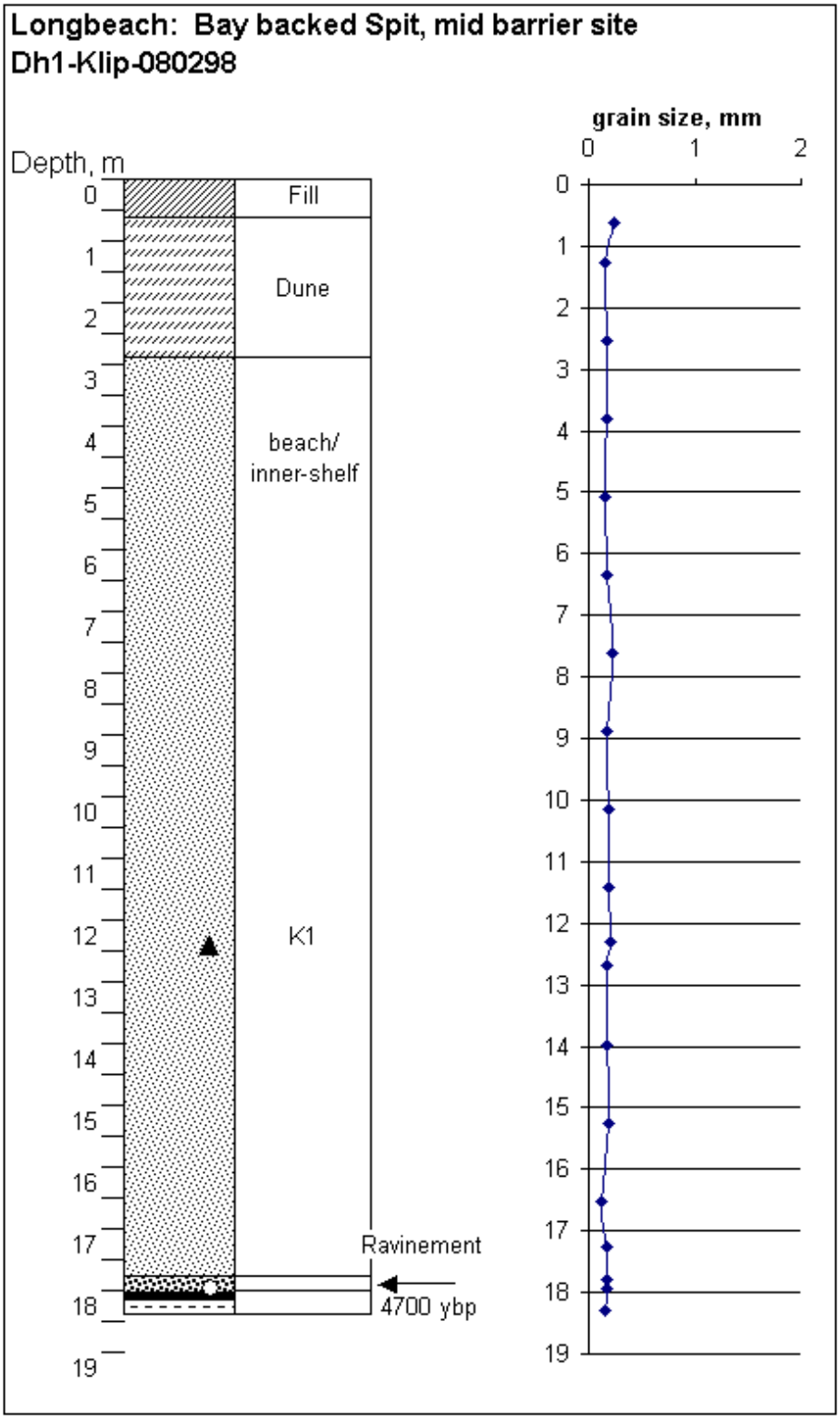

Figure 29: Klip core log: Tephra located at K1.

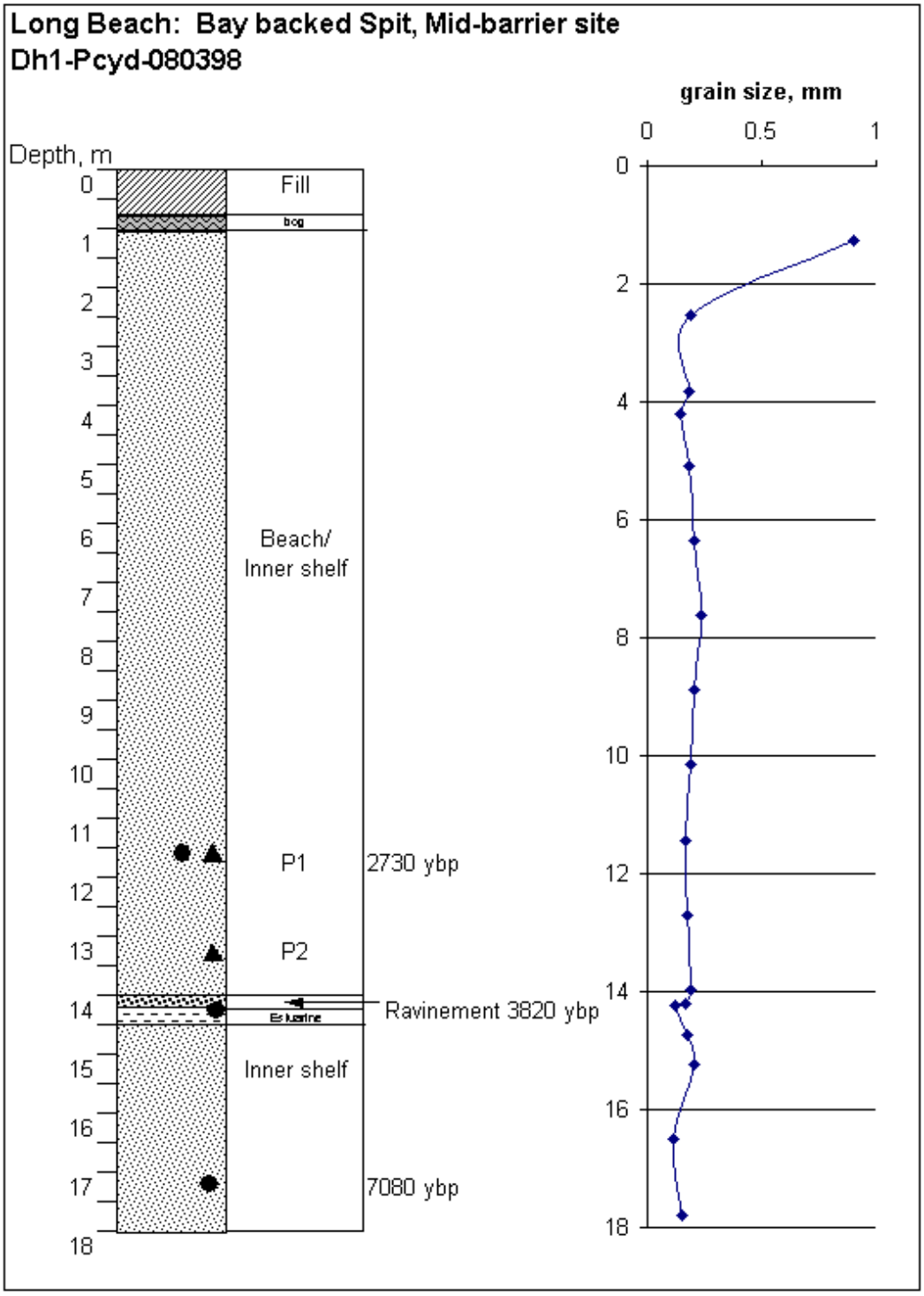

Figure 30: Pcyd core log: Tephra located at P1 and P2.

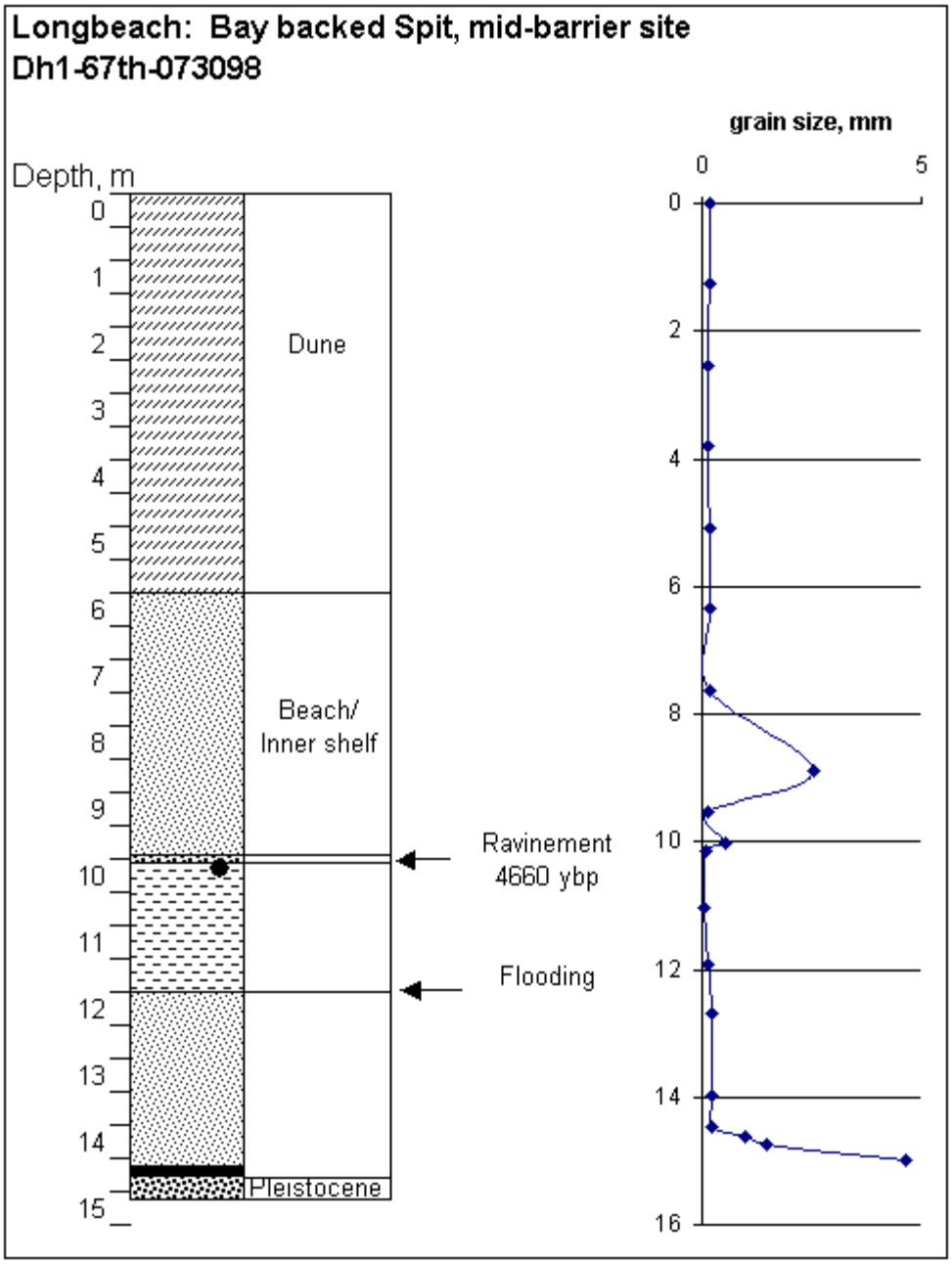

Figure 31: 67th core log.

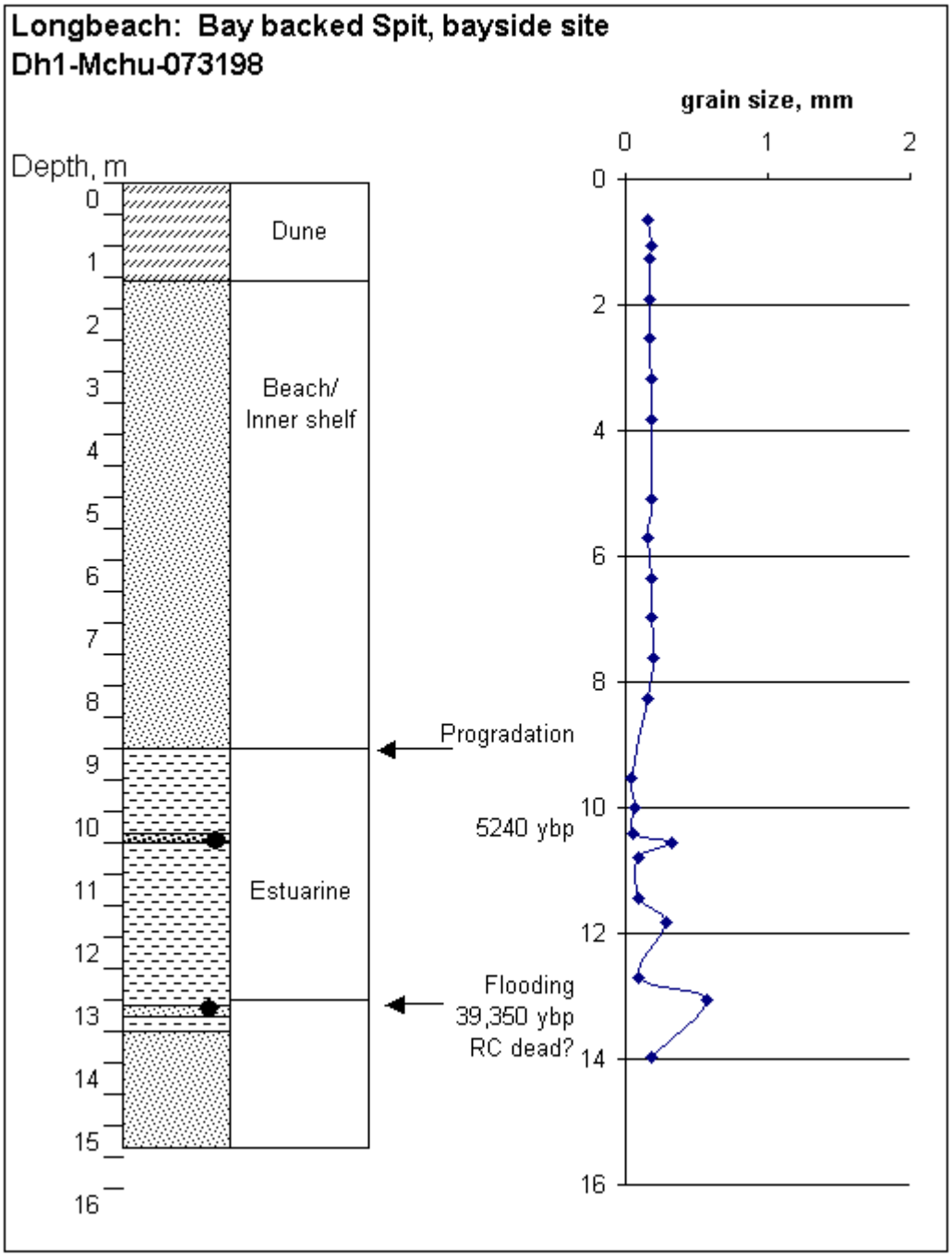

Figure 32: Mchu core log.

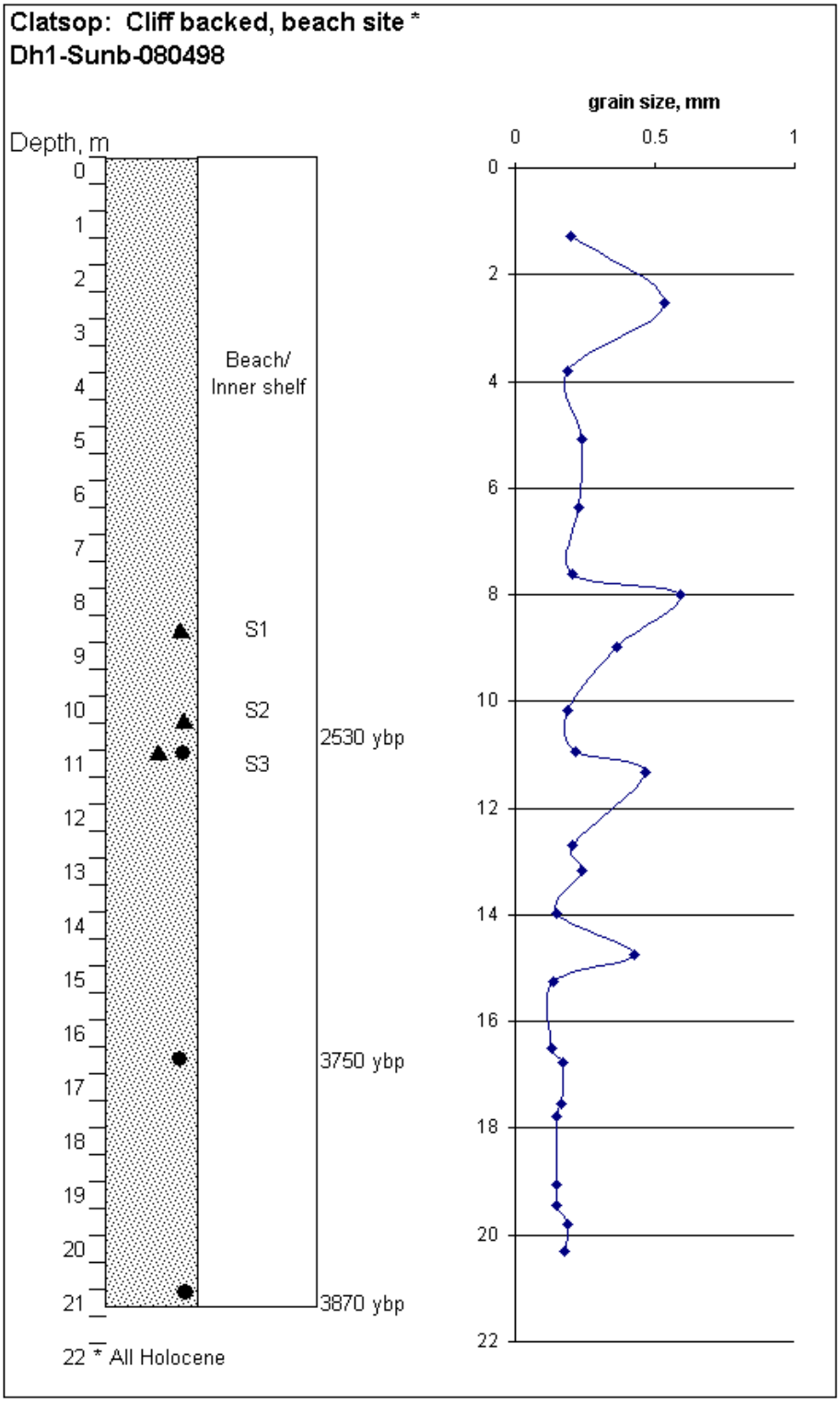

Figure 33: Sunb core log: Tephra located at S1, 2, and 3.

The Clatsop subcell also shows a time transgressive ravinement surface. The western most site, Sunb (Figure 33), has a post-ravinement age of ~3800 RCYBP at a depth of 21 m. Another site, Delr (Figure 34), on the western edge of the beach plain has a relatively shallow post-ravinement sample (13-m depth). It has a younger age of about 2000 RCYBP. The ravinement surface was below the depth of continuous coring capabilities for the rig available in this study at the western sites in the Clatsop subcell. However, one of the eastern sites, Delm (Figure 35), has a ravinement age of about 4250 RCYBP.

Channel deposits were distinguished through the use of radiocarbon dating in two subcells: Ocean Shores and Grayland. The southernmost drill hole in Ocean Shores is Oyhut-1 (Figure 36), near Grays Harbor. It shows a possible channel deposit with dates younger than expected, 520 RCYBP at 8.5 m and 860 RCYBP 11 m. The southernmost drill hole in Grays Harbor is Ncov (Figure 37) which shows possible channel deposits with the very young age of460 RCYBP at depth of 10 m.

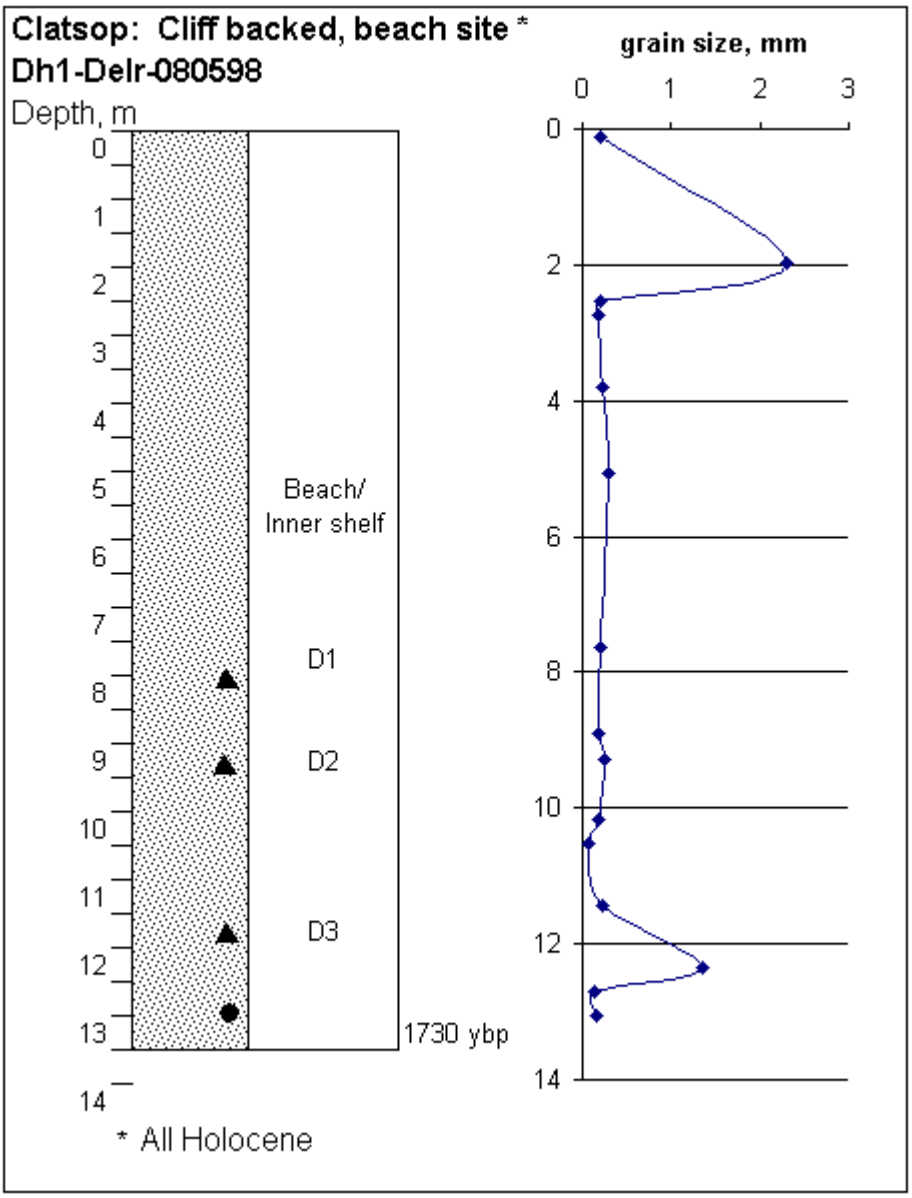

Figure 34: Delr core log: D1, 2, 3 are tephra locations in core.

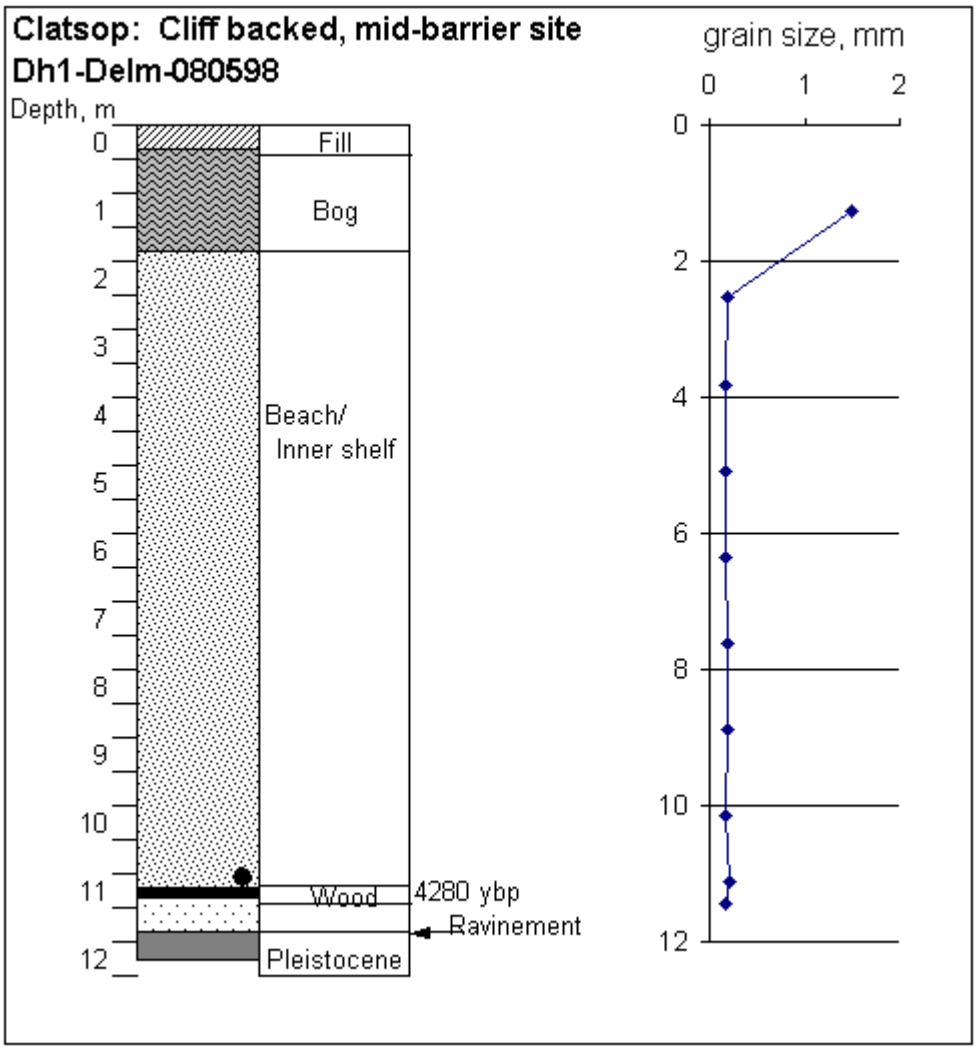

Figure 35: Delm core log.

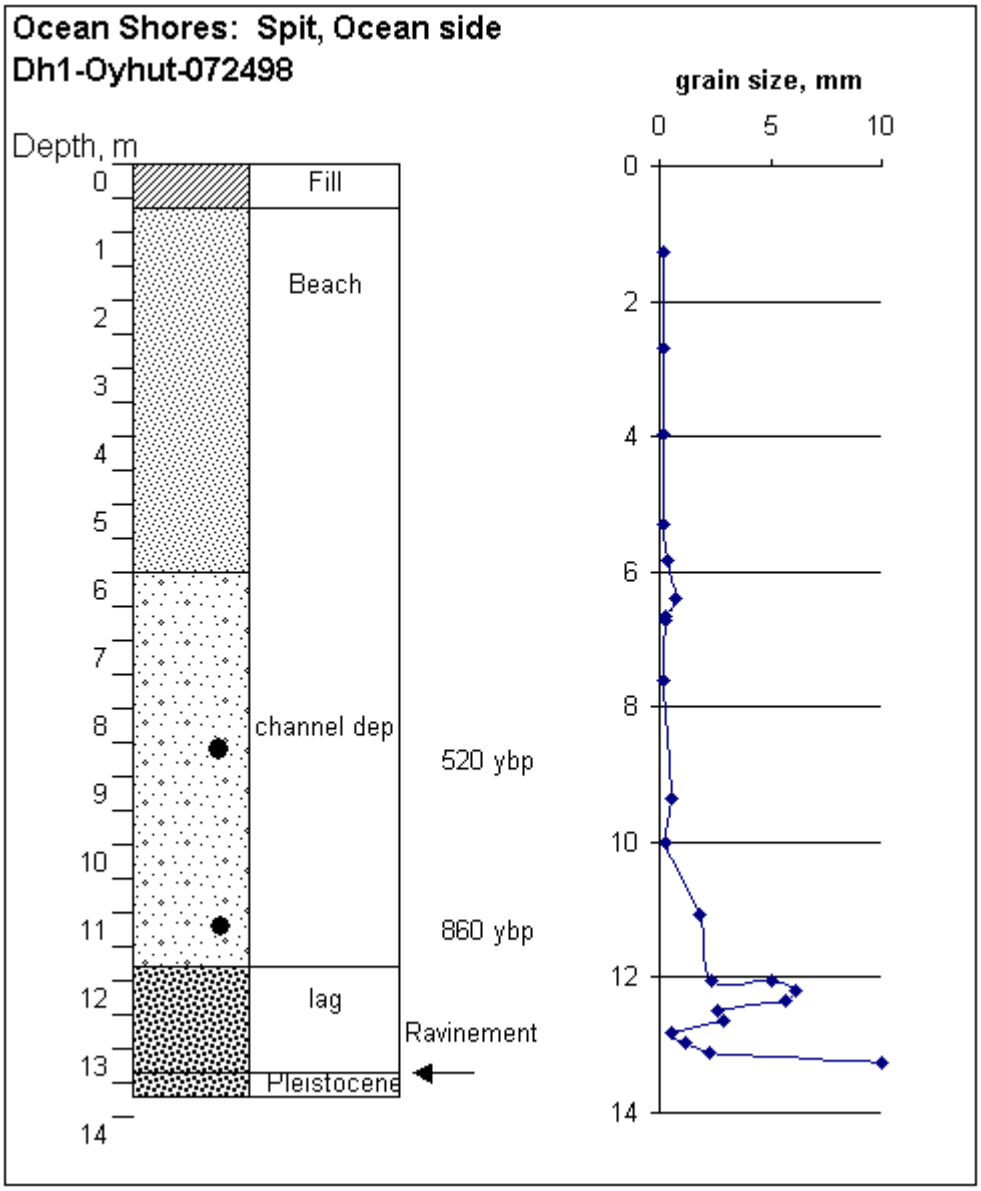

Figure 36: Oyhut core log.

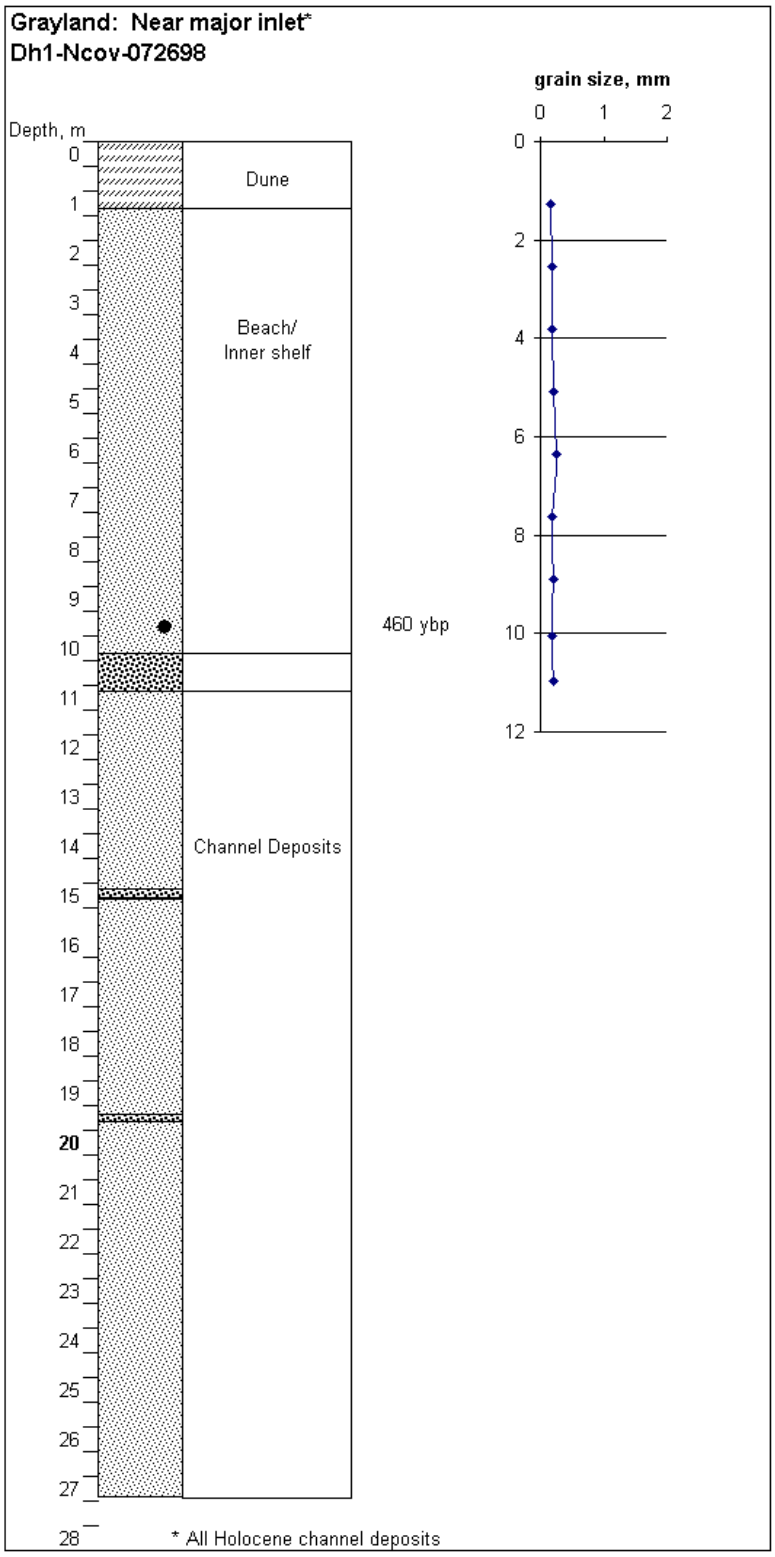

Figure 37: Ncov core log.

Tephra Deposits

Tephra laminae were found in some of the cores from the Clatsop and Longbeach subcells (Figure 38 (map); and Figures 29, 30, 33, 34 and 39 (core logs)). They were present as either single laminae or multiple laminae in thin zones, often in several depth positions down-core. This medium to coarse, pumaceous, white-gray sand was identified in the field and later checked under a petrographic microscope. Petrographic analysis of crushed grains showed shards of glass (opaque under crossed polars). Photomicrographs are shown here in Figure 40. Crystalline material was observed as enclosed grains within the tephra grains, but was not analyzed for mineralogy.

Instrumental Neutron Activation Analysis (INAA) results reveal a tendency towards Mazama chemistry as shown by Figures 41-43, but the results are not conclusive for all samples. Detailed chemical data is presented in Appendix C.

Stratigraphic positions of tephra samples, relative to radiocarbon dates, reveal that tephra deposition occurred between 3500 and 2000 years ago (See core logs in Appendix D). The age, depth and geographic positions of the tephra occurrences suggest that the tephra was supplied to the beaches by remobilization of Mazama ash sediments in the Columbia River or its interior drainage basin. The tephra was apparently transported through the Columbia River estuary and then along the shoreline by littoral processes. Tephra was not seen in the northern subcells of Grayland and Ocean Shores due to either 1) tephra was diluted in the host sand deposits and not recognized or 2) tephra broke down during transport or 3) tephra was not preserved or there was not a depositional environment (in the northern subcells) at the time of transport.

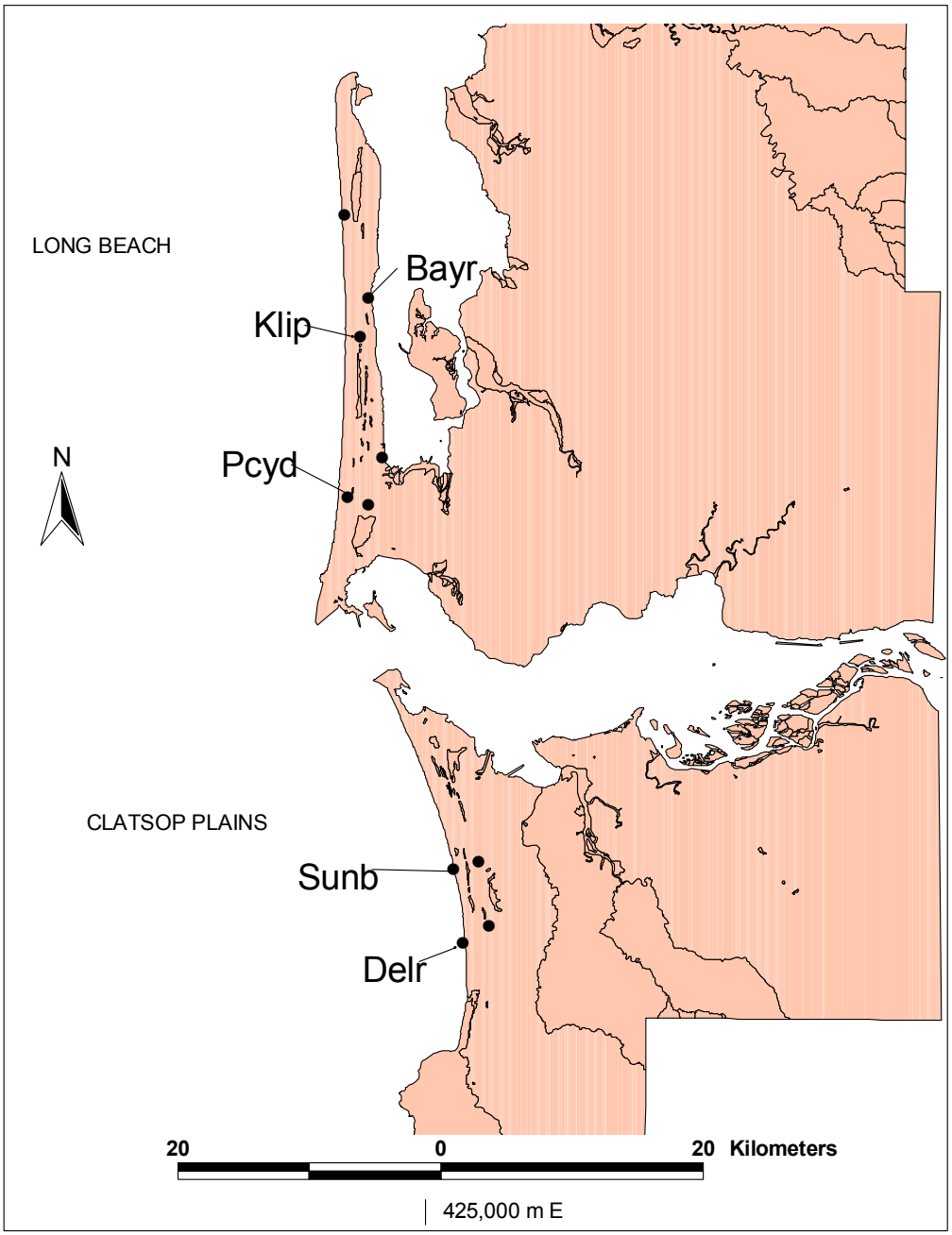

Figure 38: Map with drill sites where tephra was found.

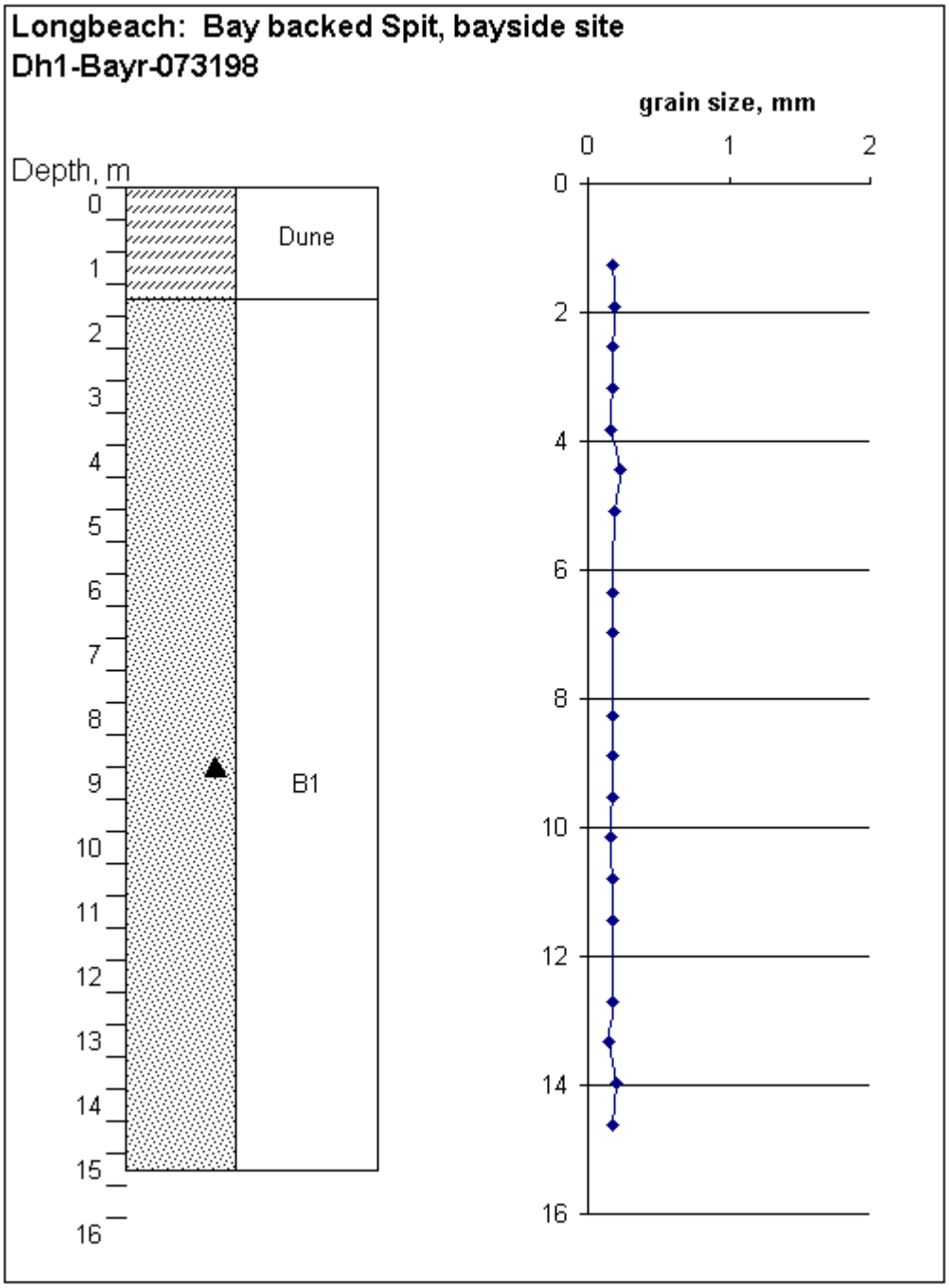

Figure 39: Bayr core log.

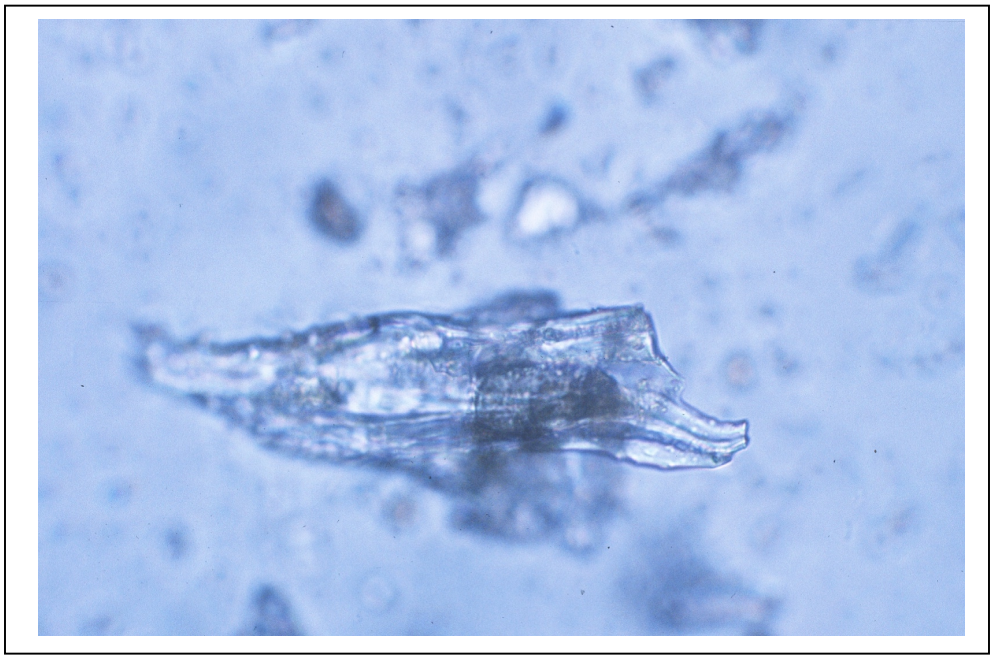

Klip-482” Flow banded tephra shard (10 x).

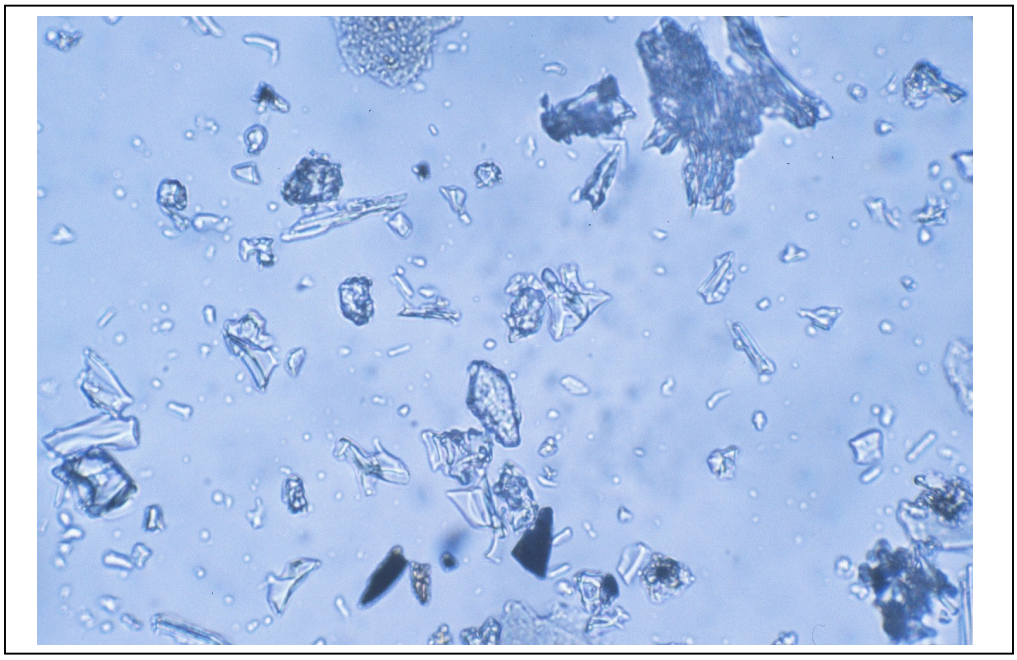

Sunb-410” Tephra shards (clear) and other particles (40 x magnification).

Figure 40: Photomicrographs of tephra from crushed samples in water mount.

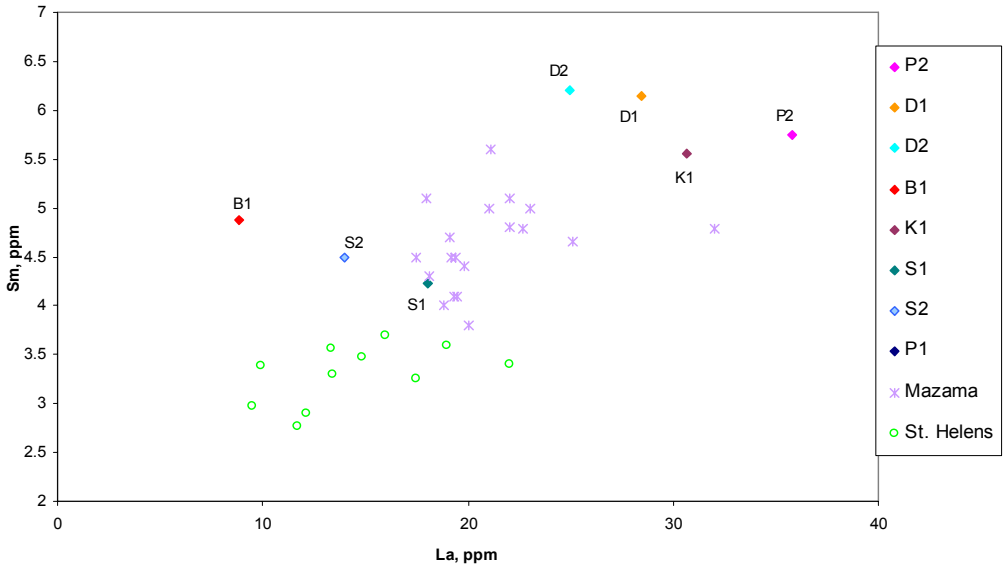

Figure 41: INAA results; plot of sample chemistry with St. Helens and Mazama eruption chemistry in order to determine source (see Appendix C for data).

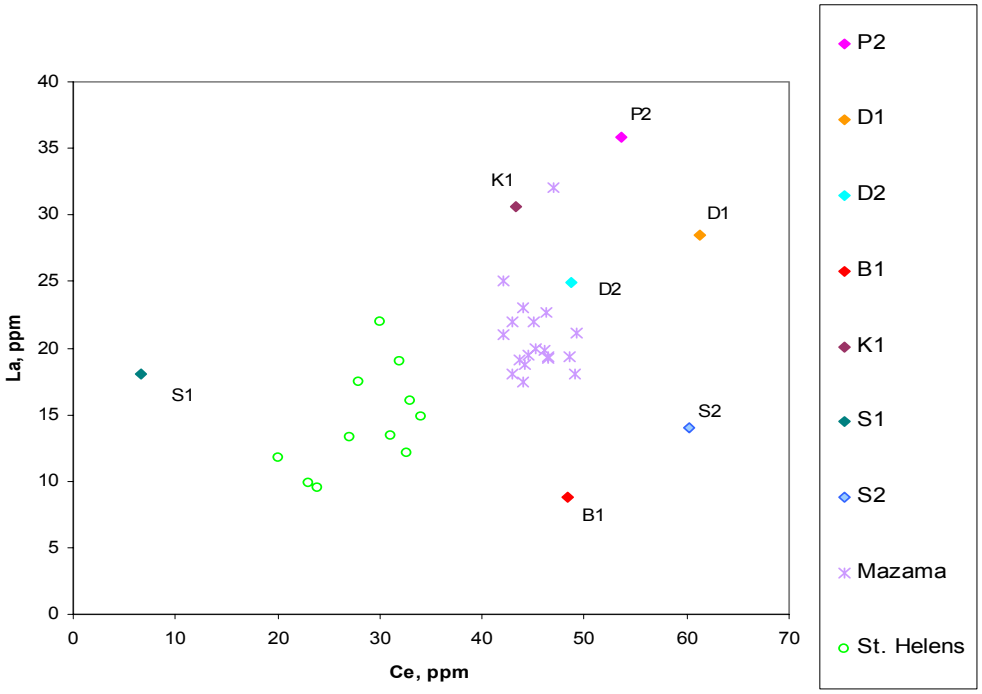

Figure 42: INAA results; plot of sample chemistry with St. Helens and Mazama eruption chemistry in order to determine source (see Appendix C for data).

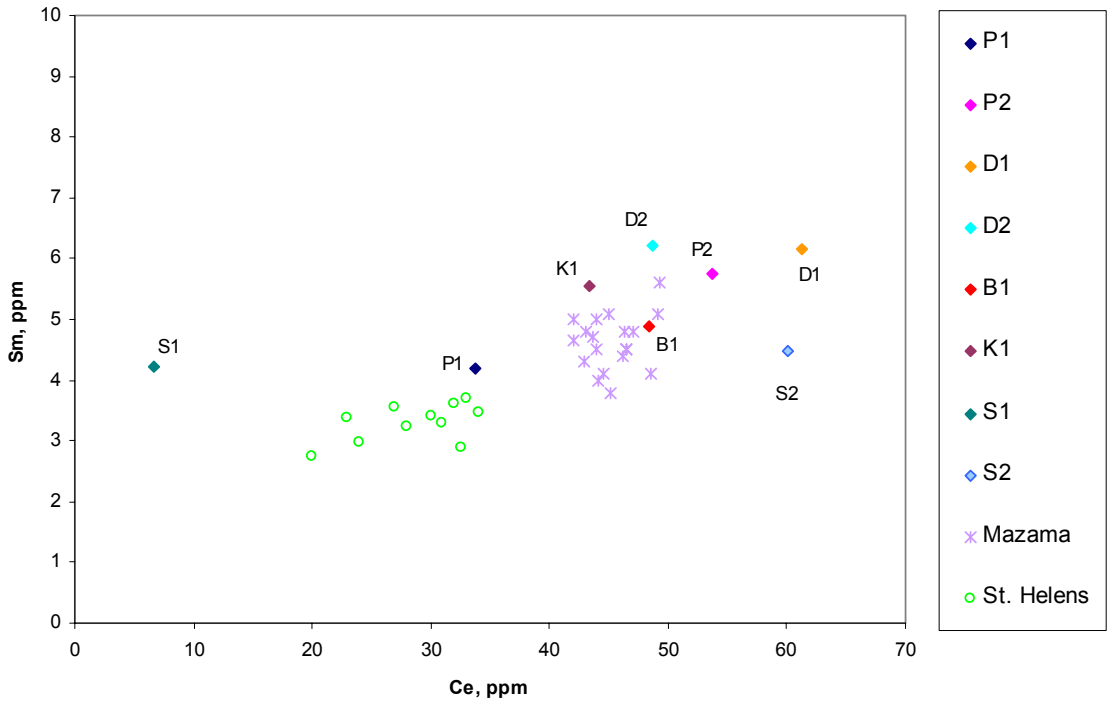

Figure 43: INAA results; plot of sample chemistry with St. Helens and Mazama eruption chemistry in order to determine source (see Appendix C for data).

Descriptive Stratigraphic Logs

The descriptive stratigraphic logs, drafted from field notes taken during the drilling of the 25 barrier auger sites are included in Appendix D. These logs are purely descriptive with field grain size estimates, shell, wood and tephra occurrences. Bedding (rarely preserved) is noted where present along with ripple laminations. This set of data is original and was used to interpret depositional environment and are simplified in the following set of interpreted logs.

Interpreted Stratigraphic Logs

Simplified logs with interpreted lithology and stratigraphic units were used to construct the lithologic cross-sections and to ground truth water well descriptive units. They provide the original data interpretations for this thesis. They are shown in Figures 24-37, 39, and 44-48. Measured grain size laboratory results are included with these logs. Radiocarbon dates and tephra sample numbers are listed on these logs as well. The Key is located below:

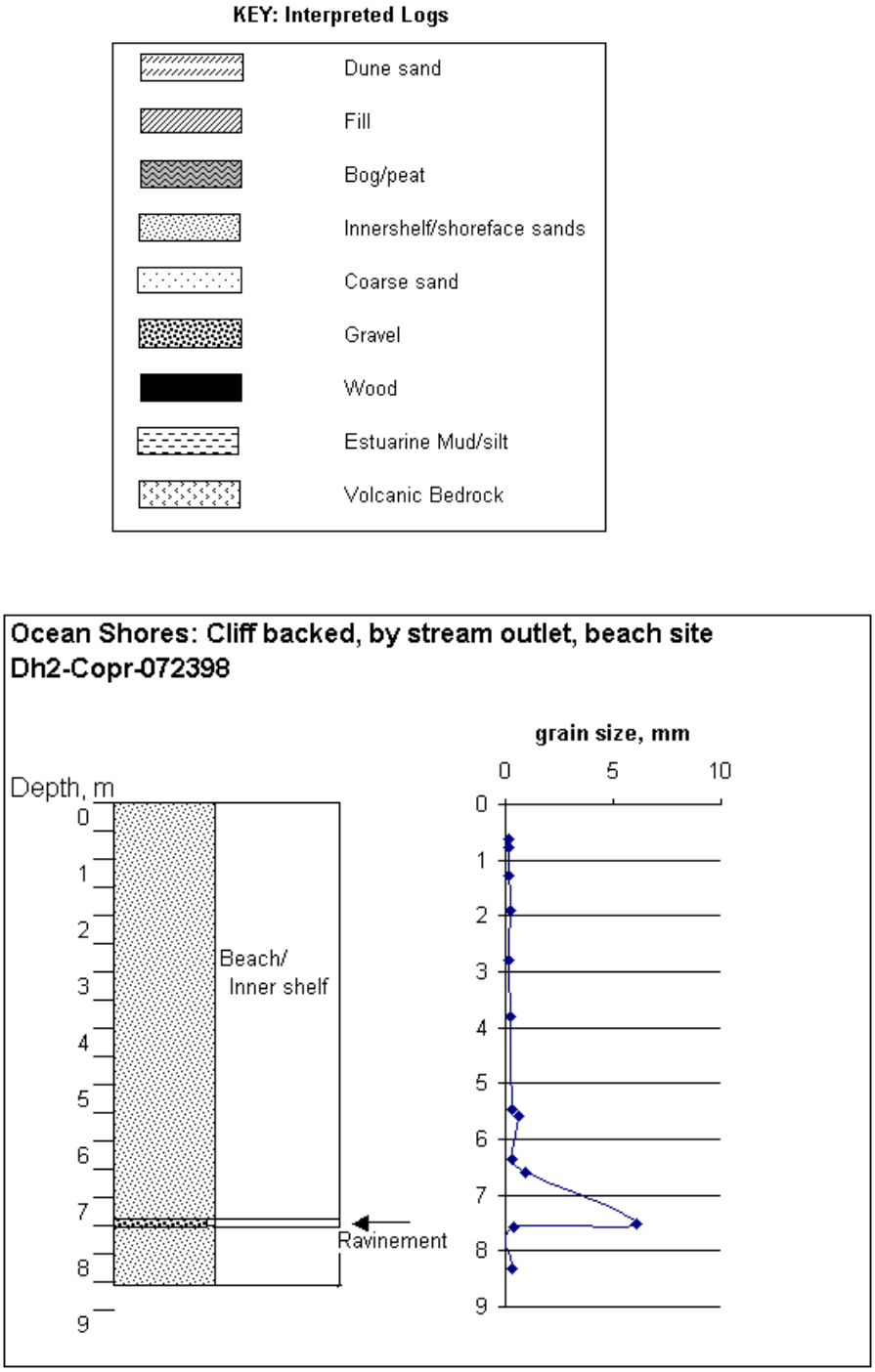

Figure 44: Copr drill site, located near Copalis River outlet.

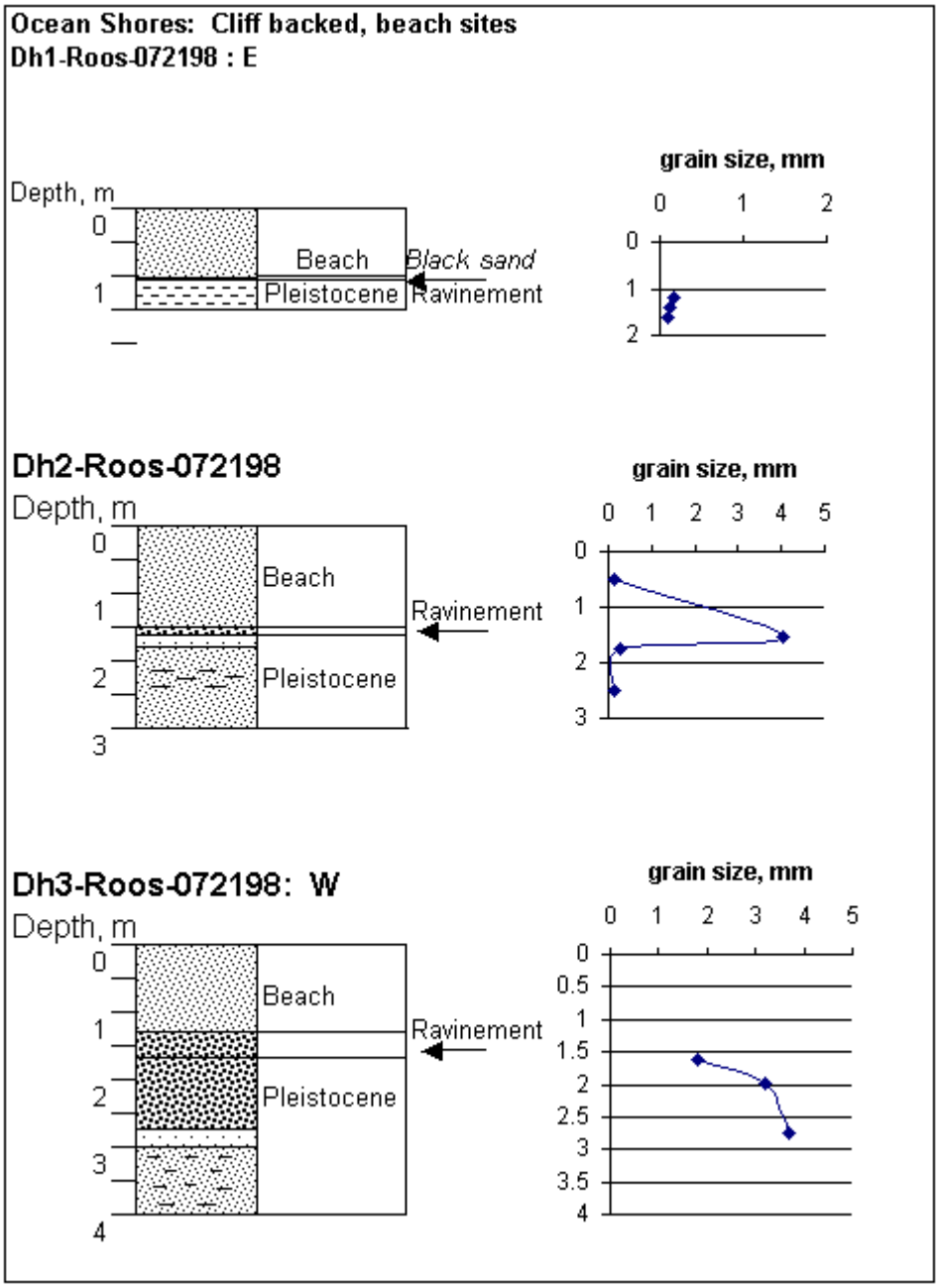

Figure 45: Roosevelt site core logs; beach transect from east to west.

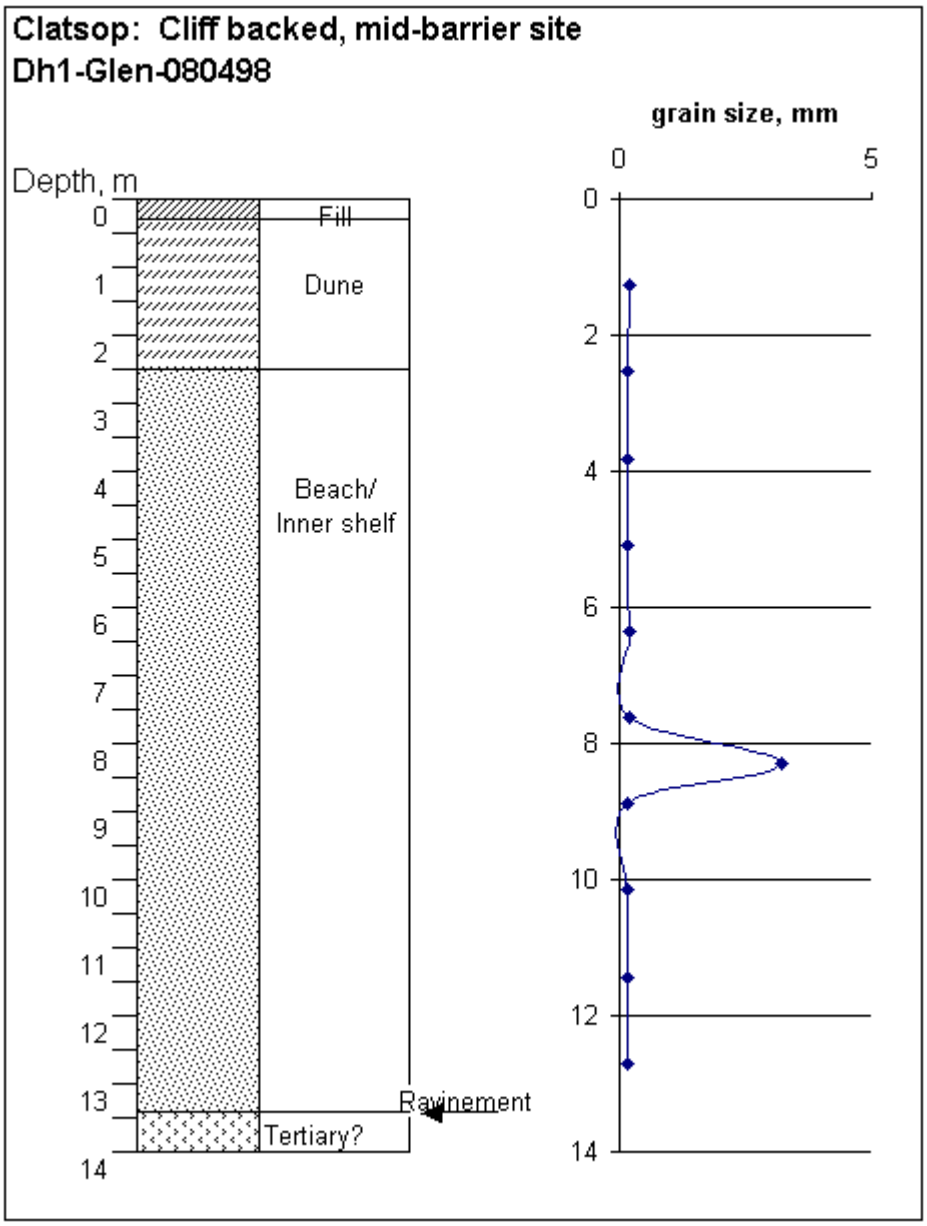

Figure 46: Core log for the one of the eastern site in Clatsop subcell (Glen), note: the base of hole is possibly Tertiary; drill could not penetrate this material.

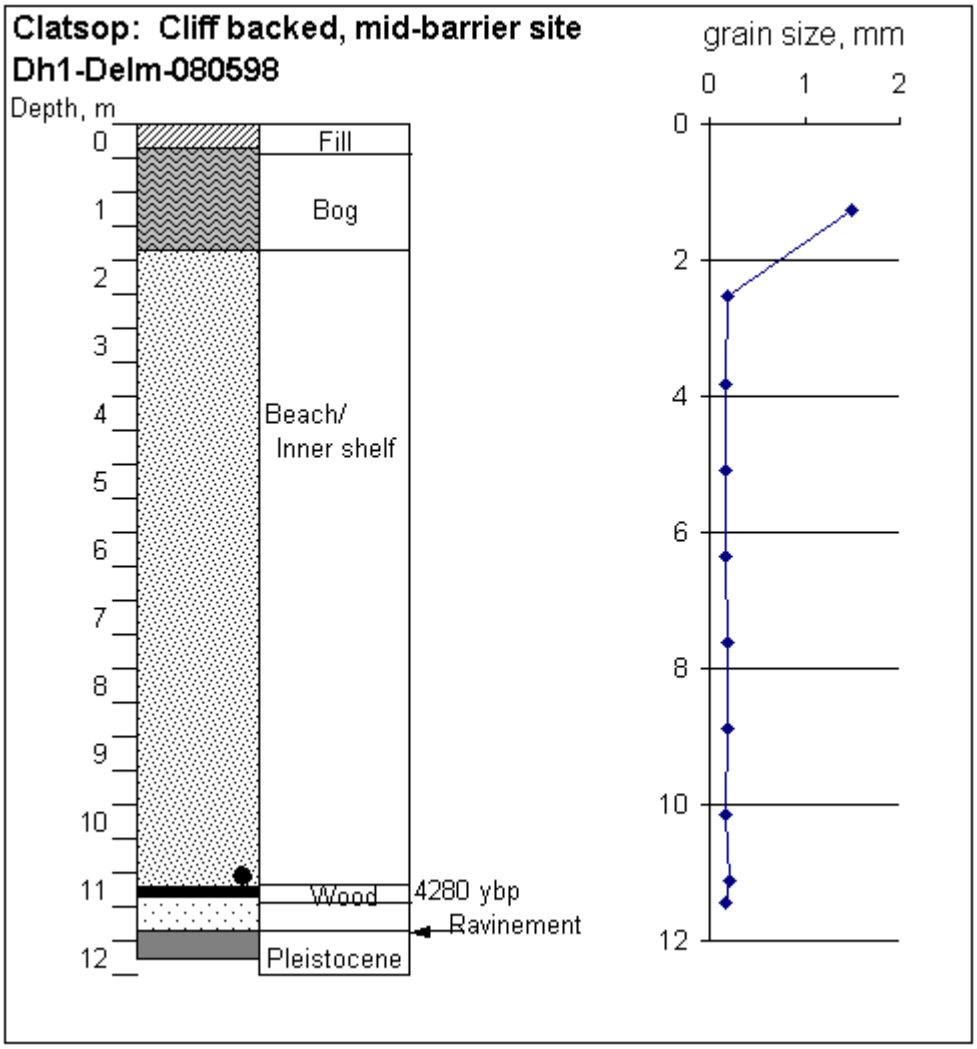

Figure 47: Eastern Clatsop subcell site core log. Grain size increases in bog material due to an increase in larger wood fragments.

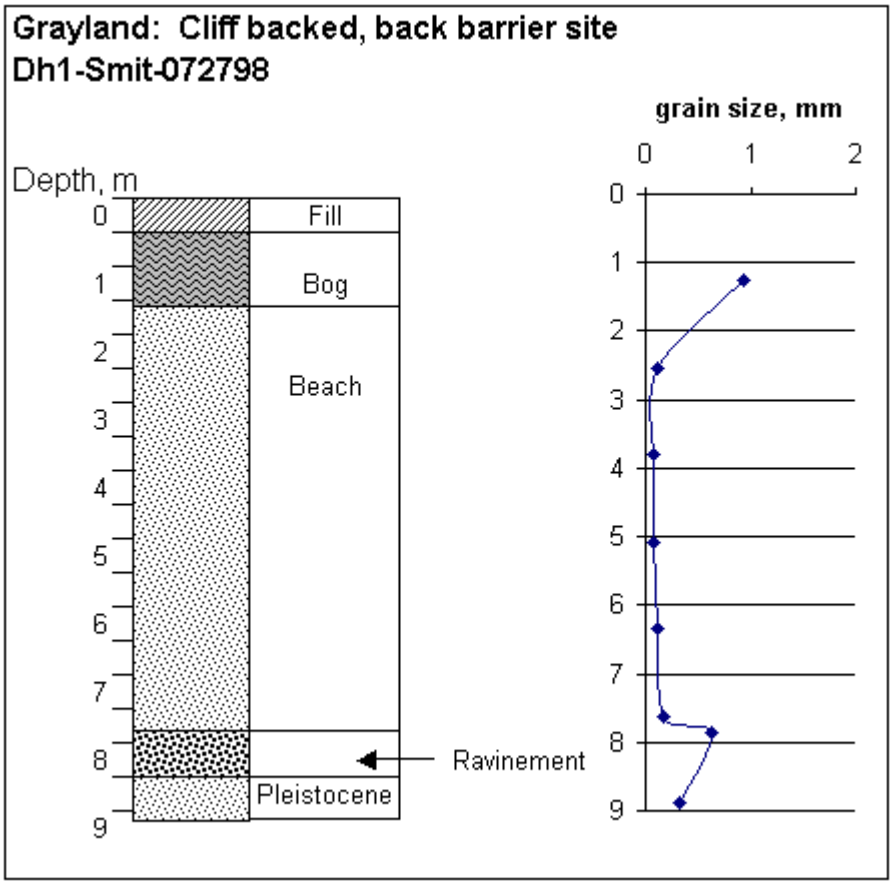

Figure 48: Core log for the eastern site in southern Grayland subcell (Smit).

Cross-section Data

Water Well and Geotechnical Borehole Data

Water well and geotechnical borehole locations and interpretations are summarized in Appendix E and are plotted on the cross-sections (Figures 49-68). Water well logs constructed by Smith (1999) are plotted on the cross-sections as well.

Ground Penetrating Radar / Offshore Seismic

Ground penetrating radar traces such as the one shown in Figure 13 were used to pick the base of the beach deposits, since field observations and grain size measurements did not provide an adequate separation of the beach and shelf units. A summary of locations and interpretations for GPR traces is included in Appendix E.

Offshore seismic interpretations (Cross *et al*., 1999) were used to plot the most westward position of the ravinement and Pleistocene surfaces (see background).

Surfzone Vibracores

Surfzone vibracores taken during the 1997 field season (Qualman *et al.*, 1999) show a bedding angle change between low angle dipping beachface bedding to flat lying bedding of the lower beach face. This change in bedding orientation is comparable to the change in GPR facies, taken in this study as the base of the beach section. A summary of recorded depth to base of the beach from vibracores is included in Appendix E.

Cross-sections

Methodology

Cross-sections have been constructed for selected locations within the Columbia River Littoral cell (Figure 14 (location map); Figures 49-68 (cross-sections)). These sections include data from various sources over and beyond the drilling program

completed for this study. The other sources are water wells, geotechnical boreholes, ground penetrating radar, surfzone vibracores and offshore seismic which have been introduced here or in the background section. All data plotted on the cross-sections were projected alongshore into the section. Data points were used as depth from surface and plotted from the DEM topography. Projection distances were less than 900 m in most cases. All of the cross-sections were placed in line with existing offshore seismic and GPR lines. Drill sites and Vibracores were designed to be directly in line with seismic and GPR lines.

All of the sections are oriented east west and partition the bay, beach, shelf, pre-ravinement and Pleistocene deposits. Where the age of deposits beneath the ravinement are known to be Pleistocene, this label is used. Where the age is not known, the label pre-ravinement is used. In many cases, the ravinement and lowstand surfaces are synonymous. Data density is represented by various symbols on the cross-sections and interpretation where no data is plotted is considered speculative. For simplification, no change in line type was used to distinguish the level of certainty.

Topography is shown at the top of the cross-sections with a solid line and extends across the bounding water surfaces with a horizontal line at 0.3 m, which is approximately sea level. Sea floor bathymetry is not shown, bay bathymetry is for visualization purposes only. Vertical exaggeration is very large for the purpose of showing detail and fitting sections easily on one page. One profile is presented at a less exaggerated scale (20 x) for visualization of more realistic slope values (Figure 49-a). Neither vertical or horizontal scales are constant from one section to the next, thus the

size of the sections cannot be compared visually in the current form. This was done in order to show detail on smaller sections.

Cross-section Clatsop-1 (Figure 49-b) is the southern most cross-section in the CRLC and will be used here as an example to explain the symbols and methodology for all of the cross-sections. Clatsop-1 (C-1) includes two drill holes (Delr and Delm; Figures 34 and 35), two geotechnical borehole logs (Gst and H2; see Appendix E), four water wells (Cw-1, 2, 3,4; see Appendix E), one vibracore (Delr; see Appendix E) and two offshore seismic line interpretations (L17s1 and L19s1; see Appendix E). GPR lines are located on the same trace as the cross-sections so the data is plotted at several positions along the section and not identified specifically like the other data sources. GPR depth calls are represented by diamond shaped markers and help delineate the beach to shelf transition. Clatsop-1 is located at 5099720 m North, UTM Zone 10 (the whole study area is UTM Zone 10). Of particular interest in this section are the pockets of muddy sediments here classified as 'lagoonal' material and the underlying pre-ravinement sands. The dashed line represents the ravinement surface. Note that the drill hole Delr terminates far short of the projected ravinement surface.

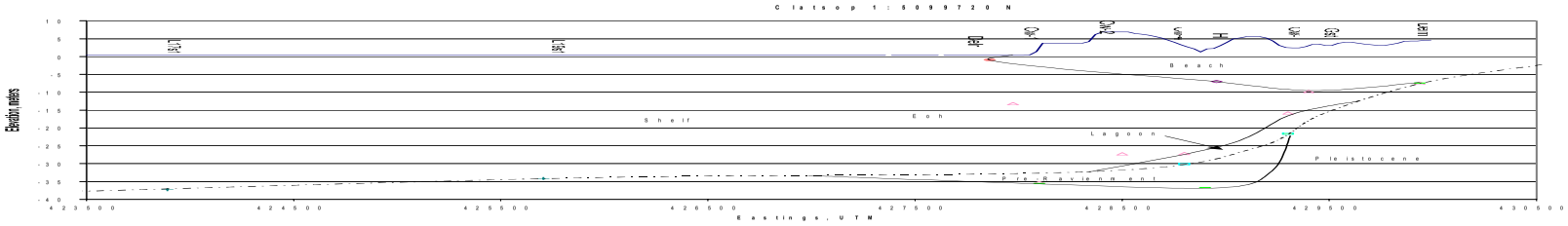

Figure 44-a: Cross-section with vertical exaggeration reduced to 20 x to show more realistic slope values and the difficulty in constructing sections at this scale.

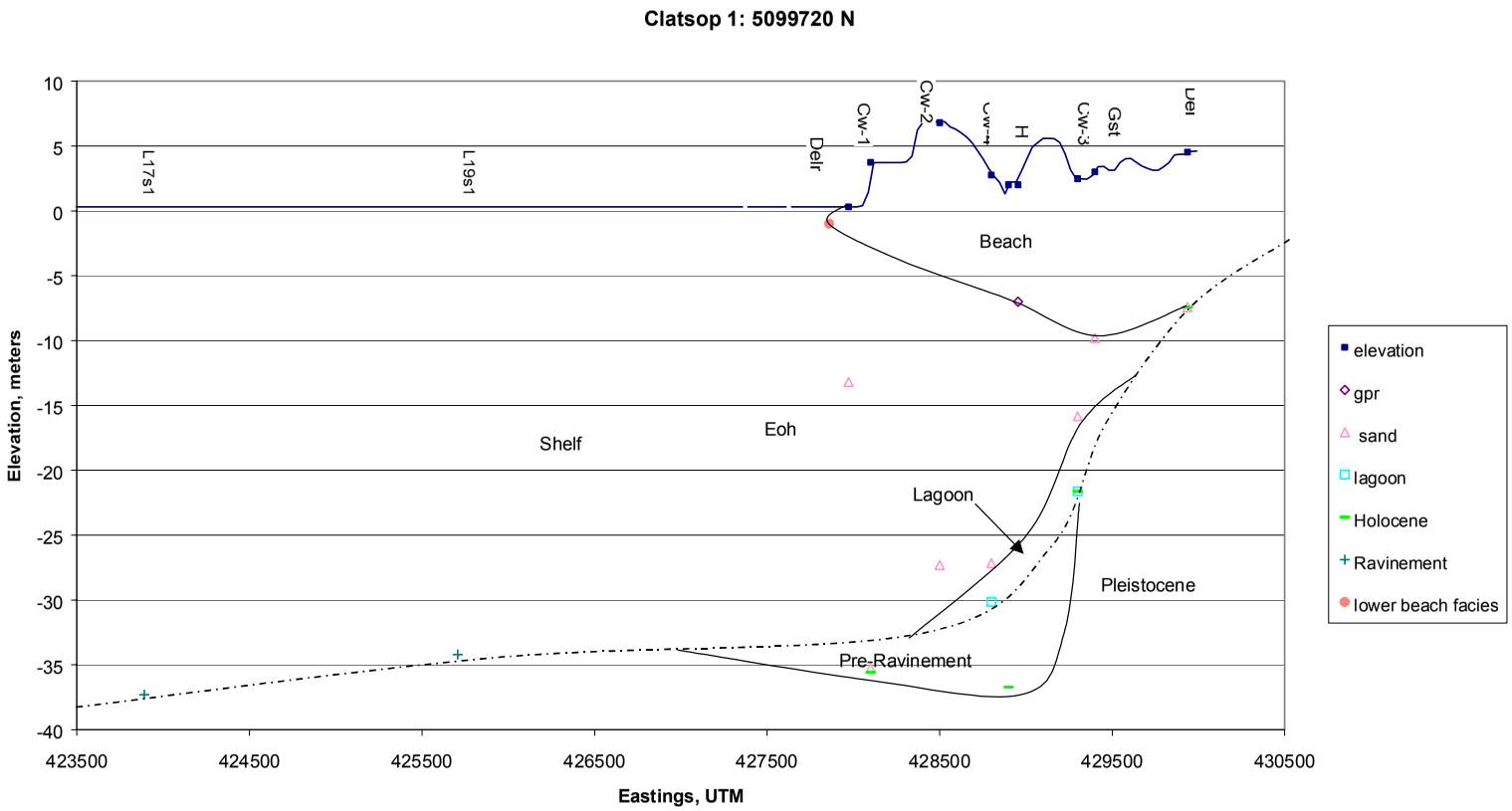

Figure 49-b: The same cross-section as presented for this thesis with greater vertical exaggeration for illustrative purposes.

Clatsop Subcell

The depth of Holocene deposits is the greatest in the Clatsop subcell. Clatsop-1 has already been mentioned (Figure 49) and has the deepest ravinement surface in the Clastsop subcell. Clatsop-2 (Figure 50) is centrally located in the Clatsop subcell. An interesting feature on Clatsop-2 is the bleb of 'lagoonal' mud within the shelf sand deposit. In similarity to Clatsop-1, the most seaward drill site, Sunb (Figure 33) does not reach the ravinement surface. Clatsop-2, however has a shallower ravinement slope than Clatsop-1, showing variability within the subcell. The northernmost cross-section in the Clatsop subcell is Clatsop-3 (Figure 51). Because Clatsop-3 is located where the shoreline trend changes to a more northwesterly orientation, it is a more oblique view of the Clatsop barrier and is consequently larger in the horizontal direction than the other Clatsop cross-sections. The far eastern edge of the section reaches the edge of the Columbia River Estuary. Only two data points exist for defining the ravinement surface in this area, thus the slope is less well constrained towards the eastern portion of the cross-section.

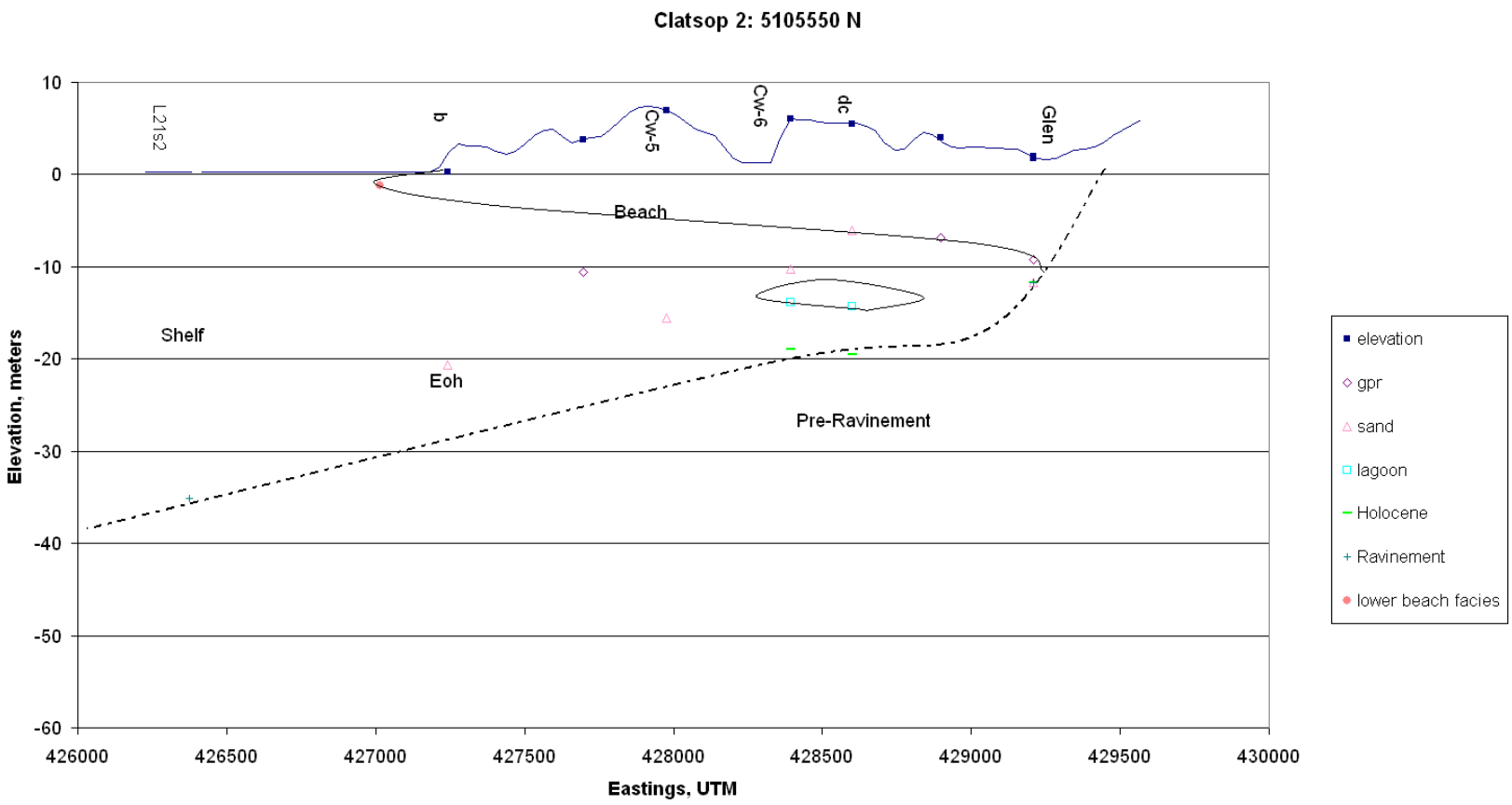

Figure 45: Mid-Clatsop subcell cross-section, note shallower ravinement than Clatsop-1.

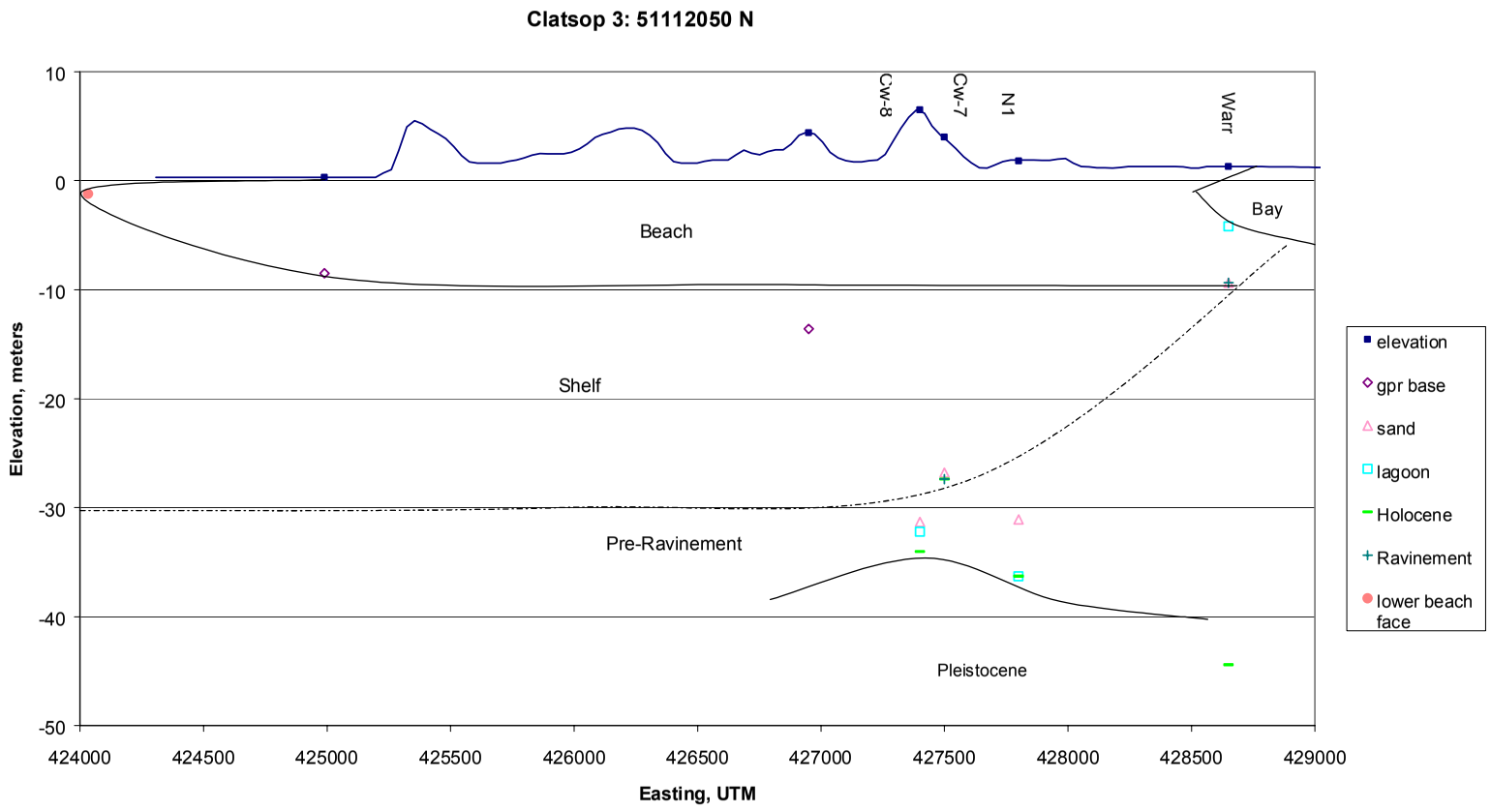

Figure 46: Northern-most cross-section in Clatsop subcell (section is oblique to shoreline).

Longbeach Subcell

The Longbeach subcell has the most bay backed area in the CRLC and the most limited spatial subsurface data coverage. Longbeach-1 (Figure 52) is the southernmost cross-section constructed for the Longbeach subcell. Pleistocene material was encountered at the drill sites 67th (Figure 31) and Pcyd (Figure 30) as well as was noted in the Ashawa well (Smith *et al*., 1999) (Figure 8). Longbeach-1 shows a Pleistocene platform in this location. It also shows a steep slope to the ravinement-lowstand surface at the western edge of the barrier.

Longbeach-2 (Figure 53) is located in the southern portion of Longbeach subcell. This cross-section shows a reverse slope (eastward) to the ravinement beneath the western edge of the barrier. Though unexpected, this trend is reasonable when compared to offshore data that show a high ravinement surface to the west of Longbeach peninsula. Pleistocene material was encountered at the drill site Mchu (Figure 32) which is located on the eastern edge of this profile. This suggests that there is another high in the ravinement at the eastern edge of the barrier.

Longbeach-3 (Figure 54) is located in the central portion of Longbeach subcell. This cross-section shows the offshore ravinement high continuing to the north and a sharp rise in the ravinement surface beneath the barrier. Pleistocene material is not encountered at this location, with data coverage available. Longbeach-4 (Figure 55) is the northernmost cross-section in the Longbeach subcell. It also shows the continued ravinement high offshore.

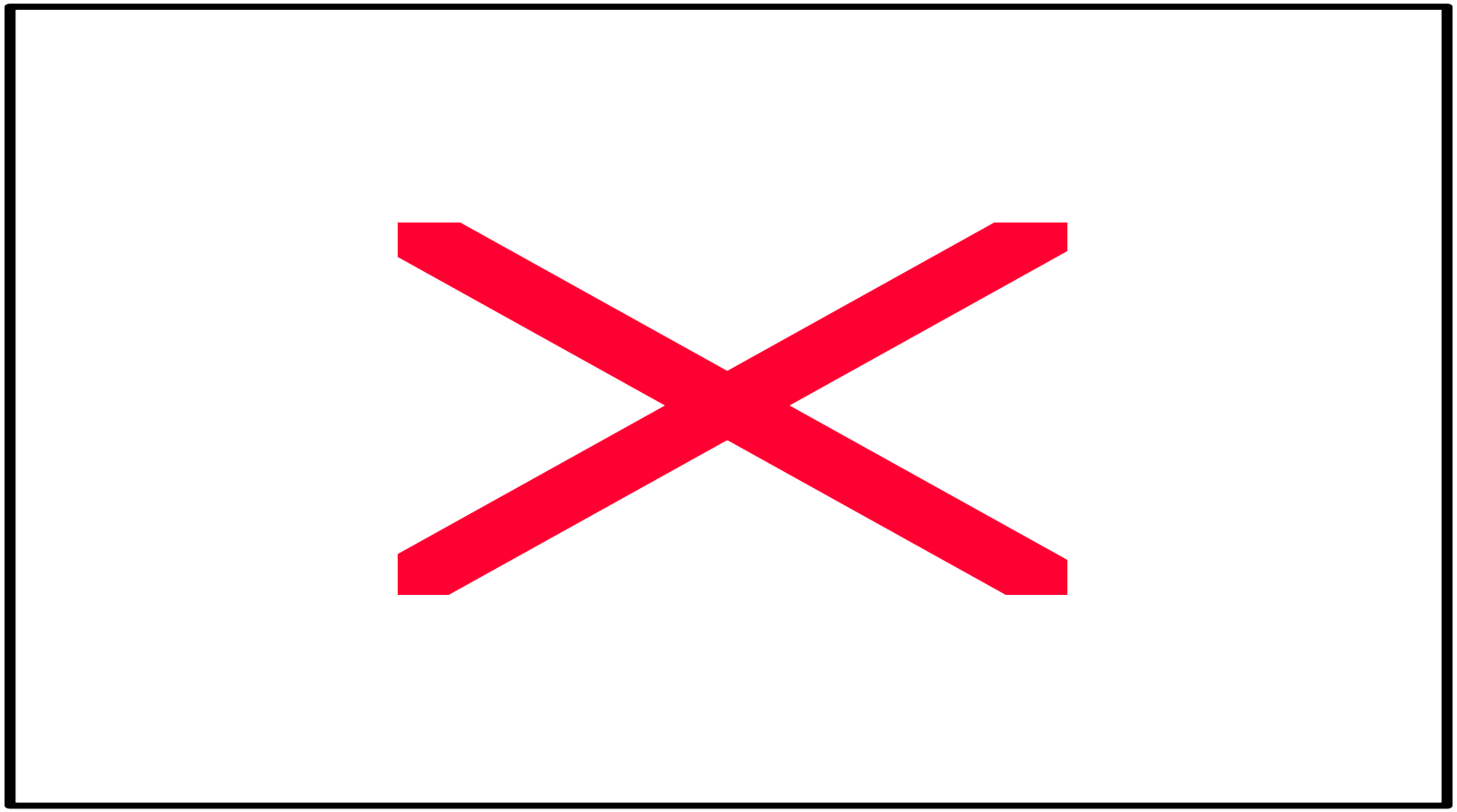

Figure 47: Southern-most cross-section in Longbeach subcell. Note the steepness of the ravinement surface.

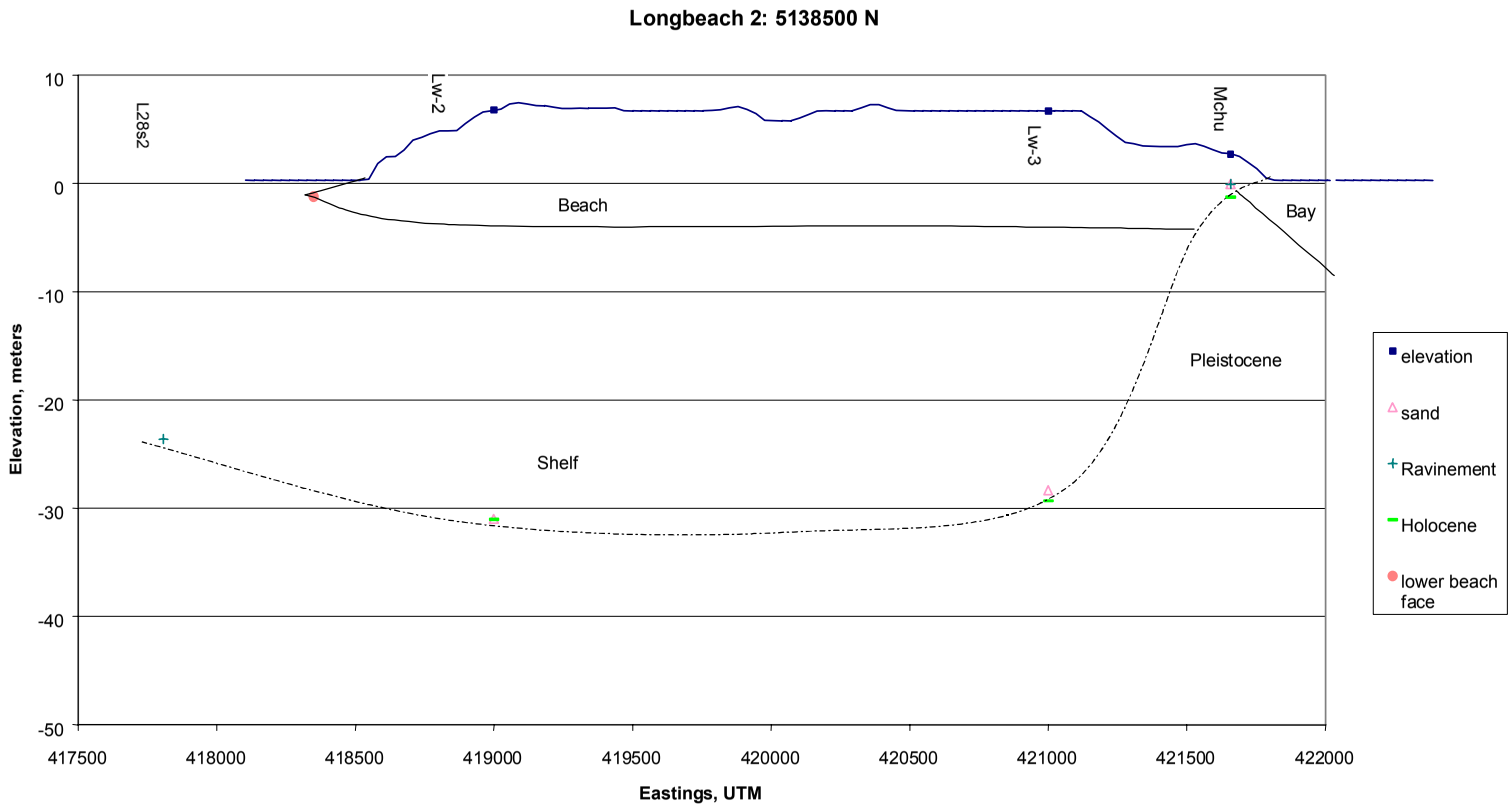

Figure 48: Mid-Longbeach subcell cross-section.

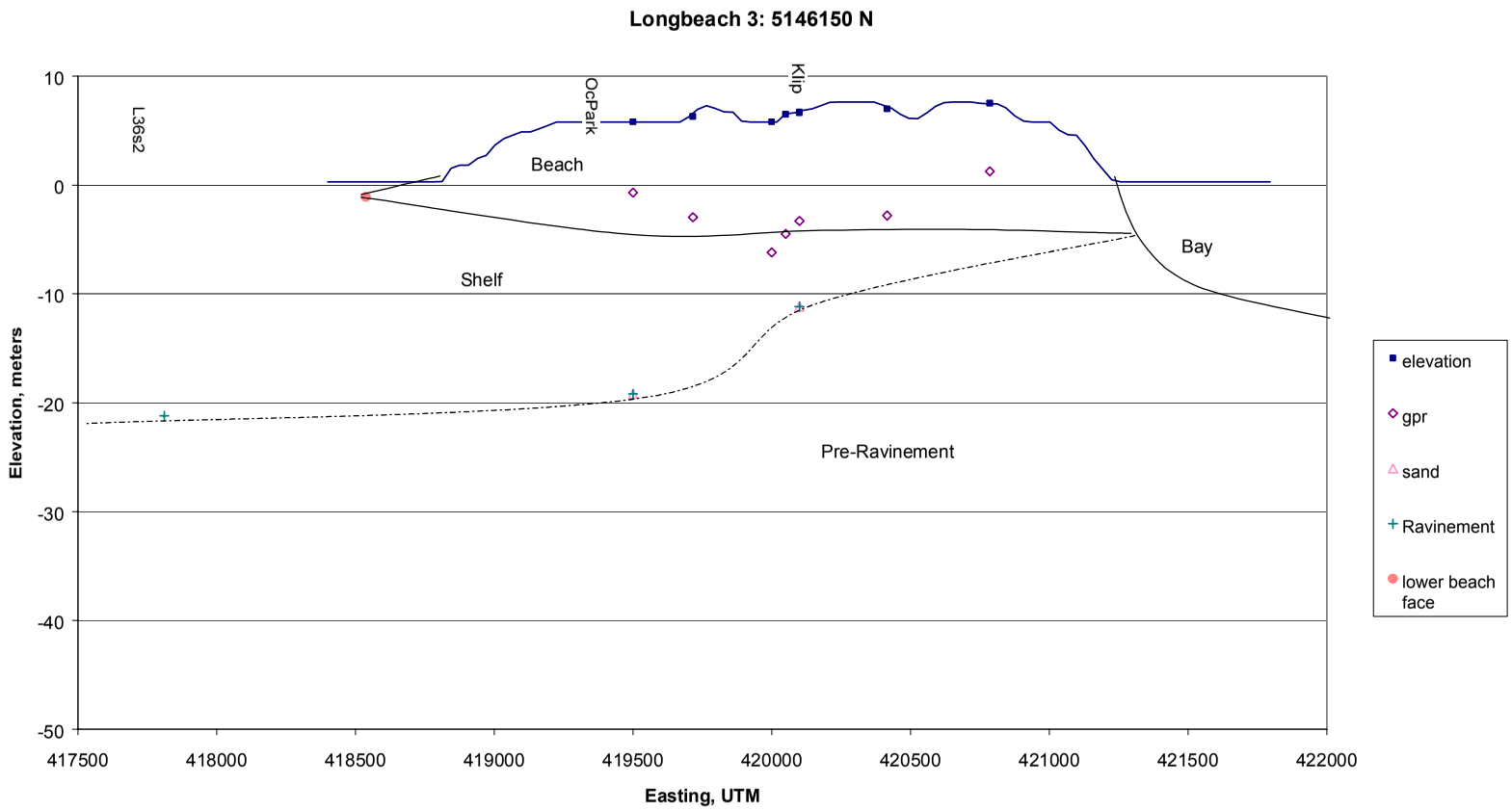

Figure 49: Mid-Longbeach subcell cross-section. Note no dip to ravinement surface.

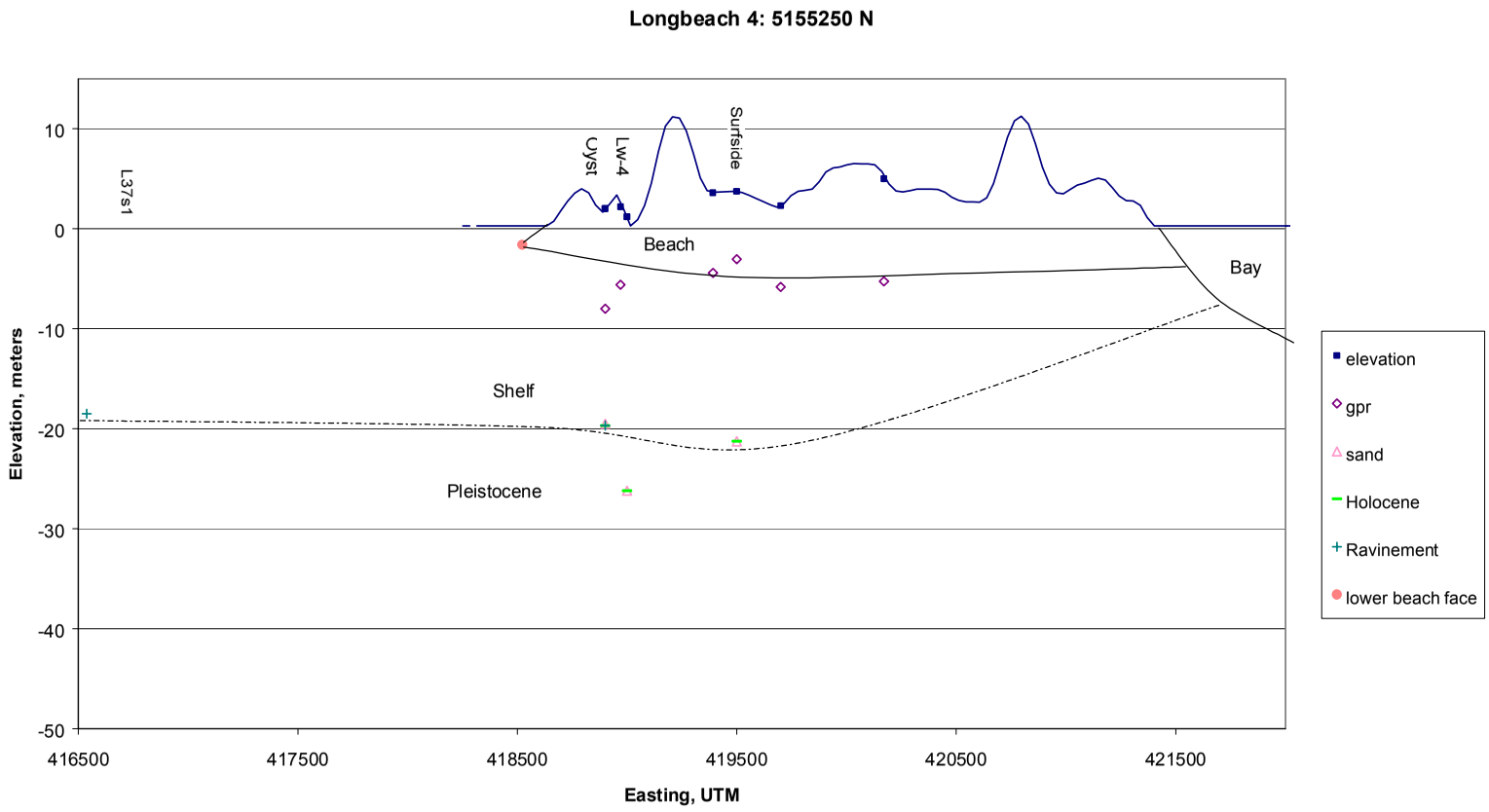

Figure 50: Northern-most cross-section in Longbeach subcell.

Grayland Subcell

Grayland subcell exhibits the most mophologically complex ravinement-lowstand surface and shows the effects of channel migrations on both the northern and southern ends. Grayland-1 (Figure 56) is the southernmost cross-section in Grayland subcell and shows the ravinement cutting through valley fill (Willapa Channel). Grayland-2 (Figure 57) is located in the central cliff backed portion of Grayland subcell. A clear low in the ravinement-lowstand occurs beneath the barrier at this location. Grayland-3 (Figure 58) is located at the southern edge of the bay backed portion of Grayland subcell. This section shows the ravinement-lowstand low continuing northward in the subcell and an offshore high in the ravinement surface. Grayland-4 (Figure 59) is the northernmost cross-section in the Grayland subcell. This cross-section, based on previous work (Peterson and Phipps, 1992) shows the effects of an actively migrating tidal inlet channel on ravinement preservation. Multiple alternations between coarse and fine sediment without the benefit of radiocarbon dates made ravinement distinction impossible in this location. It is notable that the Pleistocene surface in this area is deeper (60 m) than the rest of Grayland subcell.

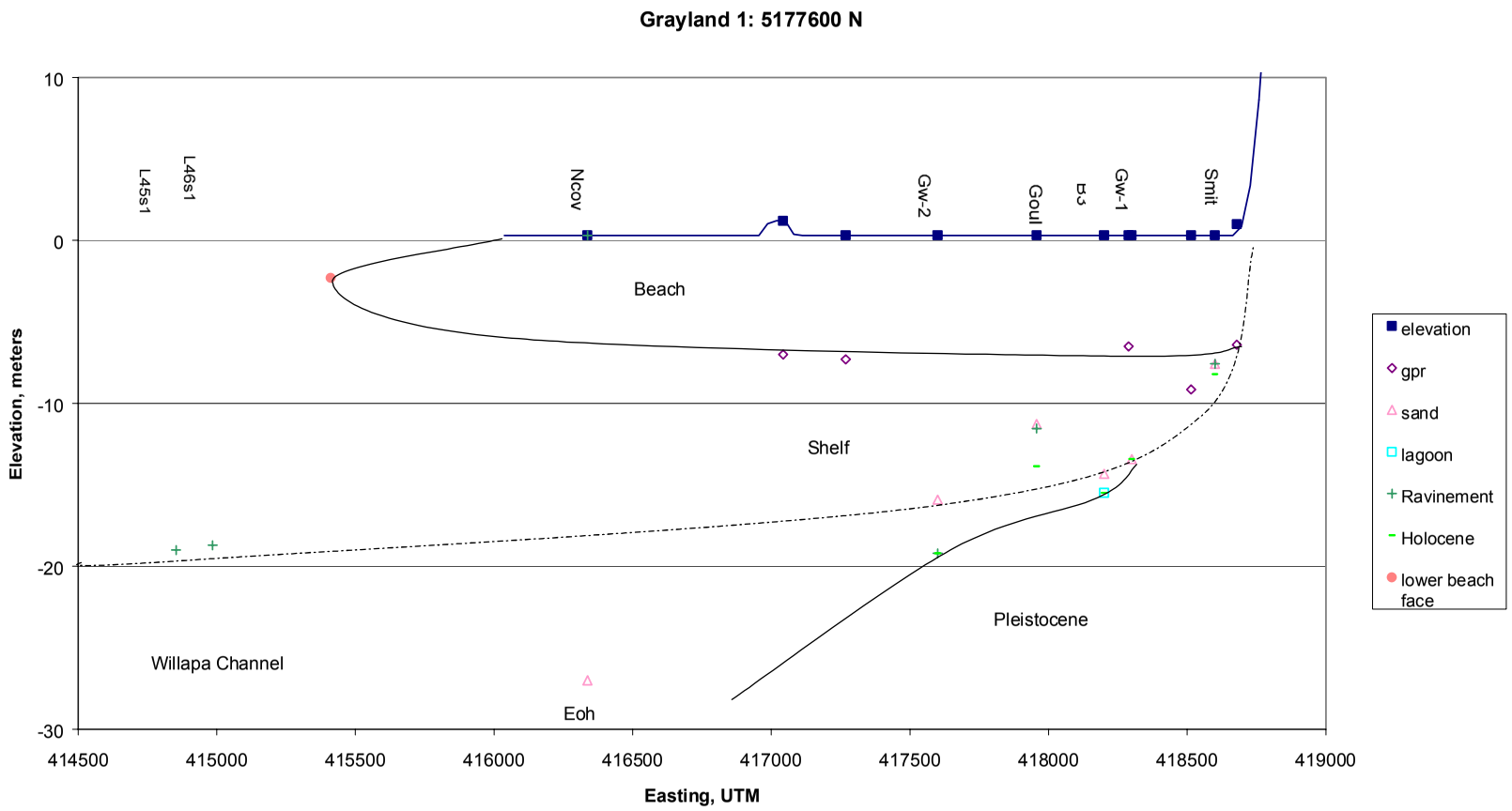

Figure 51: Southern-most cross-section in Grayland subcell. Note ravinement cutting through Willapa channel.

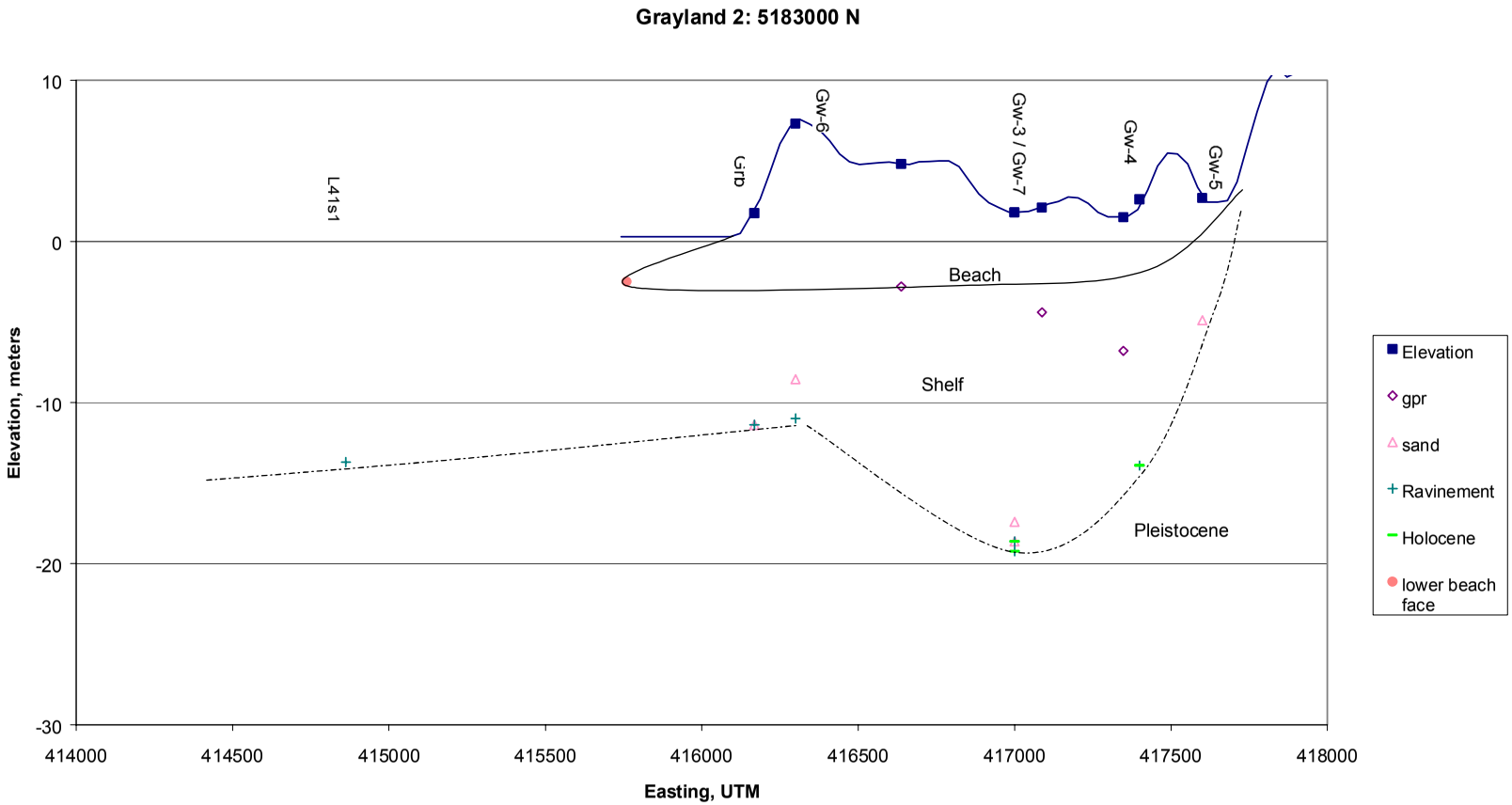

Figure 52: Mid-Grayland subcell cross-section. Note channel-like morphology of ravinement-lowstand surface.

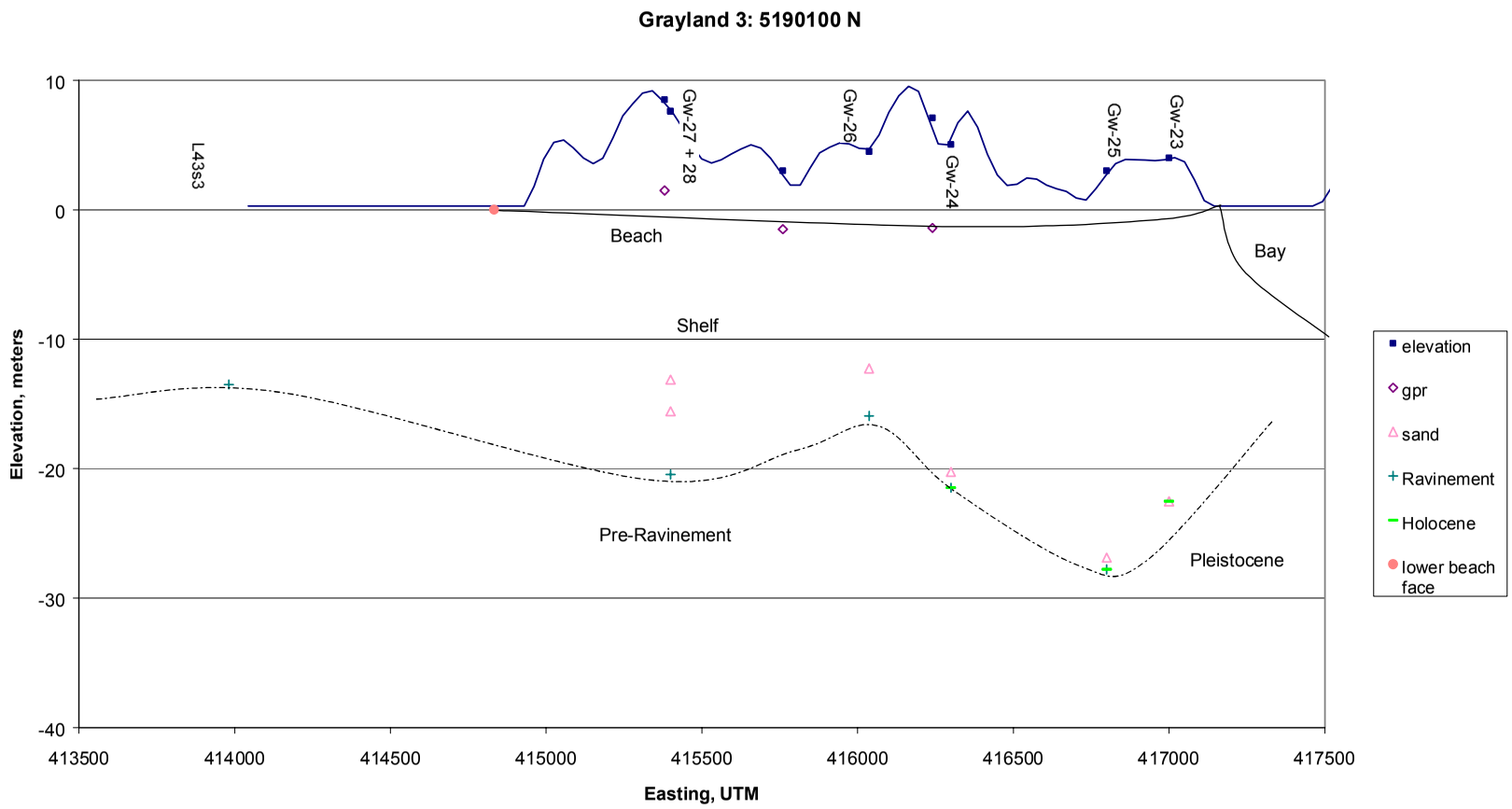

Figure 53: Mid-Grayland subcell cross-section.

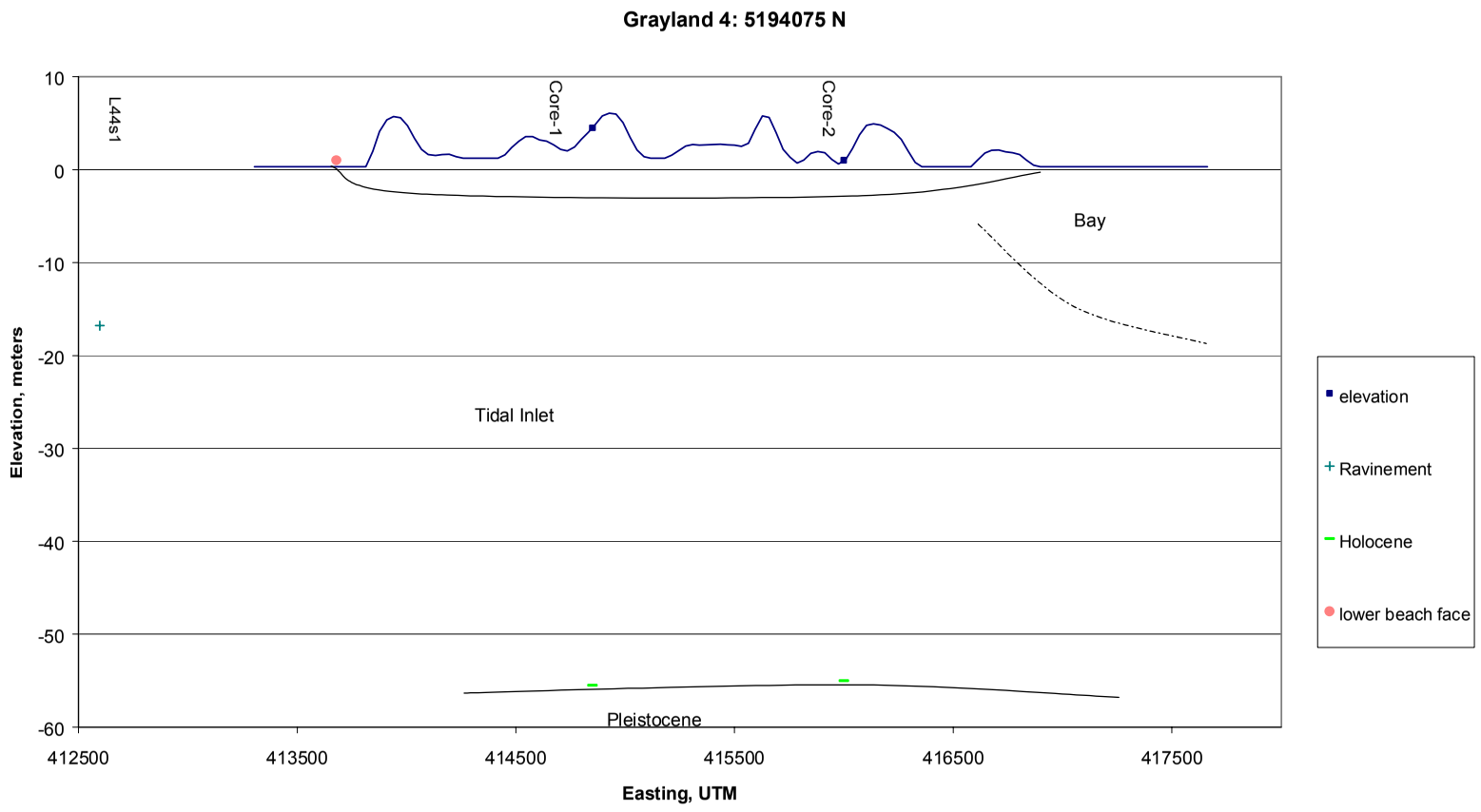

Figure 54: Northern-most Grayland cross-section. Because no radiocarbon dates were completed in this section sediment is classified as all tidal inlet below the beach deposits.

Ocean Shores Subcell

The Ocean Shores subcell shows a decrease in Holocene sediment volume from the south to the north. The southernmost cross-section for the Ocean Shores subcell is Ocean Shores-1 (Figure 60). It is located on the Ocean Shores spit and similar to Grayland-4 is based on previous work completed by Peterson and Phipps (1992) and one water well record. For the same reasons, all sediment below the base of the beach is labeled tidal inlet.

Ocean Shores-2 (Figure 61) is located further to the north on the Ocean Shores spit. A greater density of data provides definition of a sand channel within the tidal inlet material. The pre-ravinement material is much shallower (~28 m) than Ocean Shores-1 (~60 m).

Ocean Shores-3 (Figure 62) is located at the northern end of the Ocean Shores spit where it attaches to land. In this cross-section, two drill holes outline a shallow Pleistocene surface (2-8 m) and a shallow shelf sequence below the beach deposits. The sand channel deposits from Ocean Shores-2 possibly extend into this section as younger than expected radiocarbon dates were found in drill hole Oyhut-1 (Figure 35).

Ocean Shores-4 (Figure 63) the southernmost cross-section of the cliff backed portion of the subcell, is constructed with three water wells. A definite Pleistocene surface was identified about 10 m below sea level. Possible lagoonal muds exist in the landward portion of the shelf deposits. Without radiocarbon dates it is not certain that these deposits are Holocene in age.

Ocean Shores-5 and 6 (Figures 64 and 65) show the thinning shelf deposits to the

north. Ocean Shores-6 is located just south of the Copalis River. The slightly deeper shelf in this location is attributed to river incision. This section has the northernmost occurrence of dune forms.

Ocean Shores-7, 8 and 9 (Figures 66-68) are the northern beaches. They do not have dune forms, but have wide (~50 m) beaches. Data is limited in this region and the DEM topography shows a drop from the Pleistocene cliff to sea level. This made data location on the cross-sections difficult. In the case of Ocean Shores-7 surfzone and beach drill sites plotted east of the terrace cliff. Beach deposits in the northern beaches lie directly on a wave cut platform with no shelf deposits present.

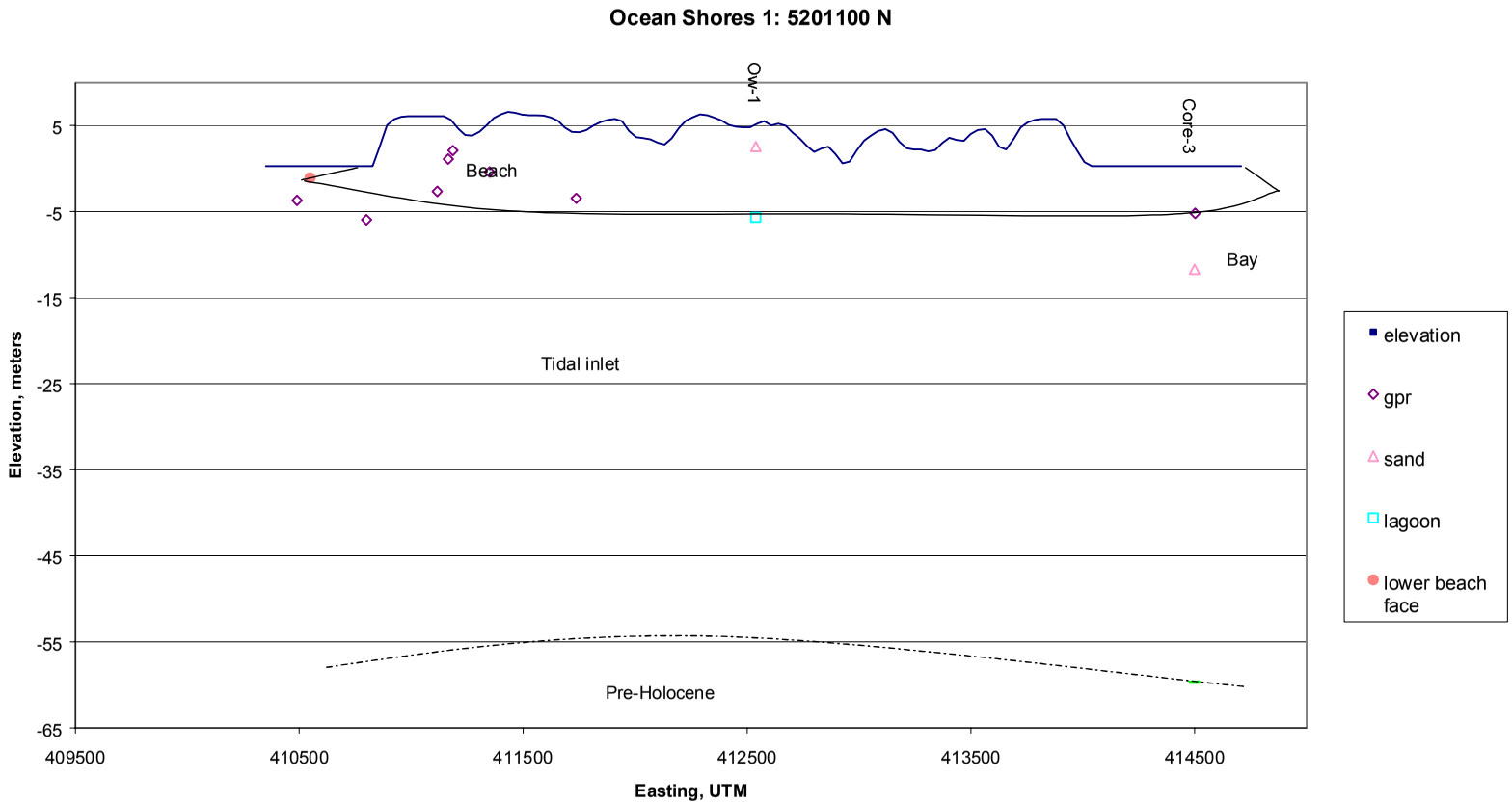

Figure 55: Southern-most Ocean Shores subcell cross-section. Tidal inlet is used due to a lack of radiocarbon dating in this area.

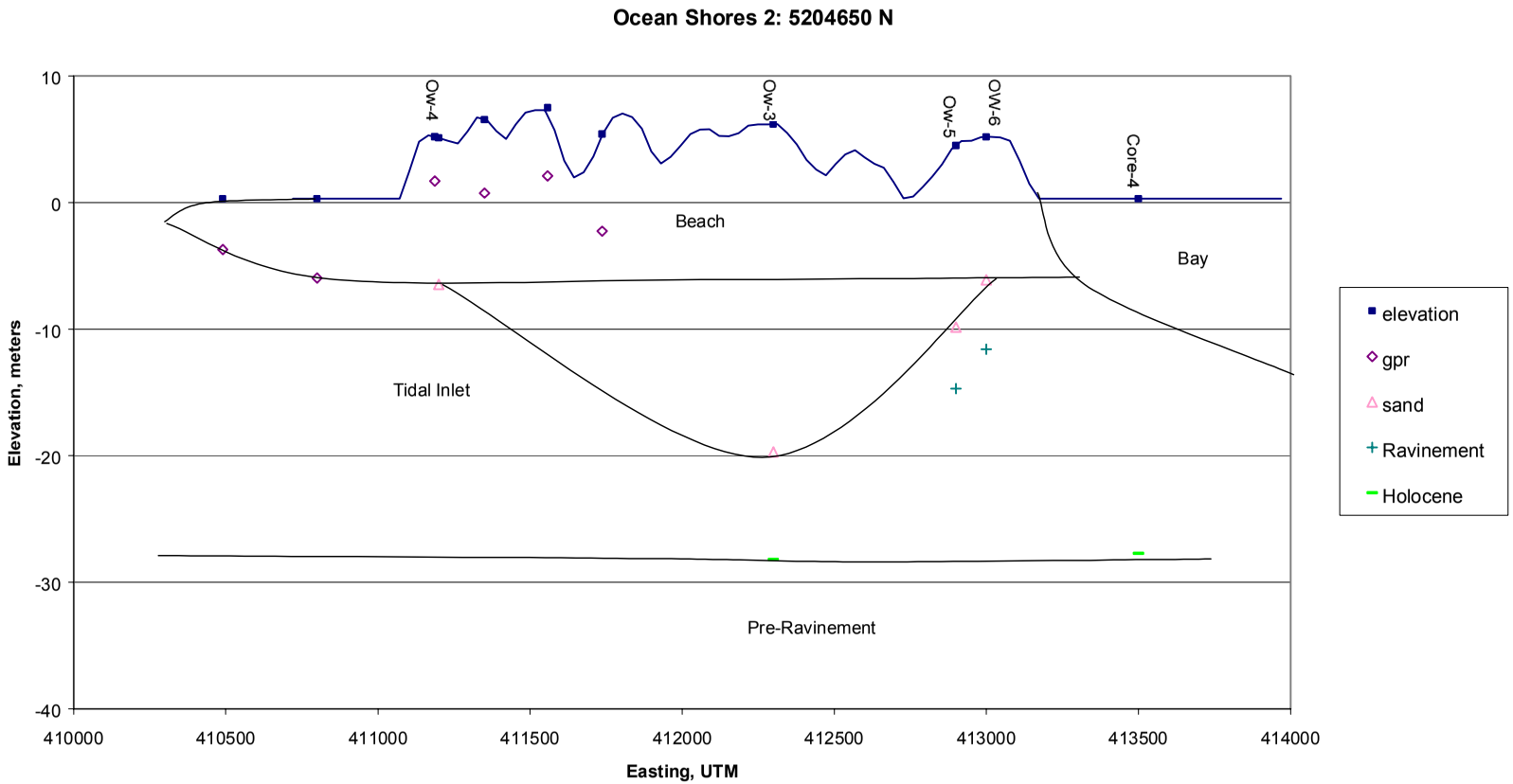

Figure 56: Mid-spit Ocean Shores cross-section. Note channel-like morphology of sand deposit within the tidal inlet deposits.

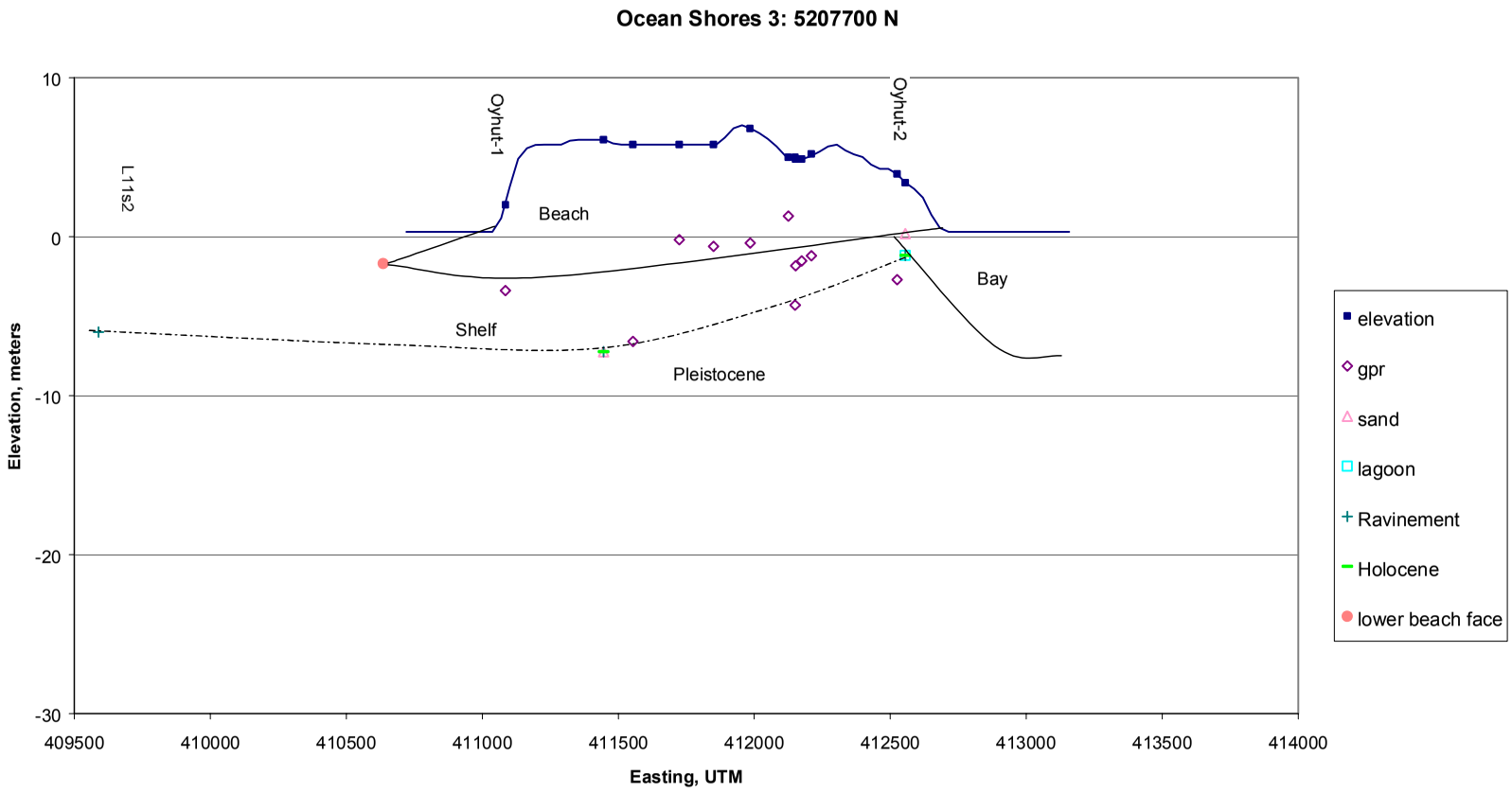

Figure 57: Ocean Shores subcell cross-section located along Damon Road, Ocean Shores, Washington.

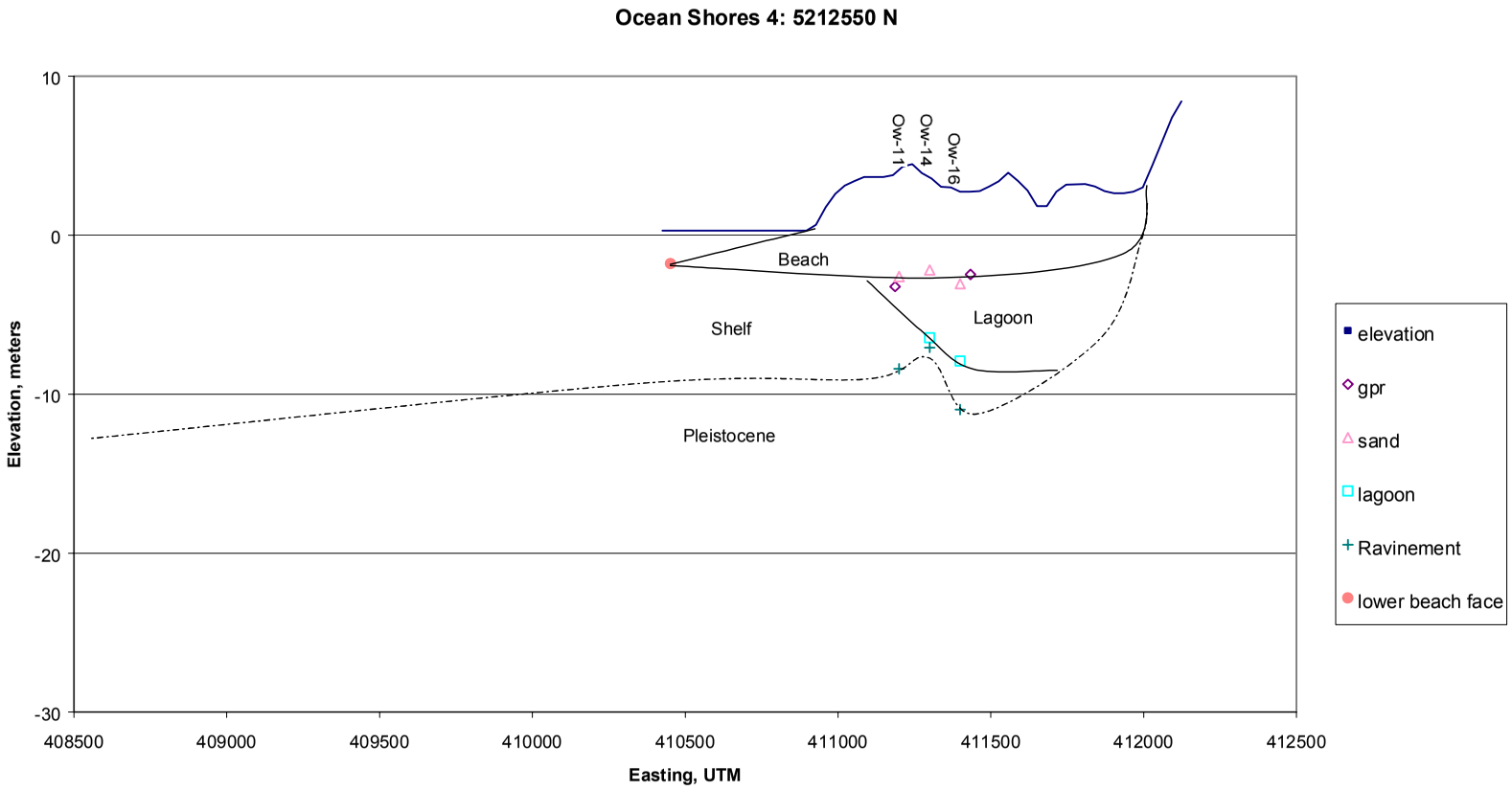

Figure 58: Southern-most dune and cliff backed Ocean Shores subcell cross-section.

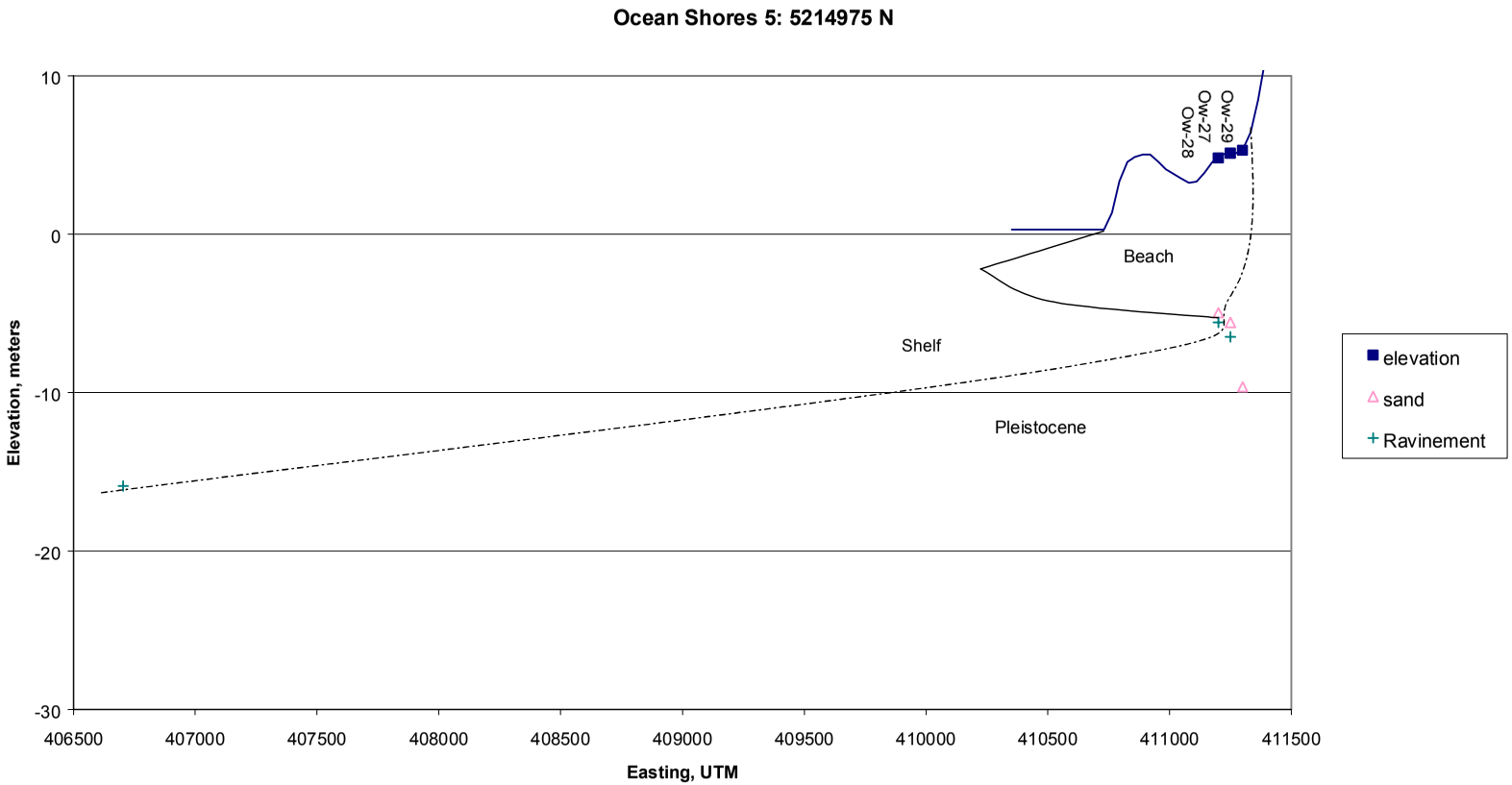

Figure 59: Ocean Shores dune and cliff backed cross-section.

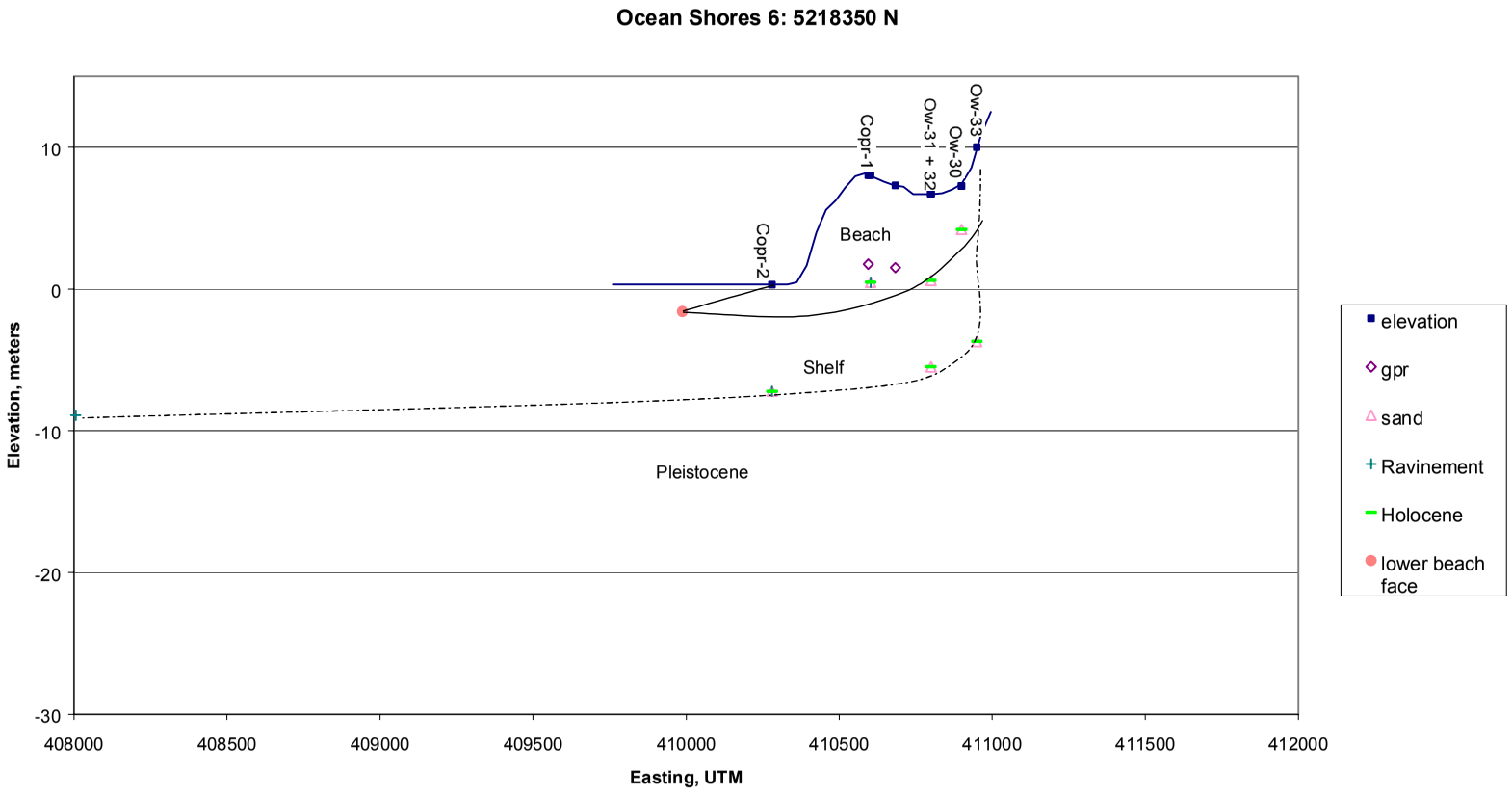

Figure 60: Copalis River cross-section, Ocean Shores subcell. (dune and cliff backed)

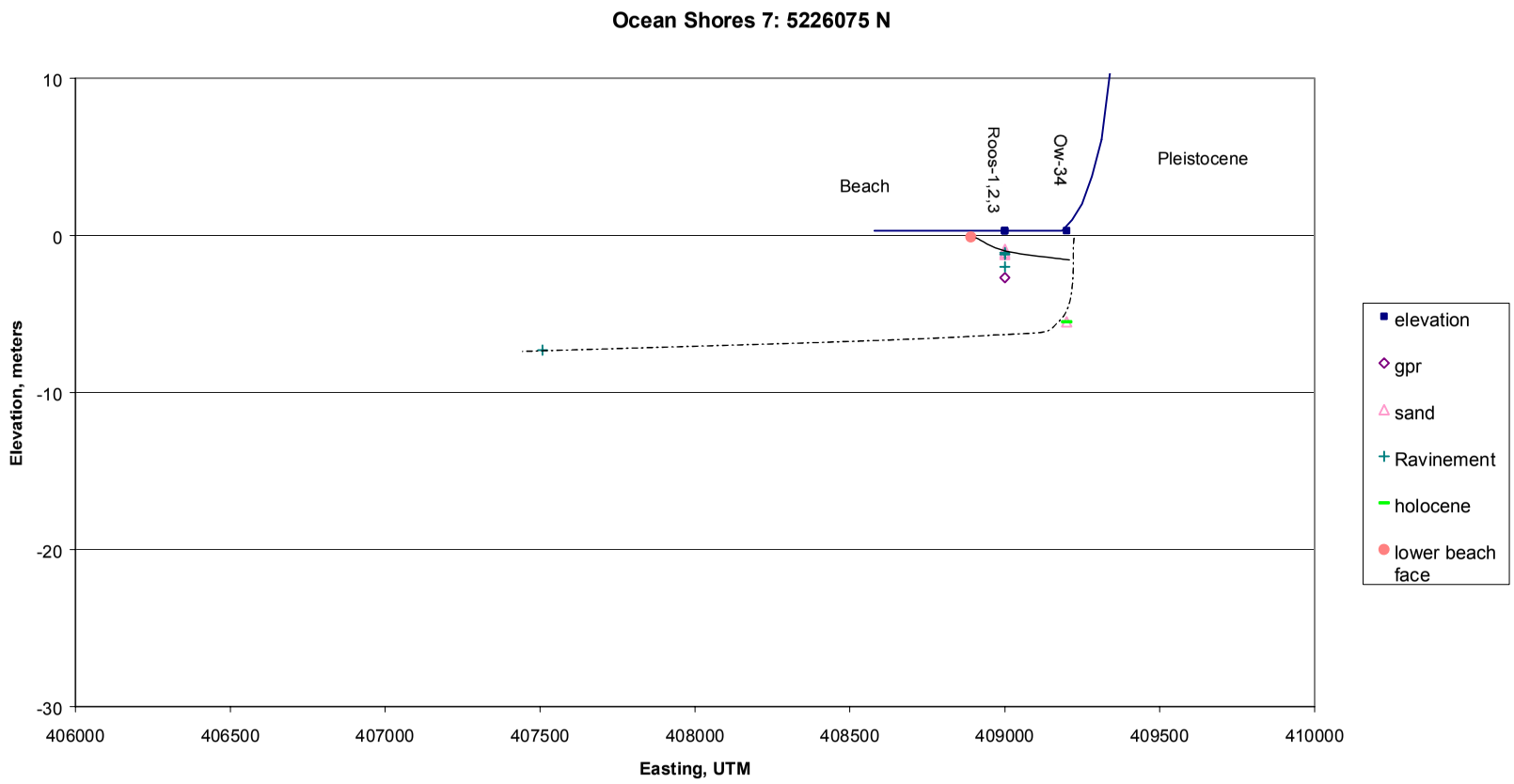

Figure 61: Cliff backed Ocean Shores subcell cross-section at Roosevelt State Park.

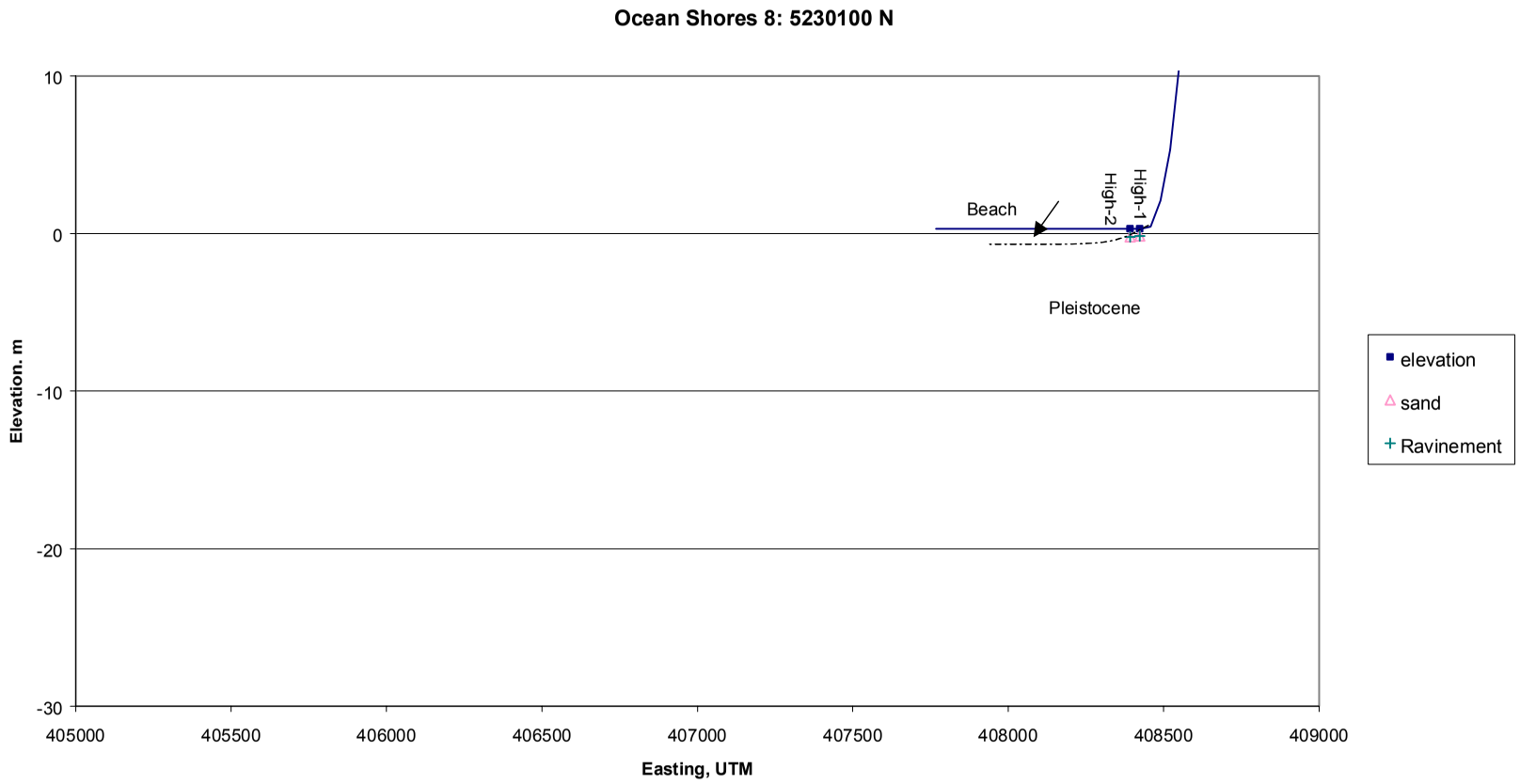

Figure 62: Cliff backed Ocean Shores subcell cross-section just north of the Pacific Naval Facility.

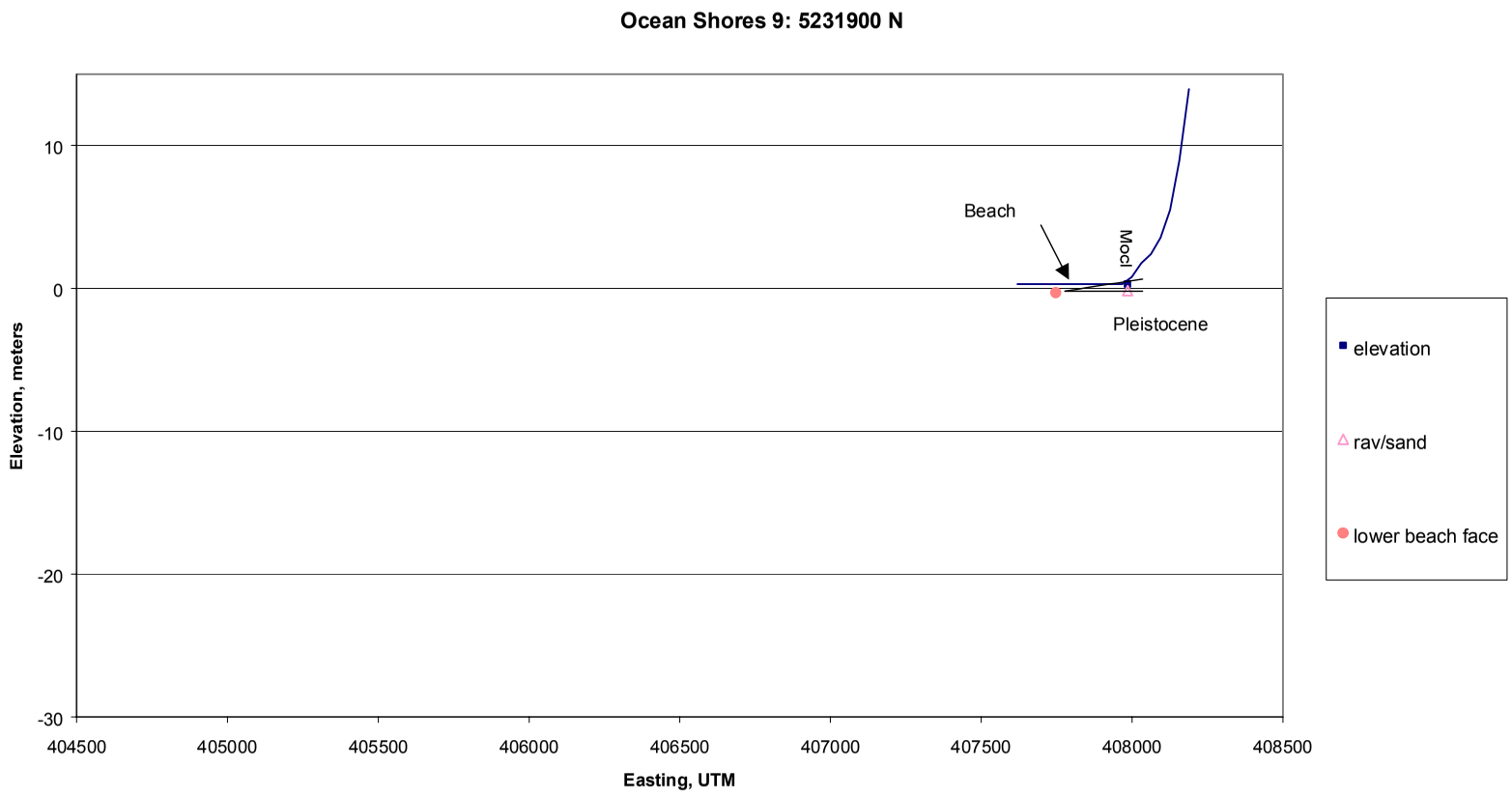

Figure 63: Northern-most cross section in the Ocean Shores subcell near Moclips, Washington.

DISCUSSION

The goals of this study are 1) to determine the amount of sand that accumulated in the inner shelf and beach-dune facies of the barrier beach plains and 2) to establish the time intervals during which the sand accumulation occurred.

Depths to beach, shelf, ravinement and Pleistocene deposits have been integrated with the construction of 20 cross-shore cross-sections. These cross-sections were digitized to compute cross-sectional areas of both the beach and shelf units. The cross-sectional areas have been multiplied by alongshore distance to yield sediment volumes. Total sediment volumes have been normalized by average total years of deposition (6000 yrs) in order to obtain a sedimentation rate for the Columbia River Littoral cell. This sedimentation rate will be compared to sediment supply rates predicted for the Columbia River in pre-historic times. Such a comparison is valid because the sand mineralogy matches the Columbia River signature throughout the entire Columbia River Littoral cell (see background).

Transgressive Stratigraphy

Near the back edge of the beach ridge plains, the shallow depth to Pleistocene material shows that the transgression cut down at least to the lowstand surface. Holocene shelf or beach deposits are found directly overlying Pleistocene or older materials at drill sites: Smit, Glen, and Delm as well as most of the northern Ocean Shores sites. In general, the likelihood of shelf or beach deposits directly overlying Pleistocene deposits decreases seaward. In many places the ravinement surface overlies Holocene deposits that predate ravinement and postdate Pleistocene deposits. These Holocene sediments were deposited

during lowstand in terrestrial or in protected marine settings.

In addition to the cross-sections presented in the results section, I have constructed several correlative plots in both the east-west and north-south directions (Appendix G) to illustrate the ravinement surface in a more conventional way. These sections are less detailed and contain only the drill hole information, in order to show facies relations.

As sea level rose, erosion of the shoreline created a low angle westward dipping ravinement surface described here as a basal lag in the shelf or beach deposits. However, in some places the ravinement did not erode a planar surface. The Grayland subcell has a Pleistocene contact that has a shore parallel, channel like morphology (Figures 57 and 58). This morphology can be explained as either a low-stand channel that filled with sediment during sea level rise, or, it could be resistant Pleistocene terrace deposits that did not erode evenly with sea level rise. In the Clatsop and Grayland subcells, isolated sea stacks are apparent (USGS 1:24,000 topographic maps: Warrenton, Gearhart, North Cove and Grayland Quadrangles) but are not included in the cross-sections shown here. In either case, the ravinement did not leave a westward dipping surface beneath some parts of the present day barrier beach plains.

Transgressive erosion does not remove the pre-existing terrain in all cases as was just shown. Nor does it cut into the landscape at a uniform rate creating a linear shoreline. The transgressive shoreline at any given time would have been as complex as the shoreline is today. In addition, the large tidal inlet channels continued lateral migration, cutting into existing sediments and replacing them with channel deposits (Figure 59-61). Because channel deposits have a basal lag similar to the ravinement surface, it is difficult

to tell if an actual ravinement occurred or whether the deposits reflect the migration, or several migrations of a channel. Thus, recognition of transgression within possible tidal channel deposits requires dating the sediments. Often, the record will be altered so that any evidence of ravinement in the area is now gone. In some cases a gradual deepening of water provides no erosive surface and a specific horizon representing transgression is not distinguishable in the tidal inlet setting.

The barrier spits fronting Grays Harbor (southern Ocean Shores and northern Grayland) have a high volume of Holocene sediment placed by tidal inlet channel migrations. Long Beach, which fronts Willapa Bay, does not exhibit obvious channel deposits and radiocarbon dates show the sediment to be old (>3000 RCYBP). Thus, most of Longbeach is not interpreted as channel deposits. However, sandy channel deposits were observed at southern Grayland, on the northern edge of the Willapa Bay mouth. These presumed beach plain deposits are otherwise identified as bay mouth deposits with radiocarbon dates of less than 1000 RCYBP. These deposits suggest that the Willapa channel migrated north of its present location within the last 1000 years. There is no evidence for tidal channel migration south into the Longbeach spit at any of the drill sites reported, south of Oysterville, within this same time period.

Cross-sections within the barriers, that are not influenced by lateral tidal inlet channel migrations, are suitable for determination of ravinement surfaces (Table 6).

TABLE 6-CROSS-SECTIONS UNAFFECTED BY TIDAL INLET CHANNEL MIGRATIONS

Cross-section # *	Northing(m), UTM Zone 10
C-1	5099720
C-2	5105550
C-3	5112050
L-1	5133400
L-3	5146150
L-4	5155250
G-1	5177600
G-2	5183000
G-3	5190100
OC-3	5207700
OC-4	5212550
OC-5	5214975
OC-6	5218350
OC-7	5226075
OC-8	5230100
OC-9	5231900

* Cross-sections are numbered according to subcell (from south to north): C = Clatsop, L = Longbeach, G = Grayland and OC = Ocean Shores.

Sediment Volumes

Cell wide variations in ravinement depth and resulting post-ravinement sediment volume reveal long-term sediment dispersal mechanisms for the Columbia River Littoral cell (CRLC). Sediment volume calculations are based on cross-sectional areas at several positions in the CRLC and provide a rough estimate of long term sedimentation rates. Calculated volumes for each subcell are presented in Table 7. For the purposes of this thesis, the sediment has been divided into two units. Dune and beach sand, including the

upper beach face, are represented as the 'beach'. The lower beach face and inner shelf sediments, including the basal lag, are referred to as 'shelf'. The shelf incorporates tidal inlet sequences that lie below the modern barriers as well For comparison purposes, the average cross-sectional area of sediment, per meter alongshore, has been calculated for each subcell and the whole littoral cell (see Appendix F for detailed data). These values are presented in Table 7.

The total volume of sediment accumulated in the CRLC above the ravinement surface is 7.8 x 10^9 m^3. Beach and dune sand comprises 2.4 x 10^9 m^3 of this sediment. Shelf and tidal inlet deposits account for 5.4 x 10^9 m^3.

TABLE 7- VOLUME CALCULATIONS FOR BEACH, SHELF, TOTAL AND NORAMLIZED SEDIMENT VOLUME, FOR THE COLUMBIA RIVER LITTORAL CELL, IN m3.

	Beach	Shelf	Beach + Shelf	m3/meter
Total Vols.	2.40 x 10^9	5.44 x 10^9	7.84 x 10^9	63555
Clatsop	8.22 x 10^8	1.36 x 10^9	2.18 x 10^9	87099
Longbeach	8.99 x 10^8	1.21 x 10^9	2.11 x 10^9	55493
Grayland	2.79 x 10^8	1.49 x 10^9	1.77 x 10^9	90101
Ocean Shores	3.95 x 108	9.93 x 108	1.39 x 109	34129

Note: Sediment volumes are taken from sediment directly below current barriers using the base of the upper beach face as the seaward limit. Beach consists of the facies as defined by GPR. Shelf includes all sediment below the beach to the Ravinement surface surface. Beach + Shelf includes all sediment deposited since the ravinement. The normalized units allow comparison of subcells without taking the length of the cell into account.

The total volume of sediment is greatest in the southernmost subcell, Clatsop, and it decreases to the north. There is no such trend in either of the beach or shelf sediments alone. The average amount of sediment per meter alongshore is highest in Clatsop and

Grayland. This illustrates that the area of sediment accumulation in these two subcells is greater in either depth or width than the other subcells. Longbeach has a moderate cross-sectional area and Ocean Shores has the lowest cross-sectional area. These differences can be explained in part by the proximity of both Clatsop and Grayland to lowstand river valleys that cut wider and deeper valleys than the surrounding landscape thus creating greater accommodation space.

The average depth to ravinement shallows to the north. Average ravinement depths were taken away from tidal inlets to obtain a true representational depth for each subcell. Clatsop has an average ravinement depth of 30 m, Longbeach has 20 m ravinement depth, Grayland has 16 m ravinement depth and Ocean Shores has 5-10 m ravinement depths. These ravinement depths show that Meyers (1994) was correct in his determination that CRLC barrier depths were greater than other places in North America (4-10 m). But, the greater depths reflects more than a larger wave climate. They reflect, what I believe to be, large-scale tectonic uplift that has been occurring in the northern half of the CRLC throughout the Pleistocene (and Holocene ?) time period (Peterson *et al*., 1991) as well as local antecedent river valley topography.

The greater depths to ravinement provide an adequate mechanism for early sediment trapping in the southern subcells. Regardless of whether or not sediment was being supplied to the northern subcells as early as 3000 years ago, there was little accommodation space to allow sediment accumulation.

The earliest Columbia River Littoral cell beaches started to prograde about 4000 years ago (Woxell, 1998), but sediment was accumulating in the existing offshore areas

prior to this time (between 4500-7000 ybp for Longbeach subcell). Back edge dates have decreasing ages from 4000 years ago in Clatsop and Longbeach to 2000 years ago for Grayland and 1500 years ago for Ocean Shores (Woxell, 1998). Tephra deposits in Clatsop and Longbeach have ages between 2000 and 3000 years ago. Both the back edge dates and the tephra depositional dates show that more than 3000 years ago, beach and shelf sediments were accumulating mainly in the Clatsop and Longbeach subcells.

Sediment Volume Comparison

Total beach sediment volumes are very low compared to total shelf sediment volumes. Twichell (personal communication) estimates deposition of approximately 58 x 10^9 m^3 of sediment on the inner-shelf since sea level transgressed over that area (Gelfenbaum *et al*., 1999). At first glance this huge difference in sediment volume makes the beaches look insignificant as a sediment sink in the CRLC. However, it is important to consider that the modern inner shelf has been under water for approximately 10, 000 years whereas the area beneath the modern coastal barriers has been submerged for only 4000-5000 years. Never-the-less, if sediment continues to be transported to the marine side, it is reasonable that there should be greater amounts of sediment, accumulated since ravinement, on the inner shelf than on the beaches. The question that remains is whether sand transport to the shelf has changed throughout the Holocene. Some change had to occur in order for the modern beach plains to prograde, a process that did not happen until the second half of the Holocene, when sea level rise slowed significantly. Was it just the relative slowing of sea level rise that allowed for barrier progradation? Or, was there an influx of sediment that occurred as well? Could there have been a shift from sedimentation on the shelf to

sedimentation on the barriers and in the bays in the last few thousand years?

Bedload sediment yield from the Columbia River has been estimated at 5.87 x 10^6 m^3 /yr by Gates (1994). For the estimated 6000 years of deposition in the Columbia River Littoral cell, this rate would supply 352 x 10^9 m^3 of sediment. The 1.3 x 10^6 m^3/yr needed to supply the 7.8 x 10^9 m^3 total (in and beneath the present barriers) and the 58 x 10^9 m^3 deposited on the inner shelf are easily accounted for with this total bedload estimate.

CONCLUSIONS

Ravinement Surface

The ravinement surface is a recognizable marker for the base of marine sedimentation during the last 7000 years for the subsurface area beneath the modern beach ridge spits and plains of the Columbia River Littoral cell. The surface is distinguishable from beach, shelf and estuarine sediments by larger grain size and oxidation. However, it is necessary to date material in conjunction with continuous coring, in order to distinguish where channels have cut into the section leaving a channel lag that looks similar to the ravinement surface.

Transgressive Patterns

In the case of the Columbia River Littoral cell, the transgressive surface is irregular in both the along-shore and across-shore directions. Though the surface does reflect the traditional oceanward dipping surface, it also incorporates paleo-topography and large scale tectonic warping in the alongshore direction.

Sediment Supply and Dispersal

Sediment supply to the Columbia River Littoral cell, for the last 7000 years has been primarily from the Columbia River. Preservation of sediments occurred in the subcells of Clatsop and Long beach prior to Grayland, and Ocean Shores. The mechanism of sediment partitioning was first filling of accommodation space and second dispersal of sand northward with littoral transport. In total, 2.4 km^3 (2.4×10^9 m^3) of sand has accumulated to make the modern barrier beaches and 5.4 km^3 (5.4×10^9 m^3) of sediment has accumulated beneath the modern barriers as shelf and tidal inlet deposits. The average sedimentation rate for the sediment beneath the present barriers is 1.3×10^6 m^3/yr (over 6000 yrs).

REFERENCES

Addicott, W.O., 1974, Recognition and distribution of *Mytilus condoni* Dall, a unique Pliocene and Pleistocene bivalve from the Pacific coast, Veliger v. 16, p. 354-358.

Bacon, C.R., and Druitt, T.H., 1988, Compositional evolution of the zoned calcalkaline magma chamber of Mount Mazama, Crater Lake, Oregon, Contributions to mineralogy and petrology, v. 98, p. 224-256.

Ballard, R.L., 1964, Distribution of beach sediments near the Columbia River: Department of Oceanography, University of Washington, Technical Report No. 98, 82p.

Bloom, A. L., 1983, Sea level and coastal changes, in Wright, H.E., Jr. (editor), The Holocene, Late Quaternary environments of the United States, v. 2, p. 42-51.

Boggs, S. Jr., 1995, Principles of Sedimentology and Stratigraphy-2nd ed., Prentice Hall, Englewood Cliffs, New Jersey, 774 p.

Borchardt, G.A., Harward, M.E., and Schmitt, R.A., 1970, Correlation of volcanic ash deposits by Activation Analysis of glass separates, Quaternary Research, v.1 p. 247-260.

Bourgeois, J., 1980, A transgressive shelf sequence exhibiting hummocky stratification: the Cape Sebastian Sandstone (Upper Cretaceous), southwestern Oregon: Journal of Sedimentary Petrology, v. 50, p. 681-702.

Clifton, H.E., 1983, Discrimination of subtidal and intertidal facies in Pleistocene deposits, Willapa Bay, Washington, Journal of Sedimentary Petrology, v. 53 p. 353-369.

Clifton, H.E., 1994, Preservation of transgressive and highstand Late Pleistocene valley-fill/estuarine deposits, Willapa Bay, Washington in Dalrymple, R. W. and Boyd, R., eds., Incised-valley systems; origin and sedimentary sequences, Special Publication- SEPM (Society for Sedimentary Geology) No. 51, p. 321-333.

Conyers, L.B., and Goodman, D., 1997, Ground-Penetrating Radar: An Introduction for Archaeologists, Altamira Press, Walnut Creek, California, 232 p.

Cooper, W.S., 1958, Coastal sand dunes of Washington and Oregon: Geological Society of America Memoir No. 72, 169p.

Cross, V., Twichell, D. and Parolski, K., 1999, Archive of Seismic-Reflection Data Collected Aboard RV CORLISS Cruise CRLS98014 in the Columbia River Estuary, Willapa Bay and off Southern Washington Inner Continental Shelf, U.S. Geological Survey Open-File Report 99-307.

Davis, R.A. and Clifton, H.E., 1987, Sea-level change and the preservation potential of wave-dominated and tide-dominated coastal sequences in Nummendal, D., Pilkey, O.H., and Howard, J.D., eds., Sea-Level Fluctuation and Coastal Evolution, Special Publication-SEPM (Society for Sedimentary Geology) No. 41, p. 167-178.

Demarest, J.M.II and Kraft, J.C., 1987, Stratigraphic record of Quaternary sea levels: implications for more ancient strata in Nummendal, D., Pilkey, O.H., and

Howard, J.D., eds., Sea-Level Fluctuation and Coastal Evolution, Special Publication-SEPM (Society for Sedimentary Geology) No. 41, p. 224-239.
Doyle, D.L., 1996, Beach response to subsidence following a Cascadia Subduction Zone Earthquake along the Washington-Oregon Coast: M.S. Thesis, Geology Department, Portland State University, Portland, Oregon, 113p.
Dupre, W.R., 1984, Reconstruction of paleo-wave conditions from Pleistocene marine terrace deposits, Monterey Bay, California, in Greenwood, B., and Davis, R.A., eds., Hydrodynamics and Sedimentation in Wave-Dominated Coastal Environments: Developments in Sedimentology, v. 39, Elsevier Publishing Co., New York, p. 435-454.
Frank, F.J., 1970, Groundwater resources of the Clatsop Plains sand-dune area, Clatsop County, Oregon, USGS Water Supply Paper 1899-A.
Gates, E.B., 1994, The Holocene sedimentary framework of the lower Columbia River basin, M.S. Thesis, Geology Department, Portland State University, Portland, Oregon, 210p.
Gelfenbaum, G., Kaminsky, G., Sherwood, C., and Peterson, C., 1997, Southwest Washington coastal erosion workshop report: U.S. Department of the Interior, U.S. Geological Survey, Open File Report 97-471, 101p.
Gelfenbaum, G., Sherwood, C.R., Peterson, C.D., Kaminsky, G.M., Buijsman, M., Twichell, D.C., Ruggiero. P., Gibbs, A.E., Reed, C., 1999, The Columbia River Littoral Cell: A sediment budget overview in Kraus, N.C., and McDougal, W.G., eds., Coastal Sediments '99 v. 2, p. 1660-1675.
Howell, D.G., Veddeer, J.D., McLean, J., Joyce, J.M., Clarke, S.H., Jr., and Smith, G., 1977, Review of Cretaceous geology, Salinian and Nacimiento blocks, Coast Ranges of central California: Pacific Coast Paleogeography Field Guide No. 2, Pacific Section, Society of Economic Paleontologists and Mineralogists, p. 1-46.
Johnson, R., R., 1992, Elementary Statistics-6th ed., Duxbury Press, Belmont, California, 730 p.
Jol, H., M., Peterson, C.D., Vanderburgh, S., and Phipps, J., 1998, GPR as a regional geomorphic mapping tool: shoreline accretion/erosion along the Columbia River littoral cell, Seventh International Conference on Ground-Penetrating Radar, Lawrence, Kansas, USA, v. 1, p. 257-262.
Jol, H.M., Smith, D.G., and Meyers, R.A., 1996, Digital Ground Penetrating Radar (GPR): A new geophysical tool for coastal barrier research (examples from the Atlantic, Gulf and Pacific coasts, USA), Journal of Coastal Research, v. 12, n. 4, p. 960-968.
Kaminsky, G.M., Ruggiero, P., Gelfenbaum, G., and Peterson, C.D., 1997, Long term coastal evolution and regional dynamics of a US Pacific Northwest Littoral cell: Washington Department of Ecology, 10p.
Komar, P.D., Lizarraga-Arciniega, R.D., and Terich, T.A., 1976, Oregon coast changes due to jetties, Journal of Waterways, Harbors and Coast Engineering Div., American Society of Civil Engineers, v. 102: WW1, p. 13-30.
Kvenvolden, K., A., Blunt, D.J. and Clifton H.E., 1979, Amino acid racemization of Quaternary shell deposits at Willapa Bay, Washington, Geochimica Acta, v. 43,

1505-1520.
Li, M.Z., 1991, Longshore grain sorting and beach-placer formation adjacent to the Columbia River, Ph. D. Dissertation, Oceanography, Oregon State University, 232p.
Li, M.Z., and Komar, P.D., 1992, Longshore grain sorting and beach placer formation adjacent to the Columbia River, Journal of Sedimentary Petrology, v. 62 (3) p. 429-441.
Luepke, G., 1982, Heavy-mineral data from samples collected in Willapa Bay and vicinity, Washington, U.S. Geological Survey Open-File Report, OF 82-0739, p. 23, 1982.
Meyers, R.A., 1994, The Willapa Barrier Spit of S.W. Washington State: Depositional processes inferred from ground penetrating radar, M.S. Thesis, Department of Geography, The University of Calgary, Calgary Alberta, 191p.
Mitchum, R.M., Jr., Vail, P.R., and Sangree, J.B., 1977, Seismic stratigraphy and global change of sea level. Part 6: Stratigraphic interpretation of seismic reflection patterns in depositional sequences, in C.E., Payton, ed., Seismic Stratigraphy-Applications to hydrocarbon exploration: American Association of Petroleum Geologists Memoir 26, p. 135-143.
Nittrouer, C.A., 1978, The process of detrital sediment accumulation in a continental shelf environment: an examination of the Washington shelf, Ph. D. Dissertation, University of Washington, Seattle, Washington.
Nittrouer, C.A., Sternberg, R.W., Carpenter, R. and Bennett, J.T., 1979, The use of Pb-210 geochronology as a sedimentological tool: Application to the Washington continental shelf: Marine Geology, v. 31, p. 297-316.
Nummendal, D., and Swift, D.J.P., 1987, Transgressive stratigraphy at seqence-bounding unconformities: some principles derived from Holocene and Cretaceous examples in Nummendal, D., Pilkey, O.H., and Howard, J.D., eds., Sea-level Fluctuation and Coastal Evolution: Society of Economic Paleontologists and Mineralogists Special Publication No. 41, p. 241-260.
Peterson, Curt D., Darienzo, Mark E., Pettit, Don J., Jackson, Philip L., Rosenfeld, Charles L., 1991, *Littoral-cell development in the convergent Cascadia Margin of the Pacific Northwest, USA*Osborne, Robert H., *From shoreline to abyss; contributions in marine geology in honor of Francis Parker Shepard*, Special Publication - Society of Economic Paleontologists and Mineralogists, 46, p. 17-34.
Peterson, C.D., Gelfenbaum, G.R., Jol, H.R., Phipps, J.B., Reckendorf, F., Twichell, D.C., Vanderburg, S. and Woxell, L., 1999, Great earthquakes, abundant sand, and high wave energy in the Columbia Cell, USA, Coastal Sediments '99, v. 2, p.1676-1691.
Peterson, C.D., and Phipps, J.B., 1992, Holocene sedimentary framework of Grays Harbor Basin, Washington, USA in Fletcher, C.H. III and Wehmiller, J.F., eds Quaternary Coasts of the United States: Marine and Lacustrine Systems, SEPM (Society for Sedimentary Geology) Special Publication No. 48, p. 273-285.
Phipps, J.B., and Smith, J.M., 1978, Coastal accretion and erosion in southwest

Washington: Washington Department of Ecology, Report #78-12, 75p.
Phipps, J.B., 1990, Coastal accretion and erosion in Washington state 1977-1987 in Shorelands and Coastal Zone Management Program Report, Washington Department of Ecology, 33p.
Posamentier, H.W., Jervey, M.T., and Vail, P.R., 1988, Eustatic controls on clastic deposition 1-Conceptaul framework, in C.K. Wilgus, B.S. Hastings, D.G. St. C. Kendall, H.W. Posamentier, C.A. Ross, and J.C. Van Wagoner, eds., Sea-Level changes: An integrated approach: Society for Economic Paleontologists and Mineralogists Special Publication 42, p. 109-124.
Qualman, D. and Peterson, C.D., 1999, Vibracore study of surf-zone facies and response to 1997-98 El Nino, Columbia River Littoral Cell, NW Oregon- SW Washington, USA, EOS Transactions of the American Geophysical Union, v. 79, no. 45, Fall 1998, p. 451.
Rankin, D.C., 1983, Holocene geologic history of the Clatsop Plains foredune ridge complex, M.S. Thesis, Geology Department, Portland State University, Portland, Oregon, 189p.
Randle, K., Goles, G.G., and Kittleman, L.R., 1971, Geochemical and petrological characterization of ash samples from Cascade Range volcanoes: Quaternary Research, v. 1, p. 261-282.
Sarna-Wojcicki, A.M., Champion, D.E., and Davis, J.O., 1983, Holocene volcanism in the conterminous United States and the role of silicic volcanic ash layers in correlation of latest Pleistocene and Holocene deposits in Wright, H.E., Jr., ed., Late Quaternary environments of the United States, v. 2, the Holocene: Minneapolis, University of Minnesota Press, p. 52-77.
Scheidegger, K.F., Kulm, L.D., and Runge, E.J., 1971, Sediment sources and dispersal patterns of Oregon continental shelf sands, Journal of Sedimentary Petrology, v. 41, 112-1120.
Scheidegger, K.F., and Phipps, J.B., 1976, Dispersal patterns of sands in Grays Harbor Estuary, Washington: Journal of Sedimentary Petrology, v. 46, no. 1, p. 163-166.
Schlicker, H.G., Deacon, R.J., Beaulieu, J.D., and Olcott, G.W., 1972, Environmental Geology of the Coastal Region of Tillamook and Clatsop Counties, Oregon, Oregon Department of Geology and Mineral Industries Bulletin 74, 164p.
Smith, D.G., Meyers, R.A., and Jol, H.M., 1999, Sedimentology of an upper-mesotidal (3.7m) Holocene barrier, Willapa Bay, SW Washington, U.S.A., Journal of Sedimentary Research, v. 69, no. 6, p. 1290-1296.
Stamp, L.D., 1922, An outline of the Tertiary geology of Burma: Geology Magazine v. 59, p. 481-501.
Sternberg, R.W., 1986, Transport and accumulation of river-derived sediment on the Washington continental shelf, USA: Journal of the Geological Society, London, v. 143, p. 945-956.
Swift, D.J.P., 1968, Coastal erosion and transgressive stratigraphy: Journal of Geology, v. 76, p. 444-456.
Terich, T.A., and Schwartz, M.L., 1991, A geomorphic classification of Washington State's Pacific Coast: Shore and Beach, v. 49, no. 3, p. 21-27.

Twichell, D., 1997, Offshore geological investigations, in Kaminsky, G., ed. 1997 Abstracts of Work in Progress, Southwest Washington Coastal Erosion Study, Washington Department of Ecology, p. 28-29.

Van Wagoner, J.C., Posamentier, H.W., Mitchum, R.M., Vail, P.R., Sarg, J.F., Loutit, T.S., and Hardenbol, J., 1988, An overview of the fundamentals of sequence stratigraphy and key definitions, in C.K. Wilgus, B.S. Hastings, D.G. St. C. Kendall, H.W. Posamentier, C.A. Ross, and J.C. Van Wagoner, eds., Sea-Level changes: An integrated approach SEPM (Society for Sedimentary Geology) Special Publication 42, p. 39-45.

Van Wagoner, J.C., Mitchum, R.M., Campion, K.M., and Rahmanian, V.D., 1990, Siliciclastic sequence stratigraphy in well logs, cores and outcrops; concepts for high-resolution correlation of time and facies, American Association of Petroleum Geologists, Methods in Exploration Series No. 7, Tulsa, Oklahoma, 55 p.

Whetten, J.T., Kelley, J.C., and Hanson, L.G., 1969, Characteristics of Columbia River sediment and sediment transport: Journal of Sedimentary Petrology, V. 39, p. 1149-1166.

White, S.M., 1970, Mineralogy and geochemistry of continental shelf sediments off the Washington-Oregon coast: Journal of Sedimentary Petrology, v. 40, no. 1, p. 38-54.

Woxell, L.K., 1998, Prehistoric beach accretion rates and long-term response to sediment depletion in the Columbia River littoral system, USA, M.S. Thesis, Geology Department, Portland State University, Portland, Oregon, USA, 199 p.

APPENDIX A

* Note: all grain size values are reported in mm.

MEAN GRAIN SIZE VALUES FOR LAGOON-BAY DEPOSITS

Lagoon: means	sample depth (in)	mean	st dev	skewness	kurtosis
Goul	550	0.166	0.169	19.039	520.774
67th	435	0.044	0.044	5.284	45.160
Estuarine					
Klip	720	0.148	0.167	3.157	17.925
Oyhut-2	126	0.189	0.315	6.605	84.921
Oyhut-2	168	0.063	0.118	5.466	38.029
Pcyd	560	0.124	0.136	1.586	4.716
Pcyd	580	0.177	0.075	0.432	14.576
Mchu	390	0.064	0.258	17.064	321.963
Mchu	465	0.287	1.071	4.161	18.367
	mean	0.140	0.262	6.977	118.492
	st dev	0.078	0.347	5.526	113.597
	var	0.006	0.121	30.539	12904.301

MODE VALUES FOR MOST COMMON GRAIN SIZE AND WEIGHT PERCENT FOR LAGOON-BAY DEPOSITS

Lagoon: modes	1	wt %	2	wt %	3	wt %
Goul	0.163	26.39	0.0315	15.15		
67th	0.0315	88.68				
Estuarine						
Klip	0.0315	43.47	0.163	15.57		
Oyhut-2	0.0315	54.88	0.274	6.79		
Oyhut-2	0.0315	87.32				
Pcyd	0.0315	51.47	0.163	5.34	0.23	3.89
Pcyd	0.194	27.29	0.0315	11.86		
Mchu	0.0315	90.06				
Mchu	0.0315	87.7				
mean	0.064	61.918	0.133	10.942		
st dev	0.061	25.130	0.099	4.707		
var	0.004	631.516	0.010	22.152		

MEAN GRAIN SIZE FOR BEACH SAMPLES

	sample depth (in)	mean	st dev	skewness	kurtosis
copr-1	75	0.168	0.054	-0.881	4.648
copr-2	30	0.168	0.061	-0.150	5.212
oyhut-1	106	0.166	0.038	-1.009	7.490
oyhut-2	78	0.296	0.586	6.002	46.149
ncov	50	0.160	0.051	-0.573	6.816
goul	100	0.167	0.056	-0.981	3.975
smit	100	0.106	0.079	1.174	11.050
grbe	150	0.154	0.056	-1.096	3.446
67th	100	0.148	0.217	-0.025	0.003
oyst	150	0.167	0.077	-0.624	2.302
klip	150	0.169	0.062	-1.042	3.422
pcyd	100	0.188	0.058	-0.941	4.146
mchu	100	0.163	0.069	0.148	19.219
bayr	100	0.171	0.068	-0.979	3.050
glen	100	0.159	0.062	-0.572	4.095
sunb	150	0.187	0.081	-0.691	2.528
delr	100	0.204	0.085	-0.172	3.755
delm	100	0.181	0.061	-0.223	8.477
	mean	0.173	0.101	-0.146	7.766
	st dev	0.037	0.127	1.637	10.480
	var	0.001	0.016	2.680	109.841

MODE AND WEIGHT PERCENT FOR BEACH SAMPLES

	1	wt %	2	wt %	3	wt %
copr-1	0.194	33.17	0.0315	7.54		
copr-2	0.163	29.04	0.0315	8.43		
oyhut-1	0.163	41.81				
oyhut-2	0.0315	32.17	0.163	9.27	0.274	7.93
ncov		35.08	0.0315	7.82		
goul	0.194	35.03	0.0315	8.83		
smit	0.0315	41.73	0.163	10.34		
grbe	0.194	33.92	0.0315	12.24		
67th	0.194	34.53	0.0315	15.85		
oyst	0.194	26.59	0.0315	17.21		
klip	0.194	34.65	0.0315	11.36		
pcyd	0.194	36.05				
mchu	0.194	36.74	0.0315	14.17		
bayr	0.194	35.9	0.0315	13.47		
glen	0.194	28.81	0.0315	11.9		
sunb	0.274	22.82	0.0315	13.08		
delr	0.274	23.39	0.0315	9.29		
delm	0.23	30.84	0.0315	7.12		
mean	0.183	32.904	0.048	11.120		
st dev	0.065	5.288	0.045	3.051		
var	0.004	27.966	0.002	9.308		

MEAN GRAIN SIZE FOR SHELF SAMPLES

	sample depth (in)	mean	st dev	skewness	kurtosis
copr-1	262	0.865	1.701	2.009	5.060
copr-2	250	0.297	0.658	6.631	46.997
oyhut-1	394	0.278	0.597	7.028	0.000
oyhut-2	117	0.325	0.340	9.957	134.048
ncov	396	0.192	0.037	1.005	16.443
goul	400	0.178	0.258	17.711	330.014
smit	250	0.115	0.111	1.471	5.480
grbe	450	0.140	0.099	22.409	1085.743
67th	300	0.160	0.048	-1.166	5.047
oyst	700	0.171	0.066	-0.222	6.208
klip	650	0.119	0.076	0.251	2.938
pcyd	500	0.177	0.075	-0.433	3.295
mchu	325	0.155	0.069	-0.702	2.451
bayr	575	0.171	0.069	-0.715	3.291
glen	500	0.168	0.075	-0.426	2.907
sunb	800	0.177	0.058	-0.547	5.376
delr	486	1.345	3.152	2.374	6.659
delm	400	0.169	0.085	0.492	6.998
	mean	0.289	0.421	3.729	92.720
	st dev	0.313	0.793	6.749	260.513
	var	0.098	0.628	45.544	67866.934

MODE AND WEIGHT PERCENT FOR SHELF SAMPLES

	1	wt %	2	wt %	3	wt %
copr-1	0.163	31.02	5	14.42	0.0315	8.24
copr-2	0.194	35.51	5	1.8		
oyhut-1	0.163	39.11				
oyhut-2	0.274	20.31	0.383	14.63	0.0315	8.5
ncov	0.194	45.08				
goul	0.163	38.9				
smit	0.0315	53.46	0.163	9.05		
grbe	0.163	25.51	0.0315	21.33		
67th	0.163	38.37	0.0315	7.26		
oyst	0.194	33.28	0.0315	10.78		
klip	0.0315	36.56	0.194	24.61		
pcyd	0.194	27.31	0.0315	12.46		
mchu	0.194	33.94	0.0315	17.95		
bayr	0.194	32.8	0.0315	13.08		
glen	0.194	26.11	0.0315	15.31		
sunb	0.194	34.41	0.0315	7.06		
delr	0.194	22.46	10	11.68		
delm	0.194	22.03	0.0315	16.01		
mean	0.172	33.121	1.402	13.162	0.032	8.370
st dev	0.057	8.470	2.937	5.755	0.000	0.184
var	0.003	71.739	8.625	33.114	0.000	0.034

MEAN GRAIN SIZE FOR RAVINEMENT SAMPLES

means	sample depth (in)	mean	st dev	skewness	kurtosis
copr-1	282	1.157	1.894	1.510	3.330
copr-2	296	6.084	5.872	0.012	1.005
oyhut-1	498	2.848	2.361	-0.205	8.322E-09
Goul	460	7.603	7.253	0.033	1.012
smit	310	0.634	2.100	4.152	18.581
grbe	515	0.190	0.081	5.229	86.048
67th	395	0.526	1.190	3.376	12.769
oyst	852	1.970	0.066	-0.023	4.395
klip	706	0.179	0.068	-0.577	3.837
pcyd	550	0.191	0.067	0.727	26.803
delm	438-439	0.212	0.066	-0.501	7.480
	mean	1.963	1.911	1.248	15.024
	st dev	2.580	2.489	2.056	25.002
	var	6.659	6.194	4.226	625.119

MODE AND WEIGHT PERCENT FOR RAVINEMENT SAMPLES

ravienment	1	wt %	2	wt %	3	wt %
copr-1	0.194	22.43	5	19.43		
copr-2	12	49.6	0.163	15.32		
oyhut-1	5	54.32	0.163	20.16		
Goul	15	48.94	0.0315	8.92	0.163	7.24
smit	0.0315	52.78	0.163	8.3	10	4.69
grbe	0.194	31.84				
67th	0.194	19.23	0.0315	14.81	5	6.38
oyst	0.194	25.7				
klip	0.194	31.13	0.0315	10.05		
pcyd	0.194	30	0.0315	6.86		
delm	0.274	27.79				
mean	3.043	35.796	0.702	12.981	5.054	6.103
st dev	5.408	12.981	1.738	5.160	4.919	1.297
var	29.246	168.503	3.020	26.629	24.194	1.683

Grain Size Analysis: 1 of 5

Hole name	Sample Depth inches	Gravel wt %	Sand wt %	Mud wt %
Dh1-ROOS-072198	47	0.00	95.19	4.81
	47-55	0.10	75.64	24.26
	55-63	0.00	62.06	37.94
Dh2-ROOS-072198	19.7	0.00	95.64	4.36
	60	79.38	19.12	1.50
	69	2.02	84.98	12.99
	98	1.11	65.89	33.00
Dh3-ROOS-072198	64	31.30	66.17	2.53
	78	57.99	39.85	2.16
	108	71.43	27.17	1.40
Dh1-MOCL-072298	20	0.00	85.26	14.74
	33	1.25	93.91	6.09
	50	25.53	72.26	2.21
	90	10.35	87.68	1.97
	150	3.50	85.44	11.06
Dh1-HIGH-072298	84	48.45	48.66	2.89
	148	24.18	45.24	3.07
	180	43.32	54.45	2.23
	185	50.53	92.65	4.23
Dh2-HIGH-072298	13	0.09	92.65	7.26
	24	0.00	90.96	9.04
	37	0.00	94.59	5.41
	72	36.60	53.33	10.06
	78	22.65	72.41	4.94
Dh1-COPR-072398	25	0.08	88.84	11.08
	50	0.01	91.61	8.39
	75	0.00	92.46	7.54
	100	0.00	94.59	5.41
	168	10.99	85.37	3.64
	193	0.63	96.41	2.95
	210	0.00	96.65	3.35
	220	3.06	80.98	15.97
	262	14.42	77.35	8.24
	282-285	19.32	77.47	3.19
	315	19.80	68.46	11.74
Dh2-COPR-072398	25	0.00	93.79	6.21
	30	0.00	91.57	8.43
	50	0.00	68.08	31.92
	75	0.54	94.23	5.22
	110	0.00	93.79	6.21
	150	0.78	94.57	4.65
	215	1.37	93.21	6.42
	220	7.61	84.84	7.55
	250	1.80	94.6	3.61
	260	13.29	83.71	3.00
	296	49.60	49.11	1.29
	298	3.78	91.44	4.79
	328	1.72	95.08	3.20
Dh1-OYHUT-072498	50	0.00	97.19	2.81
	106	0.00	96.77	3.23
	156	0.00	97.4	2.60
	209	0.20	96.11	3.70
	229	4.66	91.96	3.38
	252	10.01	84.9	5.09
	262	0.54	94.14	5.31
	264	1.17	95.24	3.59
	300	0.03	97.47	2.50
	368	3.50	96	0.50
	394	1.39	93.87	4.73
	436	29.88	67.51	2.62
	474	44.26	54.13	1.61
	474-480	40.62	57.48	1.90
	480-486	49.81	48.61	1.58
	486-492	46.01	52.18	1.81
	492-498	49.39	48.9	1.72

Grain Size Analysis: 2 of 5

Hole name	Sample Depth inches	Gravel wt %	Sand wt %	Mud wt %
	498-504	54.32	44.58	1.10
	504-510	5.99	91.25	2.76
	510-516	18.68	79.77	1.56
	516-522	40.92	55.9	3.18
	522-534	48.92	43.65	7.44
Dh2-OYHUT-072498	66-69	32.19	60.98	6.84
	78	1.09	66.75	32.17
	108	0.24	82.39	17.36
	117	0.37	91.13	8.50
	126	0.15	44.97	54.88
	160	0.00	97.22	2.78
	168	0.00	12.68	87.32
	180	60.98	14.74	24.28
	192	67.34	29.6	3.06
	220	7.61	84.84	7.55
	250	4.08	92.28	9.73
	260	12.63	84.64	8.34
	288	49.03	46.5	4.47
	296	49.60	49.11	1.29
	298	3.78	91.44	4.79
	474	40.62	57.48	1.90
Dh1-NCOV-072698	50	0.00	92.18	7.82
	100	0.00	99.32	0.68
	150	0.00	98.72	1.28
	200	0.00	97.26	2.74
	250	1.16	94.03	4.81
	300	0.16	94.96	4.88
	350	0.17	97.07	2.76
	396	0.00	99.54	0.46
	432	0.73	74.38	24.89
Dh1-GOUL-072798	14-16	11.17	68.74	20.08
	50	0.72	96.84	2.45
	100	0.00	91.17	8.83
	150	0.05	93.78	6.17
	200	0.11	95.12	4.76
	250	0.00	97.31	2.69
	300	0.23	96.9	2.86
	350	0.24	97.78	1.98
	400	0.27	95.35	4.38
	450	0.35	86.73	12.92
	460	48.94	42.14	8.92
	470	5.71	90.32	3.97
	500	0.00	86.46	13.54
	550	0.08	84.78	15.15
	558	20.59	64.25	15.15
	592-594	1.11	85.26	13.63
Dh1-SMIT-072798	50	8.03	88.59	2.59
	100	0.00	58.27	41.73
	150	0.00	34.97	65.03
	200	0.00	33.44	66.56
	250	0.00	46.54	53.46
	300	0.00	95.93	4.07
	310-334	4.69	42.52	52.78
	350	3.12	85.92	10.93
Dh1-GRBE-072898	50	0.86	92.82	7.18
	100	0.00	91.66	8.34
	150	0.00	87.76	12.24
	182	2.98	95.39	1.63
	200	0.00	88.5	11.50
	250	0.00	93.33	6.67
	300	0.00	97.88	2.12
	350	0.11	85.83	14.06
	400	0.03	89.75	10.21

Grain Size Analysis: 3 of 5

Hole name	Sample Depth inches	Gravel wt %	Sand wt %	Mud wt %
	450	0.02	78.65	21.33
	515-517	0.00	95.38	4.62
	585	3.04	82.38	14.18
Dh1-67th-073098	0	0.00	94.03	5.97
	50	0.00	90.56	9.44
	100	0.00	84.15	15.85
	150	0.00	79.52	20.48
	200	0.00	87.18	12.82
	250	0.00	93.7	6.30
	300	0.00	92.74	7.26
	350	24.33	64.23	11.44
	375	0.00	83.42	16.58
	395-397	6.38	78.8	14.81
	400	0.08	30.82	69.10
	435	0.00	11.32	88.68
	470	0.00	60.58	39.42
	500	0.00	98.06	12.94
	550	0.12	70.93	28.95
	570	0.00	71.29	28.71
	576-581	15.54	49.28	35.18
	581-583	10.31	60.13	29.56
	590-594	22.42	52.13	25.45
Dh1-OYST-080198	100	0.00	94.73	5.27
	150	0.00	82.79	17.21
	200	0.00	85.55	14.45
	250	0.00	94.85	5.15
	300	0.00	95.39	4.61
	350	0.00	88.8	11.20
	400	0.00	86.72	13.28
	426-430	0.20	92.14	7.67
	450	0.11	82.5	17.39
	457-461	0.33	91.61	8.06
	500	0.02	90.43	9.57
	550	0.52	89.01	10.47
	600	0.06	97.49	2.45
	615	4.87	85.76	9.37
	630-633	3.37	82.27	14.36
	650	0.05	81.05	18.90
	700	0.00	89.22	10.78
	852-864	0.00	95.77	4.23
	864	6.81	89.9	3.28
Dh1-KLIP-080298	24	0.05	92.44	7.51
	50	0.00	74.93	25.07
	100	0.00	91.44	8.56
	150	0.00	88.64	11.36
	200	0.00	82.58	17.42
	250	0.00	81.52	18.48
	300	0.00	93.23	6.77
	350	0.00	81.97	18.03
	400	0.00	92.86	7.14
	450	0.00	94.74	5.26
	484	0.02	92.2	7.78
	500	0.00	86.39	13.61
	550	0.00	83.84	16.16
	600	0.00	84.5	15.50
	650	0.00	63.44	36.56
	680	0.00	89.7	10.30
	700	0.00	86.79	13.21
	706-712	0.00	89.95	10.05
	720	0.00	56.53	43.47
Dh1-PCYD-080398	50	14.45	78.67	6.88
	100	0.00	94.11	5.89
	150	0.00	91.41	8.59
	166-169	0.00	82.77	17.23
	200	0.00	86.1	13.90
	250	0.00	90.37	9.63
	300	0.00	93.37	6.07

Grain Size Analysis: 4 of 5

Hole name	Sample Depth inches	Gravel wt %	Sand wt %	Mud wt %
	350	0.00	91.9	8.10
	375	0.00	80.76	19.24
	400	0.00	89.36	10.64
	450	0.00	82.38	17.62
	500	0.00	87.54	12.46
	550	0.00	93.14	6.86
	559	0.00	74.37	25.63
	560	0.00	0	100.00
	580	0.00	88.14	11.86
	600	0.00	90.24	9.76
	650	0.00	62.87	37.13
	700	0.02	85.78	14.20
Dh1-MCHU-073198	25	0.00	90.14	9.51
	42	0.08	93.98	5.94
	50	0.01	91.03	8.96
	75	0.00	85.65	14.34
	100	0.00	85.83	14.17
	125	0.00	94.57	5.43
	150	0.00	88.91	11.09
	200	0.04	87.73	12.23
	225	0.00	82.54	17.46
	250	0.04	85.1	14.85
	275	0.04	88.3	11.67
	300	0.00	96.06	3.94
	325	0.00	82.05	17.95
	375	0.00	6.82	93.18
	394	0.02	9.7	90.06
	410	0.00	17.15	82.85
	416	3.59	72.65	23.76
	425	0.00	29.19	70.81
	450	0.26	13.62	86.12
	465	4.90	7.41	87.70
	500	0.31	24.07	75.61
	514	8.16	65.66	26.91
	550	0.00	93.29	6.71
	575	0.02	104.36	-4.31
Dh1-BAYR-073198	50	0.00	90.67	9.33
	75	0.00	90.22	9.78
	100	0.00	86.53	13.47
	125	0.00	82.17	17.83
	150	0.00	79.56	20.44
	175	0.00	96.59	3.41
	200	0.00	89.33	10.67
	250	0.00	80.64	19.36
	275	0.00	90.75	9.25
	325	0.40	76.56	23.04
	350	0.00	84.02	15.98
	400	0.00	79.44	20.56
	425	0.00	80.1	19.90
	450	0.00	83.43	16.57
	500	0.00	86.16	13.84
	525	0.00	83.41	16.59
	550	0.00	92.48	7.52
	575	0.00	86.92	13.08
Dh1-GLEN-080498	50	0.00	95.63	4.37
	100	0.00	88.1	11.90
	150	0.00	87.04	12.96
	200	0.00	87.68	12.32
	250	0.00	90.51	9.49
	300	0.00	94.23	5.77
	326	20.15	68.58	11.26
	350	0.00	85.88	14.12
	400	0.00	85.56	14.44
	450	0.00	83.06	16.94
	500	0.00	84.69	15.31

Grain Size Analysis: 5 of 5

Hole name	Sample Depth inches	Gravel wt %	Sand wt %	Mud wt %
Dh1-SUNB-080498	50	0.00	90.86	9.14
	100	6.99	78.04	14.97
	150	0.00	86.12	13.38
	200	0.00	88.53	14.47
	250	0.00	89.11	10.89
	300	0.00	95.68	4.32
	315	7.92	82.81	9.27
	354	2.80	78.32	18.87
	400	0.00	87.17	12.83
	431-439	0.07	95.5	4.43
	446-451	4.06	86.33	9.60
	500	0.00	88.78	11.27
	519-522	0.65	83.87	15.48
	550	0.16	85.53	14.31
	580	5.30	79.73	14.97
	600	0.00	84.53	15.47
	650	0.00	81.56	18.44
	660-670	0.00	98.85	1.15
	690	0.06	87.66	12.28
	700	0.00	84.67	15.33
	750	0.00	85.25	14.75
	765	0.00	78.9	21.10
	780	0.00	92.24	7.76
	800	0.00	92.94	7.06
Dh1-DELR-080598	0-5	0.00	96.06	3.94
	78	9.02	80.25	10.73
	100	0.00	90.71	9.29
	108	0.00	85.9	14.10
	150	0.66	90.87	8.47
	200	0.63	92.03	7.34
	300	0.00	95.55	4.45
	350	0.00	86.21	13.79
	366	0.20	95.14	4.66
	400	0.00	86.6	13.40
	414-420	0.00	20.63	79.37
	450	0.64	87.89	11.48
	486	11.68	81.57	6.75
	500	0.00	88.69	11.31
	514	0.00	92.08	7.92
Dh1-DELM-080598	50	19.32	76.26	4.51
	100	0.00	92.88	7.12
	150	0.00	85.71	14.29
	200	0.00	82.81	17.19
	250	0.00	83.77	16.23
	300	0.00	91.12	8.88
	350	0.00	90.16	9.84
	400	0.00	83.99	16.01
	438-439	0.00	96.17	3.83
	450	0.00	86.59	13.41
mean wt %		**5.73**	**80.15**	**14.27**
st. dev.		**14.04**	**20.13**	**17.26**

GRAIN SIZE EQUATIONS

Mean $\bar{x} = \frac{\sum fm}{n}$

Standard deviation $\sigma = \sqrt{\frac{\sum f(m-\bar{x})^2}{100}}$

Skewness $Sk = \frac{\sum f(m-\bar{x})^3}{100\sigma^3}$

Kurtosis $K = \frac{\sum f(m-\bar{x})^4}{100\sigma^4}$

F = weight percent
M = midpoint of each grain size grade
N = total number in sample

Moment Statistics from Boggs, 1995

APPENDIX B

Table B-1. Radiocarbon dates, locations and depths to samples for CRLC, 1998.

Sample #	Depth, in	Easting	Northing	Type of sample	Dating technique	Surface Type	Measured C14	Conventional C14	C13/C12 ratio o/oo	beta #
Mocl1	50	407985.5	5231817	shell	Ams	R	114.1 +/- 0.5%	108.4 +/- 0.5%	-0.1	129512
Copr1	285	410602.9	5218502	shell	Ams	R	1300 +/- 40	1730 +/- 40	+1.5	129521
Oyhut2	108	412554.8	5207678	wood	Bulk	P	10 +/- 60	20 +/- 60	-24.4	129526
Oyhut1	336	411446.1	5207679	shell	Ams	S	520 +/- 40	930 +/- 40	0.0	129513
Oyhut1	436	411446.1	5207679	shell	Ams	<R	860 +/- 40	1290 +/- 40	1.0	129520
Grbe	310	416168.4	5184604	shell	Ams	S	1120 +/- 40	1550 +/- 40	0.0	129516
Grbe	418	416168.4	5184604	shell	Ams	S	1040 +/- 40	1460 +/- 40	+0.9	129511
Grbe	518	416168.4	5184604	peat	Bulk	R	3940 +/- 70	3920 +/- 70	-26.6	129531
Goul	470	417956.3	5178448	wood	Ams	>R	7420 +/- 60	7400 +/- 60	-26.5	129524
Ncov	384	416337.2	5177600	shell	Ams	S	460 +/- 40	870 +/- 40	+1.0	129515
Oyst	864	5155330	418900	wood	Ams	R	7530 +/- 60	7520 +/- 60	-25.7	129514
Klip	706	5146050	420100	peat	Bulk	R	4700 +/- 70	4710 +/- 70	-24.8	129519
Mchu	416	5136900	421850	wood	Bulk	E	5240 +/- 60	5240 +/- 60	-25.4	129525
Mchu	514	5136900	421850	wood	Ams	F	39,350 +/- 530	39,300 +/- 530	28.2	129518
67th	397	520794.7	5133592	wood	Ams	R	4660 +/- 50	4630 +/- 50	-27.0	129523
Pcyd	457	419212.2	5133841	wood	Ams	S	2730 +/-50	3170 +/- 50	+1.6	129517
Pcyd	559	419212.2	5133841	peat	Bulk	R	3820 +/- 80	3780 +/- 80	-27.4	129530
Pcyd	600	419212.2	5133841	shell	Ams	>R	7080 +/- 110	7060 +/- 110	-26.4	131122
Sunb	431	427241.9	5105427	wood	Bulk	S	2530 +/- 60	2520 +/- 60	-25.5	129529
Sunb	660	427241.9	5105427	peat	Bulk	S	3750 +/- 80	3740 +/- 80	-25.7	129527
Sunb	827	427241.9	5105427	wood	Ams	S	3870 +/- 50	3840 +/- 50	-26.8	129522
Delm	438	529936.7	5101122	peat	Bulk	<R	4280 +/- 80	4260 +/- 80	-25.9	129532
Delr	514	427972.7	5099877	shell	Ams	S	1730 +/- 40	2160 +/- 40	+1.1	129509

<R Just above Ravienment
R At Ravienment
>R Just below Ravienment

E Estuarine
F Flooding Surface
S Shelf deposits

APPENDIX C

Tephra from Columbia River Littoral cell

Hole name	Depth, m	Easting	Northing
Dh1-Bayr-073198	8.92	420762	5149177
Dh1-Klip-080298	12.24	420100	5146050
Dh1-Pcyd-080398	11.06 13.23	419212	5133592
Dh1-Sunb-080498	8.89 10.41	427242	5105427
Dh1-Delr-080598	7.87 9.25	427973	5099877

INAA Run #1: Chemistry

Sample #	Nuclide(ppm)	Error										
	Na-24		Sc-46		La-140		Sm-153		Eu-152		Pa-233	
08P1	3.34	0.09	5.74	1.26	112.22	14.17	4.18	0.15	17.00	4.11	6.11	2.53
02P2	3.57	0.09	8.42	0.85	35.81	8.44	5.74	0.19	10.92*	0.00	9.51	2.89
07D1	3.83	0.09	7.50	1.15	28.43	4.11	6.15	0.14	5.23*	0.00	5.07	1.30
11D2	4.28	0.10	8.14	0.44	24.94	3.73	6.21	0.14	5.79*	0.00	8.36	1.32
05B1	3.27	0.08	7.49	0.45	8.83	0.00	4.88	0.12	4.74*	0.00	7.54	1.31
06K1	3.74	0.09	7.04	0.45	30.68	4.41	5.56	0.14	8.11	1.81	6.04	1.36
12S1	3.49	0.08	7.41	0.26	18.03	1.73	4.22	0.09	6.10	1.35	3.98	0.64
04S2	3.60	0.08	7.24	0.25	14.00	1.93	4.49	0.10	6.17	1.37	4.37	0.59
CFA	0.17		38.60		79.10		16.83		3.58		24.70	

INAA Run #2: Chemistry

Sample #	SC-46	error	CR-51		FE-59		CO-60		ZN-65		SR-85 #		BA-131	
08p1	19.02	0.45	472.83	11.73	4.46	0.13	30.65	1.06	84.12	7.66	201.79	96.05	373.01	49.09
02p2	7.84	0.35	12.80	6.07	3.15	0.18	13.27	1.76	72.95	18.54	408.21	0.00	384.43	0.00
07d1	7.15	0.31	16.27	0.00	3.77	0.17	14.57	1.33	74.33	21.83	654.18	0.00	690.09	149.82
11d2	5.11	0.13	3.23	1.55	0.66	0.04	1.12	0.24	26.60	4.12	73.27	0.00	146.24	50.79
05b1	8.24	0.30	26.53	5.92	2.79	0.16	16.10	1.26	66.26	18.87	400.36	0.00	1702.40	409.77
06k1	8.23	0.25	10.63	2.30	1.52	0.08	10.25	0.69	45.99	7.77	468.63	94.34	559.01	68.14
12s1	24.28	0.62	38.36	3.41	6.62	0.19	38.43	1.45	114.39	10.86	311.84	154.11	395.78	127.60
04s2	6.87	0.27	18.00	5.76	3.17	0.18	10.43	1.29	53.59	18.43	368.96	0.00	974.72	251.48
Andesite	6.36	0.55	32.75	0.00	2.70	0.42	10.67	0.00	103.40	0.00	1318.83	0.00	1538.16	563.58
Rhyolite	8.74	0.34	22.13	4.41	2.49	0.13	9.62	1.25	70.48	14.29	350.64	0.00	844.93	150.14
Gabbro	7.96	0.26	14.33	2.26	3.35	0.11	10.32	0.70	50.80	6.97	393.61	156.30	641.11	134.83

Sample #	LA-140		CE-141		ND-147		EU-154		YB-169		YB-175		LU-177	
08p1	30.39	0.00	33.76	1.42	29.87	0.00	2.24	0.55	2.24	0.52	2.45	0.44	0.27	0.06
02p2	59.63	0.00	53.65	3.95	157.05	54.01	4.06	0.00	4.37	1.22	1.96	0.00	0.29	0.08
07d1	74.42	0.00	61.23	4.70	164.33	54.51	7.05	2.85	2.23	0.00	3.07	1.28	0.60	0.14
11d2	18.08	2.13	48.63	1.61	19.71	0.00	0.53	0.00	5.79	0.53	5.58	0.40	0.69	0.05
05b1	67.26	0.00	48.39	3.67	73.27	31.98	3.73	0.00	1.71	0.00	4.25	1.16	0.21	0.00
06k1	25.66	0.00	43.33	1.74	92.86	28.13	1.24	0.00	1.87	0.31	2.09	0.49	0.24	0.03
12s1	38.97	0.00	6.62	1.35	43.88	0.00	2.00	0.74	0.67	0.00	1.29	0.00	0.10	0.00
04s2	55.81	0.00	60.14	3.95	55.83	0.00	4.04	0.00	2.26	0.50	3.06	0.78	0.63	0.20
Andesite	107.81	0.00	21.86	8.18	327.26	131.07	10.27	0.00	4.37	0.00	5.13	0.00	0.22	0.00
Rhyolite	43.31	0.00	52.76	3.10	56.44	0.00	22.41	3.34	2.00	0.48	3.20	0.73	0.39	0.12
Gabbro	34.76	7.25	36.95	1.57	19.75	2.78	1.05	0.00	1.48	0.27	1.45	0.34	0.17	0.05

values in ppm

INAA Run #2: con't

Sample #	HF-181		TA-182		PA-233	
08p1	2.72	0.21	0.51	0.07	4.69	0.23
02p2	6.92	0.76	0.88	0.00	5.51	0.56
07d1	6.16	0.65	1.04	0.00	6.42	0.62
11d2	4.83	0.23	0.77	0.05	25.99	0.66
05b1	6.35	0.75	0.83	0.00	6.08	0.55
06k1	4.59	0.29	0.85	0.20	4.43	0.24
12s1	0.74	0.00	0.35	0.00	0.93	0.22
04s2	5.38	0.54	0.89	0.00	6.67	0.59
Andesite	5.05	1.18	1.96	0.00	4.22	1.28
Rhyolite	6.08	0.44	33.36	1.26	5.57	0.45
Gabbro	4.47	0.26	0.38	0.15	3.17	0.21

values in ppm

St. Helens Geochemistry

	Sc-46		La-140		Sm-153		Eu-152		Th		CR-51		FE-59 (%)	
H1^	5.67	0.09	12.1	0.3	2.9	0.19	0.864	0.017	2.77	0.1	6.9	0.8	2.76	0.04
Hy*	3.2	0.4	22	1	3.4	0.1	0.51	0.35	4.6	0.4	2.9	0.1	1.49	0.17
Hw*	4.2	0.5	19	2	3.6	0.1	0.66	0.12	5.4	1.3	2.1	0.9	1.37	0.1
Ht*	6.5	4.2	16	3	3.7	0.4	0.64	0.01	4.8	0.1	1.9	0.4	1.92	0.62
Hjb**	12.5	0.2	9.9	1	3.38	0.09	0.81	0.11	1.8	0.7			4.68	0.16
Hjy**	8.39	0.18	9.5	1.1	2.98	0.08	0.72	0.09	2.5	0.6			3.1	0.13
H4**	7.49	0.16	11.7	1.2	2.76	0.08	0.89	0.09	2.5	0.6			2.72	0.12
H3**	7.33	0.16	13.3	1.2	3.56	0.09	0.81	0.1	2.7	0.6			2.68	0.12
Hug**	13.3	0.2	13.4	1.2	3.3	0.1	0.91	0.11	0.7	0.7			4.13	0.15
Hlg**	12.1	0.2	14.8	1.2	3.47	0.11	1.15	0.11	1.4	0.7			3.95	0.15
Hugg**	8.14	0.19	17.5	1.4	3.25	0.1	0.92	0.12	1.9	0.7			2.99	0.14

	CO-60		BA-131		CE-141		YB		LU-177		HF-181	
H1^	7.8	0.16	390	40	32.6	1.1	0.9	0.05	0.18	0	3.76	0.1
Hy*	3.8	0.6	280	30	30	7	1	0.2	0.27	0.1	2.7	0.2
Hw*	3	0.1	44	80	32	2	2	0.3	0.37	0.1	4.9	0.4
Ht*	5.2	0.1	370	1	33	0	1.3	0.7	0.38	0.2	4.3	1.2
Hjb**	19.4	1.4	700	400	23	4			0.24	0.1	4.3	1.2
Hjy**	11.3	1.2	400	300	24	4			0.2	0.1	4.7	1.1
H4**	10.7	1	800	300	20	4			0.2	0.1	4.9	1
H3**	11	1.1	700	300	27	4			0.22	0.1	5.1	1
Hug**	20.8	1.5	600	400	31	4			0.22	0.1	3.4	1.2
Hlg**	22.4	1.5	1100	400	34	4			0.06	0.1	4.3	1.2
Hugg**	12.8	1.2	800	400	28	5			0.12	0.1	3.2	1.2

values in ppm

^ From Randle, Goles and Kittleman, 1970

* Mean elemental compostions of glassy separates, from Borchardt, Harward and Schmitt, 1971

** From Gates Thesis, 1994

Mazama Geochemistry

	Sc-46		La-140		Sm-153		Eu-152		Th-154		CR-51	
M1^	5.03	0.08	19.2	0.6	4.5	0.3	0.93	0.019	4.38	0.12	1.5	0.5
M2^	5.97	0.09	17.5	0.5	4.5	0.3	0.892	0.017	4.86	0.12	1.7	0.7
M3^	6.26	0.09	21.1	0.5	5.6	0.4	0.913	0.018	5.12	0.12	2	
M4^	6.73	0.1	18.1	0.5	4.3	0.3	0.64	0.03	5.45	0.11	4.8	1
M5^	5.72	0.09	19.3	0.7	4.1	0.2	1	0.03	5.8	0.08	2	
M6^	5.62	0.09	19.1	0.6	4.7	0.3	0.906	0.018	4.6	0.2	2.2	0.6
M7^	5.14	0.08	19.5	0.6	4.1	0.3	0.91	0.04	5.14	0.13	2	
M8^	6.34	0.1	18	0.6	5.1	0.3	0.851	0.017	4.69	0.11	2.5	0.5
M9^	5.88	0.09	19.4	0.5	4.5	0.3	0.828	0.017	4.61	0.16	1.5	0.8
M10^	5.67	0.09	20	0.5	3.8	0.3	0.875	0.018			2	
M11^	5.83	0.09	19.8	0.5	4.4	0.3	0.67	0.04	4.91	0.11	2	
M12^	6.4	0.1	18.8	0.6	4	0.3	0.944	0.018	4	0.11	5	0.7
MazC1*	6.6	0.5	22	2	5.1	0.4	0.94	0.05	6.6	0.3	1.6	0.6
MazC2*	6.2	0.3	21	2	5	0.5	0.84	0.09	6.3	0.4	1.5	0.7
Maz1**	7.46	0.15	25.1	1.4	4.66	0.08	1.16	0.09	4.9	0.5		
Maz2**	6.8	0.2	32	2	4.79	0.16	0.91	0.12	6.4	0.7		
Maz3**	6.75	0.06	22.7	1.7	4.79	0.11	1.06	0.05	5.6	0.19		
Mc-154***	6.73		23		5		0.95		5.3			
Mc1***	6.59		22		4.8		0.92		5.1			

values in ppm

^ From Randle, Goles and Kittleman, 1970

* Mean elemental compostions of glassy separates, from Borchardt, Harward and Schmitt, 1971

** From Gates Thesis, 1994

*** Data from C. R. Bacon and T. H. Druitt, 1988, in Gates Thesis, 1994.

Mazama Geochemistry: con't

	FE-59 (%)		CO-60		BA-131		CE-141		YB		LU-177		HF-181	
M1^	1.91	0.02	5.01	0.12	760	50	46.4	1.3	1.86	0.12	0.51	0.06	6	0.13
M2^	2.05	0.04	4.03	0.1	630	40	44	1.3	1.81	0.11	0.49	0.06	6.4	0.14
M3^	1.62	0.03	3.4	0.1	760	40	49.3	1.4	2.46	0.08	0.6	0.07	6.55	0.12
M4^	1.96	0.02	4.65	0.11	580	60	42.9	1	1.89	0.15	0.35	0.04	6.05	0.1
M5^	1.54	0.03	2.92	0.09	740	40	48.6	0.08	2.05	0.07	0.48	0.04	6.8	0.15
M6^	1.67	0.03	3.49	0.09	750	60	43.6	1.3	1.92	0.07	0.53	0.06	5.71	0.12
M7^	1.43	0.02	2.63	0.09	730	50	44.6	1	1.9	0.12	33	0.04	6.36	0.11
M8^	2.02	0.03	4.29	0.11	660	40	49.1	1.4	1.86	0.16	44	0.05	6.32	0.13
M9^	1.68	0.03	3.36	0.09	660	50	46.4	1.5	1.95	0.1	44	0.06	6.45	0.15
M10^	1.03	0.08	4.21	0.11	650	60	45.2	1.4					6.3	0.16
M11^	1.82	0.03	4.37	0.11	730	60	46.1	1.3	2.06	0.15	0.48	0.04	6.15	0.17
M12^	2.22	0.04	5.24	0.11	680	50	44.1	1.3	1.89	0.07	0.38	0.05	5.24	0.12
MazC1*	1.51	0.11	2.8	0.3	670	80	45	3	3.6	0.9	0.51	0.11	6.6	0.5
MazC2*	1.46	0.09	2.5	0.4	660	90	42	2	3.5	0.7	0.57	0.05	6.2	0.3
Maz1**	2.2	0.09	4.7	0.6	600	200	42	3			0.49	0.12	6.1	0.8
Maz2**	1.79	0.12	4.5	0.8	600	400	47	4			0.55	0.16	6.5	1.2
Maz3**	1.87	0.04	3.9	0.3	560	200	46.3	1.1			0.41	0.07	7	0.4
Mc-154***	1.61				766		44				0.35		5.9	
Mc1***	1.66				771		43				0.34		5.7	

values in ppm

^ From Randle, Goles and Kittleman, 1970

* Mean elemental compostions of glassy separates, from Borchardt, Harward and Schmitt, 1971

** From Gates Thesis, 1994

*** Data from C. R. Bacon and T. H. Druitt, 1988, in Gates Thesis, 1994.

APPENDIX D

APPENDIX E

Drill Hole and GPR line locations

well #	easting	northing	corrected elevation	elev.
Clatsop 1: 5099720			meters	
Dh1-Delm	429936.7	5101122	4.53	6
Delr	428955	5099660	2	
Clatsop 2: 5105550				
Dh1-Glen	429207.9	5106088	1.73	6
Glen	429208	5106088	2	
Suns	428897	5105241	4	
Suns	427697	5105241	3.8	
Clatsop 3: 5112050				
Ired	424990	5114310	8.8	
Camprilea	426950	5109451	18	
Longbeach 1: 5133400				
Dh1-67th	420479	5133592	3.36	6
Dh1-Pcyd	419212.2	5133500	2.64	6
Pcyd	419212	5133841	6	
67th	420768	5133592	9.2	
67th	420848	5133592	5.2	
67th	420868	5133592	5.2	
Longbeach 2: 5138500				
Dh1-Mchu	421657	5136900	2.7	3
Longbeach 3: 5146150				
Dh1-Klip	420100	5146050	6.618	6
Bayr	420786	5149177	6.25	
227th	419716	5146210	9.25	
227th	420416	5146210	9.8	
227th	420100	5146050	10	
227th	420050	5146050	11	
227th	420000	5146050	12	
Longbeach 4: 5154075				
Dh1-Oyst	418900	5155330	2	5
Oyst	418900	5155330	10	
Oyst1	419391	5155315	8	
Oyst1	418971	5155315	7.8	
Oyst2	419701	5155315	8.1	
Oyst2	420171	5155315	10.25	
Grayland 1: 5177600				
Dh1-Goul	417956.3	5178448	0.3	5
Dh1-Smit	418600	5177700	0.3	6
Wash1r8	418514	5177430	9.45	
Warr1r1	417043	5177366	8.2	
Wash1r7	418679	5177353	7.4	
Ash1r1	417268	5176641	7.6	

Drill Hole and GPR line locations: con't

well #	easting	northing	corrected elevation	elev.
Wash1r1	418288	5176331	6.8	
Grayland 2: 5183000				
Dh1-Grbe	416168.4	5184604	1.75	5
Coun	416638	5182669	7.6	
Coun	417088	5182669	6.5	
Coun	417348	5182669	8.3	
Grayland 3: 5190100				
Twin	415380	5189891	7	
Twin	415760	5189891	4.5	
Twin	416240	5189891	8.5	
Ocean Shores 1: 5201100				
Tauru	410490	5202600	4	
Tauru	411350	5202600	5.8	
Tauru	410800	5202600	6.25	
Tauru	411187	5202540	3.5	
Tauru	411737	5202540	7.65	
West1r4	414502	5192992	5.5	
Sport	411116	5199014	8.75	
Sport	411166	5199014	4.7	
Ocean Shores 2: 5204650				
Pacif	411558	5204942	5.4	
Tauru	410490	5202600	4	
Tauru	411350	5202600	5.8	
Tauru	410800	5202600	6.25	
Tauru	411187	5202540	3.5	
Tauru	411737	5202540	7.65	
Ocean Shores 3: 5207700				
Dh1-Oyhut	411446.1	5207679	6.1	6
Dh2-Oyhut	412554.8	5207678	3.38	4
Casi1r2	411984	5209831	7.2	
Casi1r1	411554	5209774	12.4	
Ocsp1r2	412152	5209288	6.7	
Ocsp1r1	411724	5209234	6	
Oyhut	411085	5207569	5.4	
Oyhut	412125	5207569	3.7	
Oyhut	412525	5207569	6.65	
Srain1r1	412174	5206939	6.4	
Lamar1r1	411850	5206447	6.4	
Lamar1r1	412150	5206447	9.3	
Lamar1r1	412210	5206447	6.4	

Drill Hole and GPR line locations: con't

well #	easting	northing	corrected elevation	elev.
Ocean Shores 4: 5212550				
Conn	411187	5213482	7	
Conn	411434	5213482	5.2	
Ocean Shores 6: 5218350				
Dh1-Copr	410602.9	5218502	8	6
Dh2-Copr	410280.5	5218322	0.3	4.5
Copr	410595	5218502	6.25	
Copr	410684	5218314	5.8	
Ocean Shores 7: 5226075				
Dh1-Roos	407985.5	5225284	2	4
Dh2- Roos	407985.5	5225284	2	4
Dh3-Roos-07	407985.5	5225284	2	4
Roos	409417	5225284	3	
Ocean Shores 8: 5230100				
Dh1-High	408423.2	5230301	0.3	
Dh2-High	408392.4	5230296	0.3	
Ocean Shores 9: 5231900				
Dh1-Mocl	407985.5	5231817	0.3	

References:
Dh-#: Bore Hole, this study
aaaa: GPR trace, this study, H. Jol

Water Well Locations: Clatsop

well #	easting	northing	corrected elevation	elev.	Well #
Cw-1	428100	5099600	3.74	8	Clat 231
Cw-2	428500	5100100	6.8	15	Clat 232
Cw-3	429300	5102100	2.48	9	Clat 337
Cw-4	428800	5102200	2.75	10	Clat 45
Cw-5	427978	5103300	7	1	Clat 50237
Cw-6	428392	5105300	6	1	Clat 211
Cw-7	427500	5111100	5	7.5	Clat 306
Cw-8	427400	5111500	6.5	18	Clat 305

Water Well Locations: Longbeach

well #	easting	northing	corrected elevation	elev.	Owner	County	Permit #/ Start card	ID
Lw-1	420300	5135000	3.39	6	Lushaw	Pacific		
Lw-2	419000	5138300	6.8	6	Robert Hall	Pacific	G2-25474	
Lw-3	421000	5138400	6.7	5.5	Nabiel Shawa	Pacific	13197	
Lw-4	419000	5154500	1.2	7	Surfside Homeowners		W13197	ACK098

Water Well Locations:Grayland

well #	easting	northing	corrected elevation	elev.	Owner	County	Permit #/ Start card	ID
Gw-1	418300	5178000	0.3	6.5	Martin Paulson	GH	GWA-10839	
Gw-2	417600	5178700	1.2	6.5	Ken Stephens	GH	35699	
Gw-3	417000	5181300	1.8	5.5	Bruce Johnson	GH	W19322	
Gw-4	417400	5181600	2.6	5.5	Steve Dzubay	GH	W01557	
Gw-5	417600	5182700	2.7	6.5	O.G. Lillegaard	GH	G2-21464P	
Gw-6	416300	5182900	7.3	4.5	Art Williams	GH	215719	
Gw-7	417000	5183000	1.8	6.5	Harold Tingstrom			
Gw-23	417000	5189700	4	4	Cliff Beaty	GH	4962	
Gw-24	416300	5189900	5.05	4	Westport Catholic Church	GH		
Gw-25	416800	5190400	3	3	Ocosta School Dist.	GH	G2-27120	
Gw-26	416037	5190900	4.5	3.5	City of Westport	GH		
Gw-27	415400	5191000	7.6	4.5	City of Westport	GH	W068304	ABE848
Gw-28	415400	5191000	7.6	4.5	City of Westport	GH	W068303	ABE847

Water Well Locations:Ocean Shores

well #	easting	northing	corrected elevation	elev.	Owner	County	Permit #/ Start card	ID
Ow-1	412540	5200900		5	Ralph Anderson	GH	W052097	
Ow-3	412300	5203900	6.2	5.5	Water Dist. No. 3, GH	GH	8529	
Ow-4	411200	5204000	5.12	4.5	City of Ocean Shores	GH	5021	
Ow-5	412900	5204800	4.5	5	City of Ocean Shores	GH	W069423	ACQ313
Ow-6	413000	5204800	5.18	5	City of Ocean Shores	GH	W069424	ACQ312
Ow-11	411200	5212100	4.1	4.5	Dunes Estates Inc.	GH	W13131	
Ow-14	411300	5212500	3.6	4.5	Bill Dickson	GH	W01505	
Ow-16	411400	5212500	2.74	4.5	John Halmstrom	GH	W01505	ABH 72
Ow-27	411250	5214900	5.1	5	Linda Hansen	GH	W044665	
Ow-28	411200	5214900	4.8	5	F.M. Jensen	GH	44664	
Ow-29	411300	5215200	5.3	5	Surfcrest Swanson-Dean Corp.	GH	G021929	
Ow-30	410900	5217200	7.25	5	Linda's Low Tide	GH		
Ow-31	410800	5217300	6.7	5	Sunrise Resorts	GH		
Ow-32	410800	5217800	6.7	5	Jerry Clarkhan	GH		
Ow-33	410950	5217800	10	5	Quigg-Close Trust Co.		7865	
Ow-34	409000	5228800	2	5	GH County	GH		

Water well synopsis

well #	material	meters	
Cw-1	sand	0.0	39.0
	gravel	39.0	39.3
	shale	39.3	41.1
Cw-2	sand	0.0	34.1
	clay	34.1	45.7
Cw-3	sand	0.0	18.3
	sand + clay	18.3	24.1
	clay (hard)	24.1	24.4
Cw-4	sand	0.0	29.9
	sand + clay	29.9	32.9
Cw-5	sand	0.0	22.6
	silty clay	22.6	23.8
Cw-6	sand	0.0	16.2
	sandy clay	16.2	19.8
	sand	19.8	25.0
	sandy shale	25.0	25.9
Cw-7	sand	0.0	30.8
	gravel + sand	30.8	31.4
	clay (hard)	31.4	33.5
Cw-8	sand	0.0	37.8
	wood	37.8	38.7
	mud	38.7	40.5
	clay (hard)	40.5	44.2
Lw-1	sand	0.0	20.4
	clay	20.4	23.2
	sand	23.2	26.5
Lw-2	sand	0.0	37.8
	clay + sand	37.8	52.7
	sand	52.7	62.5
Lw-3	sand	0.0	36.0
	clay	36.0	39.0
	sand	39.0	49.1
	ox sand	49.1	50.6
Lw-4	sand	0.0	27.4
	sandy silt	27.4	39.0
	ox sand	39.0	51.2
Gw-1	sand	0.0	13.7
	clay (hard)	13.7	25.9
	gravel	25.9	48.8
Gw-2	sand	0.0	16.2
	sand + gravel	16.2	19.5
	mud	19.5	42.7
	sandstone	42.7	48.8
	ox clay + gravel	48.8	50.0

Water well synopsis: con't

well #	material	meters	
Gw-3	sand	0.0	20.4
	sand + gravel	20.4	21.0
	ox clay + silt	21.0	39.0
Gw-4	peat	0.0	3.4
	sand + clay	3.4	12.5
	clay + gravel	12.5	16.5
	ox sand + clay	16.5	18.6
Gw-5	peat	0.0	1.5
	sand	1.5	7.6
	clay	7.6	12.2
	gravel	12.2	16.8
	clay	16.8	25.9
	gravel	25.9	30.5
Gw-6	sand	0.0	15.8
	gravel	15.8	18.3
Gw-7	sand	0.0	19.2
	sand + gravel	19.2	20.4
	ox sandy mud	20.4	43.3
Gw-23	sand	0.0	26.5
	mud	26.5	27.1
	sand	30.2	43.3
Gw-24	sand	0.0	25.3
	sand + gravel	25.3	26.5
	mud	26.5	31.1
Gw-25	sand	0.0	29.9
	sand + gravel	29.9	30.8
	mud	30.8	54.3
Gw-26	silty sand	0.0	16.8
	sand + gravel	16.8	20.4
	sand	20.4	21.3
Gw-27	sand	0.0	23.2
	sand + gravel	23.2	26.8
	sand	26.8	30.5
Gw-28	sand	0.0	15.8
	sand + gravel	15.8	20.7
	gravel + sand	20.7	28.0
	sand	28.0	33.8
Ow-1	sand	0.0	2.4
	clay	2.4	10.7
	sand	10.7	19.8
Ow-2	sand	0.0	32.3
	clay	32.3	35.1
	sand + gravel	35.1	36.9
	inc. ox mat.	36.9 +	

Water well synopsis: con't

well #	material	meters	
Ow-3	sand	0.0	25.9
	sand + gravel	25.9	30.2
	clay + sand	30.2	33.5
	wood	33.5	34.4
	ox gravel	34.4	45.4
Ow-4	sand	0.0	11.6
	sand + gravel	11.6	29.0
Ow-5	sand	0.0	14.3
	gravel + sand	14.3	17.7
	inc. peat	17.7	19.2
	silty clay	19.2	25.9
Ow-6	sand	0.0	11.3
	sand + gravel	11.3	16.8
	clay	16.8	25.9
Ow-11	sand	0.0	6.7
	sand + gravel	6.7	12.5
	ox sand + gravel	12.5	23.5
	Clay	23.5	25.9
Ow-14	sand	0.0	5.8
	sandy clay	5.8	6.4
	sand + gravel	6.4	9.1
	clay	9.1	10.1
Ow-16	sand	0.0	5.8
	mud	5.8	10.7
	sand +gravel	10.7	13.7
	clay + gravel	13.7	16.2
Ow-27	sand	0.0	4.6
	sand + clay	4.6	9.8
	clay	9.8	10.1
	sand	10.1	10.7
	gravel	10.7	11.6
Ow-28	sand	0.0	9.1
	sand + clay	9.1	9.8
	gravel	9.8	10.4
Ow-29	sand	0.0	14.9
	clay	14.9	21.9
Ow-30	sand	0.0	3.0
	clay + gravel	3.0	10.7
	clay	10.7	13.7
Ow-31	sand	0.0	6.1
	gravel + clay	6.1	19.8
	ox clay	19.8	24.4
Ow-32	sand	0.0	12.2
	gravel + sand	12.2	32.0

Water well synopsis: con't

well #	material	meters	
Ow-33	sand	0.0	13.7
	mud	13.7	22.9
	mud + gravel	22.9	30.2
	gravel	30.2	33.8
Ow-34	sand	0.0	5.8
	clay	5.8 +	

Geotech site locations

well #	easting	northing	corrected elevation	elev.
Clatsop 1: 5099720				
Gst	429400	5094380	3	5
H2	428900	5099800	2	14.1
Clatsop 2: 5105550				
dc	428600	5105400	5.53	?
Clatsop 3: 5112050				
N1a	427800	5108250	2	10.6
Longbeach 1: 5133400				
Ashawa	421000			
Longbeach 3: 5146150				
OcPark	419500			
Longbeach 4: 5155250				
Surfside	419500			
Grayland 1: 5177600				
B3	418200	5176800	0.3	3
Grayland 4: 5194075				
Core-1	5192500	414850	4.5	
Core-2	5193000	416000	1	
Ocean Shores 1: 5201100				
Core-3	5199300	414500	0.3	
Ocean Shores 2: 5204650				
Core-4	5204000	413500	0.3	

Geotech log synopsis

site #	material	meters	
Gst *	sand + gravel	0	7.9
	sand	7.9	12.8
	gravel	12.8	18.6
		0	0
H2 **	silty sand	0	13.7
	sand	13.7	25.0
	silty sand	25.0	36.6
	inc. granules of basalt	36.6	38.7
	silt + clay	38.7	42.7
dc **	sand	0	11.6
	sand + clay	11.6	16.2
	clay + sand	16.2	19.8
	sand	19.8	25.0
	shale	25.0	25.9
N1 **	sand	0	22.3
	inc. silt + org.	22.3	22.9
	sand	22.9	29.9
	sand + basalt pebbles + silty clay	29.9	30.5
	sand + silt	30.5	32.9
	clay	32.9	38.1
	shale	38.1	41.1
B-3 ***	sand	0	14.6
	clay	14.6	15.8
	ox Pleist. Terrace	15.8	0
Core-1 ****	sand	0	10.0
	sand + gravel	10.0	15.0
	sand	15.0	31.0
	sand + gravel	31.0	35.5
	sand	35.5	42.0
	sand + mud	42.0	45.0
	sand	45.0	58.0
	sand + mud	58.0	60.0
	pre-Holocene	60.0	

Geotech log synopsis

site #	material	meters	
Core-2 ****	sand	2.0	5.0
	sand + gravel	5.0	8.0
	sand	8.0	15.0
	gravel + sand	15.0	16.0
	sand	16.0	27.0
	sand + mud	27.0	39.0
	mud	39.0	40.0
	sand + mud	40.0	43.0
	sand	43.0	45.0
	mud + sand	45.0	50.0
	sand	50.0	51.0
	sand + mud	51.0	56.0
	pre-Holocene	56.0	
Core-3 ****	sand	6.0	12.0
	sand + gravel	12.0	13.0
	sand + mud	13.0	15.0
	sand	15.0	16.0
	sand + mud	16.0	21.0
	sand + gravel	21.0	23.0
	sand	23.0	24.0
	sand + gravel	24.0	26.0
	sand + mud	26.0	40.0
	mud	40.0	43.0
	mud + sand	43.0	47.0
	sand	47.0	52.0
	sand + mud	52.0	60.0
	pre-Holocene	60.0	
Core-4 ****	sand	2.0	4.0
	sand + gravel	4.0	5.0
	sand	5.0	6.0
	sand + gravel	6.0	8.0
	sand	8.0	11.0
	mud + sand	11.0	16.0
	sand + gravel	16.0	17.0
	mud + sand	17.0	28.0
	pre-Holocene	28.0	

* ODOT
** Rankin, 1983 (various sources)
*** WDOT
**** Peterson and Phipps, 1992

Base of upper beach face from surfzone Vibracoring data

Site Name	Easting	Northing	Elevation MLLW (ft)	Elevation NAVD 88 (m)
Mocl01-980723	407747	5239310	-1.7	-0.6
Rose01-980721	409191	5232039	-0.1	-0.1
Copa01-980723	409988	5218480	-1.6	-0.5
Ocea01-980724	410453	5213319	-1.8	-0.6
Bwes01-980724	410636	5207800	-1.7	-0.6
Cond01-980724	410549	5199440	-1.1	-0.4
Sojw01-980826	413680	5194731	-1.3	-0.5
Twin01-980624	414833	5190100	0	-0.1
Grbe01-980624	415760	5184540	-2.5	-0.8
Ncov01-980625	415412	5177710	-2.3	-0.8
Oyst01-980807	418522	5155700	-1.6	-0.5
Lmcb01-980806	418537	5144202	-1.1	-0.4
Ombc01-980806	418349	5139440	-1.2	-0.4
Long01-980806	417903	5133340	-1.1	-0.4
Peti01-980808	424033	5114592	-1.2	-0.4
Sunb01-980626	427014	5105480	-1.2	-0.4
Delr01-980808	427860	5099650	-1	-0.4

Data from Qualman *et al*., 1999.

Ravienment Offshore Seismic Data

Line #	Easting	Northing	depth (m)	shot #
L17S1	423891.2	5094527.2	-37.3	3404
L19S1	425705.83	5100040.6	-34.2	535
L21S2	426374	5105650	-35.1	8094
L23S1	424539	5111102.4	-30.2	16
L24S1	420829.5	5117687	-44.3	38
L31S1	416008.33	5128894.4	-41.8	210
L33S2	417277.4	5134418.8	-35.1	9854
L28S2	417807.2	5139956.6	-23.6	8873
L36S2	417811.8	5145530.2	-21.2	3877
L34S1	416995	5151287.4	-24.3	24
L37S1	416537.6	5156744.8	-18.5	369
L29S1	415513.03	5162567.4	-27.3	20
L45S1	414985.2	5179818.6	-18.7	11397
L46S1	414853.6	5179737.4	-19	32
L41S1	414862.4	5185367.2	-13.7	34
L43S3	413981.4	5191017.8	-13.5	3230
L44S1	412597.4	5195151.4	-16.8	3216
L11S2	409589.4	5208253.4	-6	8900
L8S3	406703.9	5214587.2	-15.9	19
L7S2	408006.35	5220102.4	-8.9	4695
L5S1	407507.94	5226318.2	-7.3	2

Lines are oriented east-west and shown on Figure 6.
Depth indicates depth to feature from sea level.
Shot # indicates placement on the seismic line.

Lowstand Offshore Seismic Data

Line #	Easting	Northing	depth (m)	shot #
L17S1	423891.2	5094527	-43.4	3404
L19S1	425705.8	5100041	-34.2	535
L21S2	426374	5105650	-35.1	8094
L23S1	424539	5111102	-30.2	16
L24S1	420829.5	5117687	-44.3	38
L31S1	416009.4	5128895	-41.8	209
L33S2	417277.4	5134419	-35.1	9854
L28S2	417807.2	5139957	-23.6	8873
L36S2	417811.8	5145530	-21.2	3877
L34S1	416995	5151287	-24.3	24
L37S1	416537.6	5156745	-18.5	369
L29S1	415513	5162567	-27.3	20
L46S1	414880.6	5179735	-21.2	12
L45S1	414985.1	5179814	-29.3	11400
L41S1	414862.4	5185369	-13.7	34
L43S3	413981.4	5191018	-13.5	3230
L44S1	412599.4	5195136	-66.2	3228
L11S2	409589.4	5208253	-6	8900
L7S2	408006.4	5220102	-8.9	4695
L8S3	406703.9	5214587	-15.9	19
L5S1	407507.9	5226318	-7.3	2

Lines are oriented east-west and shown on Figure 6.
Depth indicates depth to feature from sea level.
Shot # indicates placement on the seismic line.

APPENDIX F

Volume Calculations

Section #	s utm	n utm	segment length N-S	beach area	shelf area	volume B	volume S
C-1	5092000	5102250	10250	25940.10	39134.70	2.66E+08	4.01E+08
C-2	5102250	5108350	6100	20835.91	37344.33	1.27E+08	2.28E+08
C-3	5108350	5117000	8650	49626.97	83964.49	4.29E+08	7.26E+08
L-1	5128000	5135950	7950	18207.58	32175.53	1.45E+08	2.56E+08
L-2	5135950	5142325	6375	31751.78	79163.94	2.02E+08	5.05E+08
L-3	5142325	5150700	8375	25071.22	27797.26	2.10E+08	2.33E+08
L-4	5150700	5166000	15300	22334.42	39969.77	3.42E+08	6.12E+08
G-1	5175500	5180300	4800	20983.14	31694.66	1.01E+08	1.52E+08
G-2	5180300	5186550	6250	10537.15	21910.17	6.59E+07	1.37E+08
G-3	5186550	5192087	5537	11596.91	46468.51	6.42E+07	2.57E+08
G-4	5192087	5195100	3013	16072.16	164291.22	4.84E+07	4.95E+08
OC-1	5197600	5202875	5275	32028.30	205439.61	1.69E+08	1.08E+09
OC-2	5202875	5206175	3300	25322.69	63164.64	8.36E+07	2.08E+08
OC-3	5206175	5210125	3950	11278.60	7621.16	4.46E+07	3.01E+07
OC-4	5210125	5213762	3637	6368.03	9459.34	2.32E+07	3.44E+07
OC-5	5214975	5216662	1687	6612.75	3536.87	1.12E+07	5.97E+06
OC-6	5216662	5222212	5550	11197.03	13659.48	6.21E+07	7.58E+07
OC-7	5222212	5228087	5875	188.90	0.00	1.11E+06	0.00E+00
OC-8	5228087	5231000	2913	53.32	0.00	1.55E+05	0.00E+00
OC-9	5231000	5239500	8500	66.99	0.00	5.69E+05	0.00E+00
					totals	2.40E+09	5.44E+09
					total	7.84E+09	

All values in meters. Area in meters^2. Volume in meters^3.

APPENDIX G

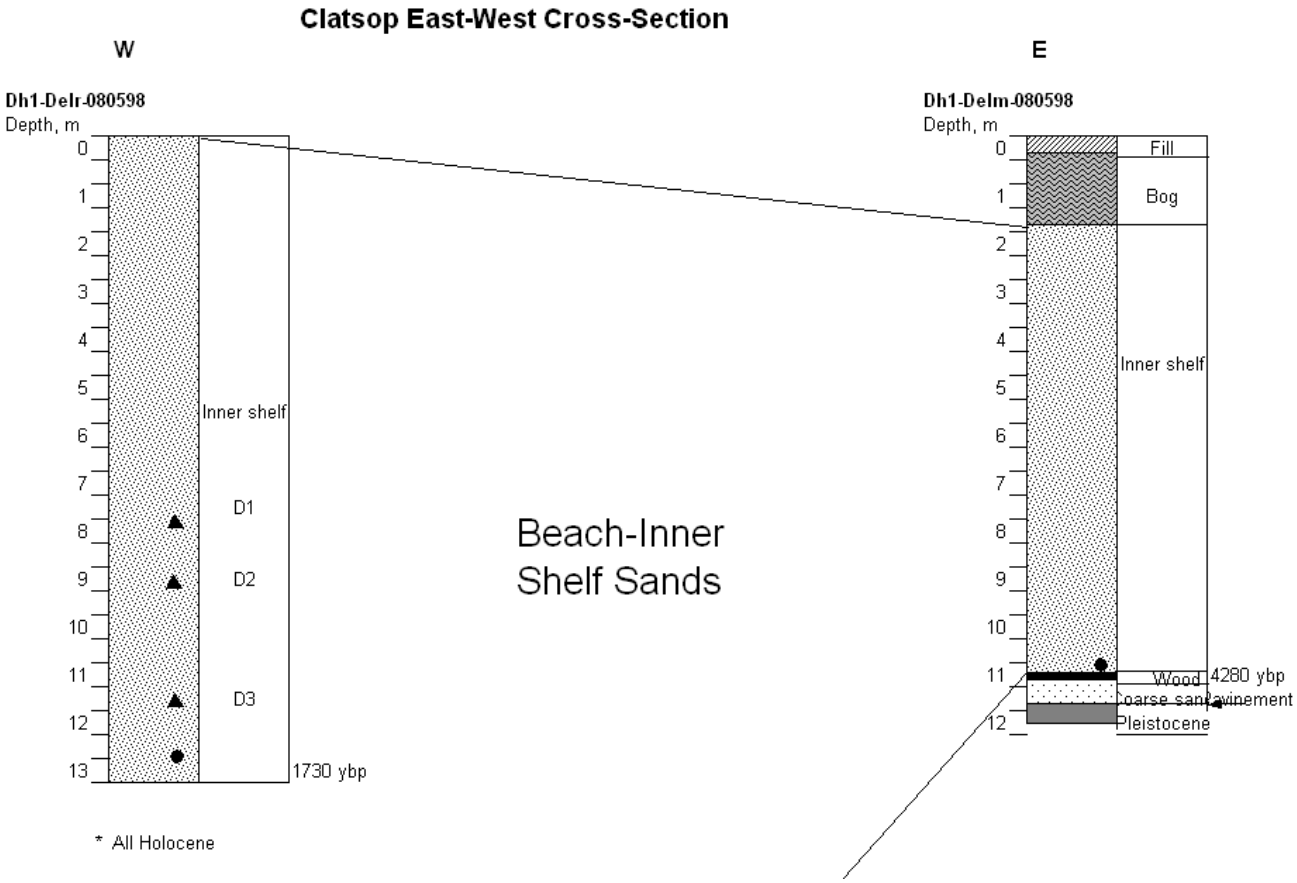
Clatsop East-West Cross-Section
W
E
Dh1-Delr-080598
Depth, m
0
1
2
3
4
5
6
7
8
9
10
11
12
13
Inner shelf
D1
D2
D3
1730 ybp
Beach-Inner
Shelf Sands
Dh1-Delm-080598
Depth, m
Fill
Bog
Inner shelf
Wood
4280 ybp
coarse sand
Pleistocene
* All Holocene

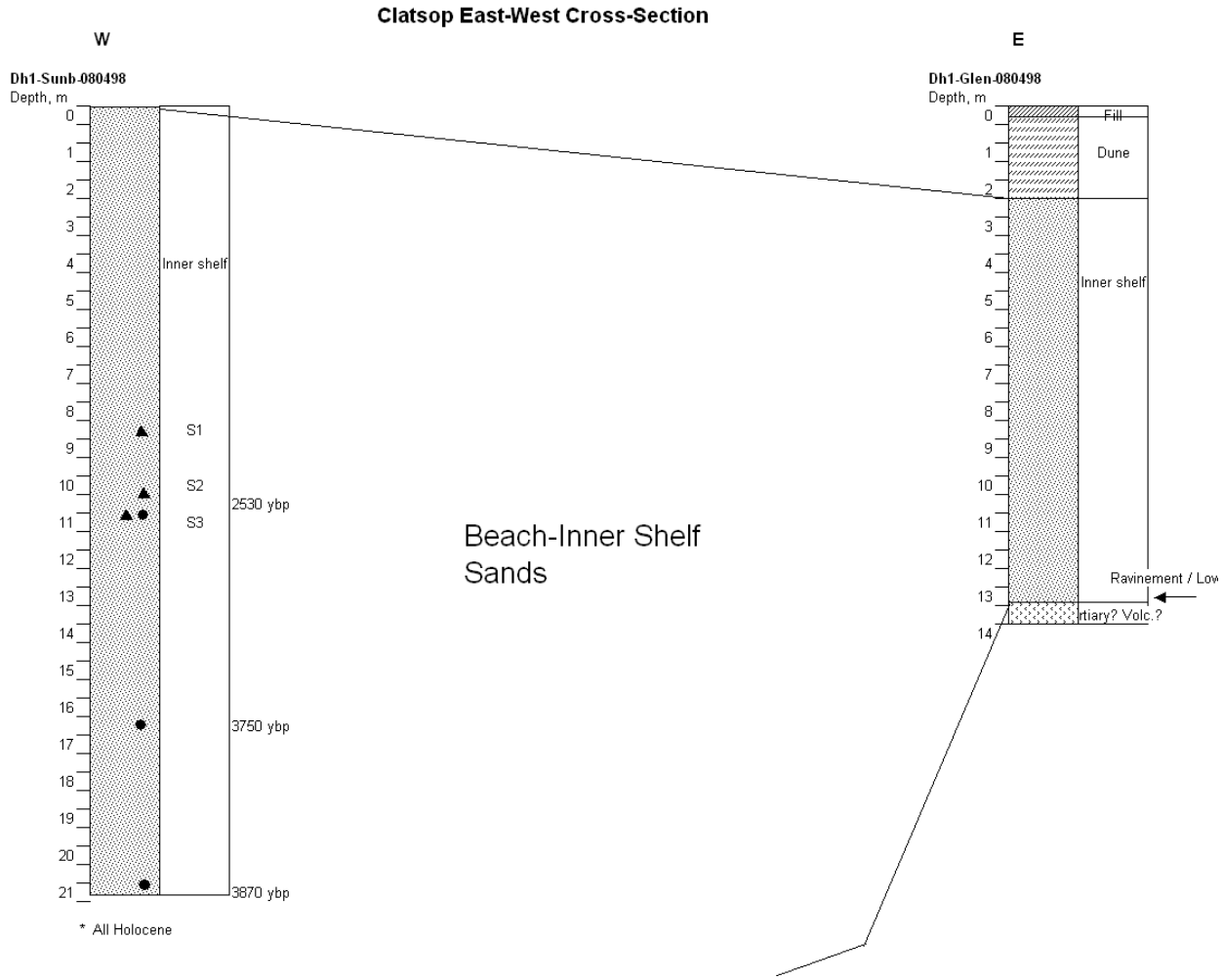
Clatsop East-West Cross-Section
W
E
Dh1-Sunb-080498
Depth, m
0
1
2
3
4
5
6
7
8
9
10
11
12
13
14
15
16
17
18
19
20
21
Inner shelf
S1
S2
S3
2530 ybp
3750 ybp
3870 ybp
* All Holocene
Beach-Inner Shelf
Sands
Dh1-Glen-080498
Depth, m
Fill
Dune
Inner shelf
Ravinement / Low
rtiary? Volc.?

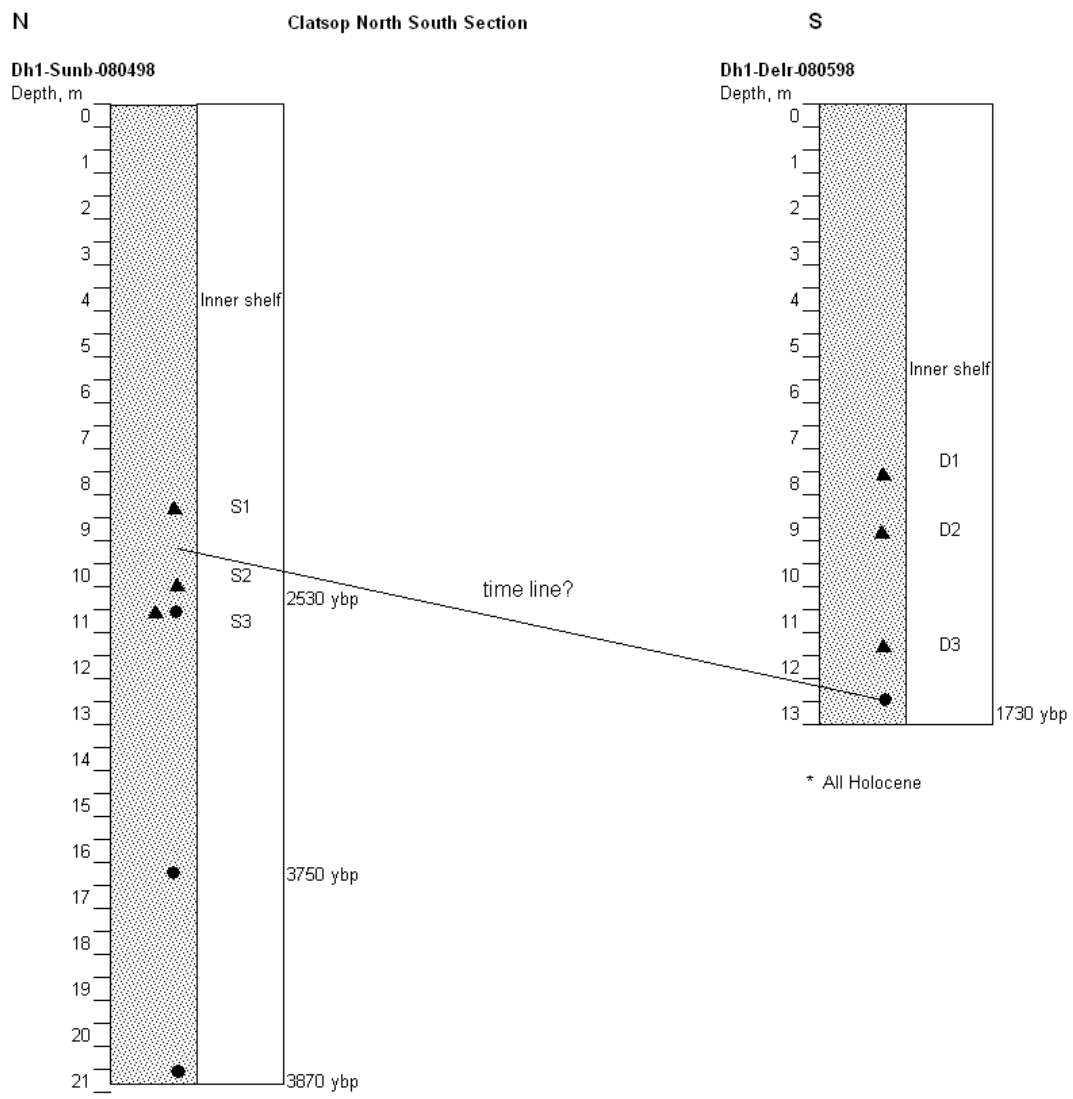
N
Clatsop North South Section
S
Dh1-Sunb-080498
Depth, m
0
1
2
3
4
5
6
7
8
9
10
11
12
13
14
15
16
17
18
19
20
21
Inner shelf
S1
S2
S3
2530 ybp
3750 ybp
3870 ybp
time line?
Dh1-Delr-080598
Depth, m
0
1
2
3
4
5
6
7
8
9
10
11
12
13
Inner shelf
D1
D2
D3
1730 ybp
* All Holocene

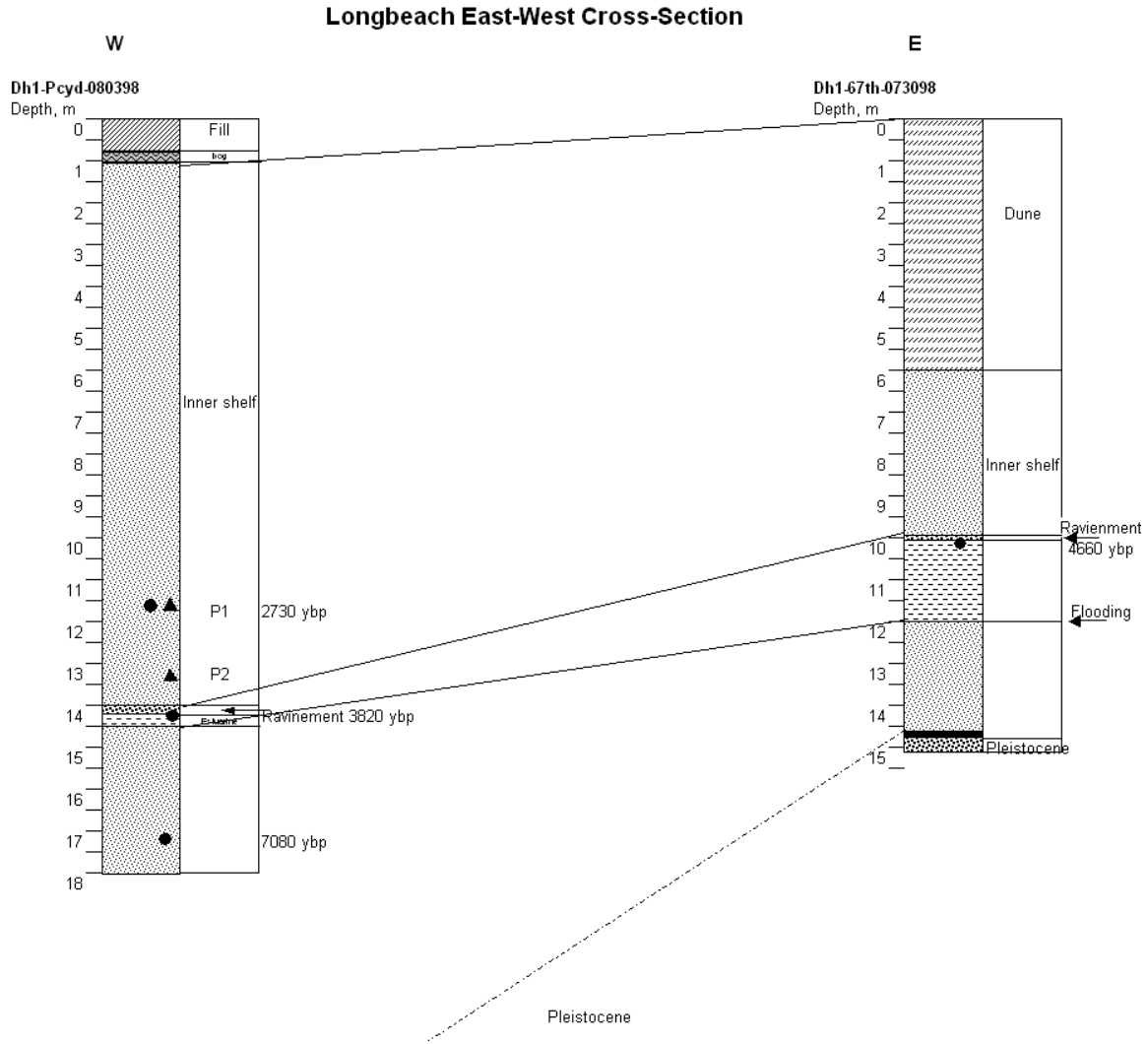
Longbeach East-West Cross-Section
W
E
Dh1-Pcyd-080398
Depth, m
Dh1-67th-073098
Depth, m
Fill
bog
Inner shelf
P1
2730 ybp
P2
Ravinement 3820 ybp
7080 ybp
Dune
Inner shelf
Ravienment
4660 ybp
Flooding
Pleistocene
Pleistocene

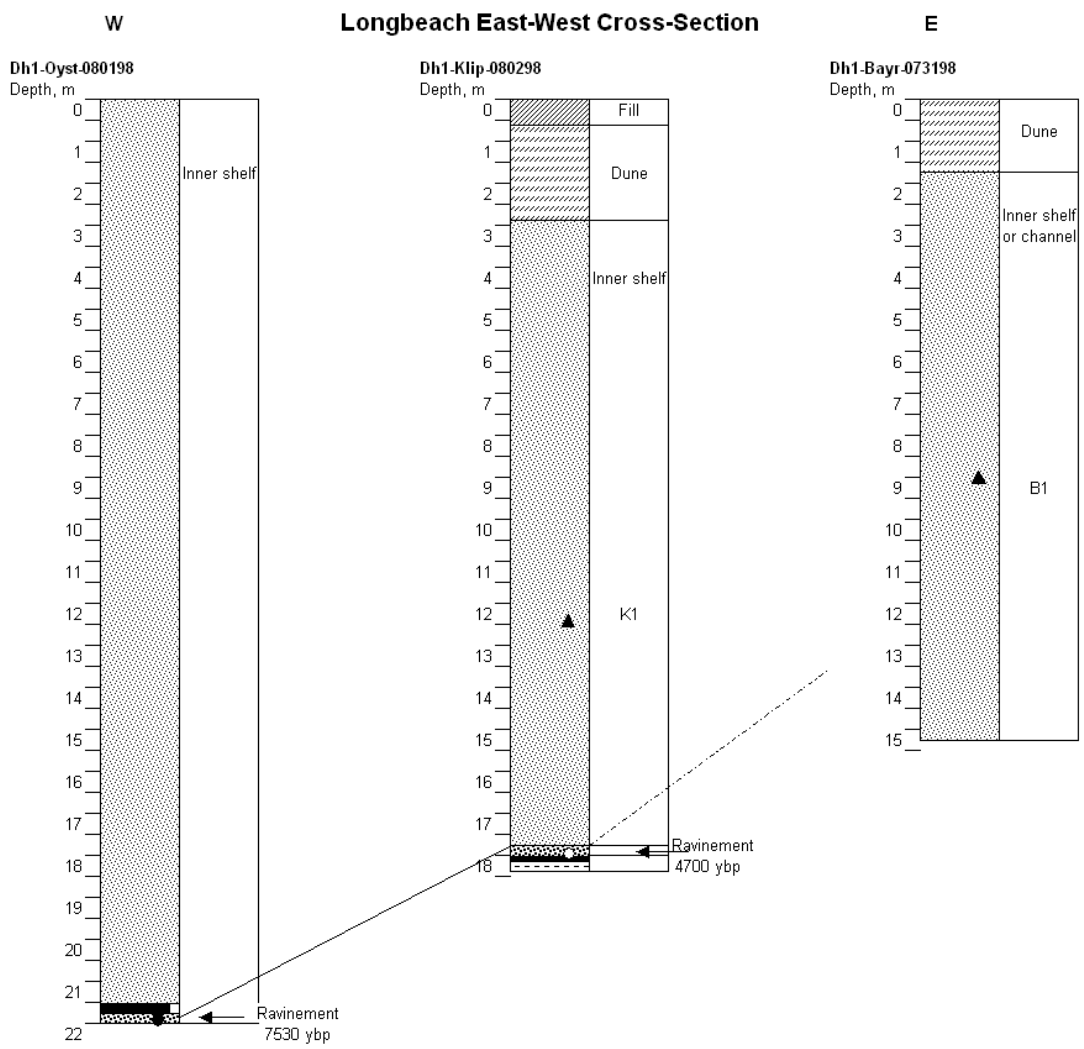
W
Longbeach East-West Cross-Section
E
Dh1-Oyst-080198
Depth, m
Inner shelf
Ravinement
7530 ybp
Dh1-Klip-080298
Depth, m
Fill
Dune
Inner shelf
K1
Ravinement
4700 ybp
Dh1-Bayr-073198
Depth, m
Dune
Inner shelf
or channel
B1

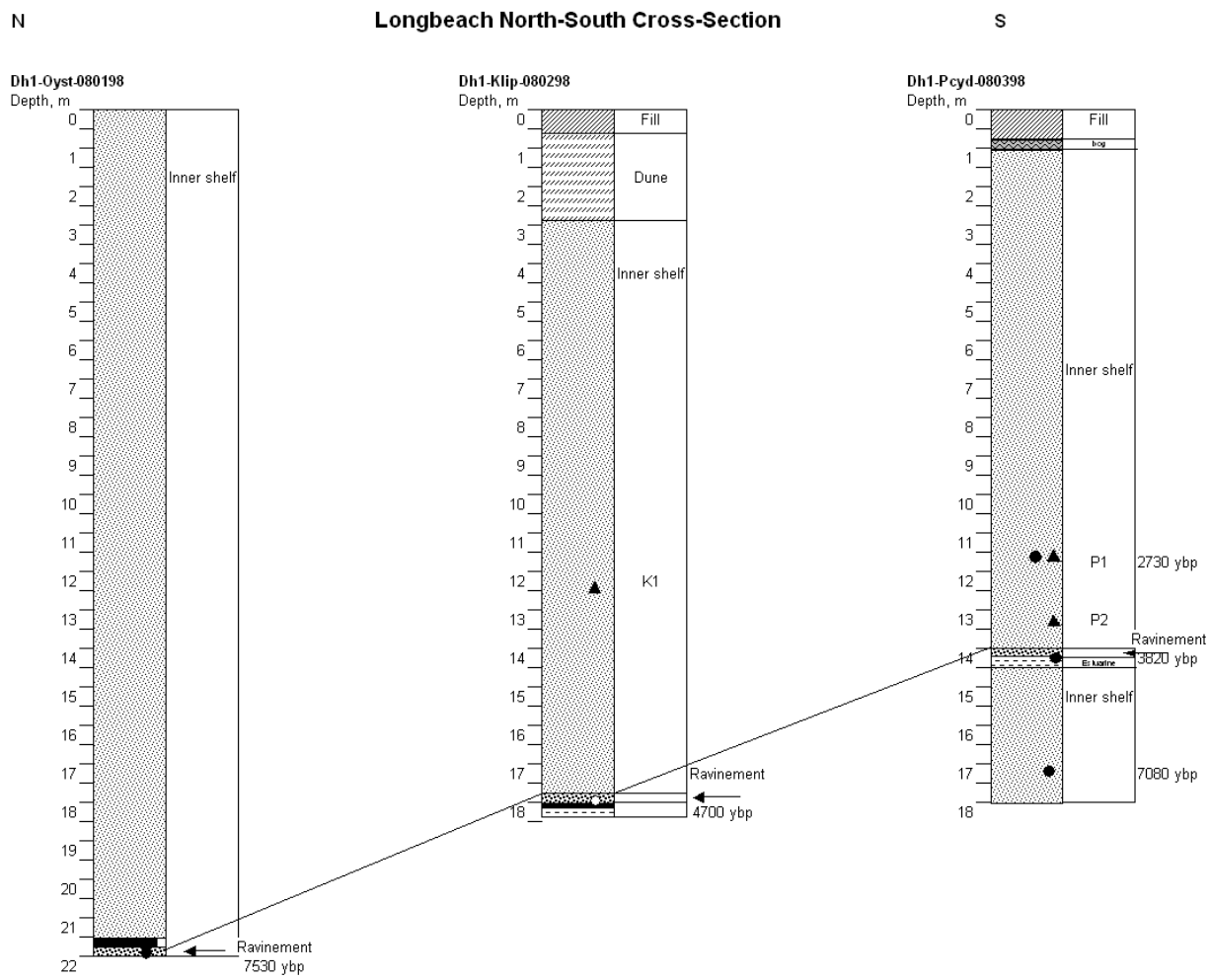
N
Longbeach North-South Cross-Section
S
Dh1-Oyst-080198
Depth, m
Inner shelf
Ravinement
7530 ybp
Dh1-Klip-080298
Depth, m
Fill
Dune
Inner shelf
K1
Ravinement
4700 ybp
Dh1-Pcyd-080398
Depth, m
Fill
Inner shelf
P1
2730 ybp
P2
Ravinement
3820 ybp
Inner shelf
7080 ybp

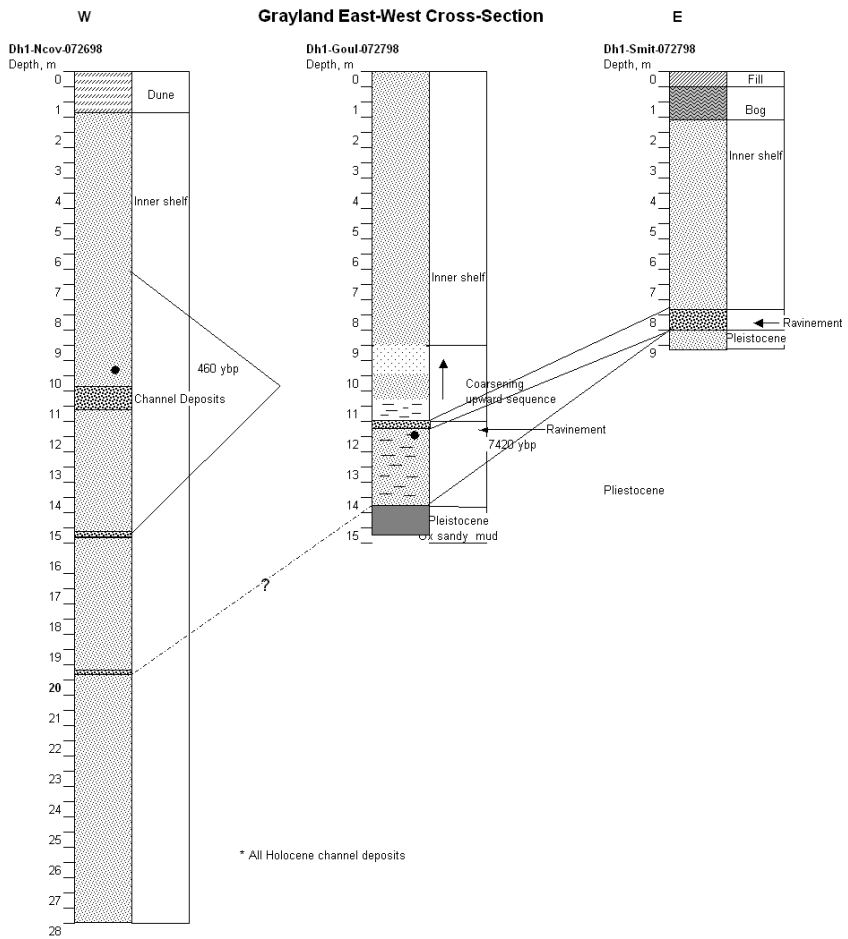
Grayland East-West Cross-Section
W
E
Dh1-Ncov-072698
Depth, m
Dh1-Goul-072798
Depth, m
Dh1-Smit-072798
Depth, m
Dune
Inner shelf
Channel Deposits
460 ybp
Inner shelf
Coarsening upward sequence
Ravinement
7420 ybp
Pleistocene
Ox sandy mud
Fill
Bog
Inner shelf
Ravinement
Pleistocene
Pliestocene
?
* All Holocene channel deposits

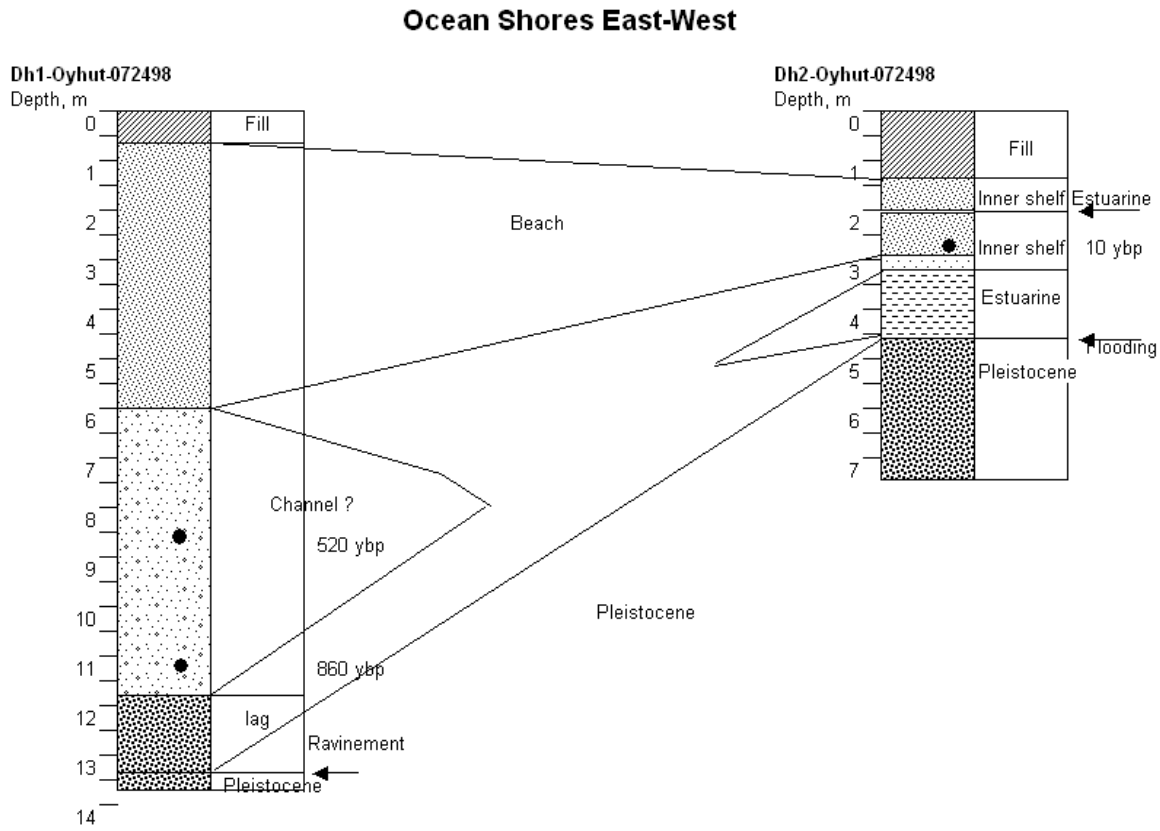
Ocean Shores East-West
Dh1-Oyhut-072498
Depth, m
0
1
2
3
4
5
6
7
8
9
10
11
12
13
14
Fill
Beach
Channel ?
520 ybp
860 ybp
lag
Ravinement
Pleistocene
Pleistocene
Dh2-Oyhut-072498
Depth, m
0
1
2
3
4
5
6
7
Fill
Inner shelf
Estuarine
Inner shelf
10 ybp
Estuarine
Flooding
Pleistocene

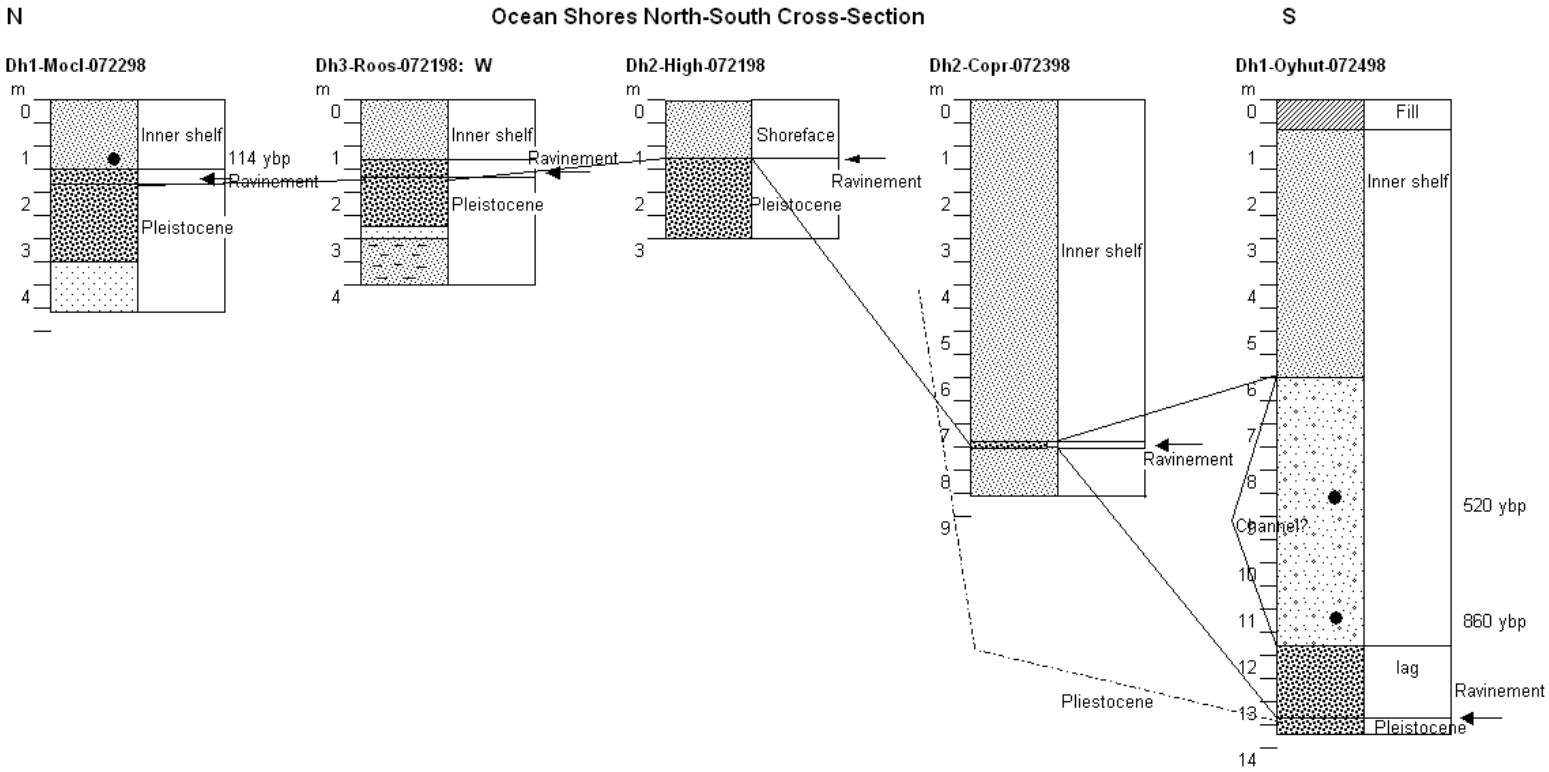
N
Ocean Shores North-South Cross-Section
S
Dh1-Mocl-072298
Dh3-Roos-072198: W
Dh2-High-072198
Dh2-Copr-072398
Dh1-Oyhut-072498
m
Inner shelf
114 ybp
Ravinement
Pleistocene
Shoreface
Fill
Channel?
520 ybp
860 ybp
lag
Pliestocene

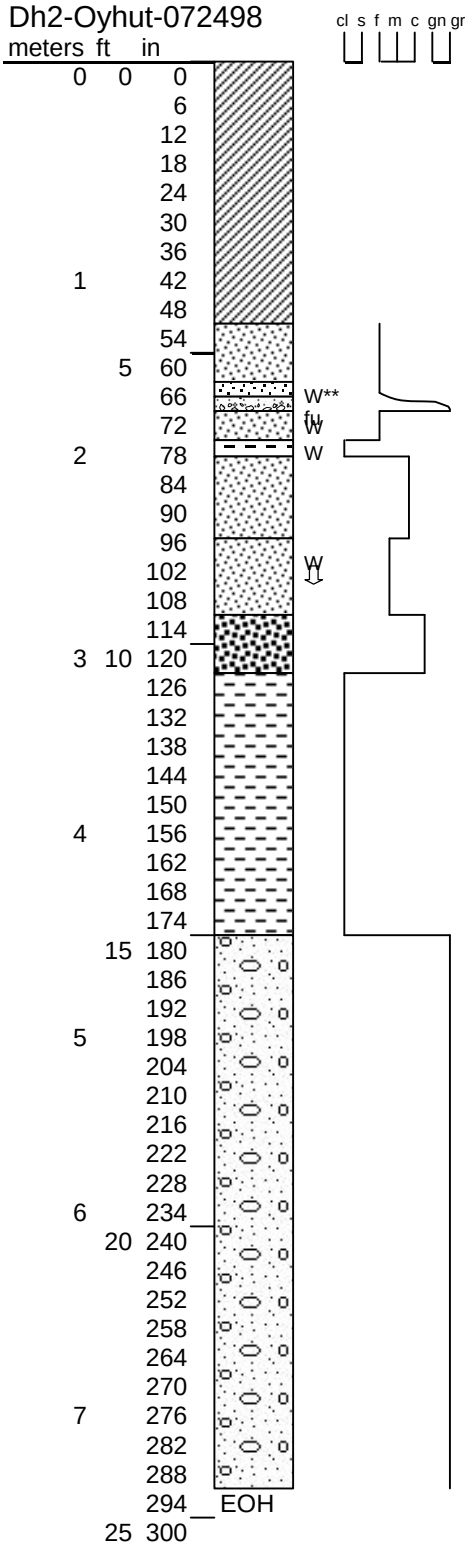
Dh2-Oyhut-072498
meters ft in
cl s f m c gn gr
W**
fw
W
W
W
W
EOH

Dh1-Ncov-072698: Page 1

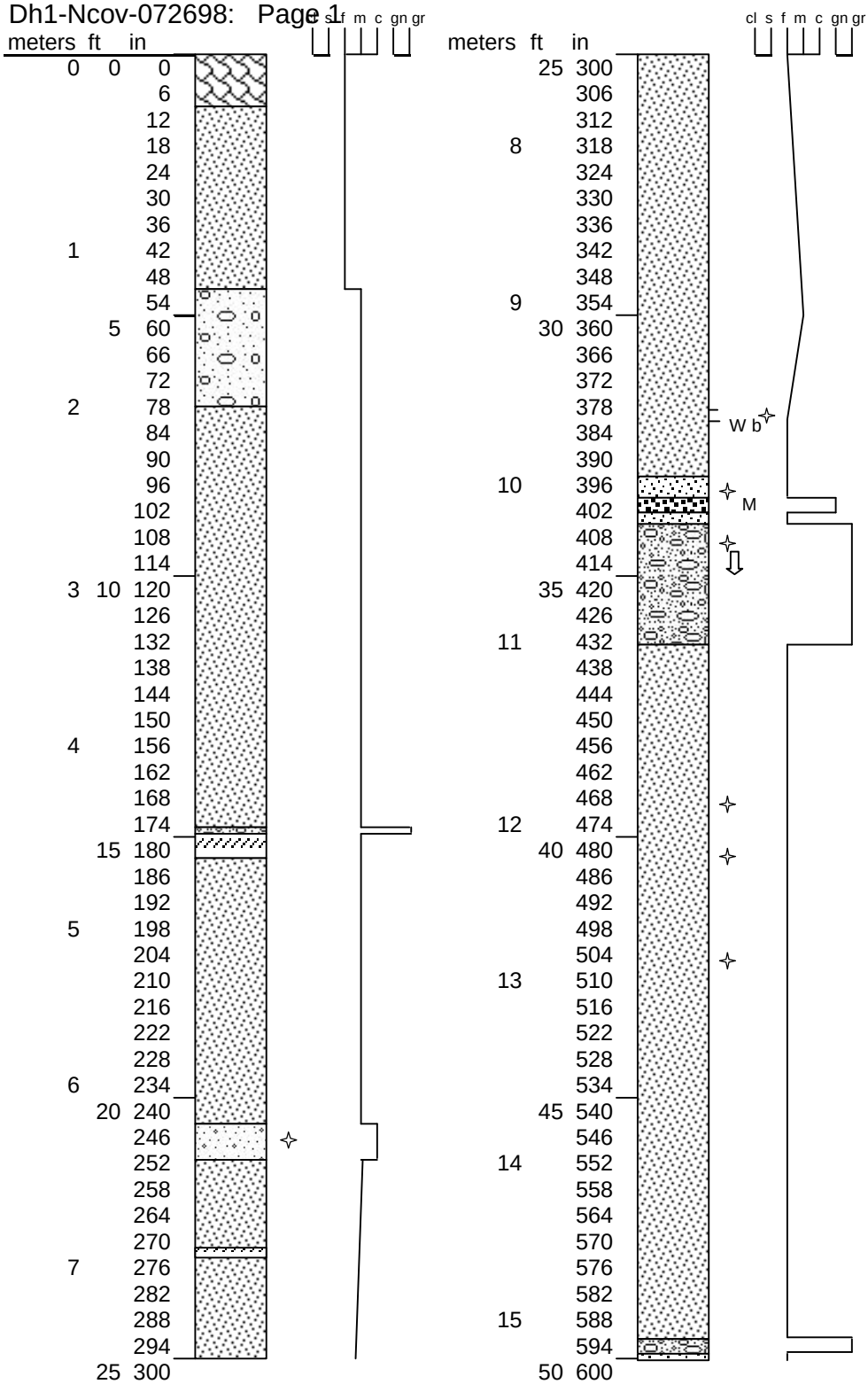

Dh1-Ncov-0726-98: Page 2

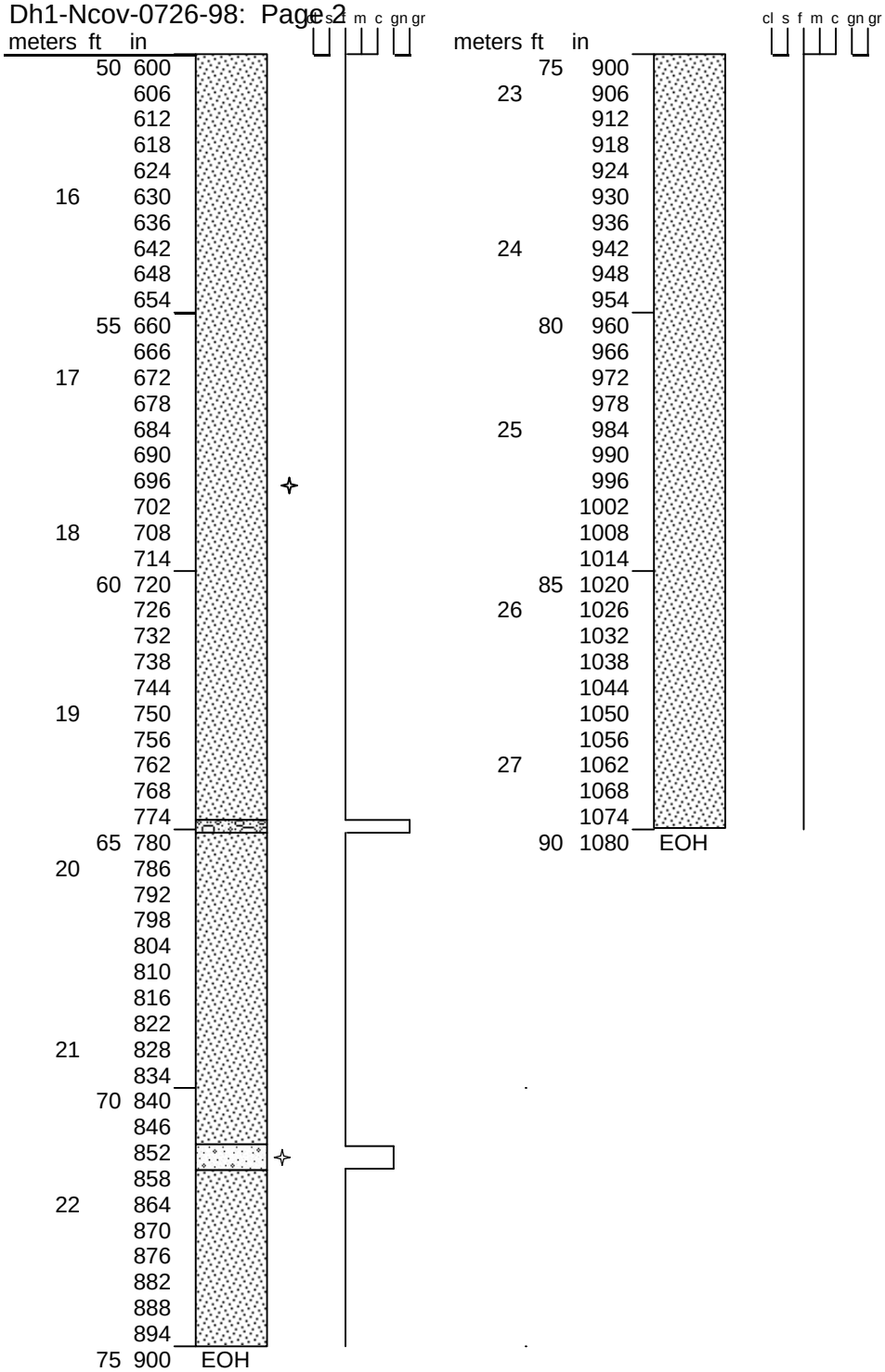

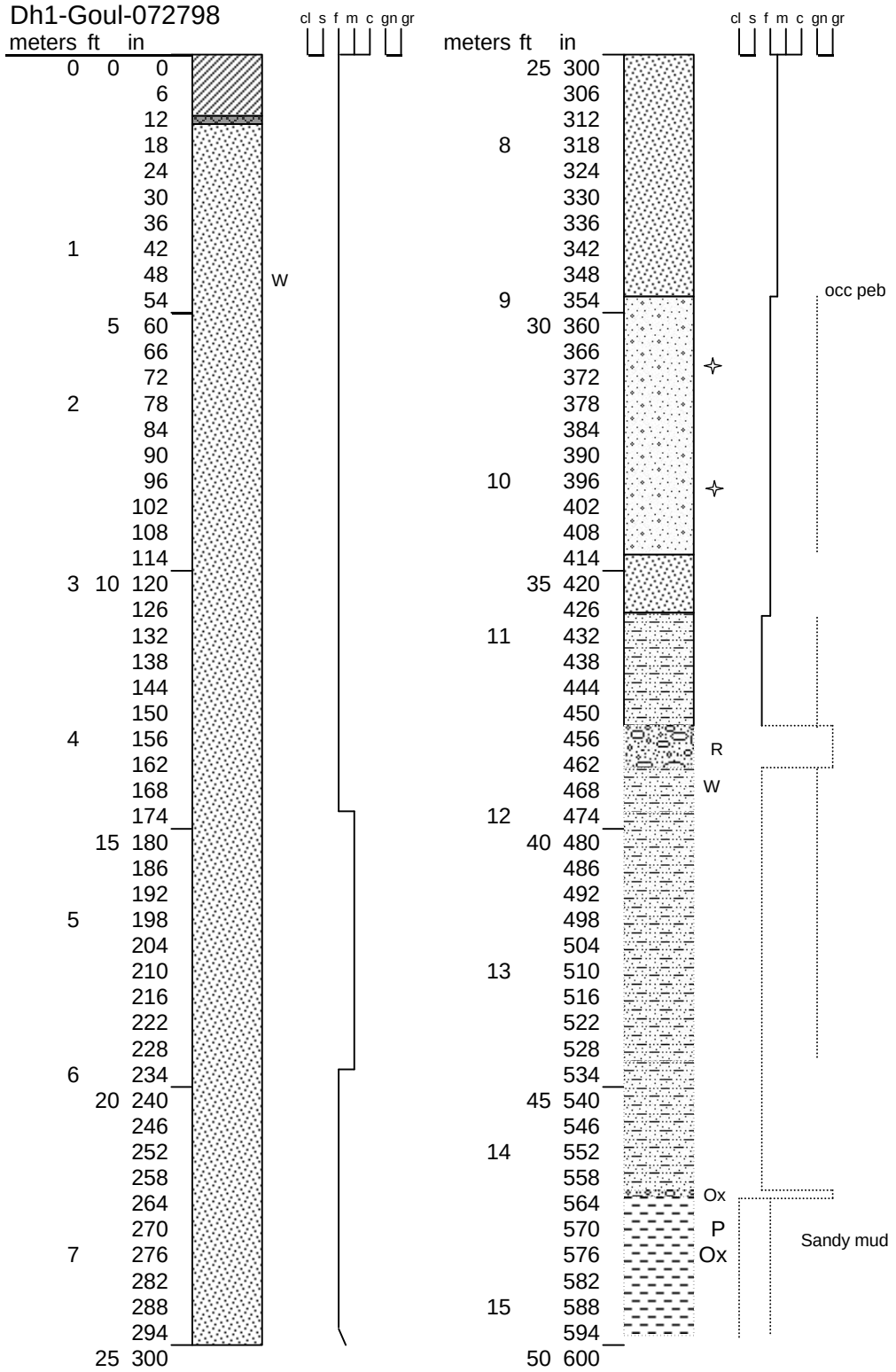
Dh1-Goul-072798
meters ft in
cl s f m c gn gr
W
occ peb
R
W
Ox
P
Ox
Sandy mud

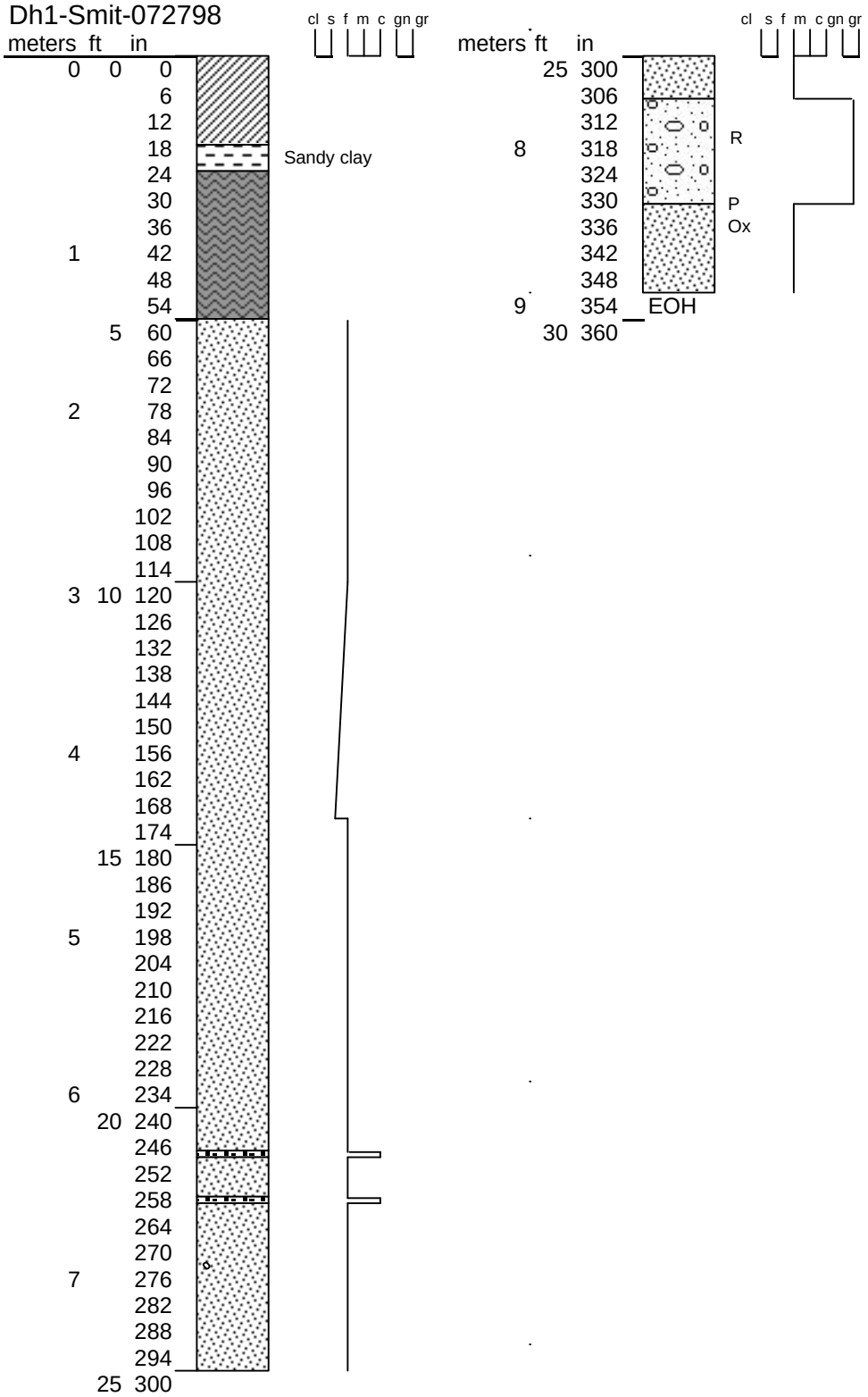
Dh1-Smit-072798
meters ft in
cl s f m c gn gr
Sandy clay
R
P
Ox
EOH

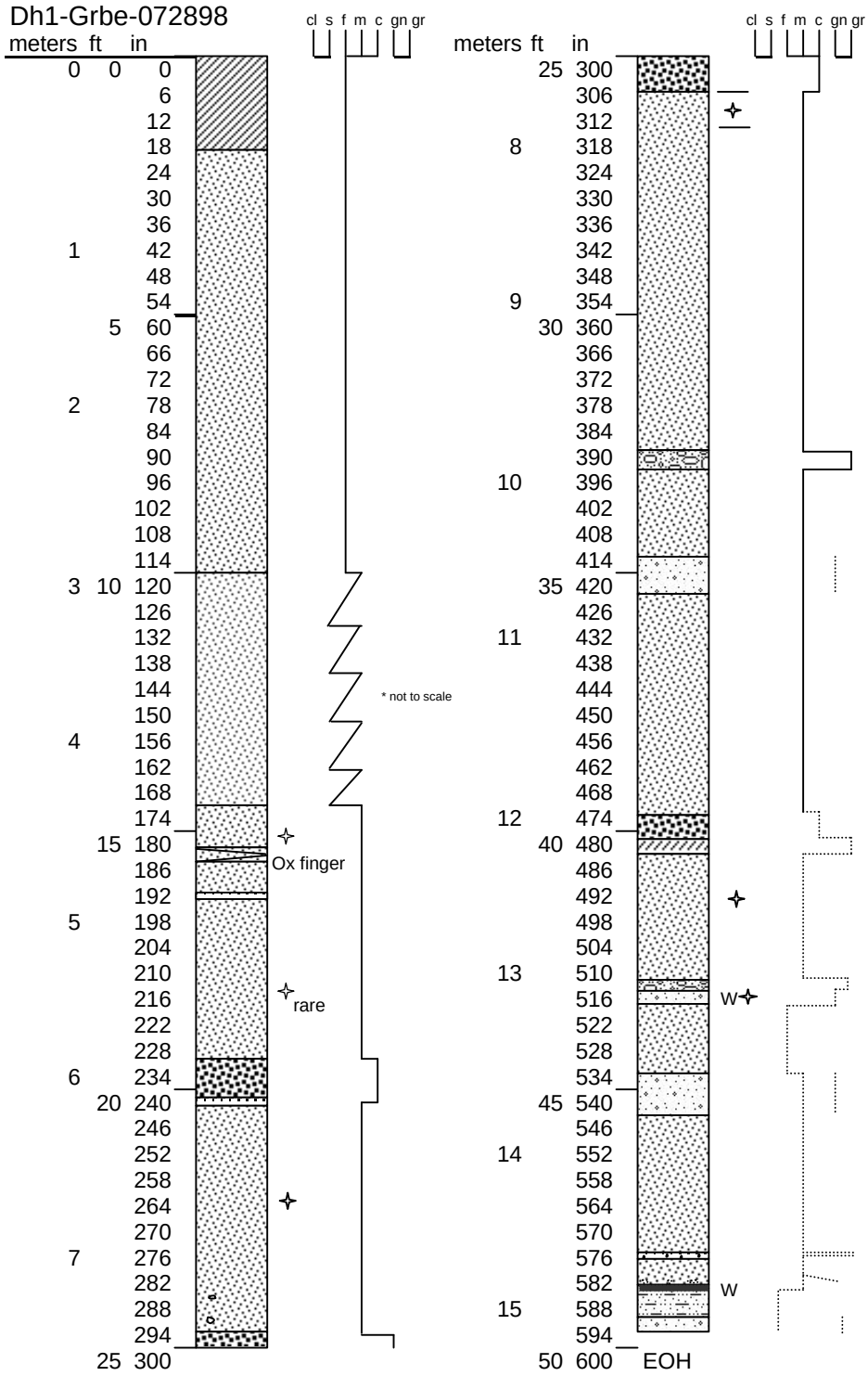
Dh1-Grbe-072898
meters ft in
cl s f m c gn gr
Ox finger
rare
* not to scale
W
W
EOH

Dh1-67th-073098

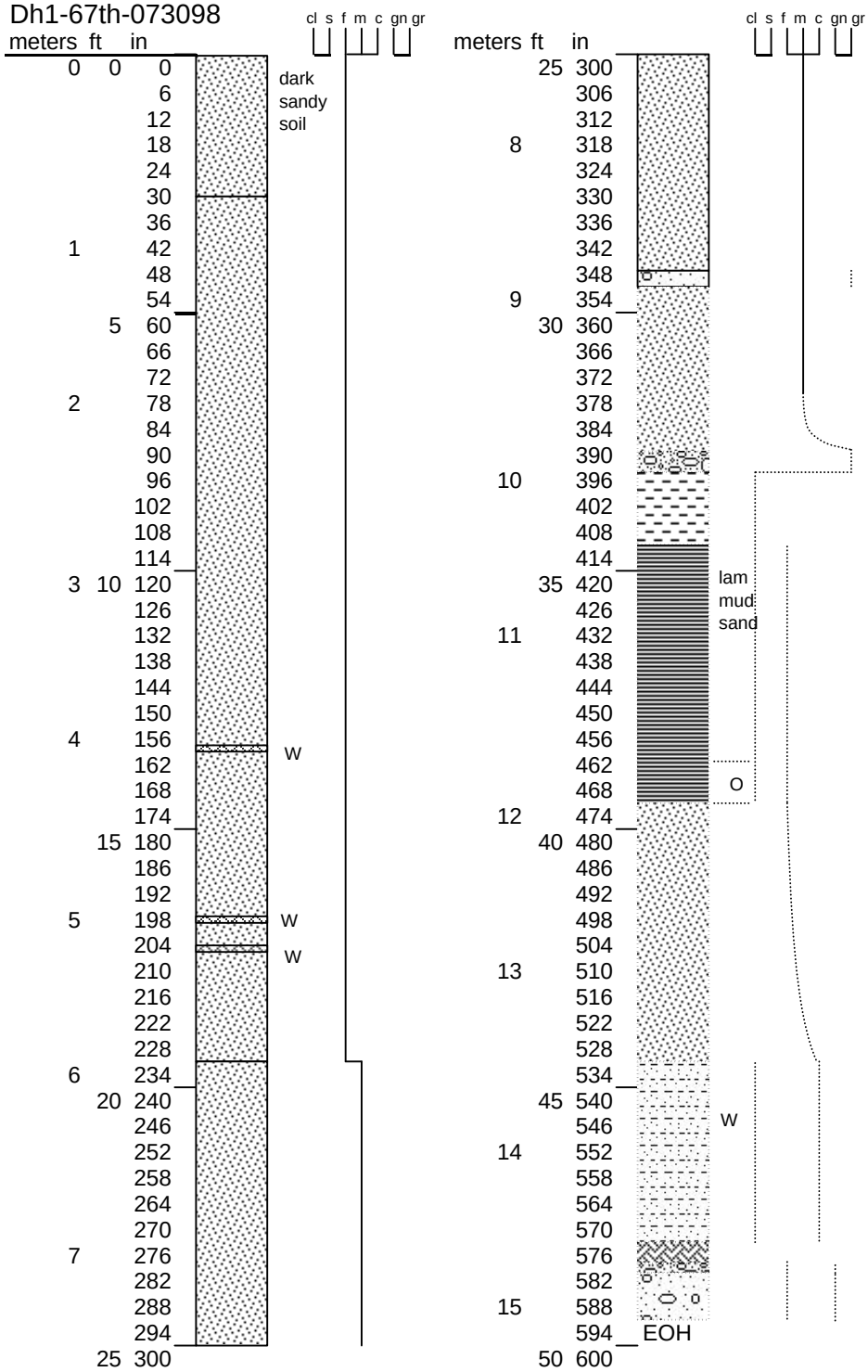

Dh1-Oyst-080198: Page 1

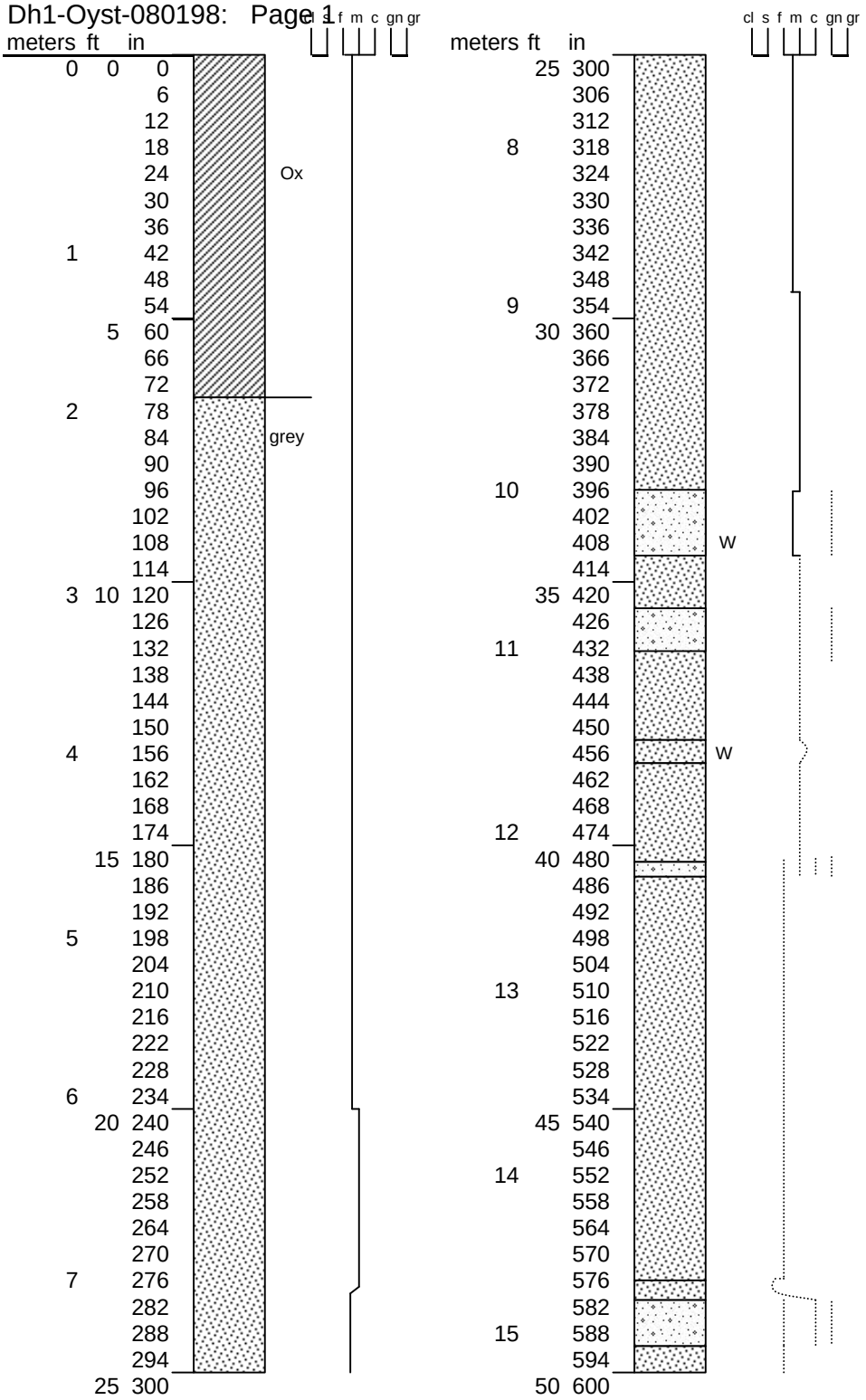

Dh1-Oyst-080198: Page 2

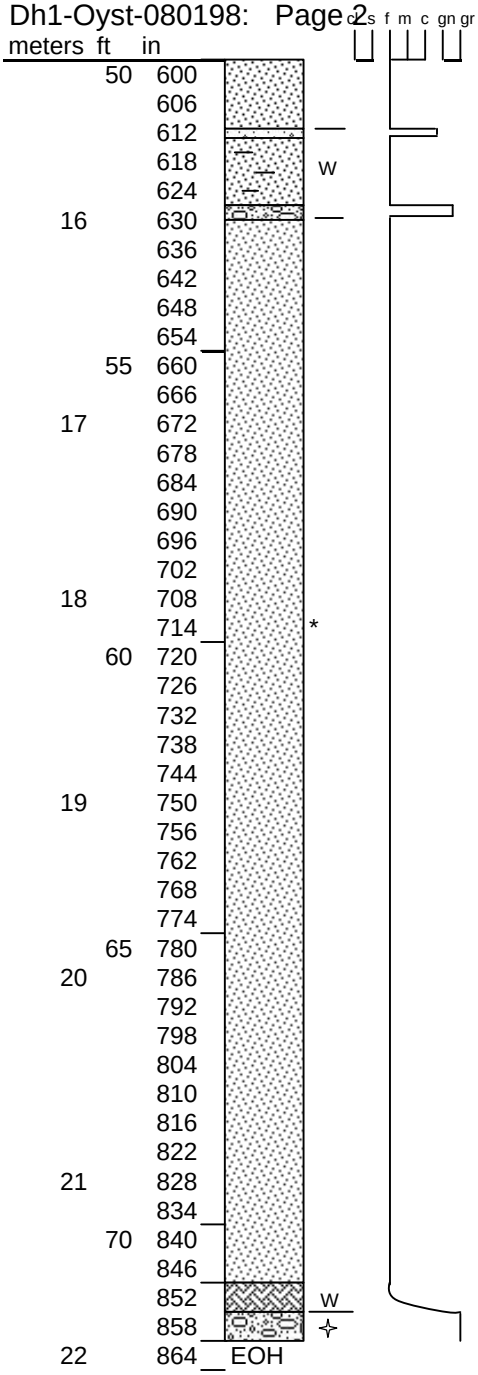

Dh1-Klip-080298: Page 1

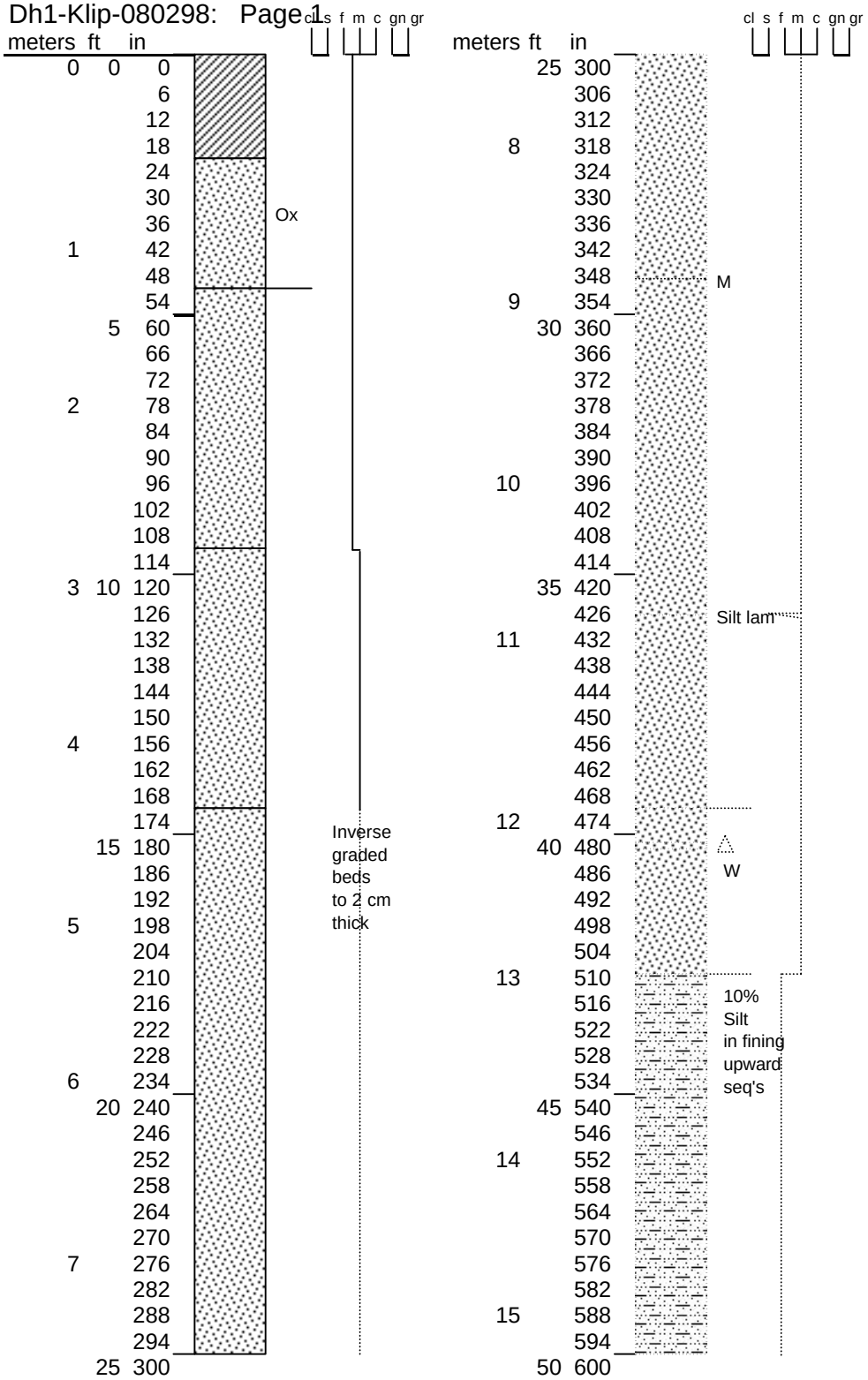

Dh1-Klip-080298: Page 2

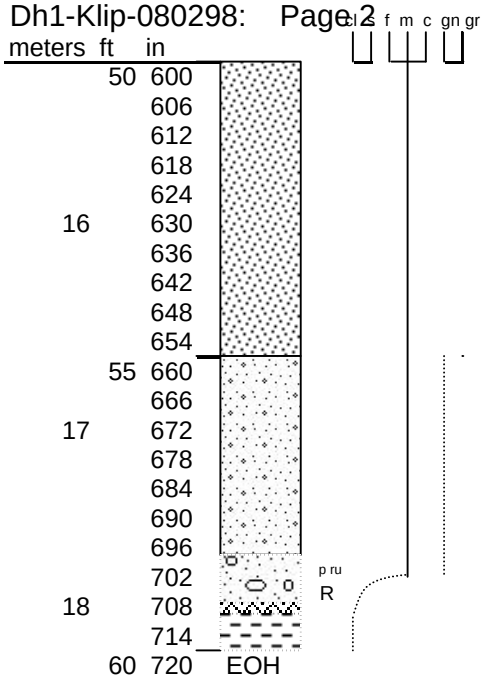

Dh1-Pcyd-080398: Page 1

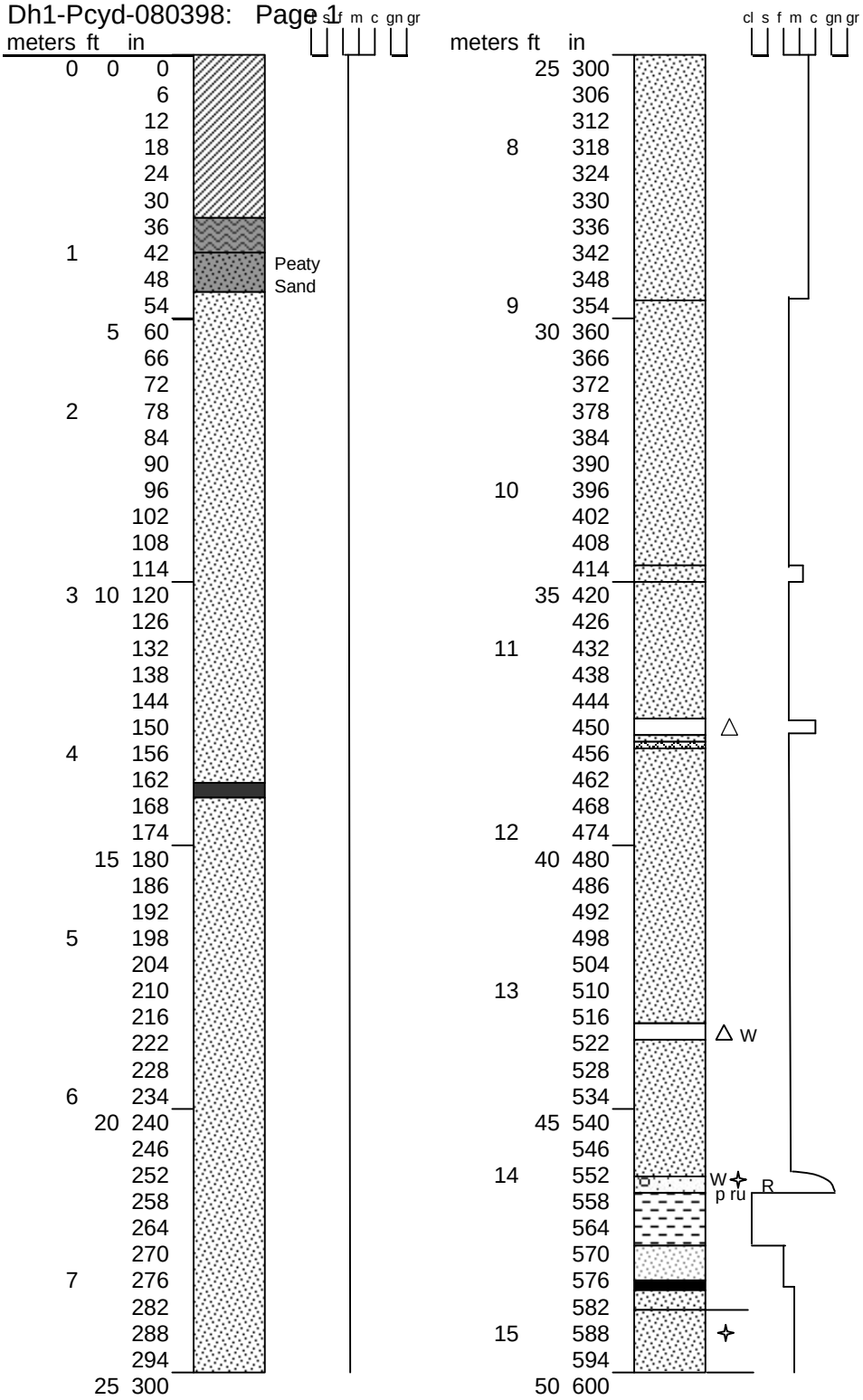

Dh1-Pcyd-080398: Page 2

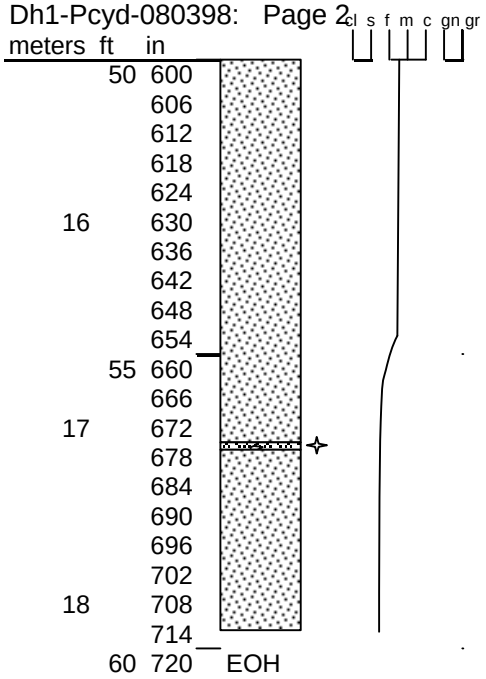

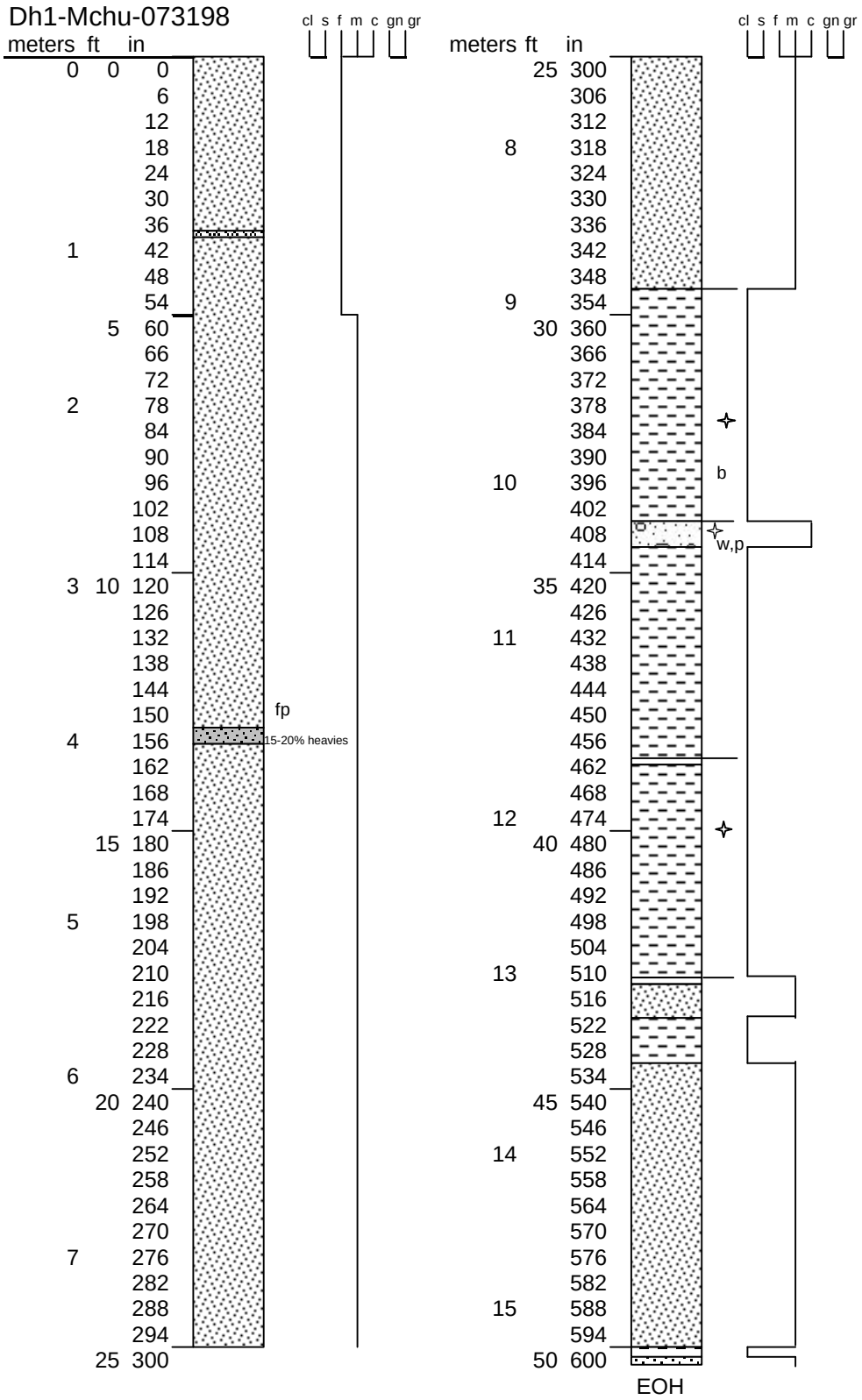
Dh1-Mchu-073198
meters ft in
cl s f m c gn gr
fp
15-20% heavies
b
w,p
EOH

Dh1-Bayr-07-3198

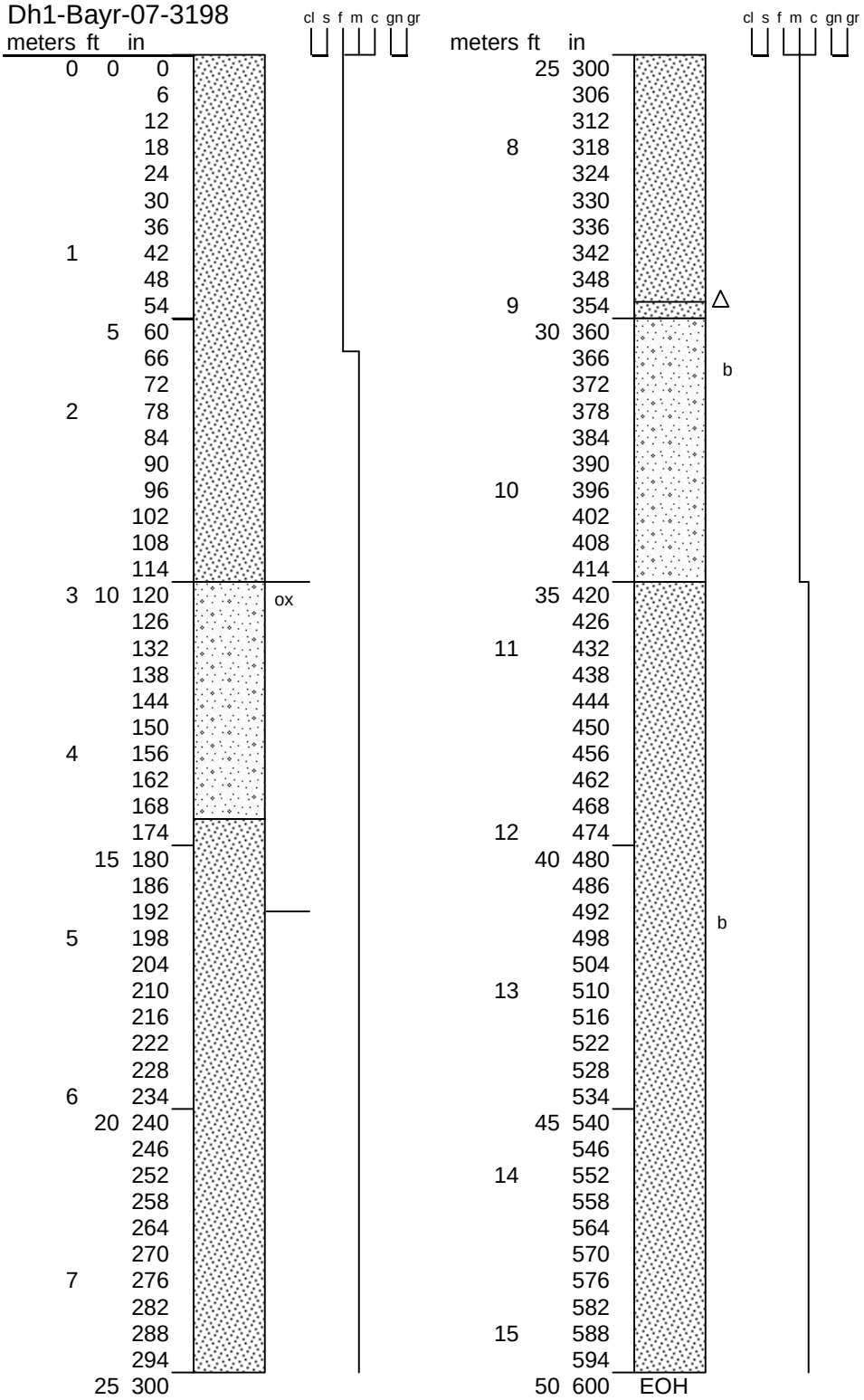

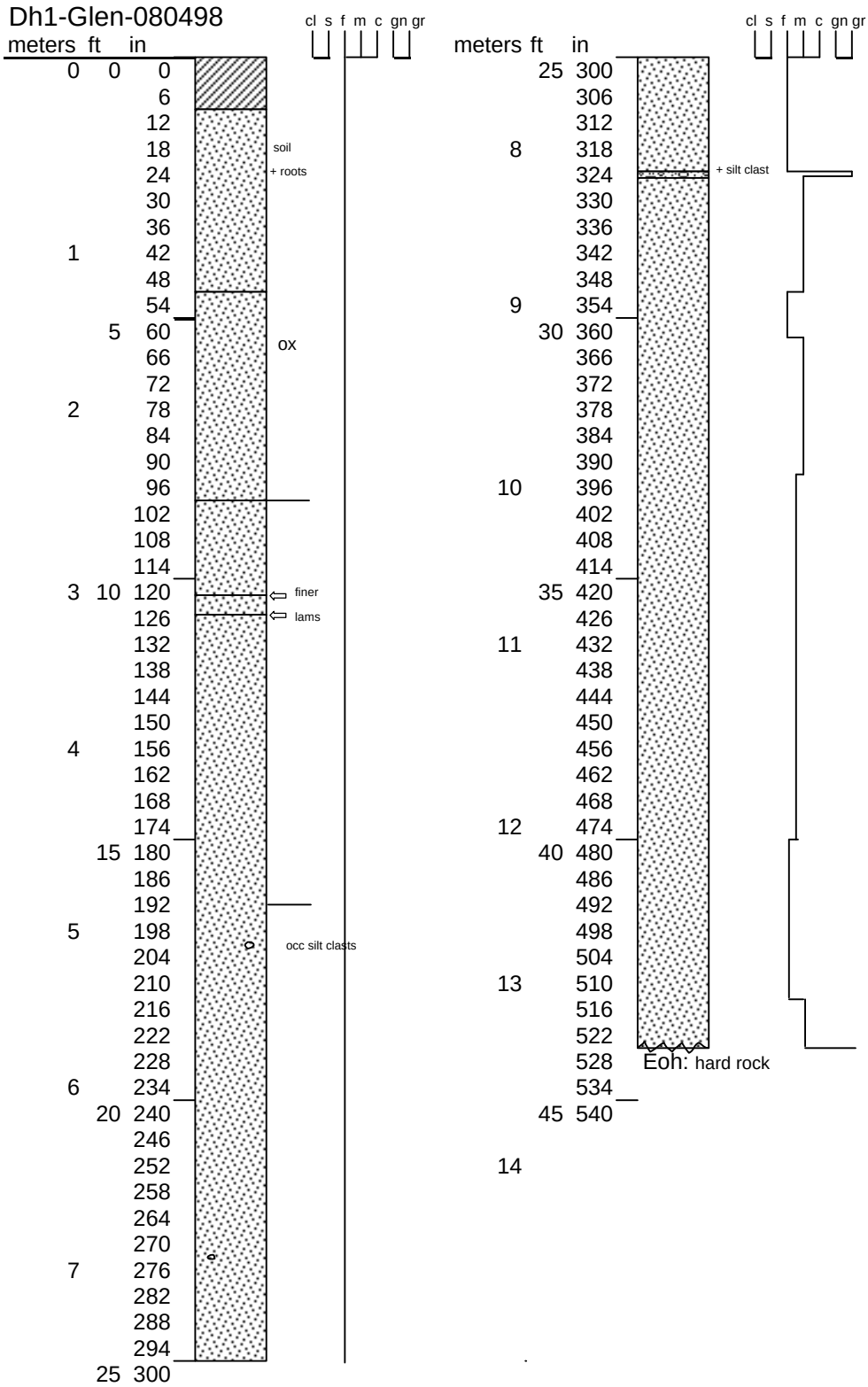
Dh1-Glen-080498
meters ft in
cl s f m c gn gr
soil
+ roots
ox
finer
lams
occ silt clasts
+ silt clast
Eoh: hard rock

Dh1-Sunb-080498: Page 1

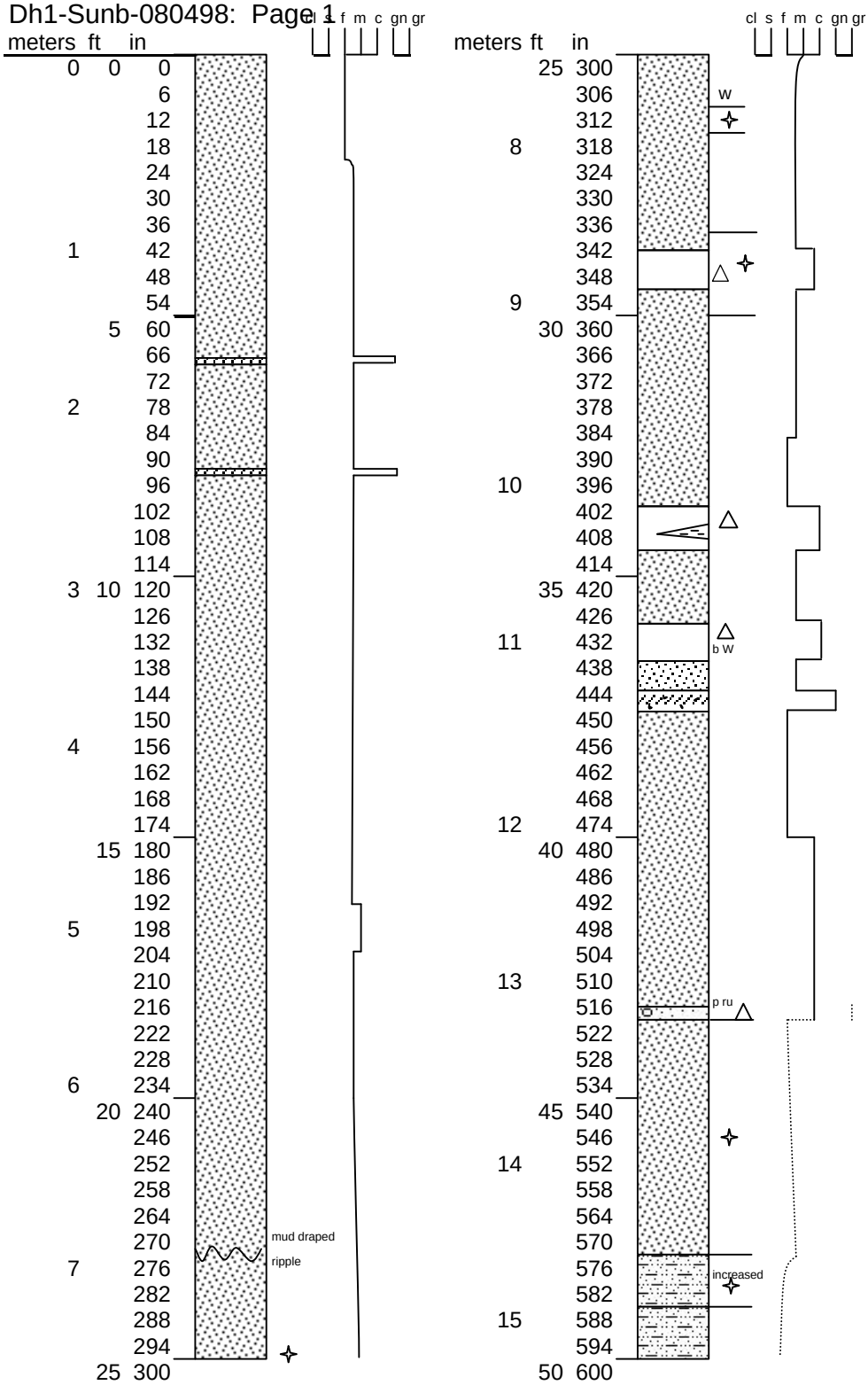

Dh1-Sunb-080498: Page 2

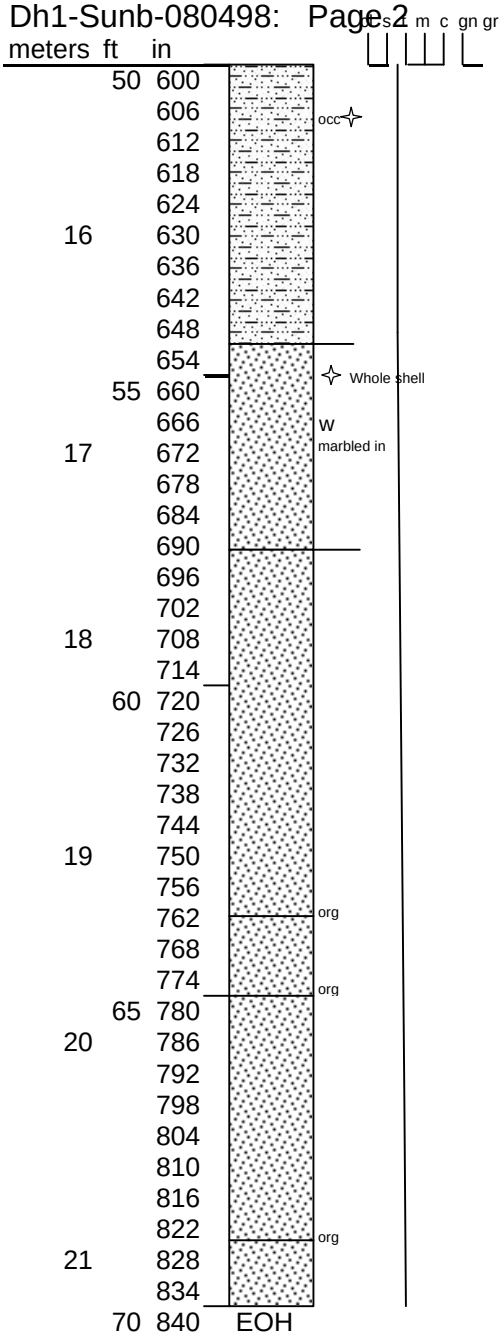

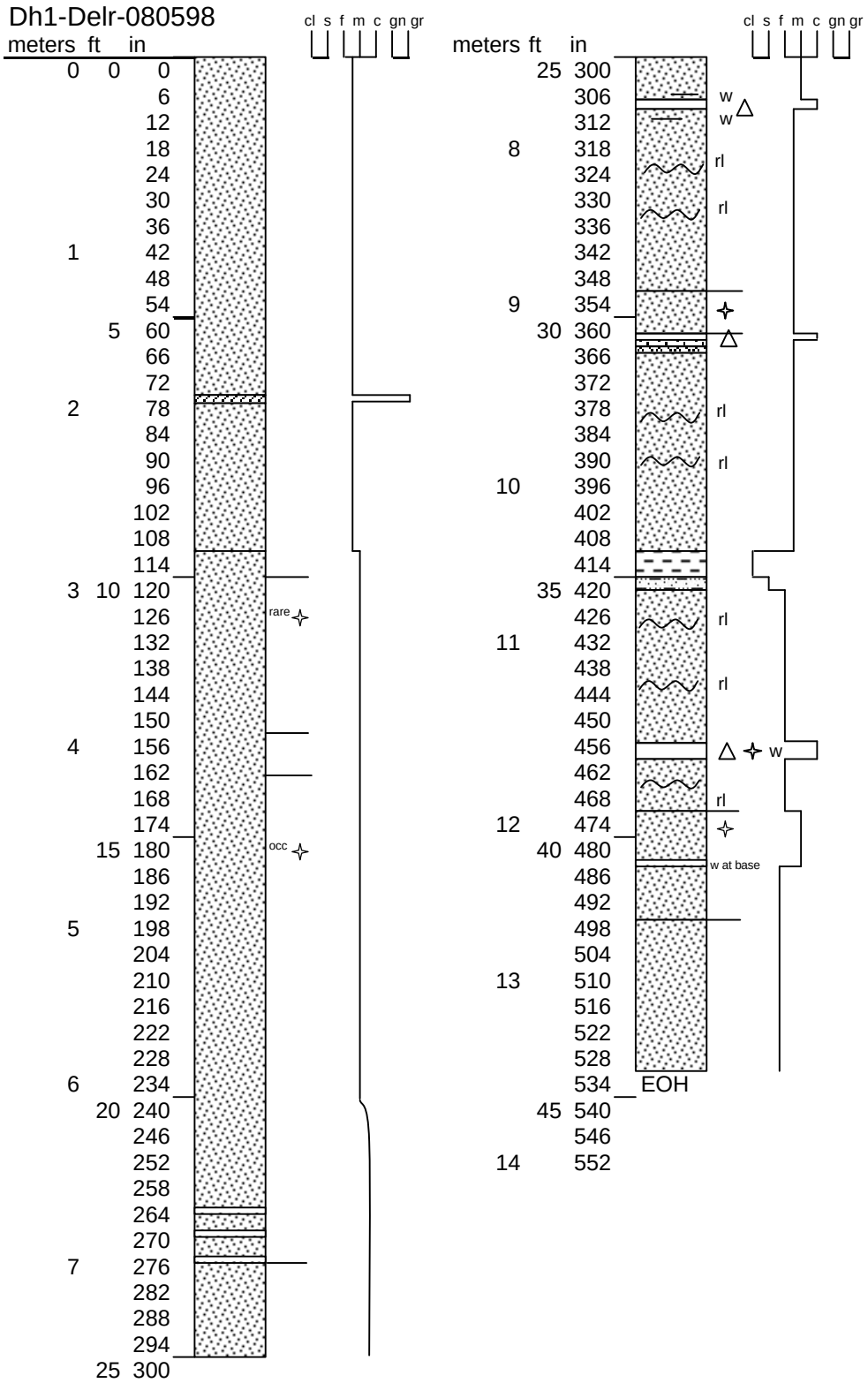
Dh1-Delr-080598
meters ft in
cl s f m c gn gr
rare
occ
w
rl
w at base
EOH

Dh1-Delm-080598

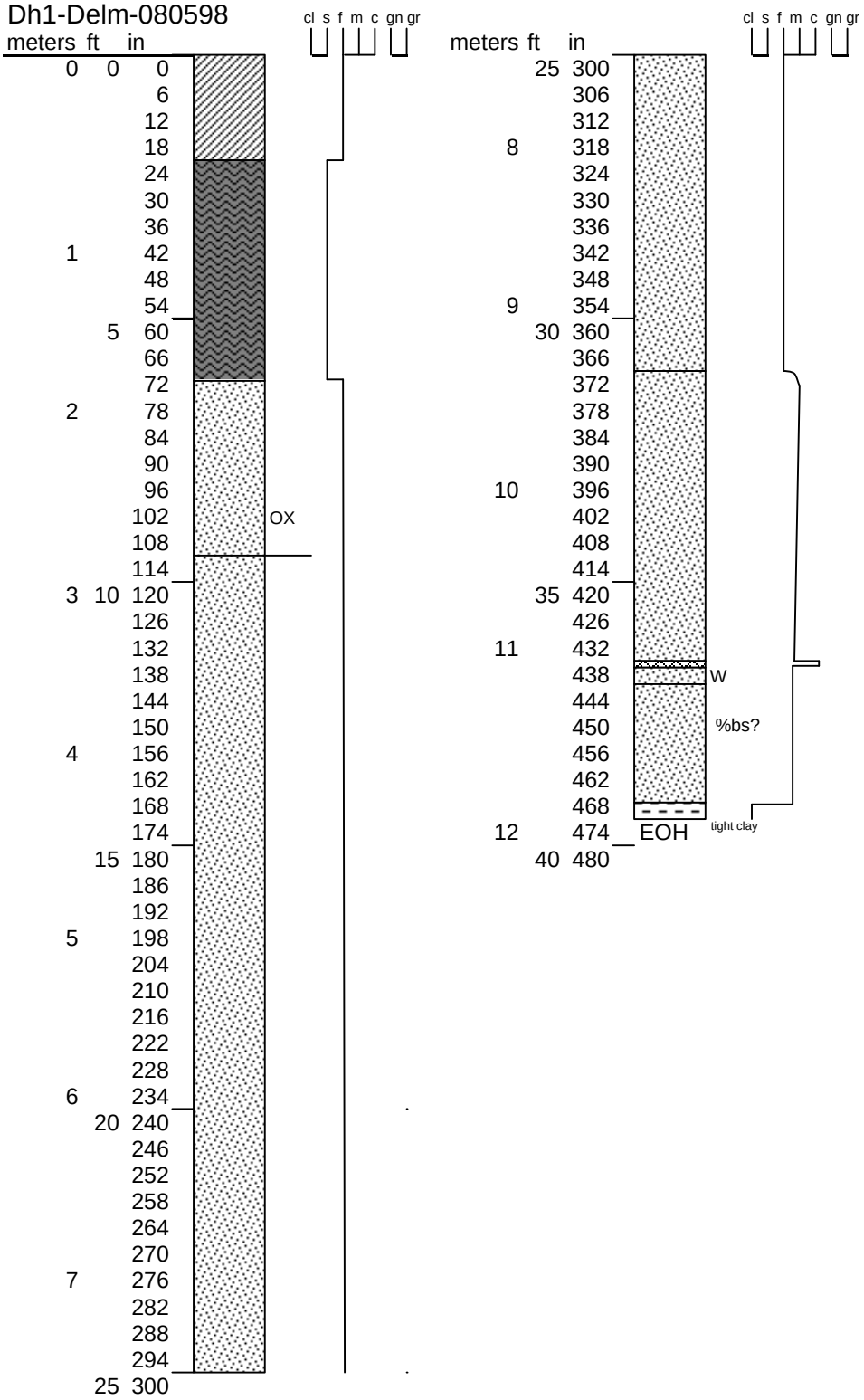

meters	ft	in
0	0	0
		6
		12
		18
		24
		30
		36
1.00		42
		48
		54
	5	60
		66
		72
2.00		78
		84
		90
		96
		102
		108
		114
3.00	10	120
		126
		132
		138
		144
		150
4.00		156
		162
		168
		174
	15	180
		186
		192
5.00		198
		204
		210
		216
		222
		228
6.00		234
	20	240
		246
		252
		258
		264
		270
7.00		276
		282
		288
		294
	25	300

cl s f m c gn gr

meters	ft	in
	25	300
		306
		312
8		318
		324
		330
		336
		342
		348
9		354
	30	360
		366
		372
		378
		384
		390
10		396
		402
		408
		414
	35	420
		426
11		432
		438
		444
		450
		456
		462
		468
12		474
	40	480
		486
		492
		498
		504
13		510
		516
		522
		528
		534
	45	540
		546
14		552
		558
		564
		570
		576
		582
15		588
		594
	50	600

cl s f m c gn gr